



HAL
open science

Low-Frequency Noise Measurements and Applications

Jean-Guy Tartarin

► **To cite this version:**

Jean-Guy Tartarin. Low-Frequency Noise Measurements and Applications: Low-Frequency Noise Metrology For The Development of High-Frequency Technologies and For High Purity Signal Generation. 102th ARFTG Microwave Measurement Symposium, Andrej Rumiantsev, Jan 2024, San Antonio (TX), United States. hal-04440695

HAL Id: hal-04440695

<https://hal.science/hal-04440695>

Submitted on 6 Feb 2024

HAL is a multi-disciplinary open access archive for the deposit and dissemination of scientific research documents, whether they are published or not. The documents may come from teaching and research institutions in France or abroad, or from public or private research centers.

L'archive ouverte pluridisciplinaire **HAL**, est destinée au dépôt et à la diffusion de documents scientifiques de niveau recherche, publiés ou non, émanant des établissements d'enseignement et de recherche français ou étrangers, des laboratoires publics ou privés.



January 21-24, 2024

102nd ARFTG
Microwave Measurement Symposium

Microwave Measurement Conference

Low-Frequency Noise Metrology For The Development of High-Frequency Technologies and For High Purity Signal Generation



Pr. J.G. TARTARIN

LAAS-CNRS & University of Toulouse (Université Paul Sabatier), France

*Manager of the European Platform for “Low Frequency and RTN Noise” labeled by Keysight
Leader of the « HF analog Devices for telecommunications» of Reliability platform PROOF*



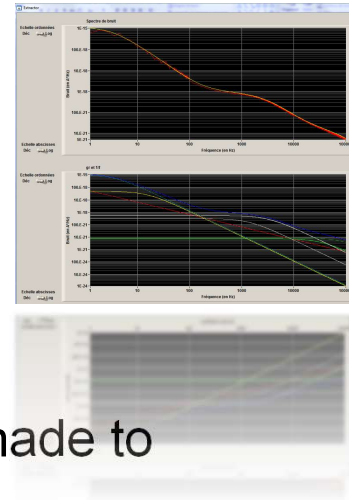
Platform of Reliability tOOls for Failure analysis dedicated to wide bandgap devices



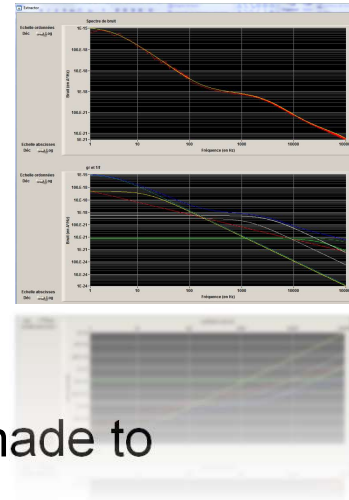
Université
de Toulouse



- ELECTRONIC NOISE: in France and at LAAS-CNRS
- LOW FREQUENCY NOISE (LFN) : metrological niche ? Not only !
- LFN EXPERIMENTAL SETUPS: a large variety of solutions from home-made to commercial solutions
- APPLICATIONS OF LFN MEASUREMENTS : defect detection, reliability analysis, non-linear RF circuit design (VCOs, Mixers).
- CONCLUSIONS and QUESTIONS



- **ELECTRONIC NOISE: in France and at LAAS-CNRS**
- **LOW FREQUENCY NOISE (LFN) : metrological niche ? Not only !**
- **LFN EXPERIMENTAL SETUPS: a large variety of solutions from home-made to commercial solutions**
- **APPLICATIONS OF LFN MEASUREMENTS : defect detection, reliability analysis, non-linear RF circuit design (VCOs, Mixers).**
- **CONCLUSIONS and QUESTIONS**



- > LF Noise meas. in France
- > HF Noise meas. in France

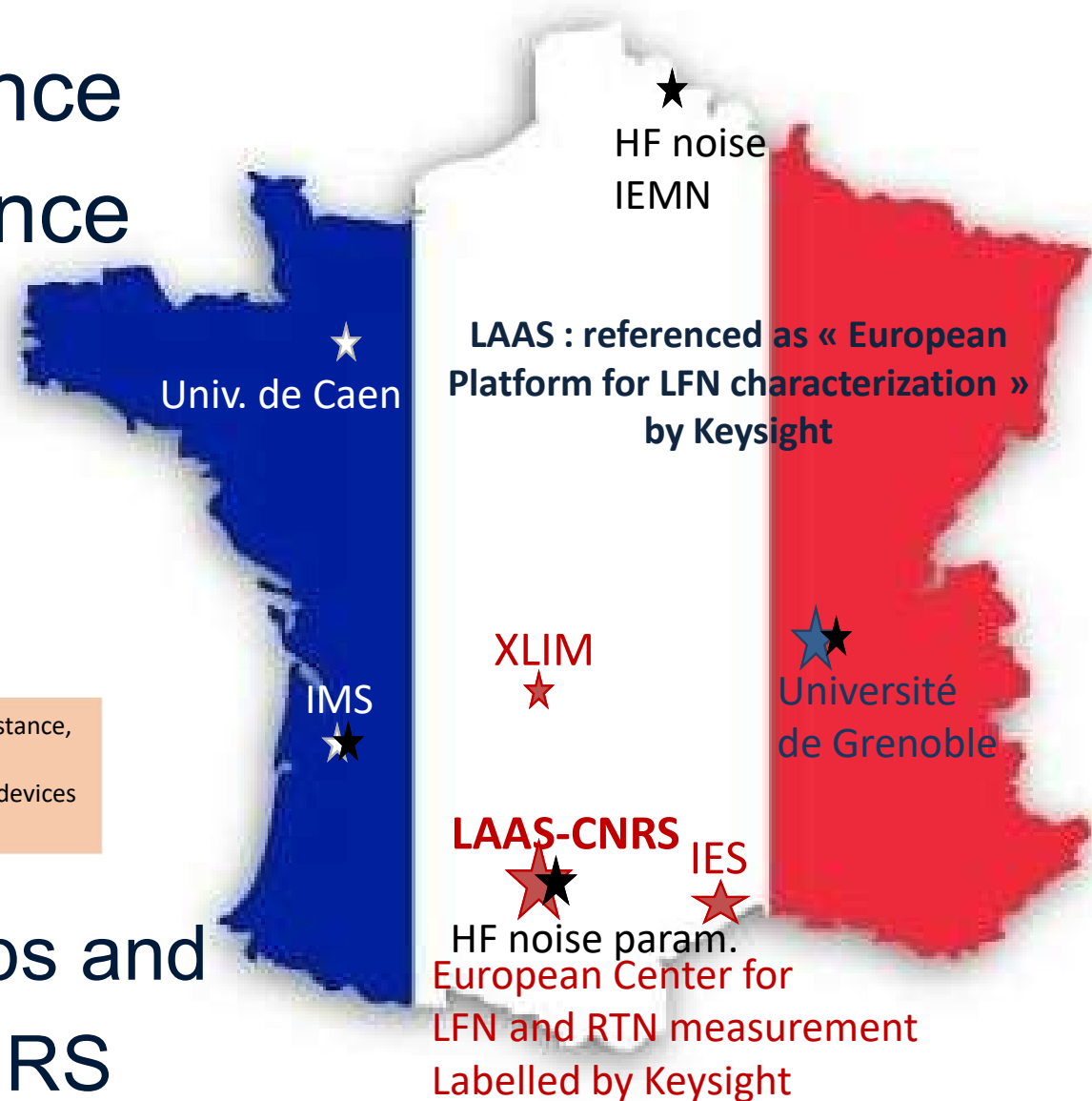
European Microwaves

From IEEE Microwave Magazine,
"European Microwaves", Sept-Oct 2012

Roberto Sorrentino
and Jan Grahm

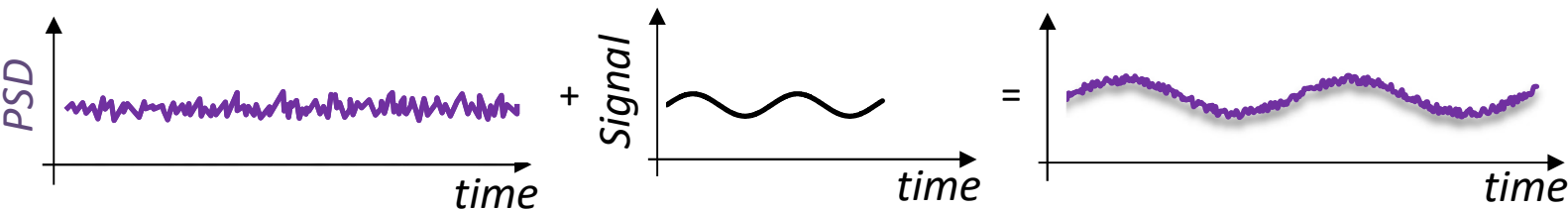


Cooperation with academic laboratories has often specialized in specific topics (for instance, **IEMN** on device processing, simulation, and characterization; **XLIM** on microwave components and systems modelling and simulation; **LAAS on noise**; **IMS** on silicon devices and reliability; **LabSTICC** on filtering; and **IETR** on antenna design and characterization

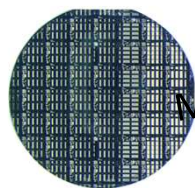
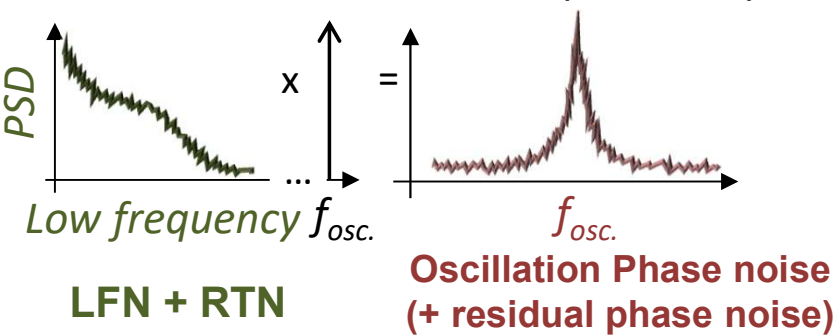


- > Electronic Noise exp. setups and related activities at LAAS-CNRS

HF noise (NF50 + 4 noise parameters) *Transient representation at a frequency f_0*

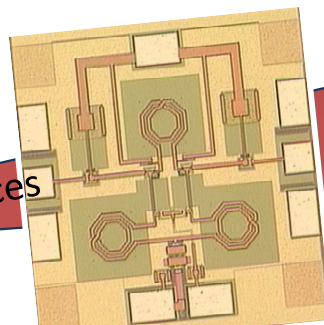


Non-Linear LF & HF noise *Spectral representation (at LF & at frequency f_0)*



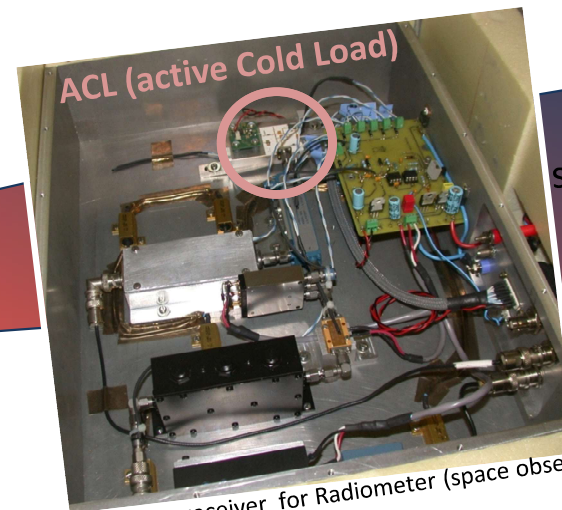
Wafer (SiGe, GaAs, GaN ...) for process optimization

Material/devices



circuits

K.W Wong, JG Tartarin, 2004 State of the art low phase noise Ka band VCO



Ultra low noise receiver for Radiometer (space observation)

systems

Measurements – models

→ **Mastering the noise from device/circuit/system**



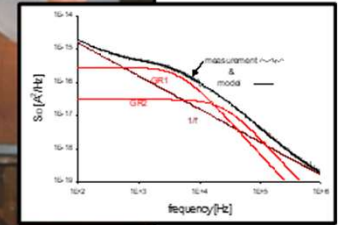
ELECTRONIC NOISE:

Noise measurement facilities at LAAS-CNRS



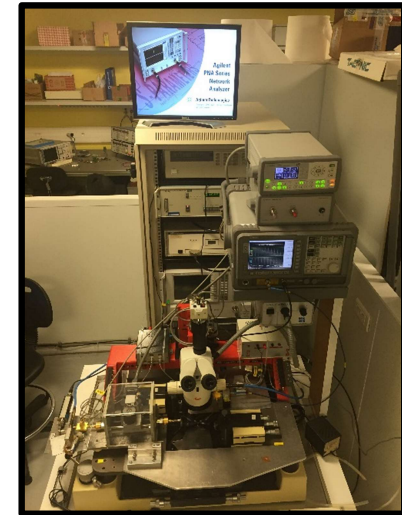
Université de Toulouse

LFN and RTN: the LAAS CNRS has been developing low frequency noise (LFN) metrology means for more than six decades, which allow it to claim very low levels of detectivity performance (10^{-28} A/Hz^{1/2}) and up to 1 MHz.



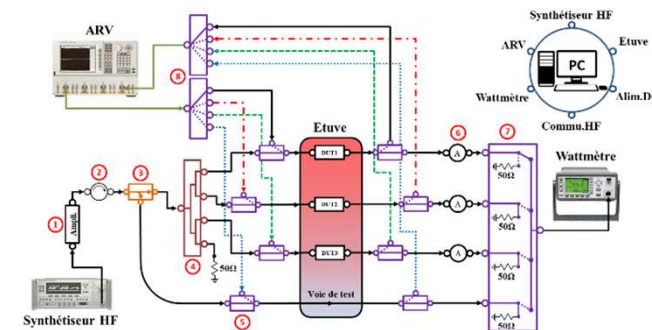
Labeled as a European Platform for LFN and RTN by Keysight since 2017

HF NF50 and 4 noise parameters: different (evolving and automated) workbenches for noise measurement from 10 MHz to 50 GHz. NFA and PNA-X option 029 from Keysight



HF NF50 NL noise under pumping signal: evolution of NF50 under aggressive EM signal (jamming, interferences)

Integration of LFN & HF noise measurements in situ - reliability testbench : The 4-channel RF and thermal test bench allows Full-DC characterization, [S] parameter characterization, NL $P_{out}-P_{in}$ AND LFN (output) spectra, and NF50 measurement without removing connectors.



Main scientific fields :

Pr. JG TARTARIN

> New devices :

- *Modelling and noise sources identification - process improvement*

> Reliability :

- *Reliability through noise measurement, at device and circuit level – process improvement*

> Linear & Nonlinear circuits and noise :

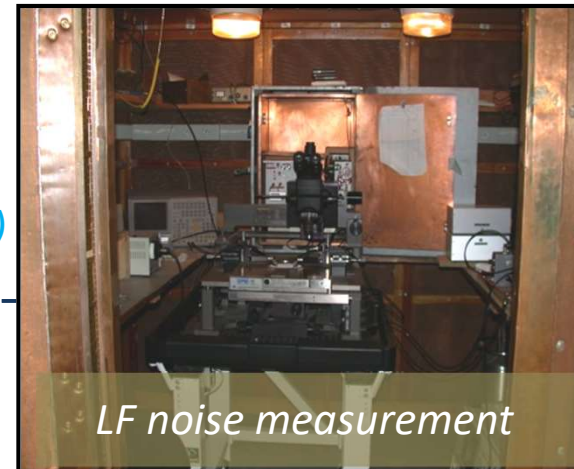
- *Noise sources modelling under nonlinear conditions*
- *Low Noise Amplifier design – harshness vs jamming (+ nonlinear noise figure)*
- *Phase noise modelling (oscillator, amplifier...)*

> Noise in complex systems :

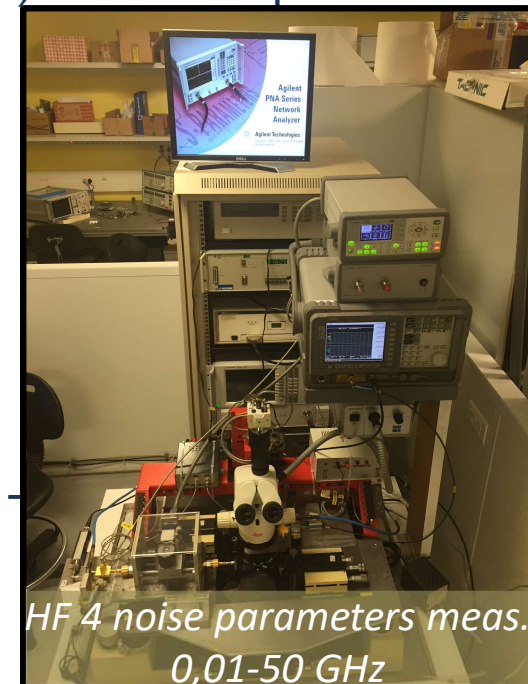
- *Noise in frequency synthesis,*
- *Noise in Tx/Rx RF links...*

> Noise metrology :

- *Low frequency noise (1/f – GR - RTN)*
- *Microwave linear noise (NF50, 4 parameters)*
- *Nonlinear HF noise*
- *Phase noise (RF and microwave sources)*
- *additive phase noise*
- *Optical noise (ex : laser RIN, Δv)*



LF noise measurement



HF 4 noise parameters meas.
0,01-50 GHz

Main scientific fields :

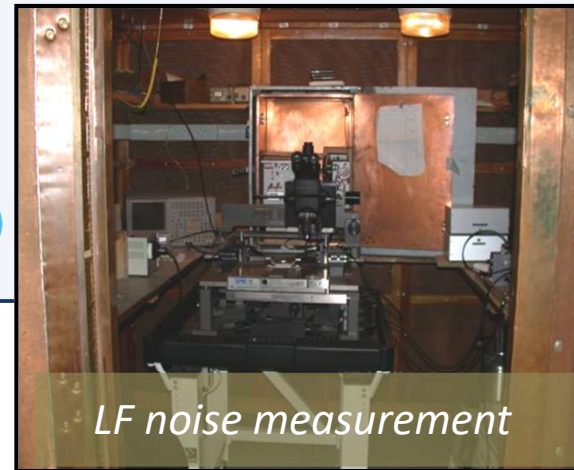
- > **New devices :**
 - *Modelling and noise sources identification - process improvement*
- > **Reliability :**
 - *Reliability through noise*
- > **Linear & Nonlinear circuits :**
 - *Noise sources modelling*
 - *Low Noise Amplifier design*
 - *Phase noise modelling (PLL)*
- > **Noise in complex systems :**
 - *Noise in frequency synthesis,*
 - *Noise in Tx/Rx RF links...*
- > **Noise metrology :**
 - *Low frequency noise (1/f – GR - RTN)*
 - *Microwave linear noise (NF50, 4 parameters)*
 - *Nonlinear HF noise*

NOISE IN ELECTRONIC DEVICES / CIRCUITS / SYSTEMS since 1998

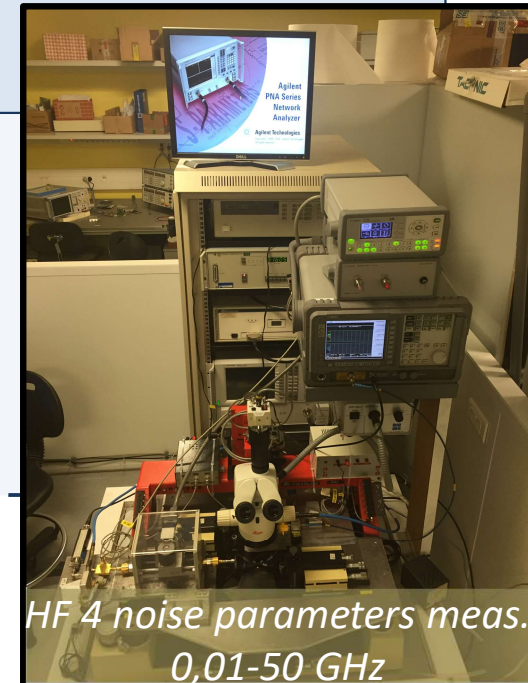
5 International or European Programs on LF noise
 1 PEPR and 10 ANR French National projects
 32 projects with Leading Industries in Europe and North America
 6 Int. Patents and 3 Software Releases
 98 Int. Publications in Journals & Symposiums

Pr. JG TARTARIN

1 Pr; 1 Research Engineer, 2-3 Ph.D. students / year



LF noise measurement



HF 4 noise parameters meas.
0,01-50 GHz



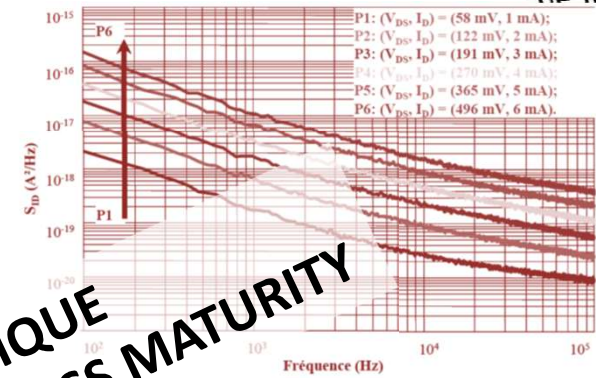
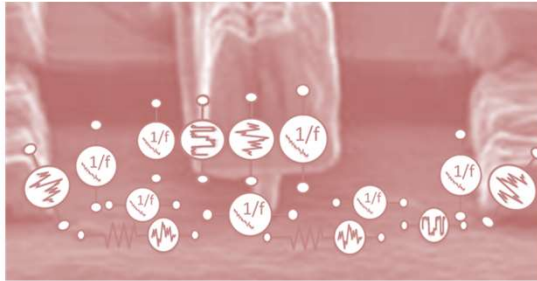
OUTLINE



Université
de Toulouse

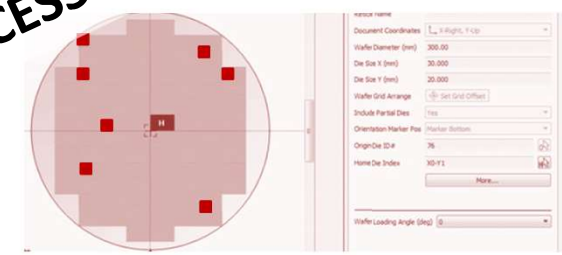
- ELECTRONIC NOISE: in France and at LAAS-CNRS
- **LOW FREQUENCY NOISE (LFN) : metrological niche ? Not only !**
- LFN EXPERIMENTAL SETUPS: a large variety of solutions from home-made to commercial solutions
- APPLICATIONS OF LFN MEASUREMENTS : defect detection, reliability analysis, non-linear RF circuit design (VCOs, Mixers).
- CONCLUSIONS and QUESTIONS

Defect analysis prior to electrical degradation

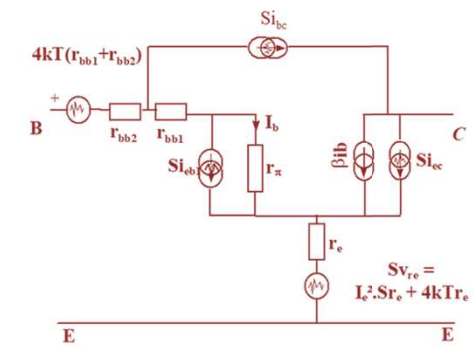


Defect analysis for reliability and SOA

NON INVASIVE – NON DESTRUCTIVE TECHNIQUE
NOT A DETERMINISTIC SIGNAL – SIGNATURE OF PROCESS MATURITY



Models for Low Phase Noise behavior
(high purity / low phase noise oscillators)



Still (and more than ever) in the race as far as there will be new technologies and signal-detection noise floor !

Is LFN old fashioned?

- International Conference on Fluctuation and Noise, since 1968 and still alive
(*Fluctuation And Noise, and other noise-dedicated conferences are out now*)

International Conference on Fluctuation and Noise 2023, Grenoble, France:

- invited paper « **Low frequency noise in qubits** » by Mark Dykman - Theory
- quantum system and noise session - Theory
- quantum devices and noise – Electronic Devices & Material
- quantum transport and superconductivity session - Theory

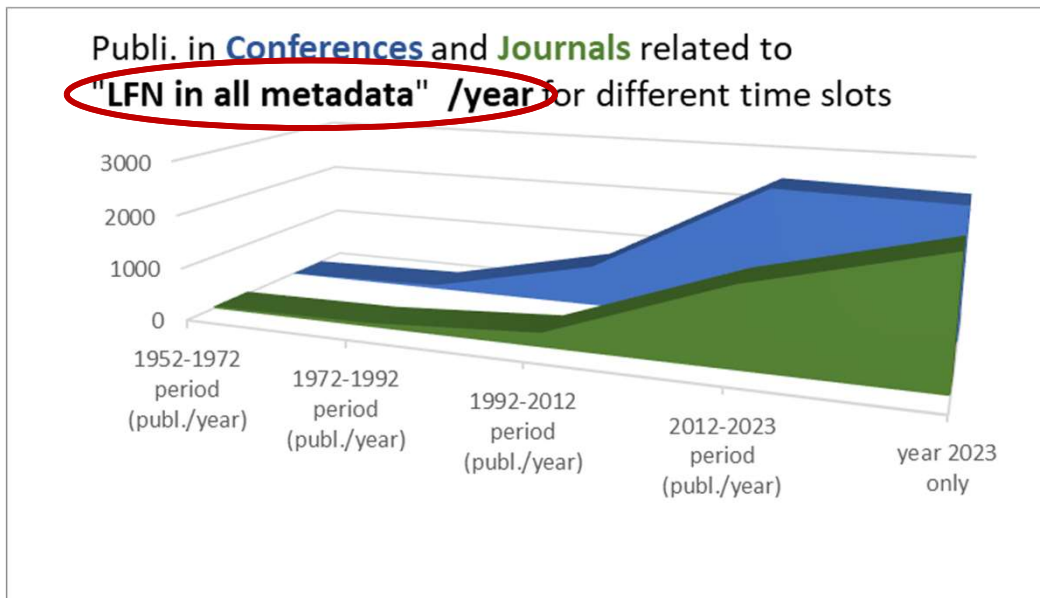
Where to find noise (and LFN) in Conferences or Journals:

- **IMS: International Microwave Symposium (USA)** – every year, sessions dedicated to low noise devices (EuMW), circuits (EuMiC) and systems (EuRAD)
- **EuMW: European Microwave Week (Europe)** – every year, almost the same format as for IMS
- **ESREF: European Symposium on Reliability of Electron Devices** – no dedicated session BUT LFN is used for failure detection and degradation analysis in (active) devices
- **RADECS: RADiations and its Effects on Components and Systems Conference (Europe)**
and many other
- *Journals: IEEE (MTT, EDL, SSE), AIP publishing, Cambridge Univ. Press, Elsevier... **ponctual publ.***

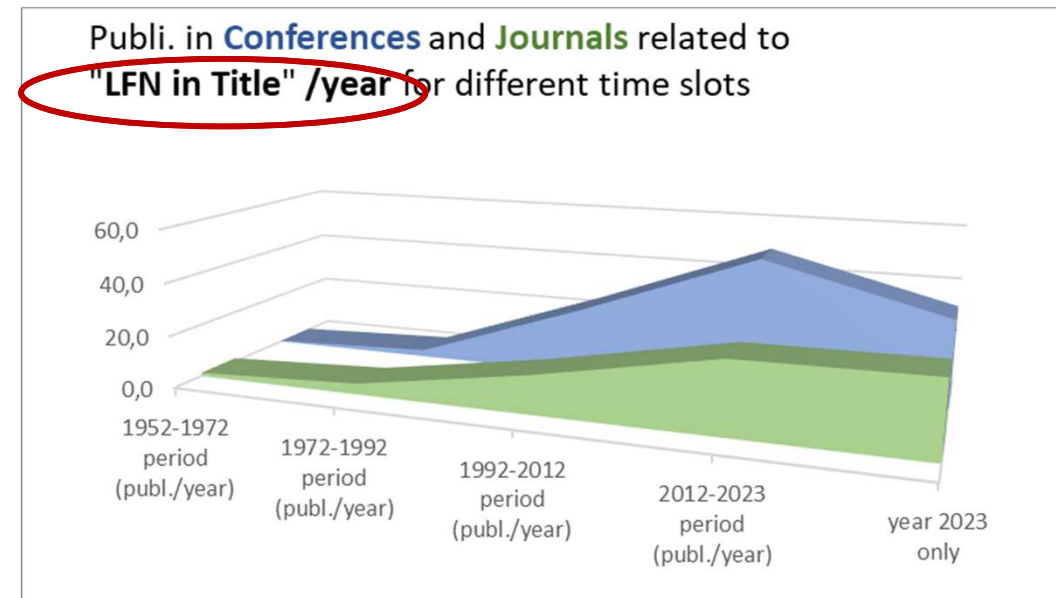
Research on data base from IEEE EXPLORE over different periods: from (1912 to) 1952 to 2023

1912-1952 : 75 journals (i.e. average of 1.8 publications/year)

1952-2023 : large increase in the use of LFN (theory/metrology/applied physics or technological assessment)



More general purpose (tool?)



Specific research in the field (expert skills)

Clearly, those who claimed the LFN was dead were geniuses 😂 – the new Nostradamus



Some of them however come back to LFN! 🤔 Quantic or whatever the technology, LFN is still in the race

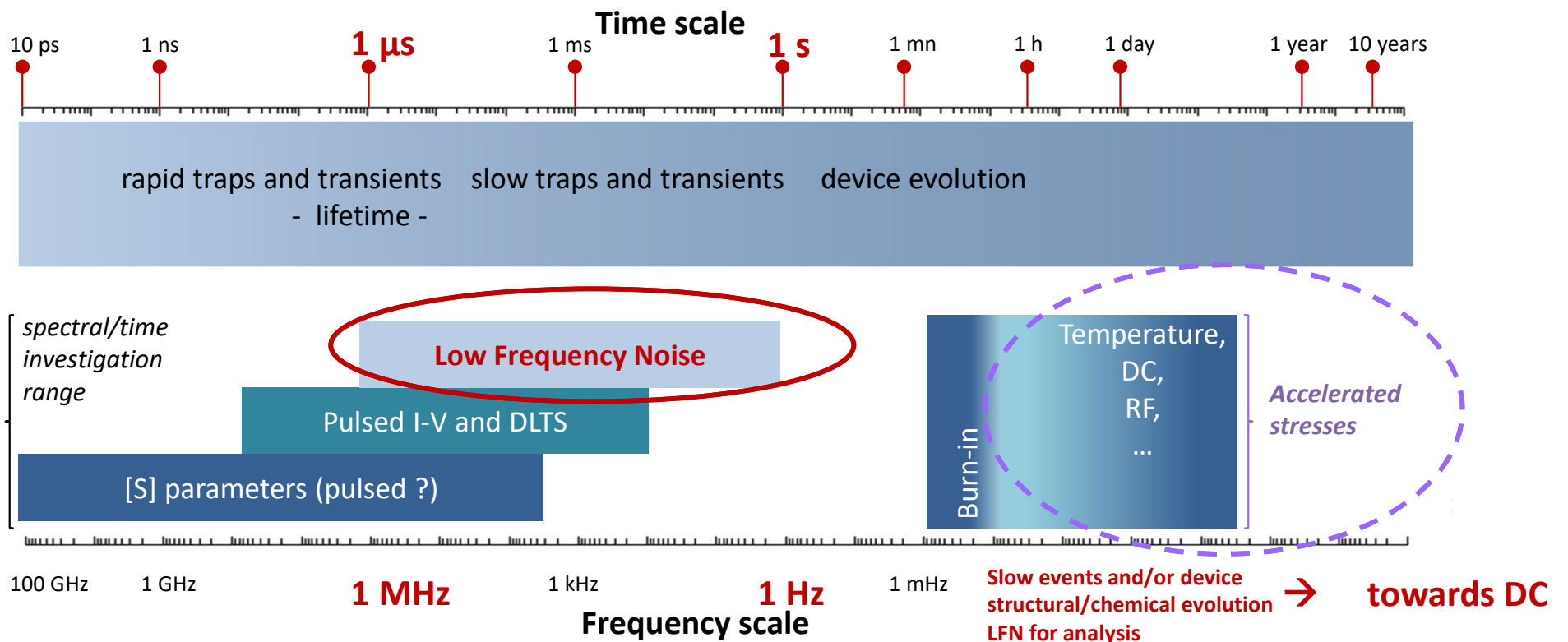
- LFN within other frequency characterization.

Discrimination between time constants / impact of the experimental setup ?

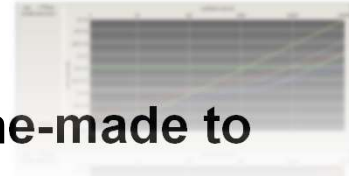
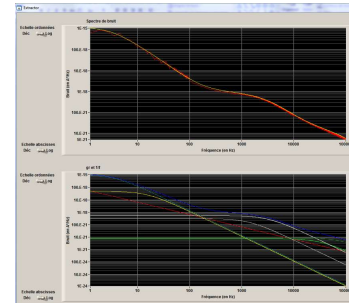
- Non invasive measurement techniques for failure analysis (LFN, pulsed electrical, DLTS, ...)

→ Investigation of technological defects at t_0

→ Evolution of the device's perf. during stress



- ELECTRONIC NOISE: in France and at LAAS-CNRS
- LOW FREQUENCY NOISE (LFN) : metrological niche ? Not only !
- **LFN EXPERIMENTAL SETUPS: a large variety of solutions from home-made to commercial solutions**
- APPLICATIONS OF LFN MEASUREMENTS : defect detection, reliability analysis, non-linear RF circuit design (VCOs, Mixers).
- CONCLUSIONS and QUESTIONS



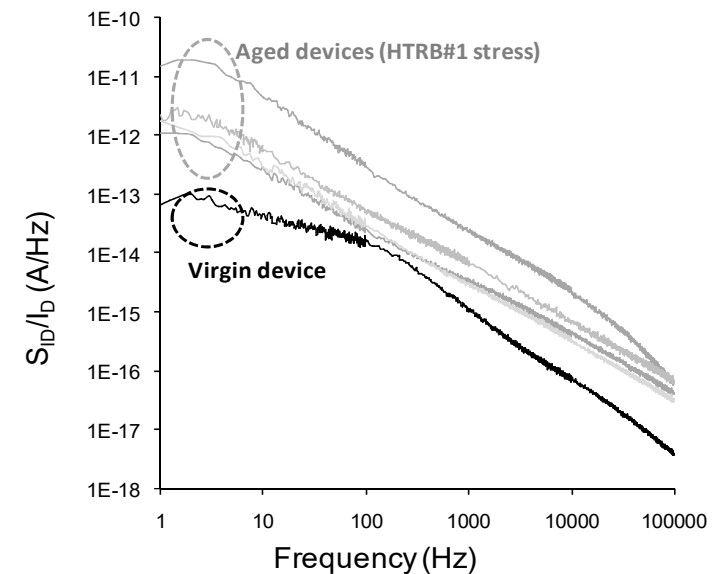
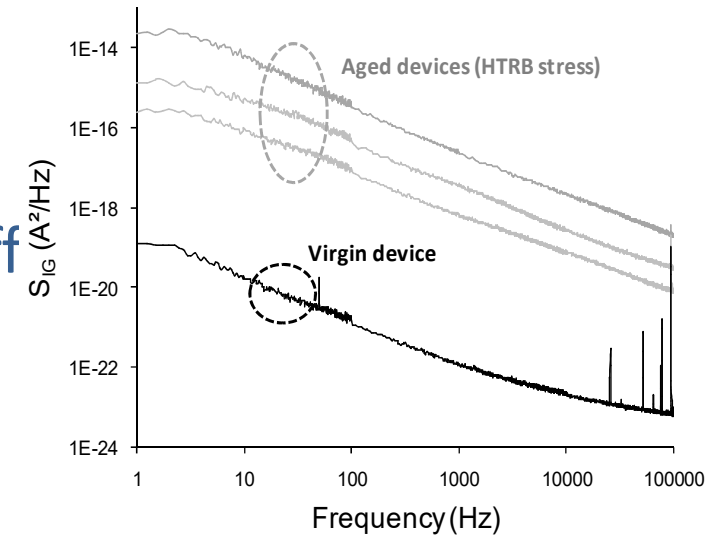
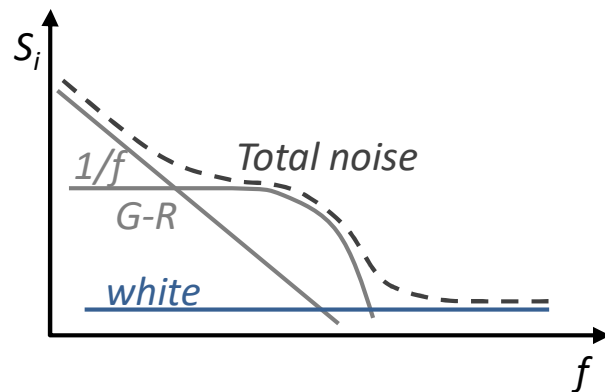
Internal noise in electronic devices:

Linear noise:

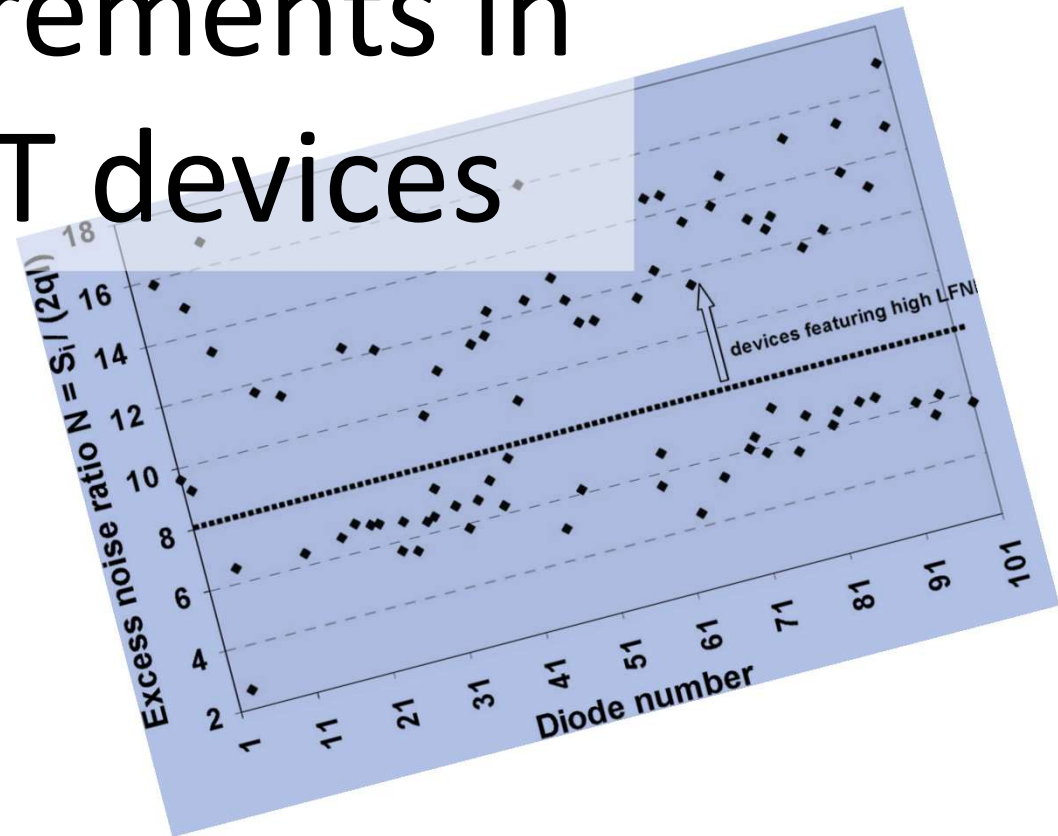
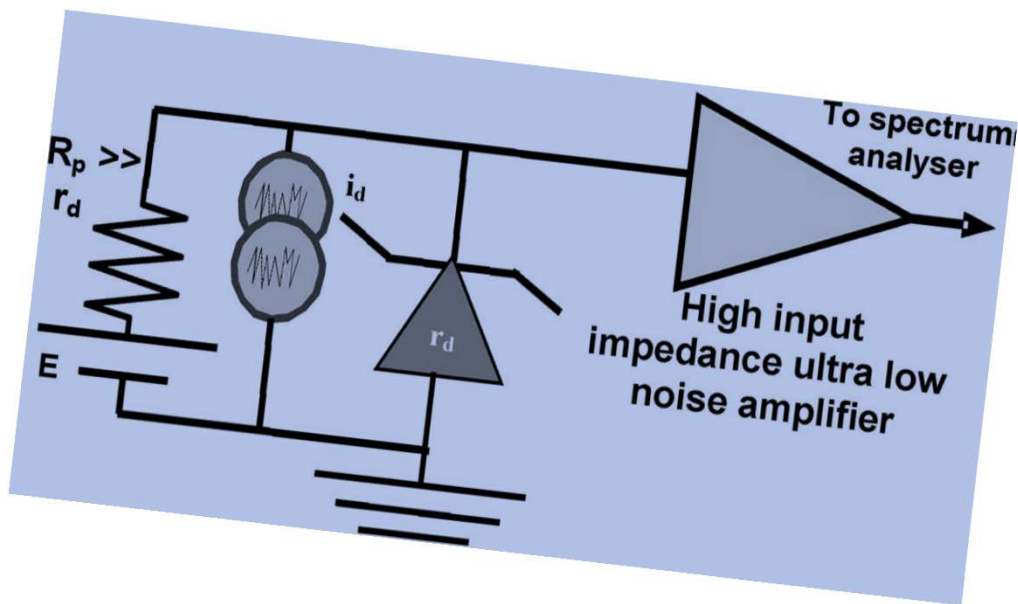
- White Noise (thermal noise, shot noise, diff

Non-linear -Excess Noise (can be reduced):

- $1/f$ noise
- Generation-recombinaison (G-R)
- Random Telegraph Noise (RTS or RTN)



LFN measurements in ONE-PORT devices

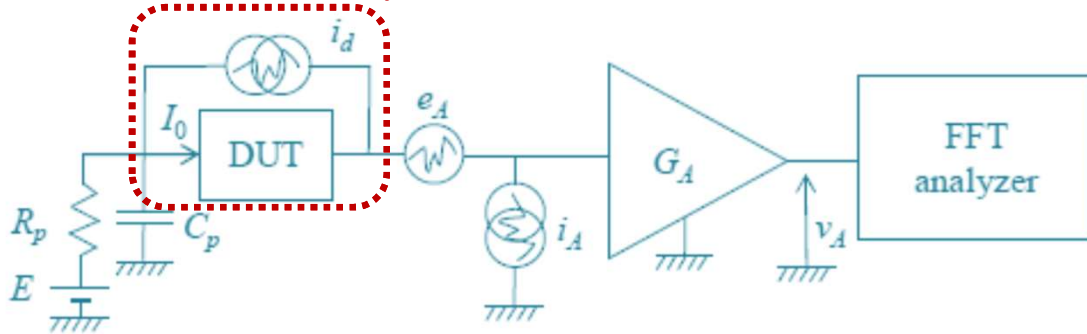


Configuration for diode measurement ; current-voltage or voltage-voltage amplifier

Two possible arrangements for one-port LFN (S_{id}) measurements;

- Current-voltage amplifier (gain G_A in V/A)
- Voltage amplifier (Gain G_V)

D.U.T : Diode or photodiode



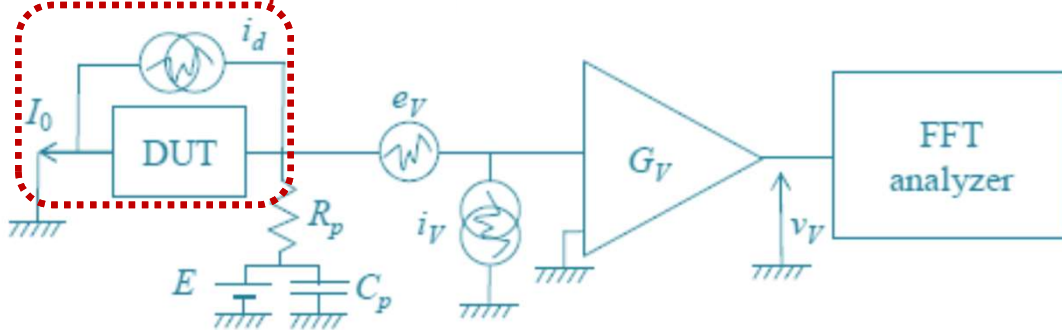
Simplified S_{vA} and S_{vV} expressions

$$S_{vA} = G_A^2 \left[\frac{R_{dut}}{(R_{dut} + R_{inA})} \right]^2 \left[S_{id} + S_{iA} + \frac{S_{eA}}{R_{dut}^2} + \frac{2S_{eiA}}{R_{dut}} \right]$$

As long as $R_{DUT} \gg R_{input A}$
and $R_{DUT} \gg (S_{eA}/S_{iA})^{1/2}$

$$S_{vA} = G_A^2 [S_{id} + S_{iA}]$$

D.U.T : Diode or photodiode



$$S_{vV} = G_V^2 \left[\frac{R_{inV}}{R_{dut} + R_{inV}} \right]^2 [R_{dut}^2 S_{id} + S_{eV} + R_{dut}^2 S_{iV} + 2R_{dut} S_{eiv}]$$

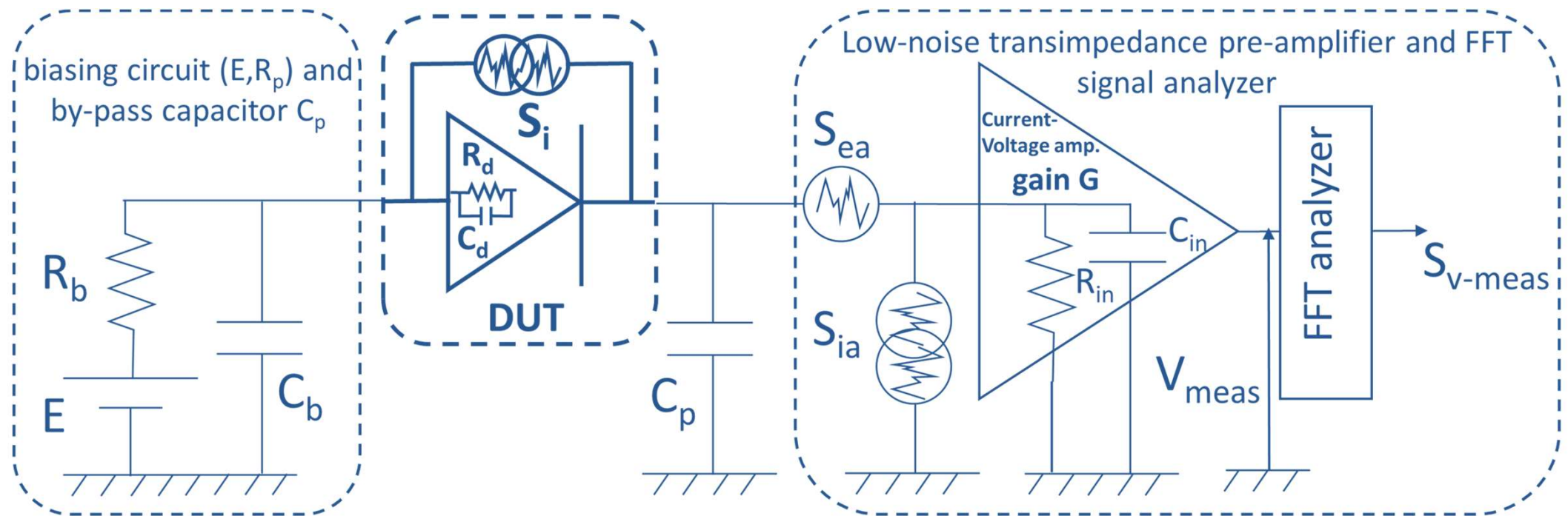
As long as $R_{DUT} \ll R_{input V}$
and $R_{DUT} \ll (S_{eV}/S_{iV})^{1/2}$

$$S_{vV} = G_V^2 [R_{dut}^2 S_{id} + S_{eV}]$$

Configuration for diode measurement ; current-voltage amplifier

DUT impedance is elevated \rightarrow transimpedance ampl. ! All the elements are measured prior to LFN meas. Below is the full expression for S_{v-meas}

$$S_{v-meas}(f) = \left(\frac{G^2 R_d^2}{(R_d + R_{in})^2 + (R_{in} R_d C_d \omega)^2} \right) \cdot \left(\frac{S_{ea} [1 + (R_d C_d \omega)^2]}{R_d^2} + S_{ia} + \frac{2 \operatorname{Re}(S_{ea} i a^*)}{R_d} + 2 \operatorname{Im}(S_{ea} i a^*) \cdot C_d \omega + S_i \right)$$

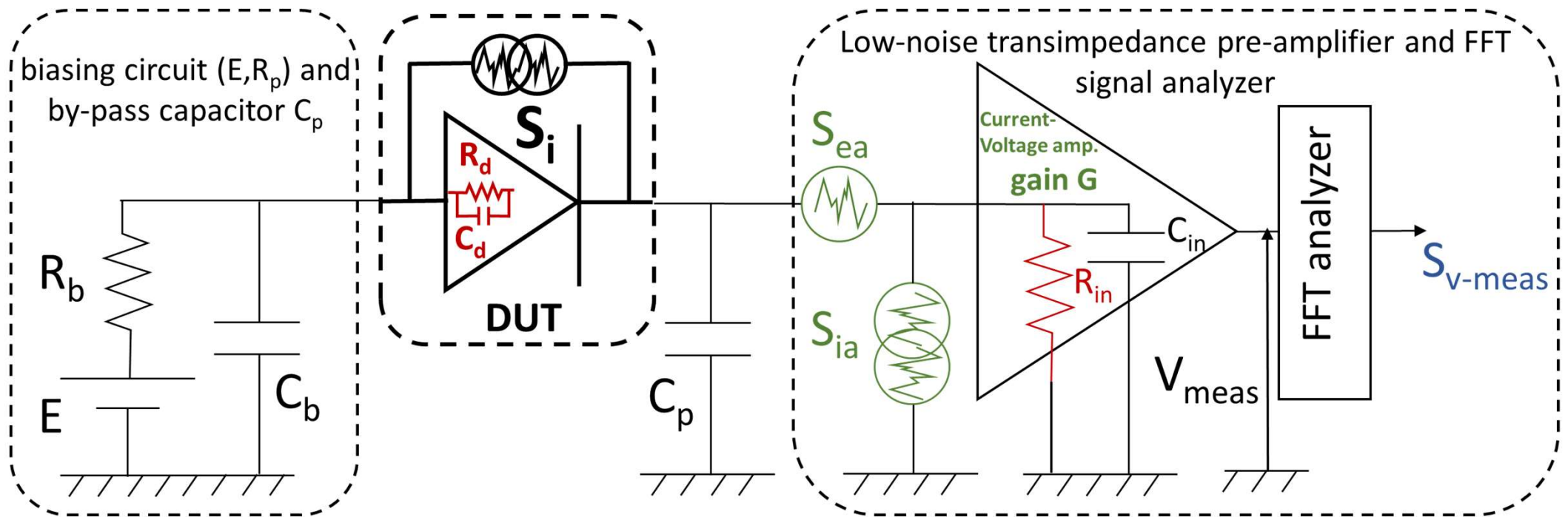


Configuration for diode measurement ; voltage or current amplifier

Experimental setups and measurement validation

After $G(f)$, $Z_{\text{ampli}}(f)$, $Z_{\text{diode}}(f)$ and $S_{ea}(f)$, $S_{ia}(f)$ measurements $\rightarrow S_i(f)$

$$S_i(f) = S_{v\text{-meas}}(f) \left(\frac{(R_d + R_{in})^2 + (R_{in}R_dC_d\omega)^2}{G^2R_d^2} \right) - \frac{S_{ea}[1 + (R_dC_d\omega)^2]}{R_d^2} - S_{ia} - \frac{2\text{Re}(S_{ea.ia^*})}{R_d} - 2\text{Im}(S_{ea.ia^*}) \cdot C_d\omega$$

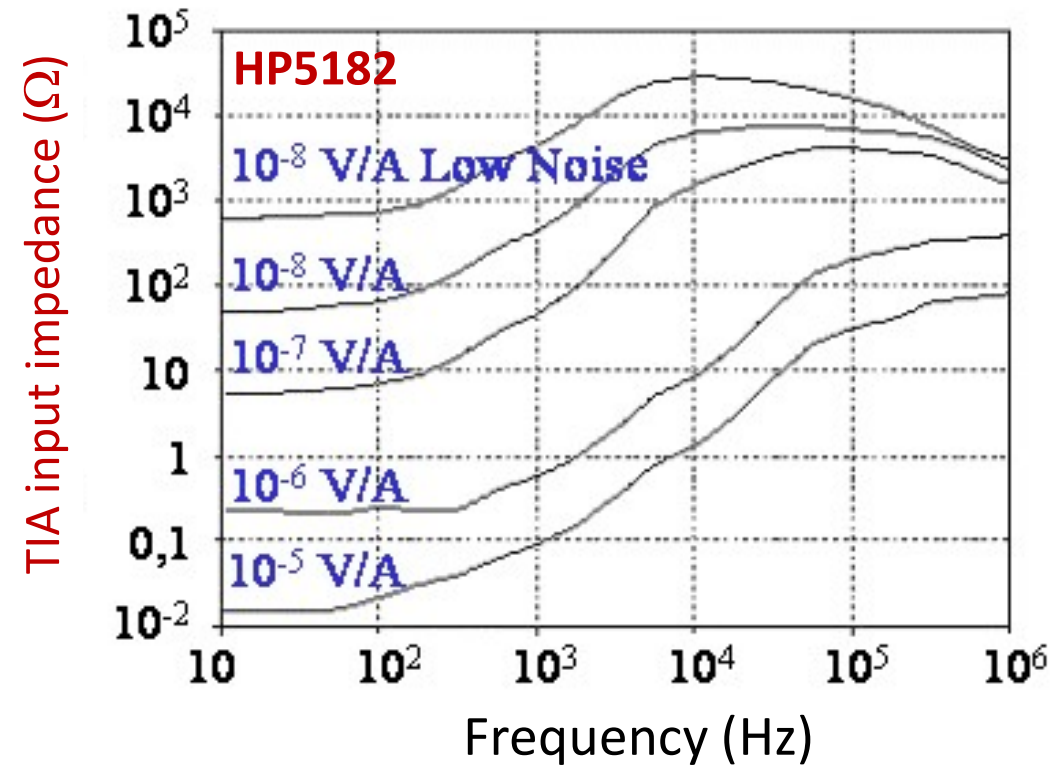
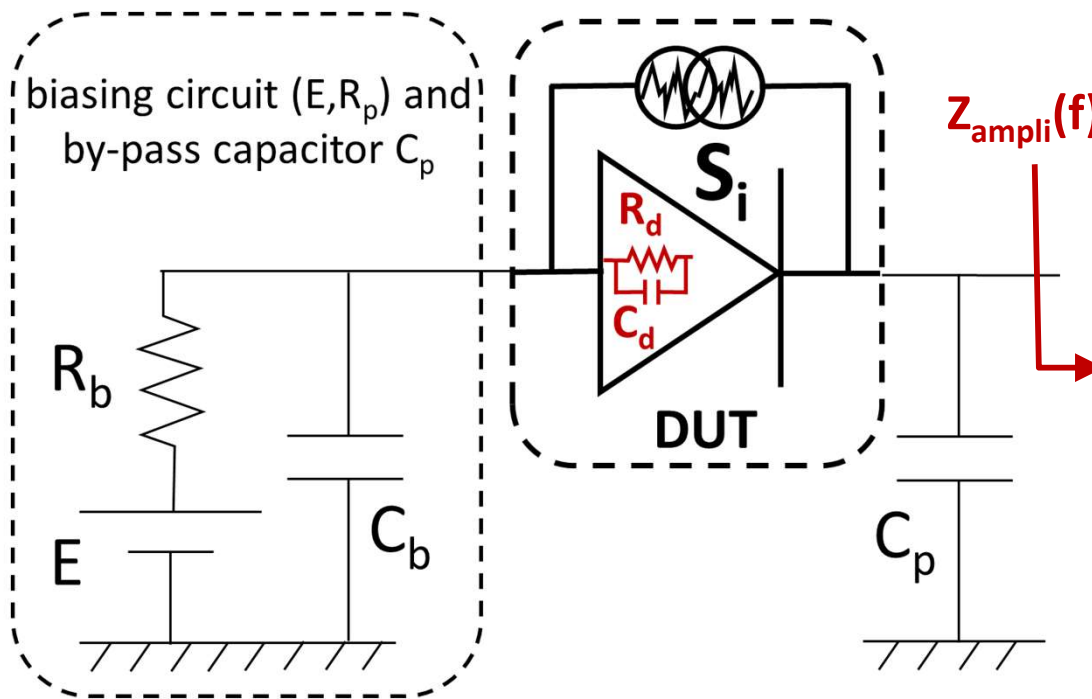


Configuration for diode measurement ; voltage or current amplifier

Experimental setups and measurement validation

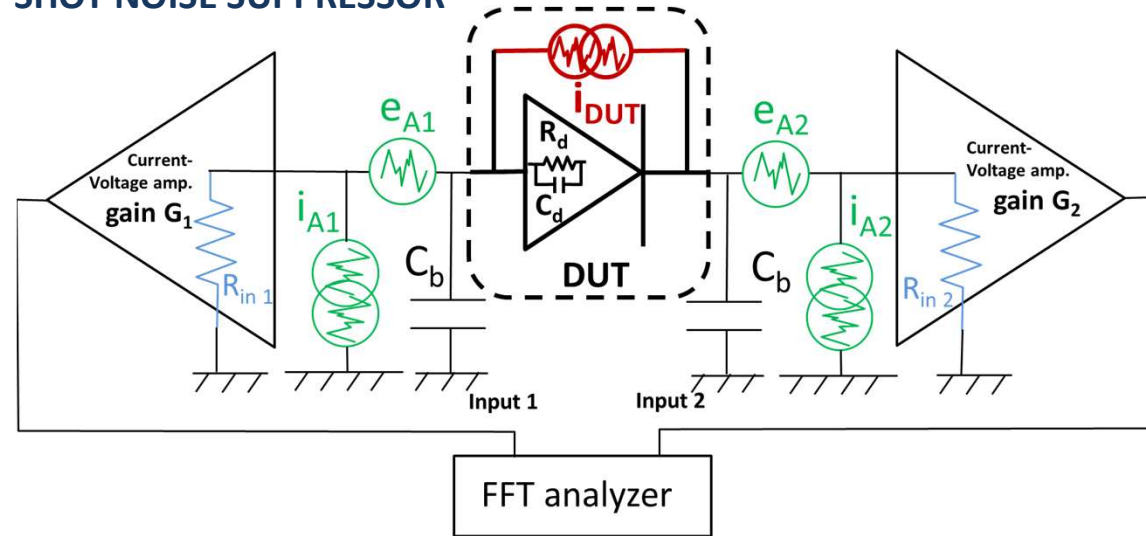
After $G(f)$, $Z_{\text{ampli}}(f)$, $Z_{\text{diode}}(f)$ and $S_{ea}(f)$, $S_{ia}(f)$ measurements $\rightarrow S_i(f)$

$$S_i(f) = S_{v\text{-meas}}(f) \left(\frac{(R_d + R_{in})^2 + (R_{in}R_dC_d\omega)^2}{G^2R_d^2} \right) - \frac{S_{ea}[1 + (R_dC_d\omega)^2]}{R_d^2} - S_{ia} - \frac{2\text{Re}(S_{ea.ia^*})}{R_d} - 2\text{Im}(S_{ea.ia^*}) \cdot C_d\omega$$



Configuration to improve the noise floor for diode measurement ; by cross-correlation technique

SHOT NOISE SUPPRESSOR



Assuming paired amplifiers T1 and T2

$$S_{eA1} = S_{eA2} = S_{eA} \quad (\text{average } 10^{-17} \text{ V}^2/\text{Hz})$$

$$S_{iA1} = S_{iA2} = S_{iA} \quad (\text{average } 10^{-23} \text{ A}^2/\text{Hz})$$

$$S_{eA1 \cdot iA1^*} = S_{eA2 \cdot iA2^*} = S_{eA \cdot iA^*}$$

$$G1 = G2 = G$$

$$R_{in1} = R_{in2} = R_{in}$$

$$S_{Vs1 \cdot Vs2^*} = G^2 \cdot S_{i1 \cdot i2^*}$$

$$i_1 = \frac{1}{Z_d + 2 \cdot R_{in}} [e_{A1} + e_{A2} + i_{A1}(Z_d + R_{in}) + i_{A2} \cdot R_{in} + \cancel{i \cdot Z_d}]$$

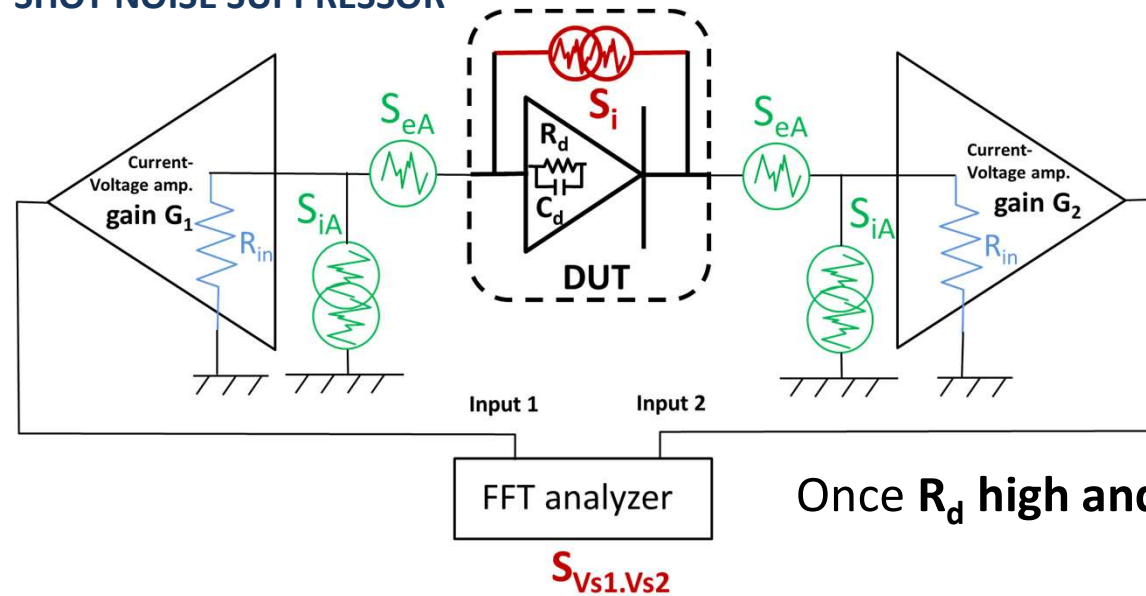
$$i_2 = \frac{1}{Z_d + 2 \cdot R_{in}} [e_{A1} + e_{A2} + i_{A1} \cdot R_{in} + i_{A2} \cdot (Z_d + R_{in}) + \cancel{i \cdot Z_d}]$$

S_{iA} noise contributor is **negligible** if $R_d \gg R_{in}$ and $R_{in} C_d \omega \ll 1$
Correlation loses of its interest for higher LFN measurement

$$S_i^{rd \rightarrow \infty} = S_{Vs1 \cdot Vs2^*} \frac{1 + (2R_{in} C_d \omega)^2}{G^2} - 2[S_{eA}(C_d \omega)^2 + \text{Real}(S_{eA \cdot iA^*})R_{in}(C_d \omega)^2 + \text{Imag}(S_{eA \cdot iA^*})(C_d \omega)]$$

Configuration to improve the noise floor for diode measurement ; by cross-correlation technique

SHOT NOISE SUPPRESSOR



From this configuration, S_{eA} (average 10^{-17} V²/Hz associated to each of the 2 amplifiers (even if paired) will produce a **current noise** $2 \cdot S_{eA} (1 + [r_d C_d \omega]^2) / r_d^2$ (if neglecting C_p and R_{in}). This noise contributor will be amplified by G_1 and G_2 , but **will not be eliminated by correlation.**

Once R_d high and $R_d C_d \omega \ll 1$, then this current noise is negligible and **correlation technique is strongly efficient**

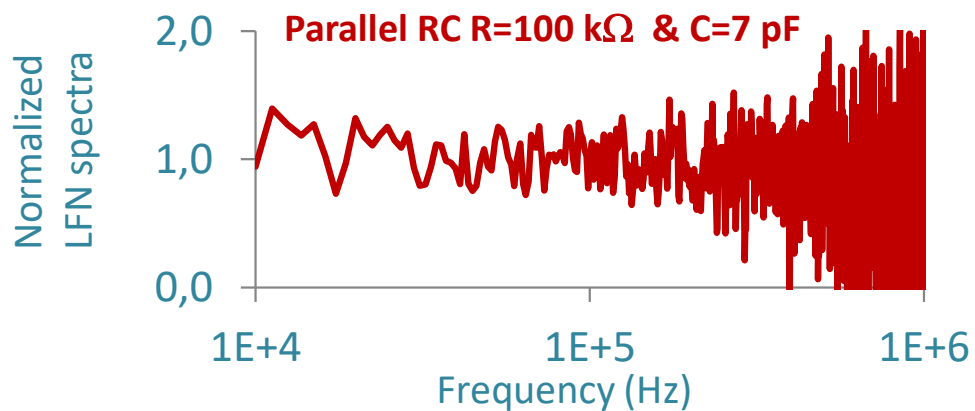
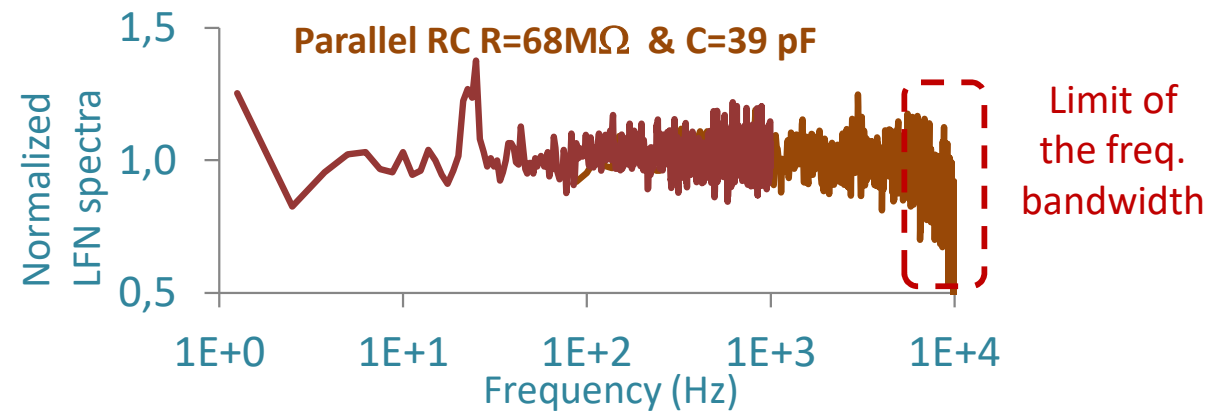
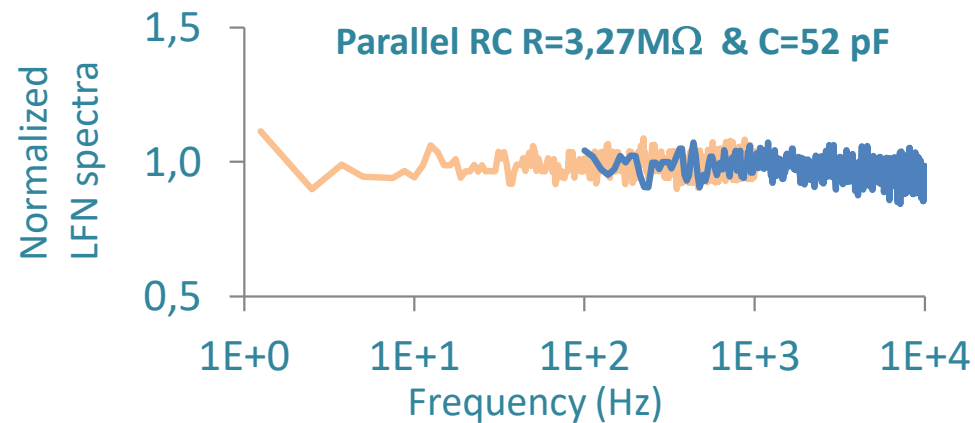
Case 1 : when **DUT (diode) is forward biased** (even at low level !), R_d should reach **30 kΩ** for example (diode biased as low as $I_d = 80$ nA) and the parasitic noise becomes $2 \cdot 10^{-17} / 9 \cdot 10^8 = 2.2 \cdot 10^{-26}$ A²/Hz
 → same as for a shot noise from a diode under 60 nA !

Case 2 : **If such diode presents $C_d = 30$ pF**, at 100 kHz $(1 + [r_d C_d \omega]^2) / r_d^2$ increases up to 10^9 :
 the parasitic noise now corresponds to a diode biased under 90 nA
 → Higher than the current noise to be measured !!!

Configuration for diode measurement ; voltage or current amplifier

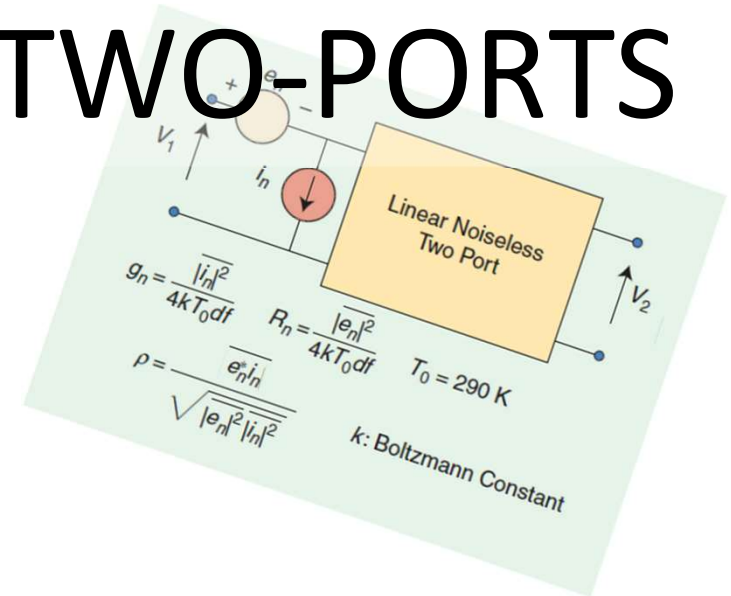
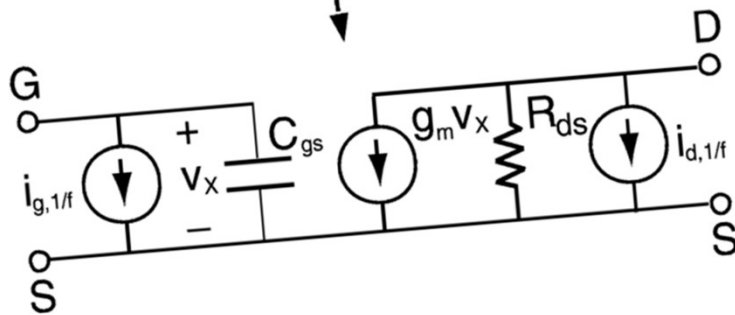
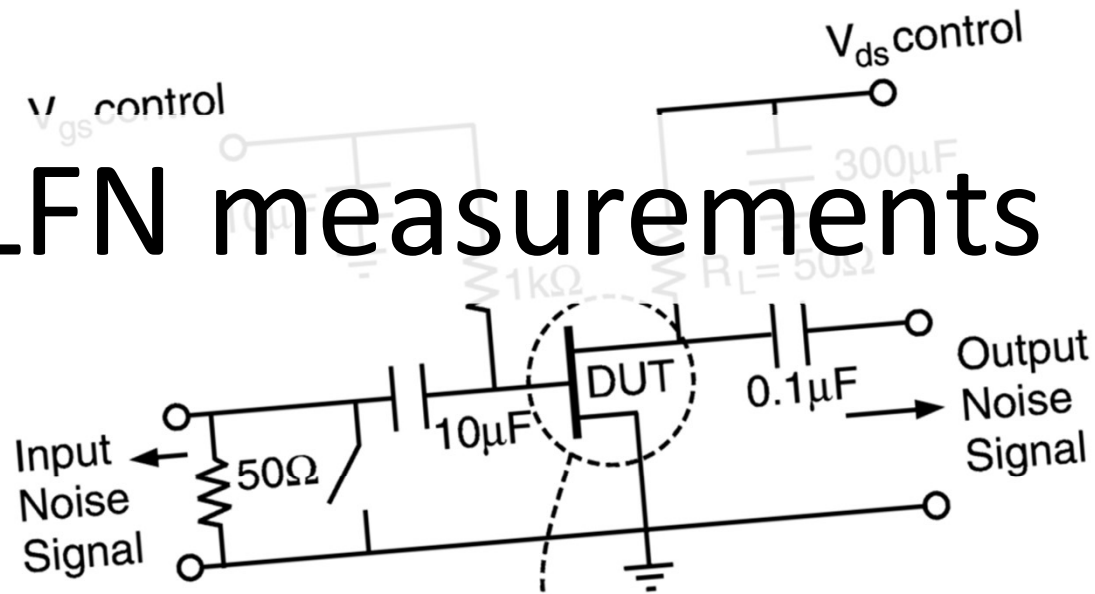
Experimental setups and measurement validation

CALIBRATION STEP – resistors and diodes

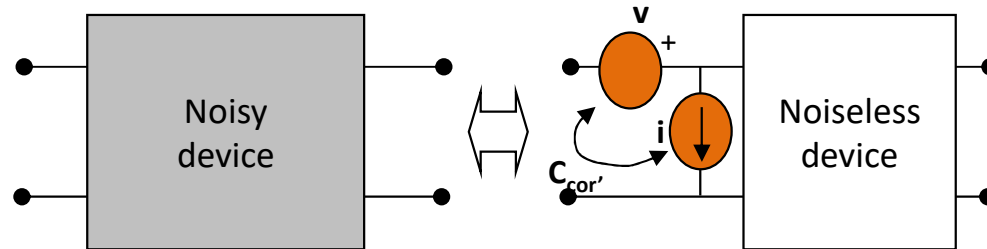


Under specific R-C values, measurement is tricky @ “elevated LF” but still around unity at higher frequencies

LFN measurements in TWO-PORTS



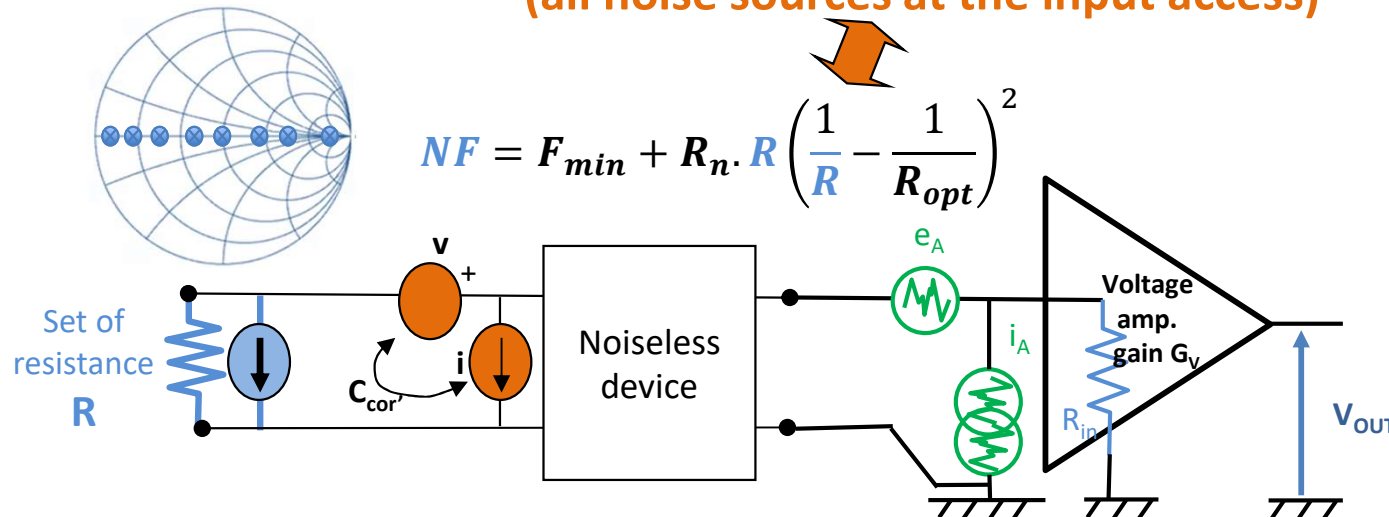
LOW FREQUENCY NOISE MEASUREMENTS: In/Out + correlation



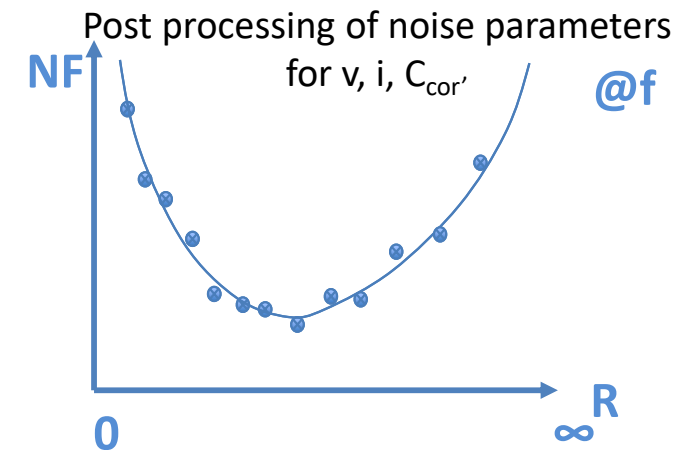
Multi-impedance setup

Usually between 12-16 resistances

(all noise sources at the input access)

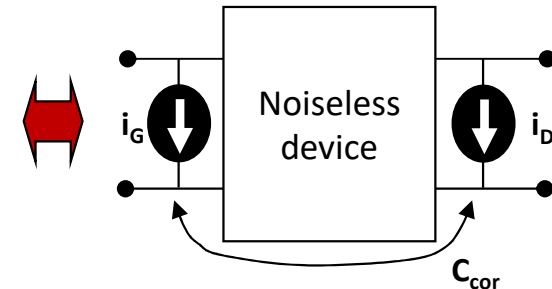
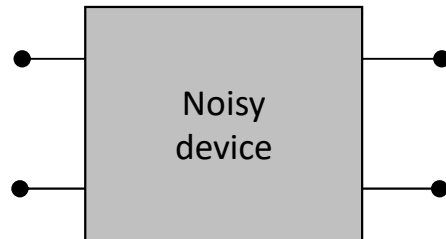


$$NF = F_{min} + R_n \cdot R \left(\frac{1}{R} - \frac{1}{R_{opt}} \right)^2$$



Also need Z_{DUT} (bias) and Z_{in} vs frequency of Ampli for all bias of the DUT
Extraction of v , i and correlation is a quite complex process

LOW FREQUENCY NOISE MEASUREMENTS: In/Out + correlation



**In/Out access characterization
(I-V or V-V low noise amplifiers)**

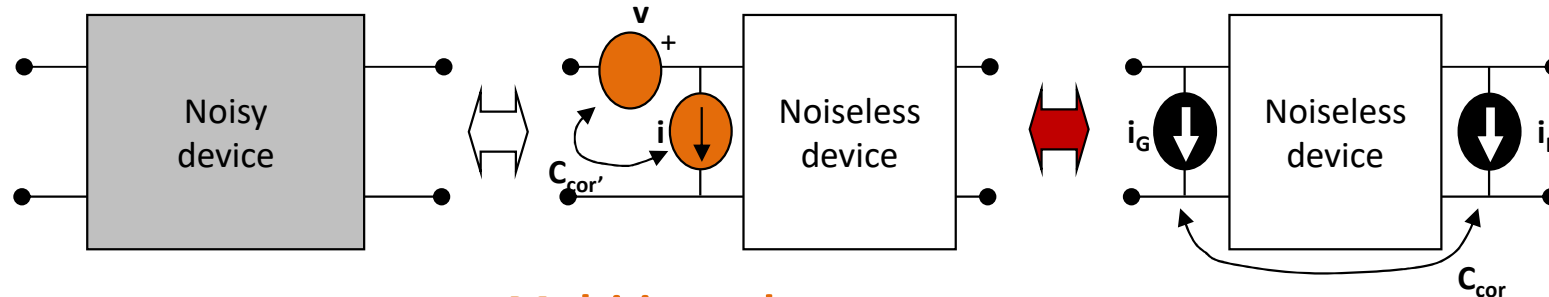


Partition of IN/OUT noise sources

Easier to develop.

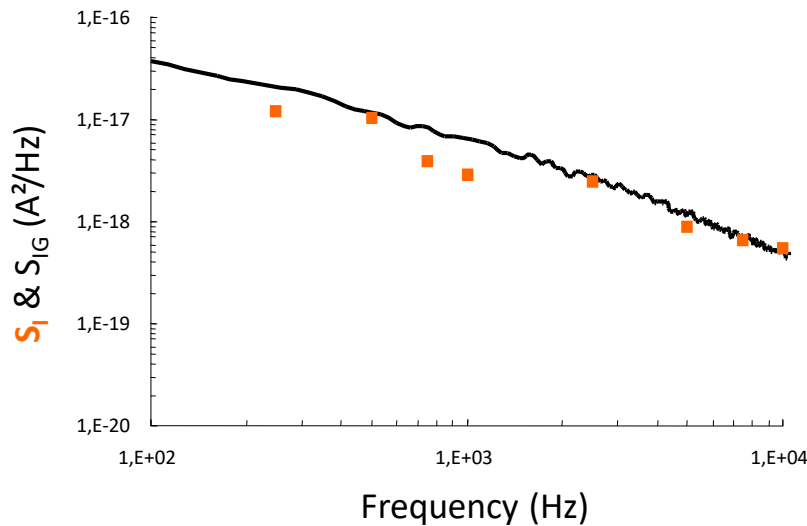
Our solution as presented in the next slides

LOW FREQUENCY NOISE MEASUREMENTS: In/Out + correlation



**Multi-impedance setup
(all noise sources at the
input access)**

**In/Out access characterization
(I-V or V-V low noise amplifiers)**

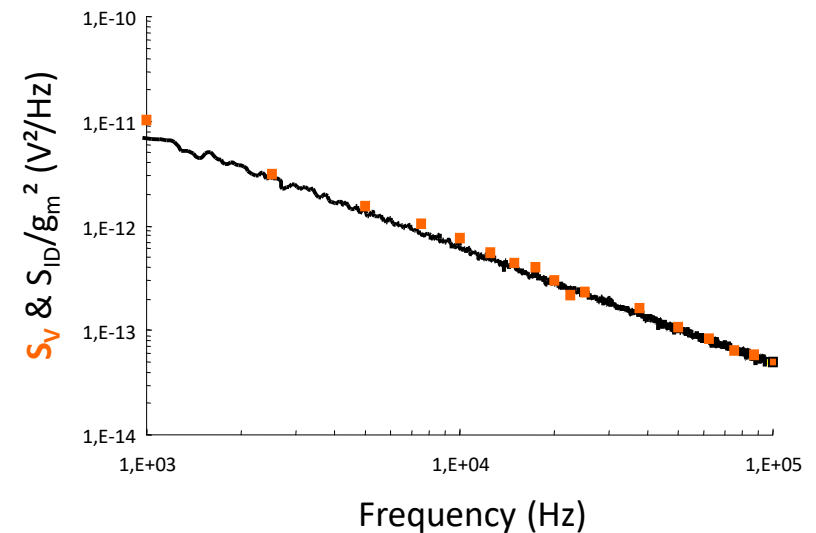


**Equivalence
relations**

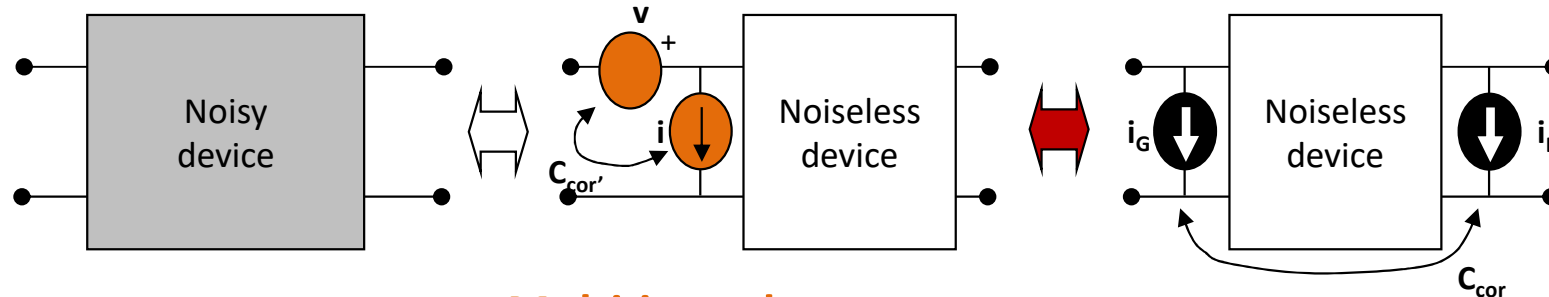
$$S_I = S_{IG}$$

$$S_V = S_{ID}/g_m^2$$

FET



LOW FREQUENCY NOISE MEASUREMENTS: In/Out + correlation



**Multi-impedance setup
(all noise sources at the
input access)**

**In/Out access characterization
(I-V or V-V low noise amplifiers)**

$$S_V = \left(\frac{Z_{\text{entrée}}}{\beta} \right)^2 S_{IC}$$

$$S_I = S_{IB} + \frac{S_{IC}}{\beta^2} + 2 \frac{\Re\{S_{IBIC^*}\}}{\beta}$$

$$S_{VI^*} = \left(\frac{Z_{\text{entrée}}}{\beta} \right) \left(\frac{S_{IC}}{\beta} + S_{IBIC^*} \right)$$

**Equivalence
relations**

**S_I & S_{IB}
 S_V & S_{IC}**

HBT

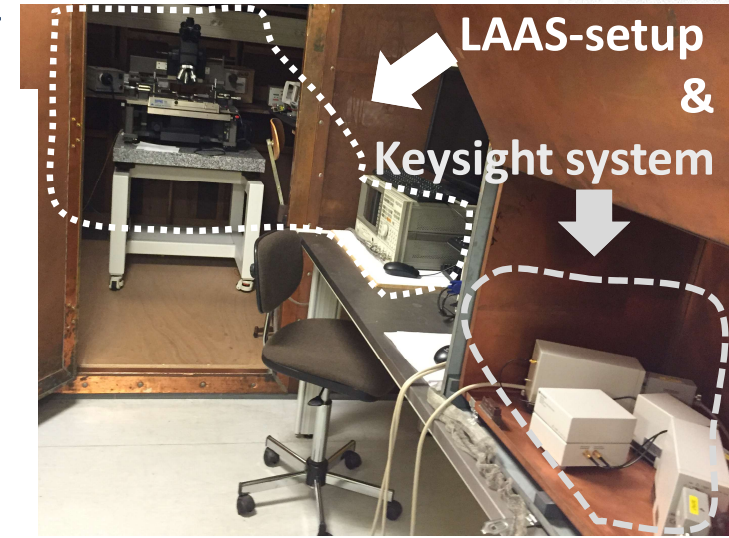
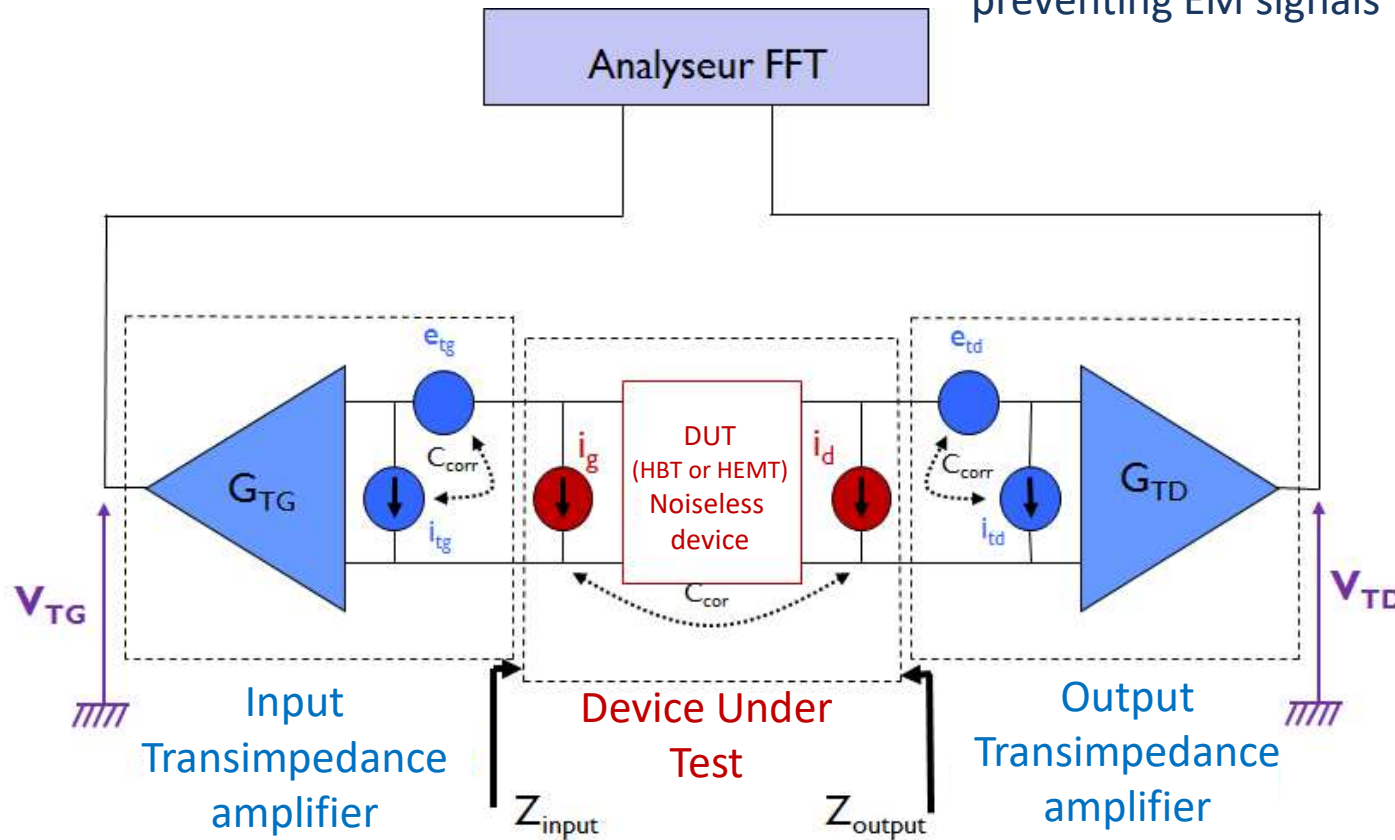
$$S_{IC} = \left(\frac{\beta}{Z_{\text{entrée}}} \right)^2 \cdot S_V$$

$$S_{IB} = S_I + \frac{S_V}{Z_{\text{entrée}}^2} + 2 \frac{\Re\{S_{VI^*}\}}{Z_{\text{entrée}}}$$

$$S_{IBIC^*} = \left(\frac{\beta}{Z_{\text{entrée}}} \right) \left(\frac{S_V}{Z_{\text{entrée}}} + S_{VI^*} \right)$$

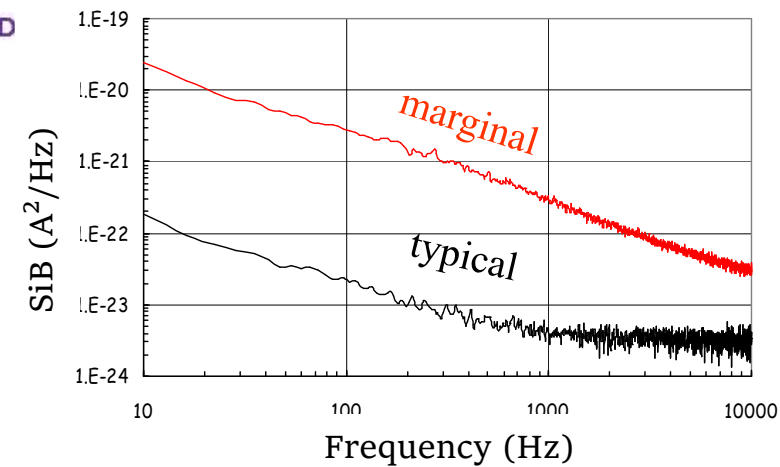
General Setup for LF noise measurement

Still in a Faraday cage for preventing EM signals



For most cases of study

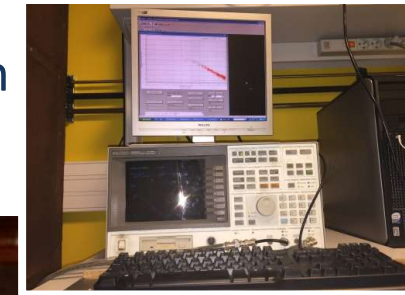
$$\overline{V_{TD}^2} = G_{TD}^2 \left(\overline{i_d^2} + \overline{i_{td}^2} + \frac{\overline{e_{td}^2}}{Z_{output}^2} + \frac{2 * \text{Re} \left\{ \overline{e_{td} i_{td}^*} \right\}}{Z_{input}} \right)$$



LOW FREQUENCY NOISE MEASUREMENTS: In/Out + correlation

Non-Linear LF noise (1Hz-1MHz, 2 exp. Tools + Keysight LFNA) :

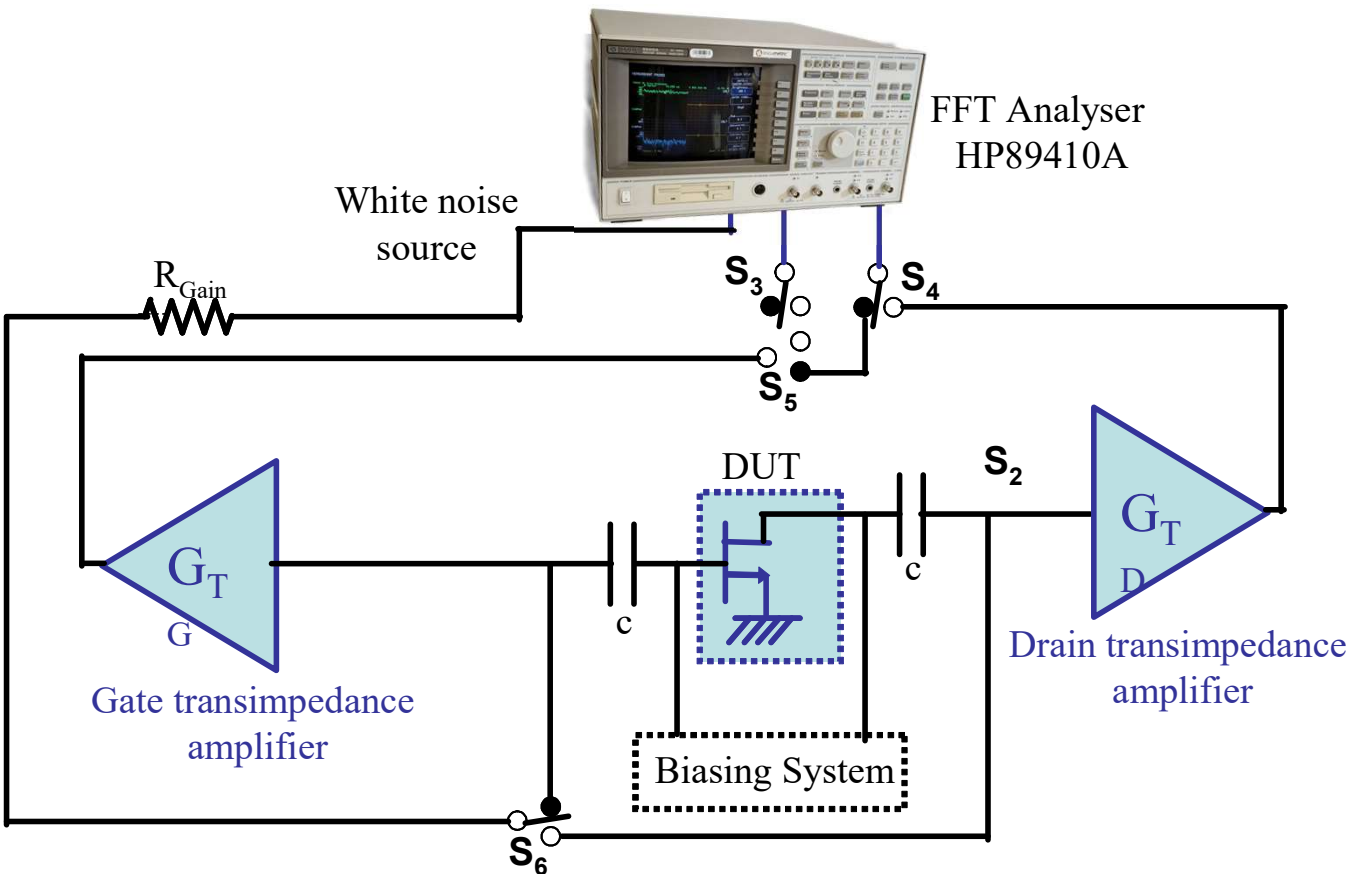
→ $S_{i_{in}} - S_{i_{out}}$ & correlation



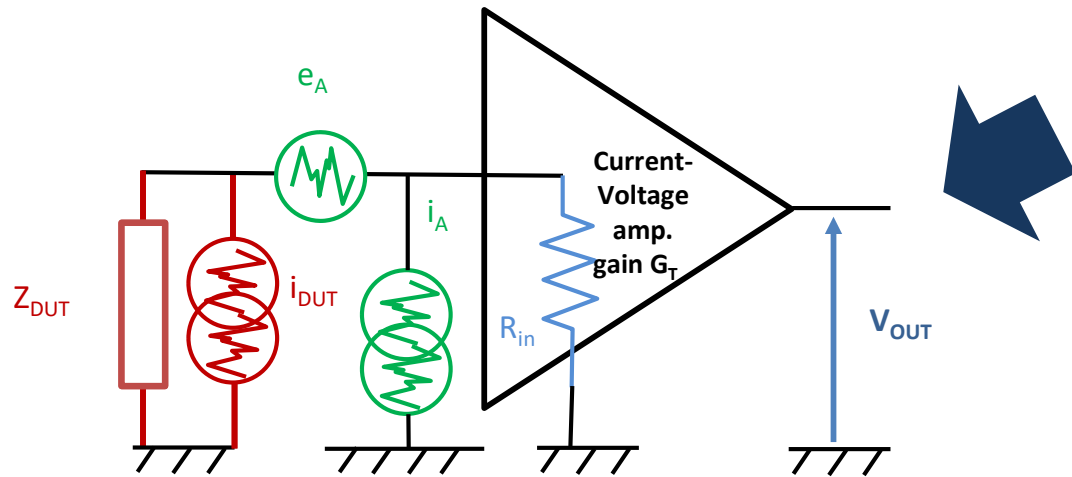
Faraday shielded room (LF noise)

A set of switches is used for the calibration of the different elements (amplifiers) and for :

- $S_{I_{IN}}$
- $S_{I_{OUT}}$
- IN-OUT correlation



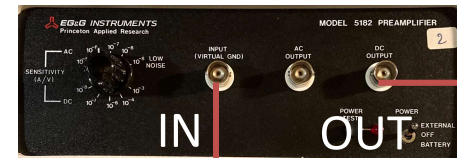
Determination of DUT spectral density for a Dipole – (2x for a Quadripole ?)



$$\overline{V_{out}^2} = G_T^2 \left(\overline{i_{DUT}^2} + \overline{i_A^2} + \frac{\overline{e_A^2}}{Z_{DUT}^2} + \frac{2\text{Re}\{\overline{e_A i_A^*}\}}{Z_{DUT}} \right)$$

$$\overline{i_{DUT}^2} = \frac{\overline{V_{out}^2}}{G_T^2} - \overline{i_A^2} - \frac{\overline{e_A^2}}{Z_{DUT}^2} - \frac{2\text{Re}\{\overline{e_A i_A^*}\}}{Z_{DUT}}$$

Signal Analyser
HP89410A
FFT

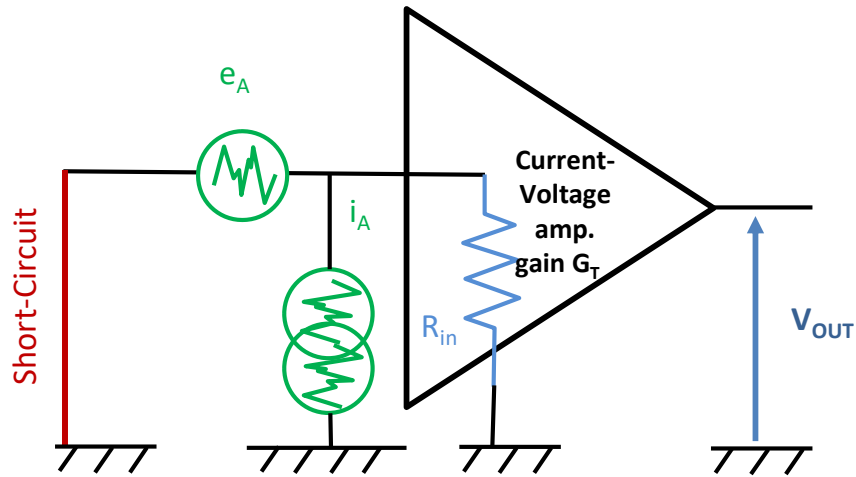


Attention :

-measurement of input/output/correlation all together is a tricky problem (output current is that of the input current, amplified. Correlation is erroneous !

→ Voltage amplifier at the input OR full characterization of the $Z_{in}(freq)$

Determination of the transimpedance noise sources and correlation



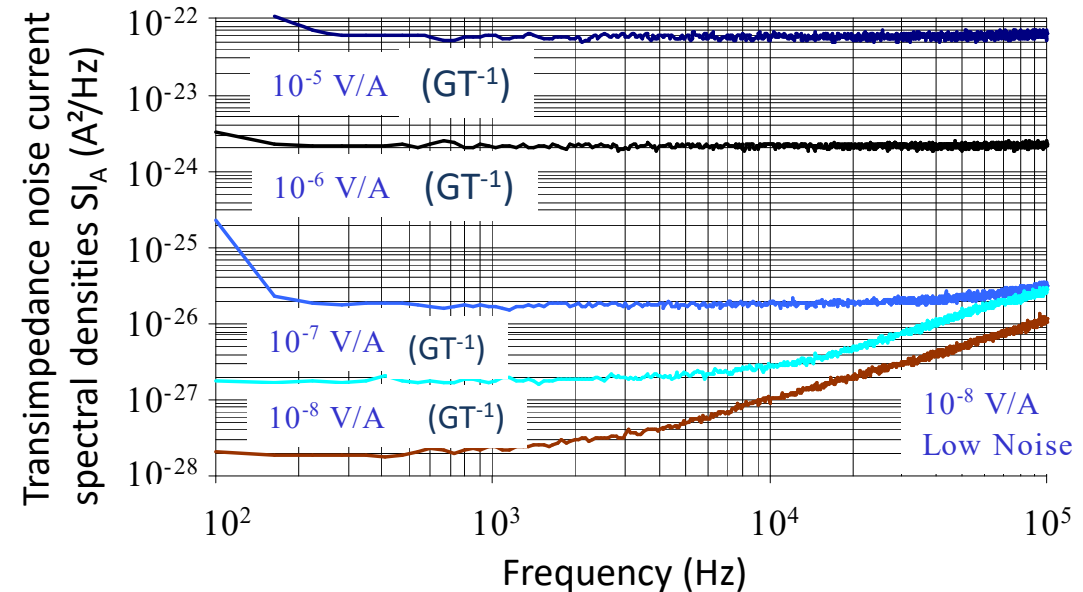
$$\overline{V_{out}^2} = G_T^2 \left(\cancel{i_{DUT}^2} + \overline{i_A^2} + \cancel{\frac{e_A^2}{Z_{DUT}^2}} + \cancel{\frac{2\text{Re}\{e_A i_A^*\}}{Z_{DUT}}} \right)$$

$$\overline{V_{out}^2} = G_T^2 \cdot \overline{i_A^2}$$

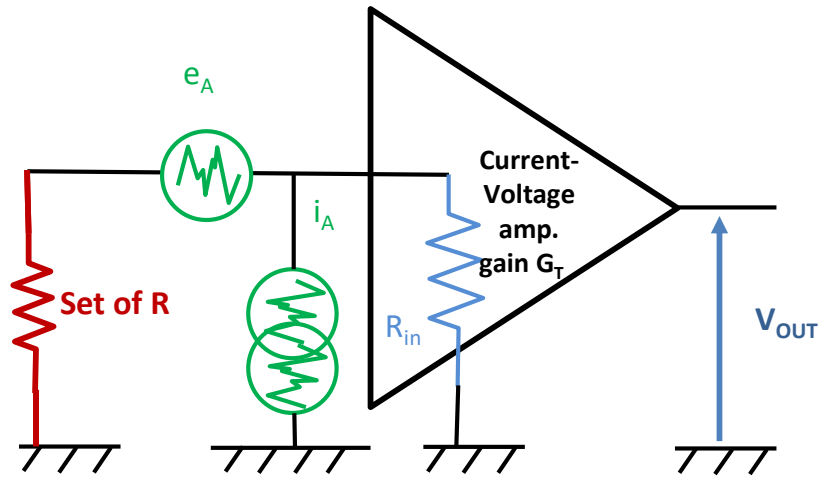
Signal Analyser
HP89410A
FFT



Short-Circuit



Determination of the transimpedance noise sources and correlation

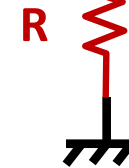


$$\overline{V_{out}^2} = G_T^2 \left(\overline{i_R^2} + \overline{i_A^2} + \frac{\overline{e_A^2}}{R^2} + \frac{2\text{Re}\{\overline{e_A i_A^*}\}}{R} \right)$$

Knowing $\overline{i_R^2} = 4kT/R$

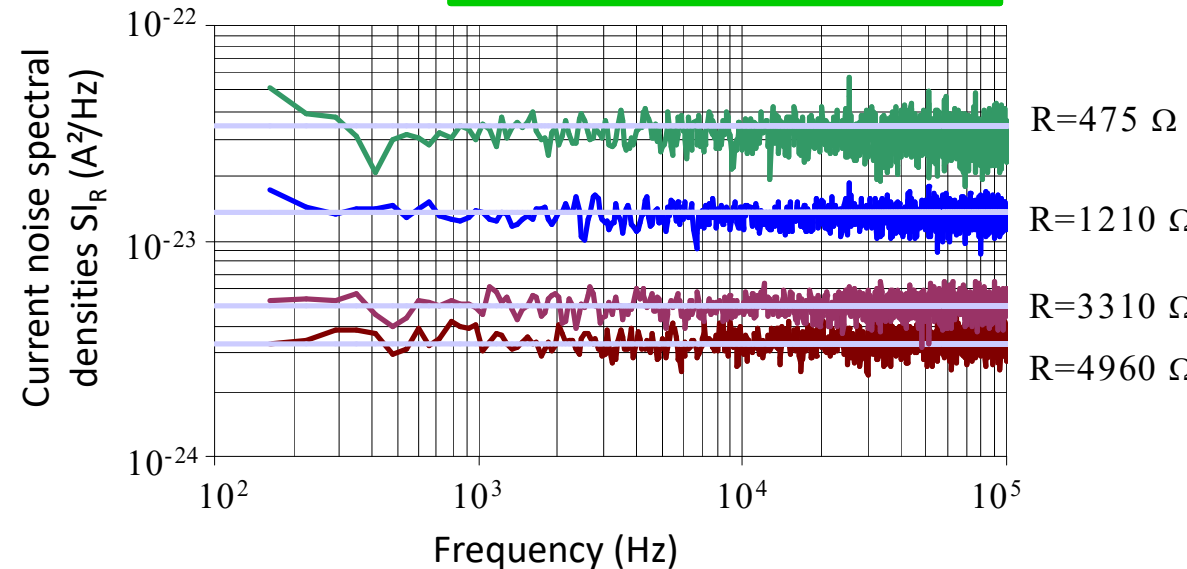
$$\overline{i_R^2} = \frac{\overline{V_{out}^2}}{G_T^2} - \overline{i_A^2} - \frac{\overline{e_A^2}}{R^2} - \frac{2\text{Re}\{\overline{e_A i_A^*}\}}{R}$$

Signal Analyser
HP89410A
FFT



$$\overline{e_t^2} = 10^{-17} \text{ V}^2/\text{Hz}$$

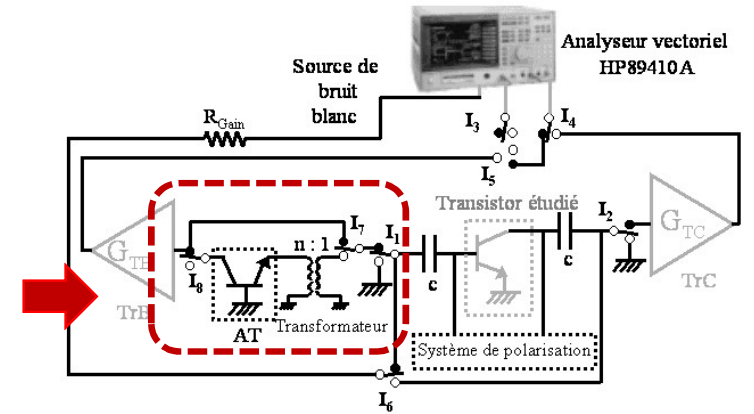
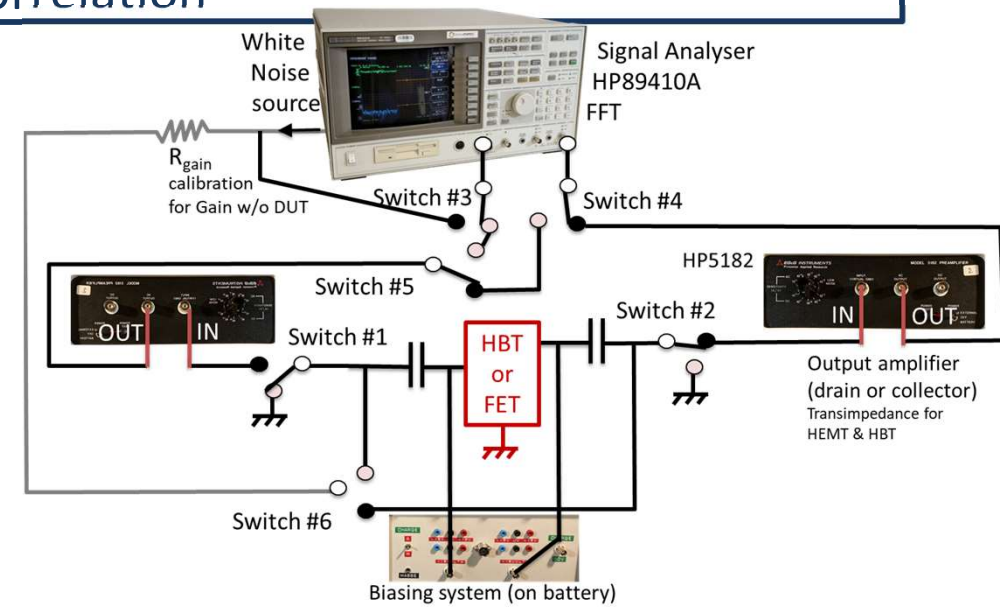
$$\text{Re}\{\overline{e_t i_t^*}\} = 1,35 \cdot 10^{-21} \text{ V}\cdot\text{A}/\text{Hz}$$



Switches configurations

LOW FREQUENCY NOISE MEASUREMENTS: In/Out + correlation

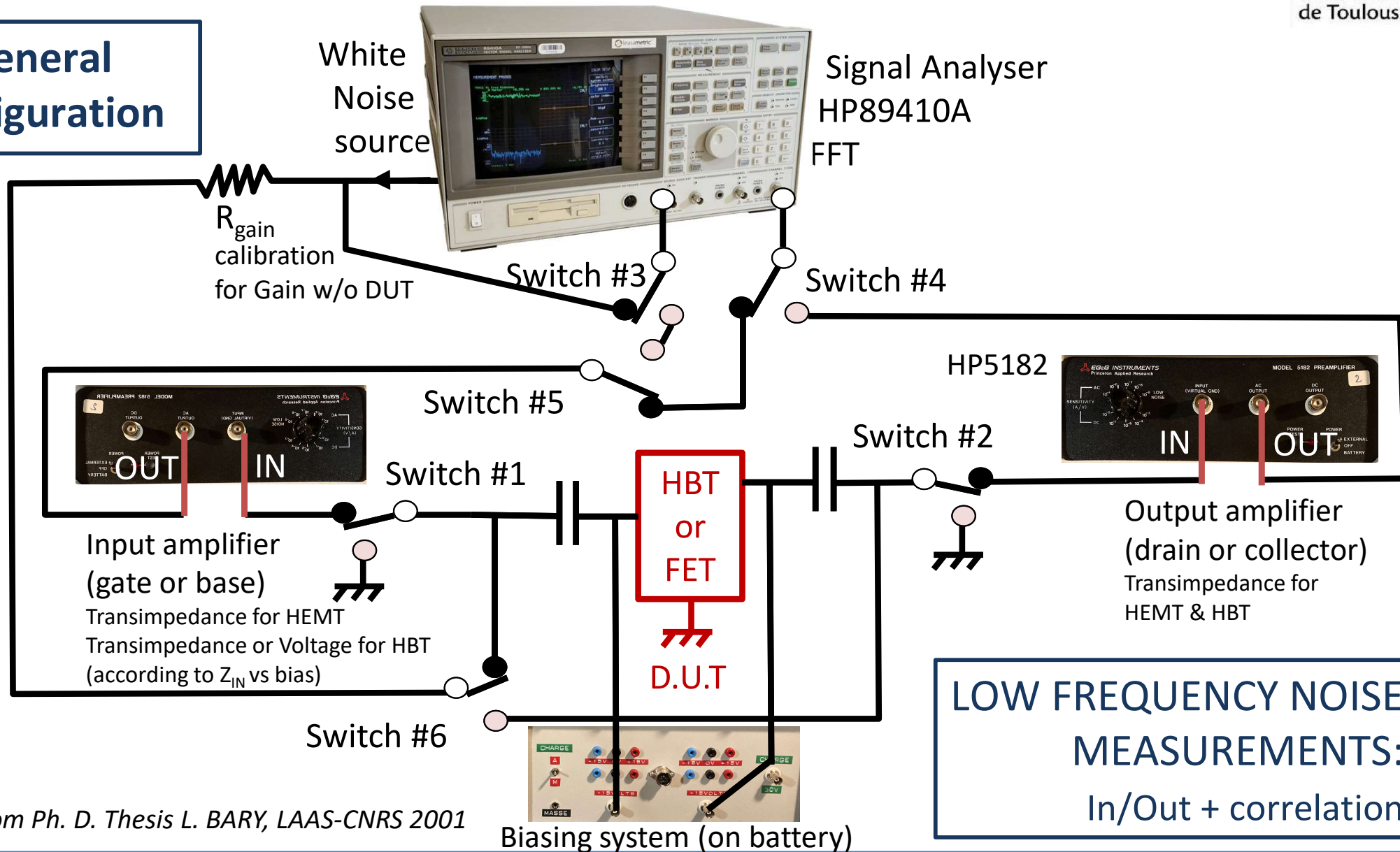
Meas. config.	SW1	SW2	SW3	SW4	SW5	SW6
Chain noise & gain	<input type="radio"/>	<input type="radio"/>	<input type="radio"/>	<input type="radio"/>	<input type="radio"/>	floating
Conversion gain of Input transimpedance G_{T_IN}	①	<input type="radio"/>	③	④	⑤	⑥
Conversion gain of Output transimpedance G_{T_OUT}	<input type="radio"/>	②	③	<input type="radio"/>	floating	<input type="radio"/>
S_{I-IN} measurement	①	<input type="radio"/>	<input type="radio"/>	④	⑤	floating
S_{I-OUT} measurement	<input type="radio"/>	②	<input type="radio"/>	<input type="radio"/>	<input type="radio"/>	⑥
$S_{I-IN, I-OUT}$ * cross-correlation measurement	①	②	<input type="radio"/>	<input type="radio"/>	<input type="radio"/>	floating



Nota : two more switches can be added to improve meas. on INPUT (between SW1 and Input amplifier-mainly Transimpedance) : using a transformer and a buffer amplifier.

Adapted from Ph. D. Thesis L. BARY, LAAS-CNRS 2001

General configuration



LOW FREQUENCY NOISE MEASUREMENTS:
In/Out + correlation

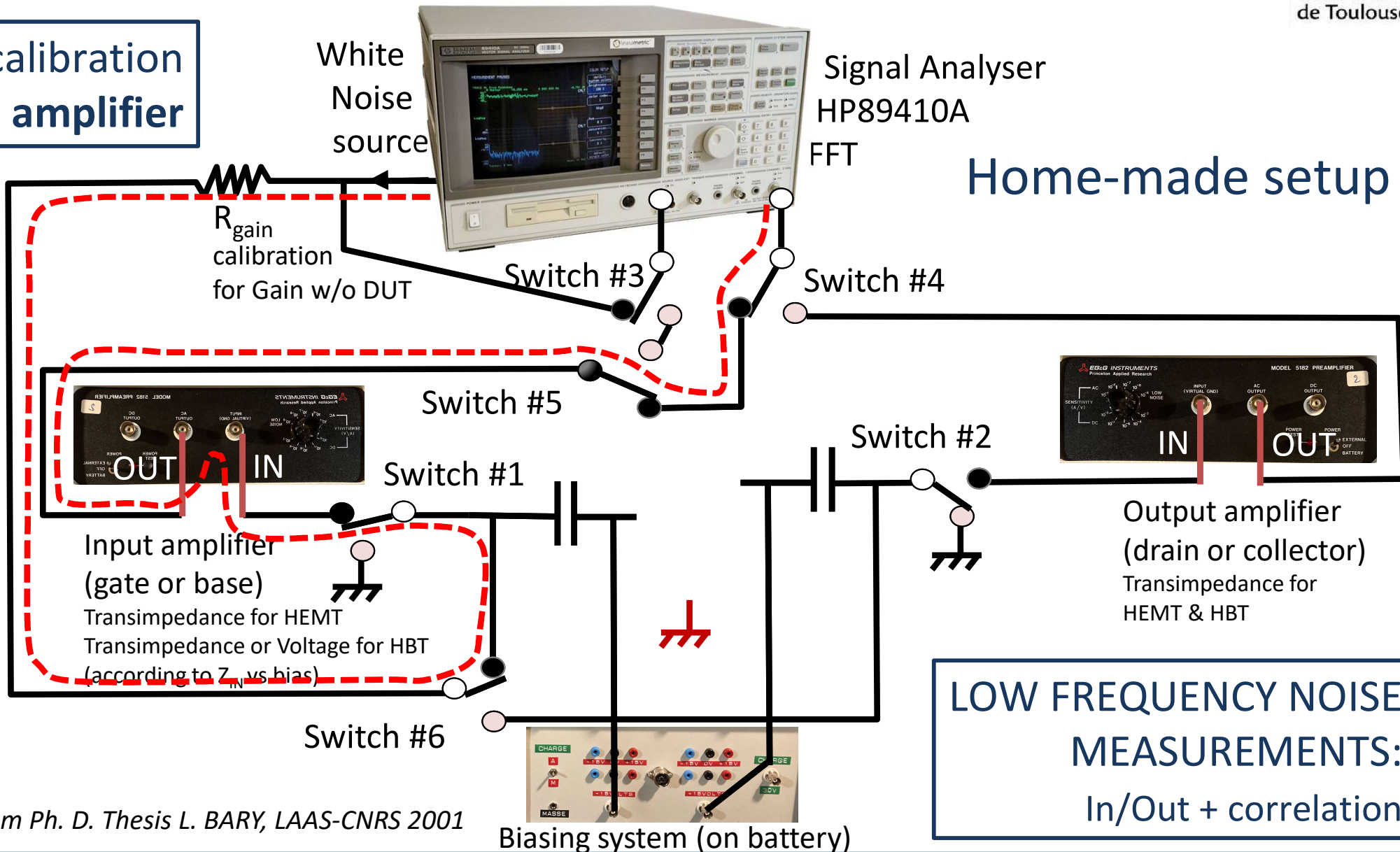
Adapted from Ph. D. Thesis L. BARY, LAAS-CNRS 2001

Gain calibration
Input amplifier

White Noise source

Signal Analyser
HP89410A
FFT

Home-made setup



LOW FREQUENCY NOISE MEASUREMENTS:
In/Out + correlation

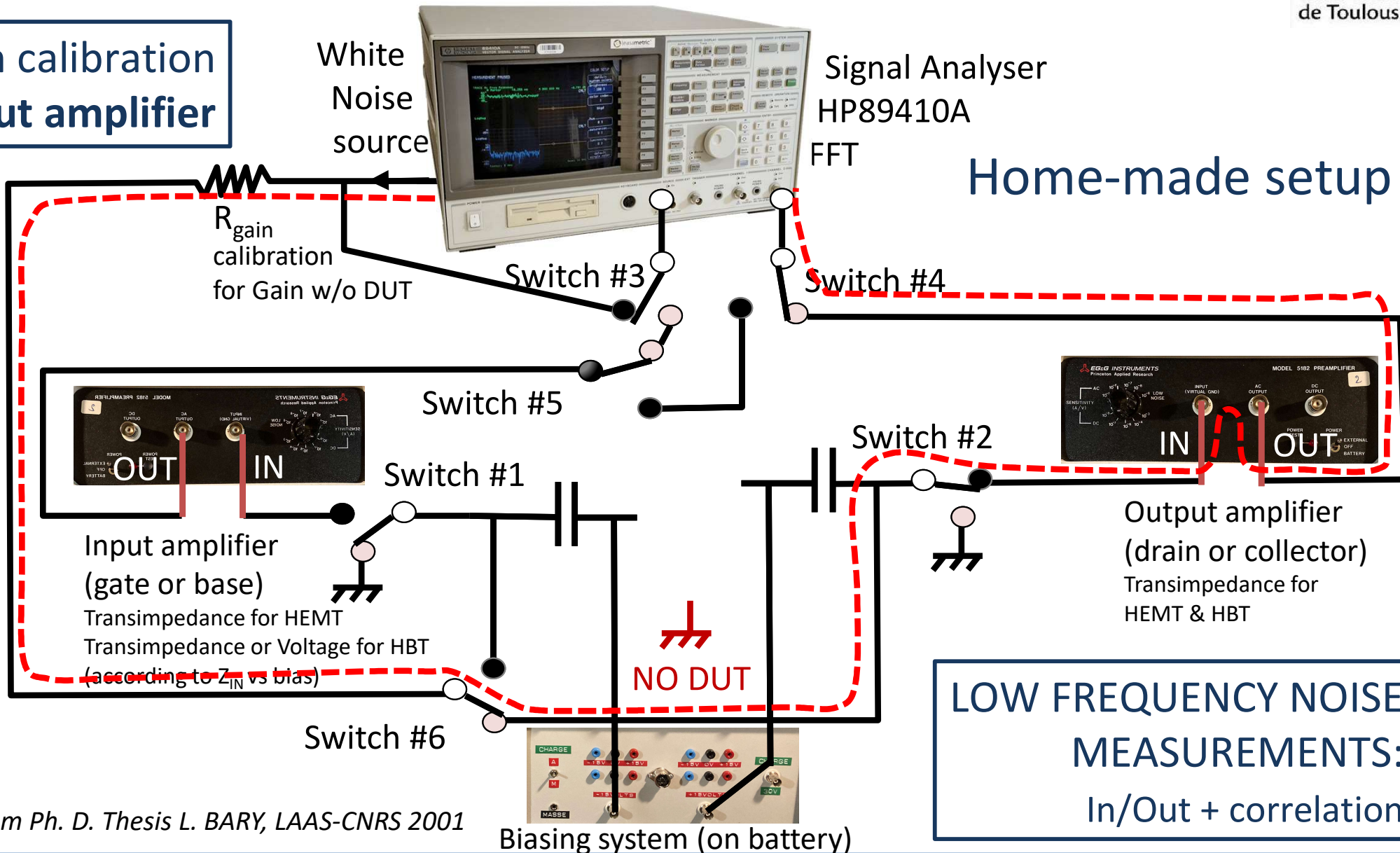
Adapted from Ph. D. Thesis L. BARY, LAAS-CNRS 2001

Gain calibration
Output amplifier

White Noise source

Signal Analyser
HP89410A
FFT

Home-made setup



LOW FREQUENCY NOISE MEASUREMENTS:
In/Out + correlation

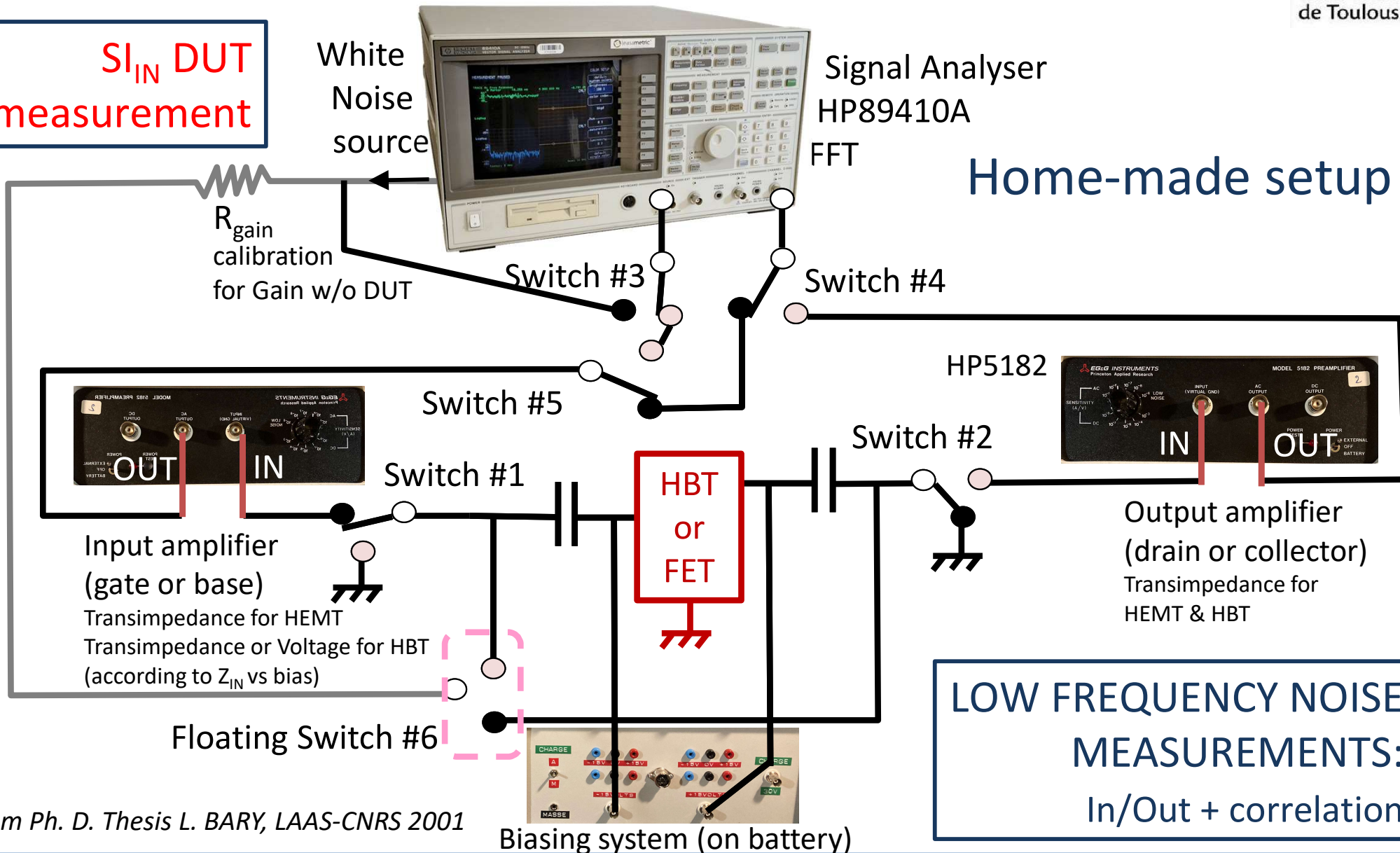
Adapted from Ph. D. Thesis L. BARY, LAAS-CNRS 2001

$S_{I_{IN}}$ DUT
measurement

White Noise source

Signal Analyser
HP89410A
FFT

Home-made setup



Adapted from Ph. D. Thesis L. BARY, LAAS-CNRS 2001

$S_{I_{OUT} DUT}$
measurement

White Noise source



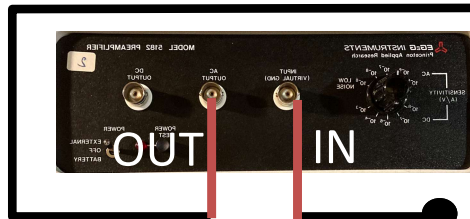
Signal Analyser
HP89410A
FFT

Home-made setup

R_{gain}
calibration
for Gain w/o DUT

Switch #3

Switch #4



Input amplifier
(gate or base)

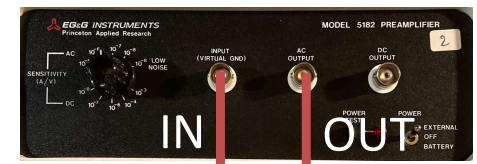
Transimpedance for HEMT
Transimpedance or Voltage for HBT
(according to Z_{IN} vs bias)

Switch #5

Switch #1

HBT
or
FET

Switch #2



Output amplifier
(drain or collector)
Transimpedance for
HEMT & HBT

Floating Switch #6



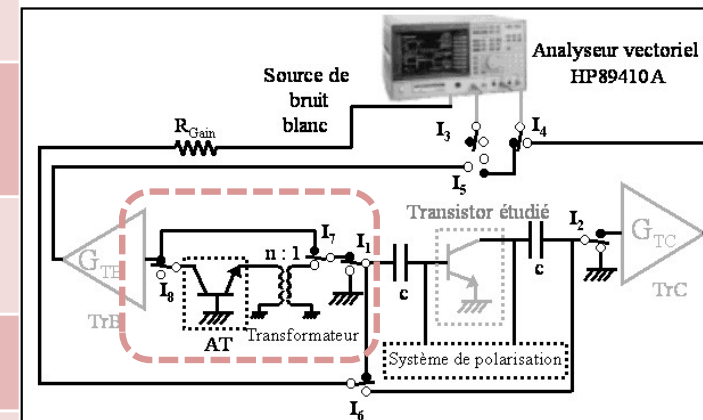
Biasing system (on battery)

LOW FREQUENCY NOISE
MEASUREMENTS:
In/Out + correlation

Adapted from Ph. D. Thesis L. BARY, LAAS-CNRS 2001

Meas. config. \ Switch	SW1	SW2	SW3	SW4	SW5	SW6	SW7 Depending on configuration	SW8 Depending on configuration
Chain noise & gain	○	○	○	○	○	floating	⑦	⑧
Conversion gain of Input transimpedance G_{T_IN}	①	○	③	④	⑤	⑥	⑦	○
Conversion gain of Output transimpedance G_{T_OUT}	○	②	③	○	floating	○	○	○
$S_{I-IN TA}$ measurement	①	②	○	④	⑤	floating	⑦	⑧
$S_{I-OUT TA}$ measurement	○	②	○	④	○	floating	○	○
$S_{I-IN, I-OUT*}$ cross-correlation measurement	①	②	○	○	○	floating	○	○

Switches configurations



Nota : two more switches can be added to improve meas. on INPUT (between SW1 and Input amplifier-mainly Transimpedance) : using a transformer and a buffer amplifier. Lower input impedance as seen by the device at its input !

THIS ALLOWS FOR S_{iout} and Correlation measurement

LOW FREQUENCY NOISE MEASUREMENTS:
In/Out + correlation

Adapted from Ph. D. Thesis L. BARY, LAAS-CNRS 2001

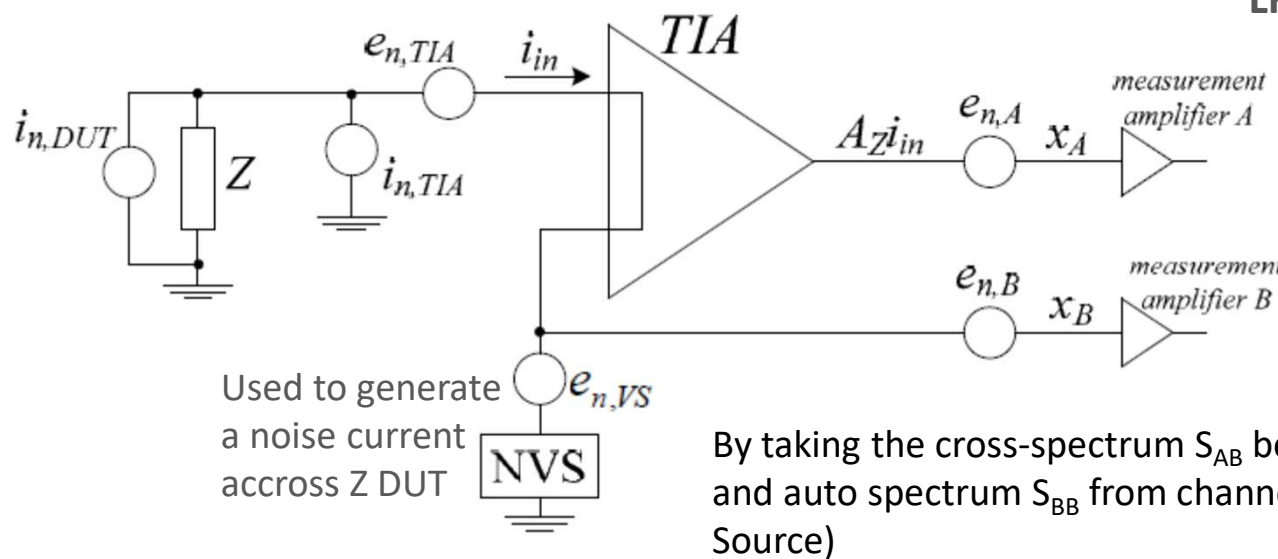
Also cf. to Integrated Method for Impedance and Low Frequency Noise Measurements, G. Giusi, G. Scandurra and C. Ciofi IEEE Instrumentation and Measurement Society

Integrated method for LFN and Impedance Measurements (IMs)

IMs are performed by means of cross-correlation LFN measurements.

Three-channel measurement system for the automatic DC, Gate or Drain low frequency noise, and impedance characterization of electron devices

Nota : correlation of In/out LFN sources are not accounted for here



LFN measurement on channel A

$$\frac{x_A}{A_Z} = i_{n,DUT} + \left[\frac{e_{nA}}{A_Z} + i_{n,TIA} + \frac{e_{n,TIA} + e_{n,VS}}{Z} \right]$$

$$\left[\frac{e_{nA}}{A_Z} + i_{n,TIA} + \frac{e_{n,TIA} + e_{n,VS}}{Z} \right]$$

Input connected to ground during LFN meas.

$$x_B = e_{nB} + e_{n,VS}$$

As low as possible to improve detectivity for LFN meas.

$$S_{AB} = e_{n,VS}^2 \frac{A_Z}{Z}$$

$$S_{BB} = e_{nB}^2 + e_{n,VS}^2 \approx e_{n,VS}^2$$

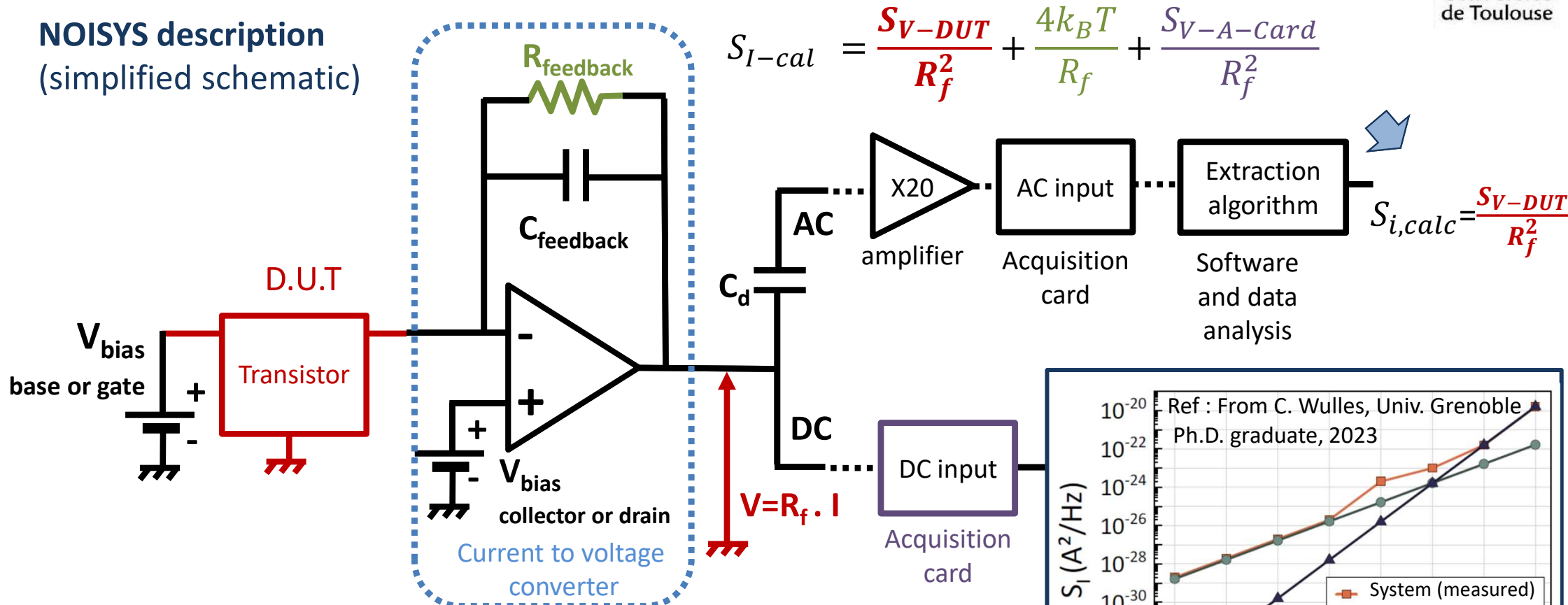
Correlation between the noise current from NVS (channel A) and the applied noise source (channel B) is used to calculate Z

$$Z \approx A_Z \frac{S_{BB}}{S_{AB}}$$

NVS is selected to be noisier than $e_{n,B}$

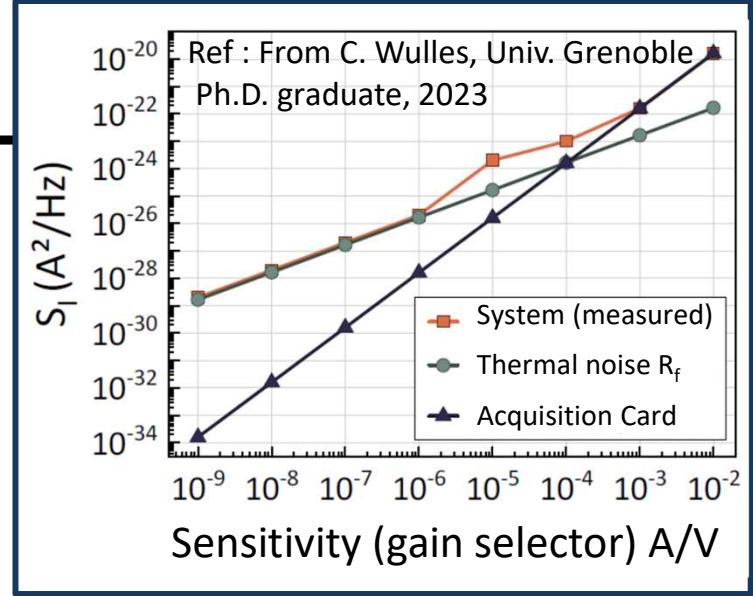
Ref: Giusi, IEEE International Instrumentation and Measurement Technology Conference (I2MTC), 2017

NOISYS description (simplified schematic)



$$S_{I-cal} = \frac{S_{V-DUT}}{R_f^2} + \frac{4k_B T}{R_f} + \frac{S_{V-A-Card}}{R_f^2}$$

$$S_{i,calc} = \frac{S_{V-DUT}}{R_f^2}$$



Noise of the Acquisition card :
 $S_{V-A-Card} = 2.10^{-16} \text{ V}^2/\text{Hz}$

i.e. $V_{CA} = 4,5 \text{ nV}/\text{Hz}^{1/2}$

Ref: http://www.synergie-concept.fr/index_fichiers/Page1212.htm

- Programmable Gain from 1×10^3 to 1×10^8 V/A
 - Bandwidth DC / 1 Hz... 500 kHz
 - Two Programmable Voltage Outputs for Biasing
- Equ. Input Noise Voltage : 4 nV / Hz (@ 100 Hz)
 Input Bias Current : 1 pA typ. (maximum 3 pA)
 Output Voltage: ± 10 V (@ 10 k Load)
 Output Voltage for Biasing ± 5 V (0.1% Precision)
 Output Impedance : 50

E4727B Advanced Low-Frequency Noise Analyzer



What is said by Keysight
 → LNA for better sensitivity in low current biasing conditions
 → High power device noise measurement **even in the high current like 1A** (wide bandgap technologies at open channel operating modes)



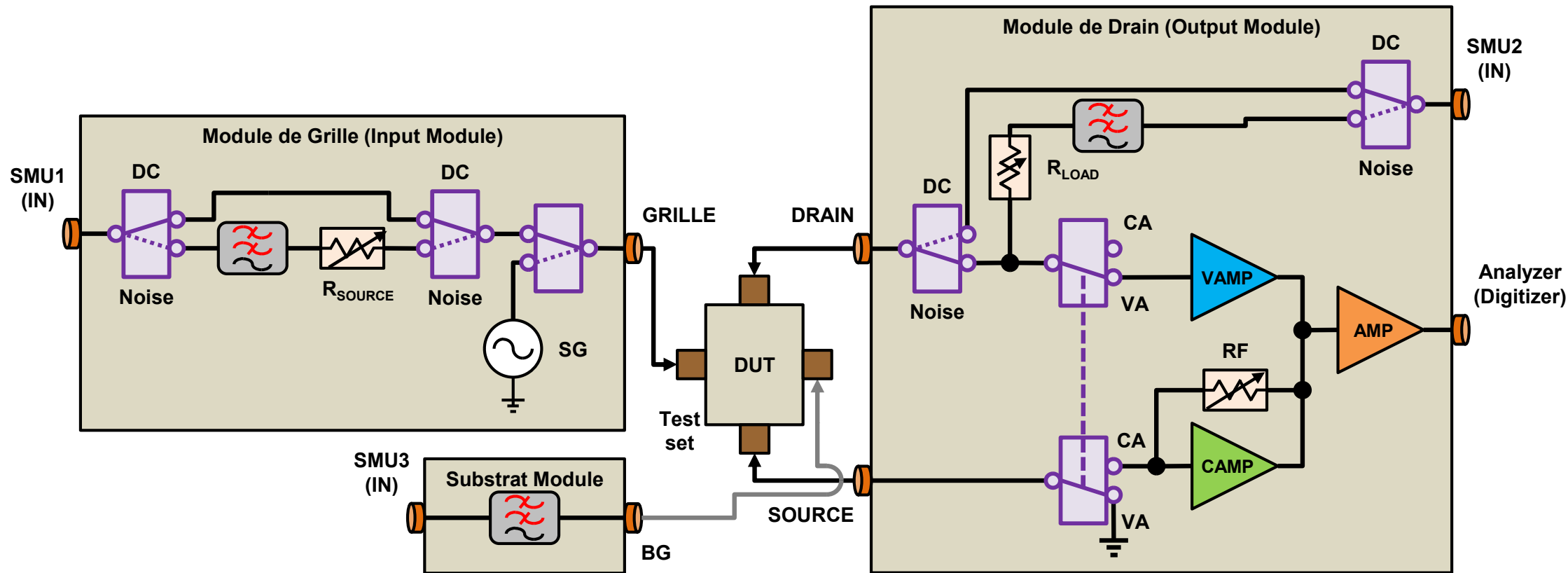
DCP-HTR Series Probe DCP 100 Series Probe

- Grounded probes closer to the device (limit ground loops from EMI/FRI) (GSG for RF devices for example, or dedicated probes with 1 contact)
- Shielded Environment Faraday or Probe station → FormFactor's CM300xi-ULN probe station to address these measurements with low noise floor level (-190 dBVrms/Hz^{0,5} spectral noise)

Ref: <https://www.keysight.com/us/en/product/E4727B/e4727b-advanced-low-frequency-noise-analyzer.html>

Ref: <https://www.formfactor.com/applications/semiconductor-r-d-test/low-frequency-noise/>

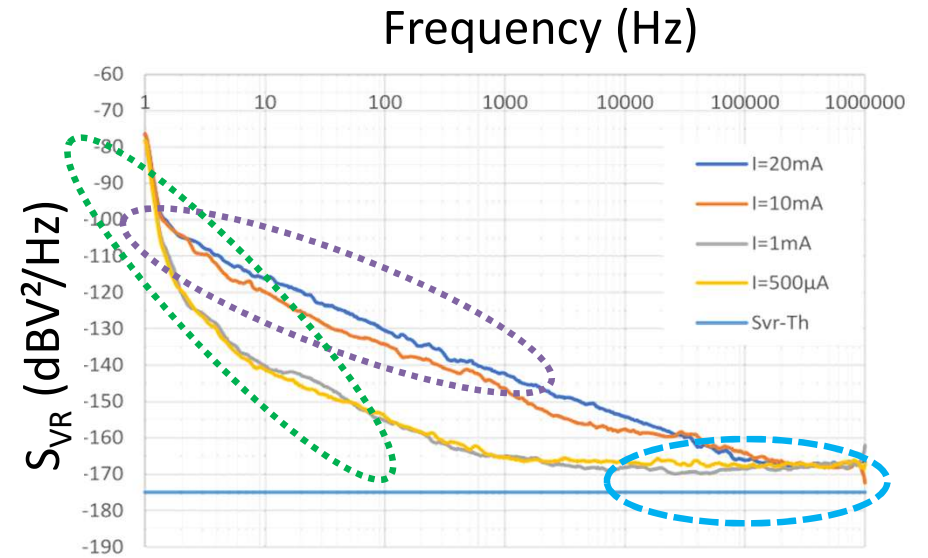
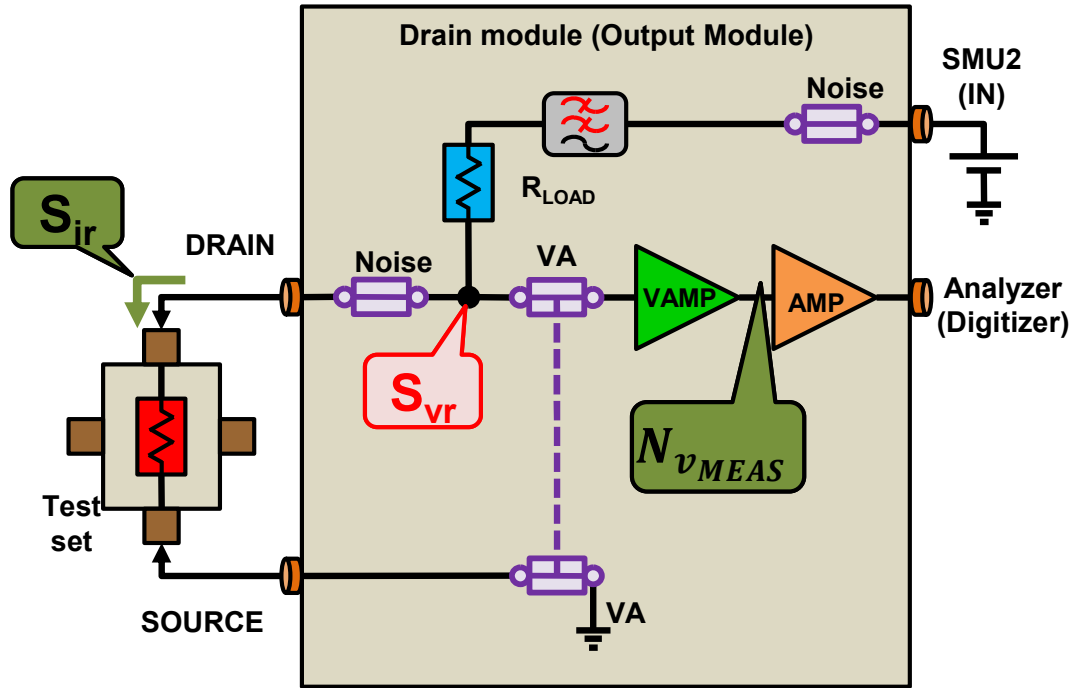
E4727A or B Advanced Low-Frequency Noise Analyzer



- LFNA as it is ! Commercialized version
- Development for Extended measurements – limits and confidence interval - studies by LAAS-CNRS

With modified equations (consideration of all noise sources of the setup)

Calibration using a large set of Resistors and Diodes



Thermal noise of a $R=200 \Omega$ resistance

Keysight Equation – V-A-M-P

Noise voltage
DUT

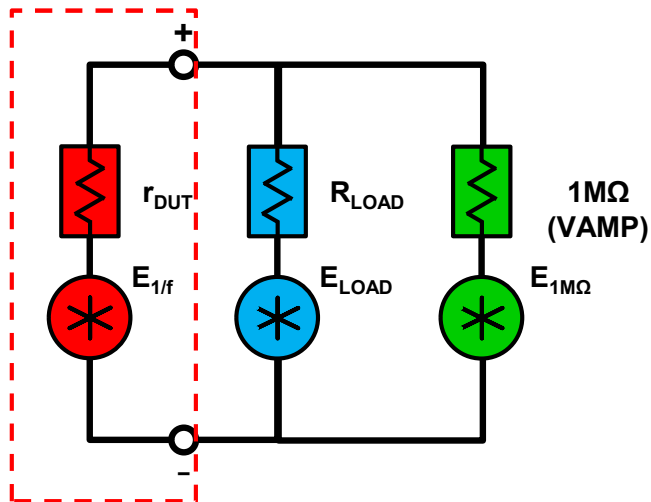
$$S_{vr} [V^2/Hz] = \left\{ \left(\frac{N_{V_{MEAS}} [V/\sqrt{Hz}]}{G_{V_{VAMP}}} \right)^2 - 4kTR_{LOAD} \cdot \left(\frac{\frac{1}{\frac{1}{r_{DUT}} + \frac{1}{1M}}}}{\frac{1}{\frac{1}{r_{DUT}} + \frac{1}{1M}} + R_{LOAD}} \right)^2 - 4kT \cdot 1M \cdot \left(\frac{\frac{1}{\frac{1}{r_{DUT}} + \frac{1}{R_{LOAD}}}}}{\frac{1}{\frac{1}{r_{DUT}} + \frac{1}{R_{LOAD}} + 1M}} \right)^2 \right\} \left(\frac{r_{DUT} + \frac{1}{\frac{1}{R_{LOAD}} + \frac{1}{1M}}}}{\frac{1}{\frac{1}{R_{LOAD}} + \frac{1}{1M}}} \right)^2$$

All the considered noise sources are thermal noise

With modified equations (consideration of all noise sources of the setup)

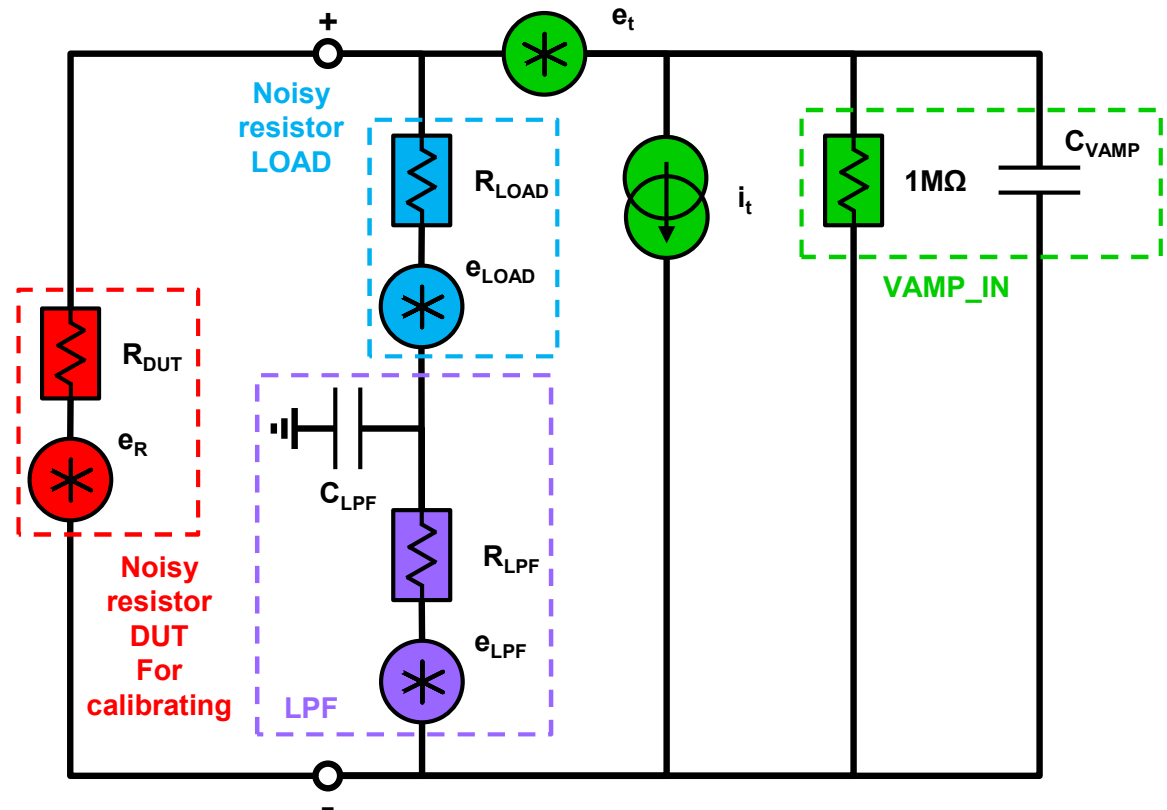
Calibration using a large set of Resistors and Diodes

Keysight equivalent model



Noisy resistor
DUT
for calibrating
 $S_i = 4kT/R_{DUT}$

Our complete chain representation using VAMP with noise sources at the input,
and with R_{DUT}



e_t and i_t : noise sources voltage/current for VAMP

e_R et e_{LOAD} : voltage noise sources for the noisy resistors R_{DUT} and R_{LOAD}

e_{LPF} : voltage noise source for the resistor of the LPF

With modified equations (consideration of all noise sources of the setup)

Calibration a large set of Resistors and Diodes

Keysight equivalent model

$$S_{vr} [V^2/Hz] = \left\{ \left(\frac{N_{VMEAS} [V/\sqrt{Hz}]}{G_{VVAMP}} \right)^2 - 4kTR_{LOAD} \cdot \left(\frac{\frac{1}{r_{DUT}} + \frac{1}{1M}}{\frac{1}{r_{DUT}} + \frac{1}{1M} + R_{LOAD}} \right)^2 - 4kT \cdot 1M \cdot \left(\frac{\frac{1}{r_{DUT}} + \frac{1}{R_{LOAD}}}{\frac{1}{r_{DUT}} + \frac{1}{R_{LOAD}} + 1M} \right)^2 \right\} \left(r_{DUT} + \frac{1}{\frac{1}{R_{LOAD}} + \frac{1}{1M}} \right)^2$$

Noisy resistor
DUT
for calibrating
 $S_i = 4kT/R_{DUT}$

Our complete chain representation using VAMP with noise sources at the input, and with R_{DUT}

$$S_{vr} \left(\frac{V^2}{Hz} \right) = \left[\frac{N_{vmeas}^2 \left(\frac{V^2}{Hz} \right)}{G_v^2} \cdot \left(1 + \frac{1}{|Z_{in}|} \cdot \frac{R_{Load} \cdot |Z_{DUT}|}{R_{Load} + |Z_{DUT}|} \right)^2 - (e_{R_{Load}}^2 + e_{SMU}^2) \cdot \left(\frac{|Z_{DUT}|}{R_{Load} + |Z_{DUT}|} \right)^2 \right. \\ \left. - e_v^2 - i_v^2 \cdot \left(\frac{R_{Load} \cdot |Z_{DUT}|}{R_{Load} + |Z_{DUT}|} \right)^2 - 2Re \left\{ e_v \cdot i_v^* \cdot \frac{R_{Load} \cdot |Z_{DUT}|}{R_{Load} + |Z_{DUT}|} \right\} \right] \cdot \left[\frac{R_{Load} + |Z_{DUT}|}{R_{Load}} \right]^2$$

Noisy resistor
LOAD

Noisy resistor
DUT
For calibrating

VAMP_IN

VAMP noise sources should be determined for VAMP configuration (also with $e_v \cdot i_v^*$)

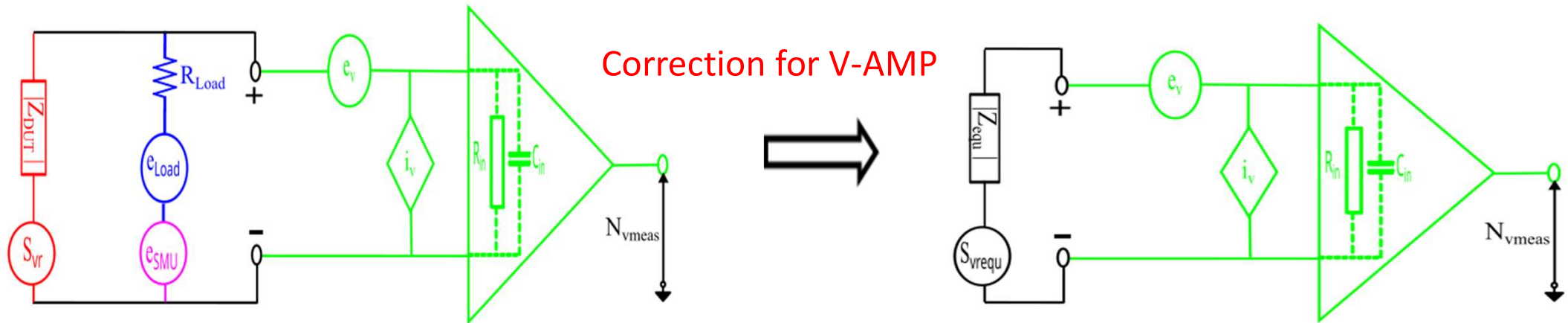
Noise sources of SMU can be managed with Rload configuration in a certain limit ($R_{Load} \gg |Z_{DUT}|$)

With modified equations (consideration of all noise sources of the setup)

Calibration a large set of Resistors and Diodes

Integrated formula : LFNA from Keysight

$$S_{vr}[V^2/Hz] = \left\{ \left(\frac{N_{VMEAS}[V/\sqrt{Hz}]}{G_{VAMP}} \right)^2 - 4kTR_{Load} \cdot \left(\frac{\frac{1}{r_{DUT} + \frac{1}{1M}}}{\frac{1}{r_{DUT} + \frac{1}{1M}} + R_{Load}} \right)^2 - 4kT \cdot 1M \cdot \left(\frac{\frac{1}{r_{DUT} + R_{LOAD}}}{\frac{1}{r_{DUT} + R_{LOAD}} + 1M} \right)^2 \right\} \left(\frac{r_{DUT} + \frac{1}{\frac{1}{R_{Load}} + \frac{1}{1M}}}}{\frac{1}{\frac{1}{R_{Load}} + \frac{1}{1M}}} \right)^2$$



Our full equation :

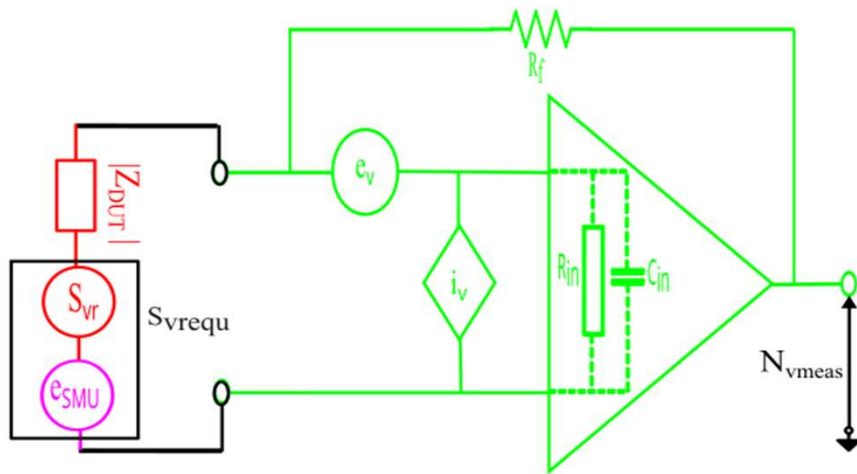
$$S_{vr} \left(\frac{V^2}{Hz} \right) = \left[\frac{N_{vmeas}^2 \left(\frac{V^2}{Hz} \right)}{G_v^2} \cdot \left(1 + \frac{1}{|Z_{in}|} \cdot \frac{R_{Load} \cdot |Z_{DUT}|}{R_{Load} + |Z_{DUT}|} \right)^2 - (e_{R_{Load}}^2 + e_{SMU}^2) \cdot \left(\frac{|Z_{DUT}|}{R_{Load} + |Z_{DUT}|} \right)^2 \right. \\ \left. - e_v^2 - i_v^2 \cdot \left(\frac{R_{Load} \cdot |Z_{DUT}|}{R_{Load} + |Z_{DUT}|} \right)^2 - 2Re \left\{ e_v \cdot i_v^* \cdot \frac{R_{Load} \cdot |Z_{DUT}|}{R_{Load} + |Z_{DUT}|} \right\} \right] \cdot \left[\frac{R_{Load} + |Z_{DUT}|}{R_{Load}} \right]^2$$

With modified equations (consideration of all noise sources of the setup)

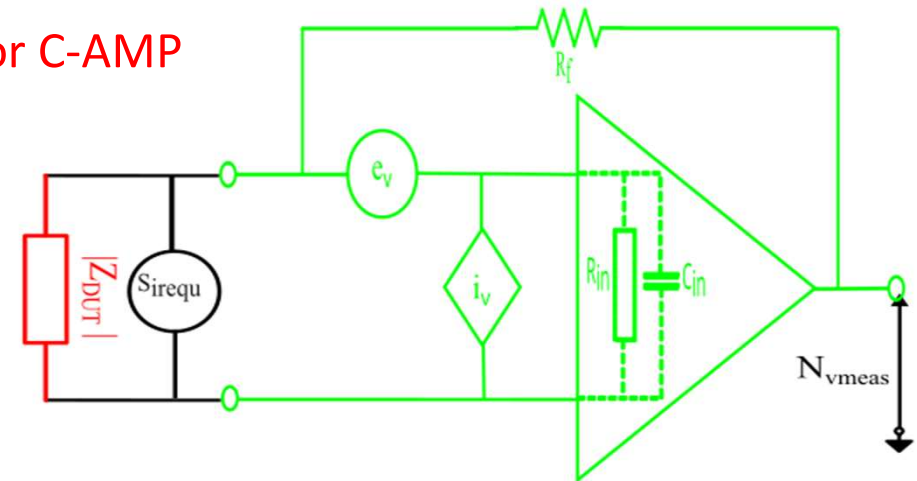
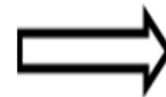
Calibration a large set of Resistors and Diodes

Integrated formula : LFNA from Keysight

$$S_{ia}(A^2/Hz) = \frac{N_{vmeas}^2(V^2/Hz)}{R_f^2}$$



Correction for C-AMP

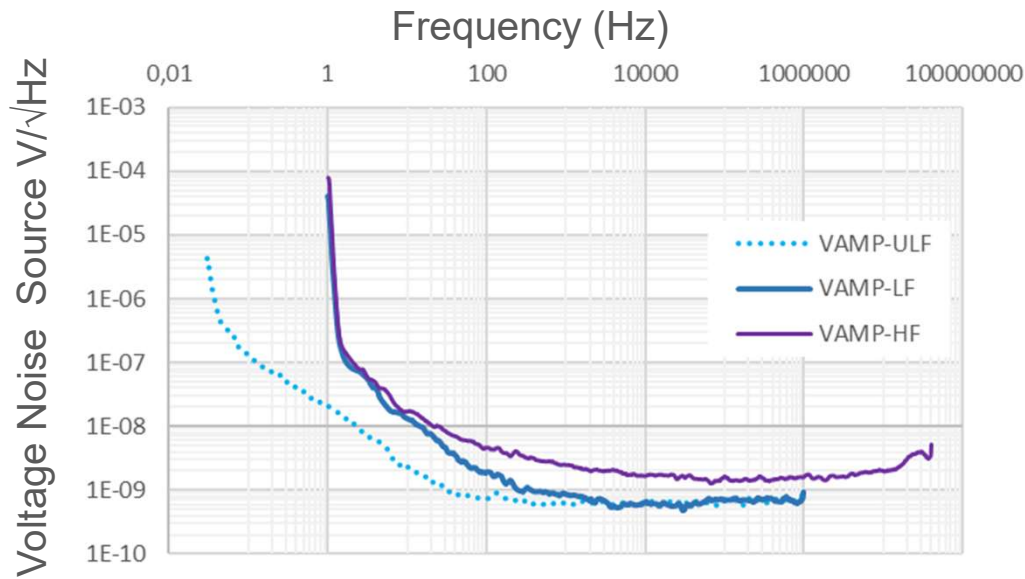


Our full equation :

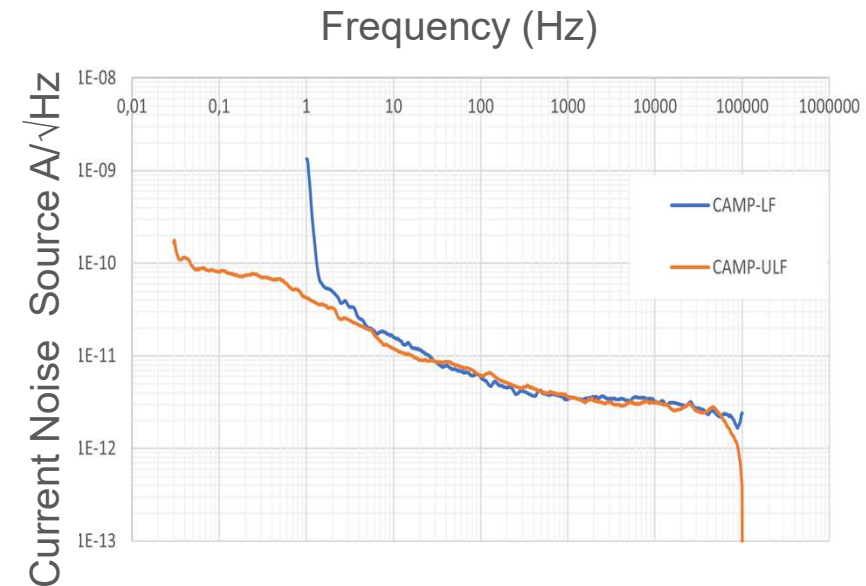
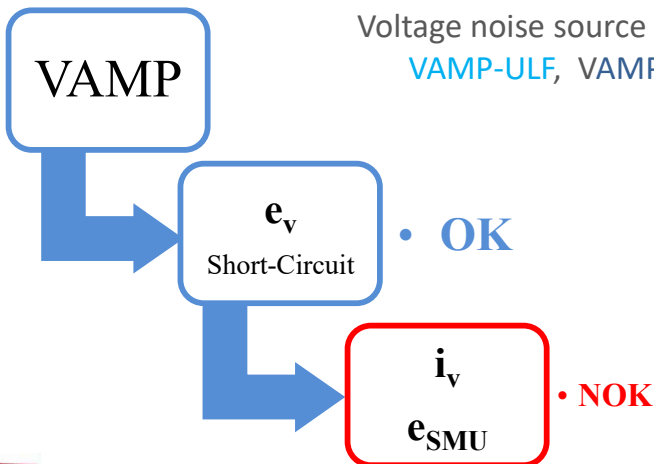
$$S_{iDUT}\left(\frac{A^2}{Hz}\right) = \frac{N_{vmeas}^2\left(\frac{V^2}{Hz}\right)}{R_f^2} \cdot \left[\frac{|Z_{in}| + |Z_{DUT}|}{|Z_{DUT}|}\right]^2 - \frac{e_{SMU}^2}{|Z_{DUT}|^2} - i_A^2 - \frac{e_A^2}{|Z_{DUT}|^2} - 2\text{Re}\left\{i_A^* \cdot \frac{e_A}{|Z_{DUT}|}\right\}$$

With modified equations (consideration of all noise sources of the setup)

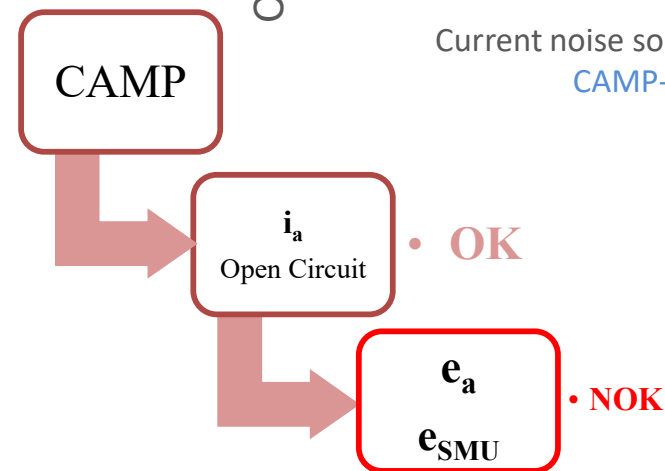
Calibration of noise sources of V-AMP and C-AMP (needed for the extraction of the DUT noise source)



Voltage noise source characterization for VAMP-ULF, VAMP-LF & VAMP-HF

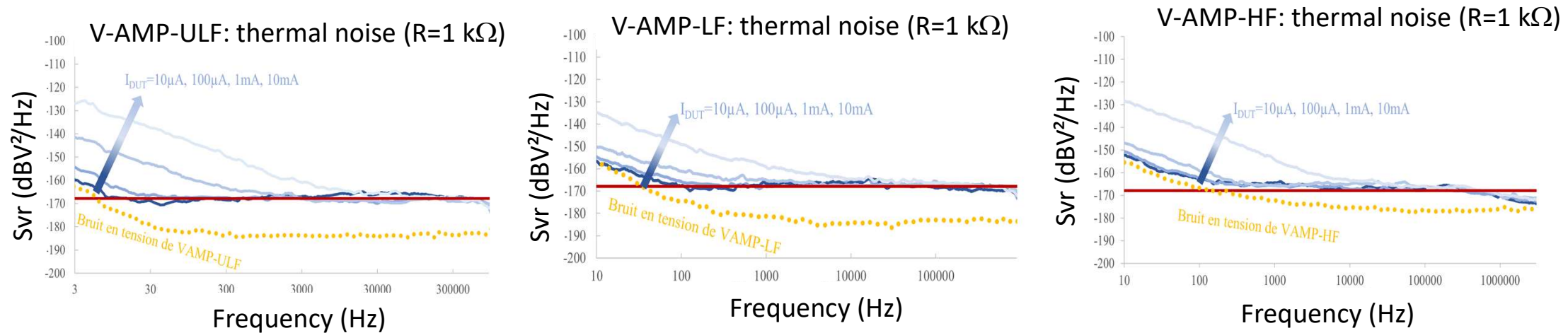


Current noise source characterization for CAMP-LF, CAMP-ULF



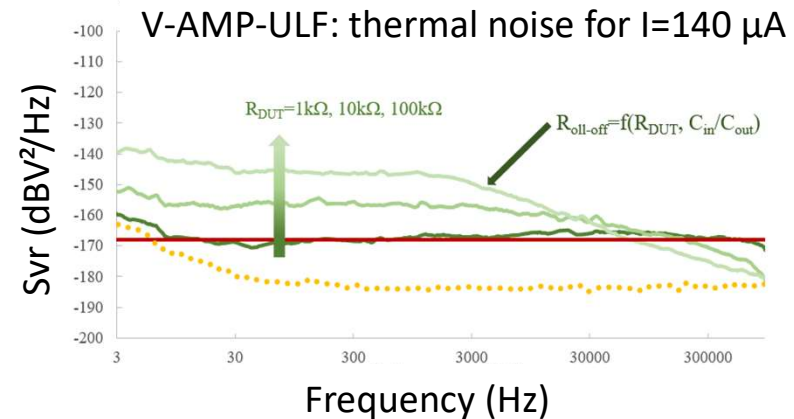
Interval of confidence for LFN measurements with E4727A

Calibration for thermal noise versus R_{bias} for V-AMP configurations



definition of a reliable data exploitation zone
with template(Δf , noise floor) :

Detection limit and DUT biasing impact on
data post-processing





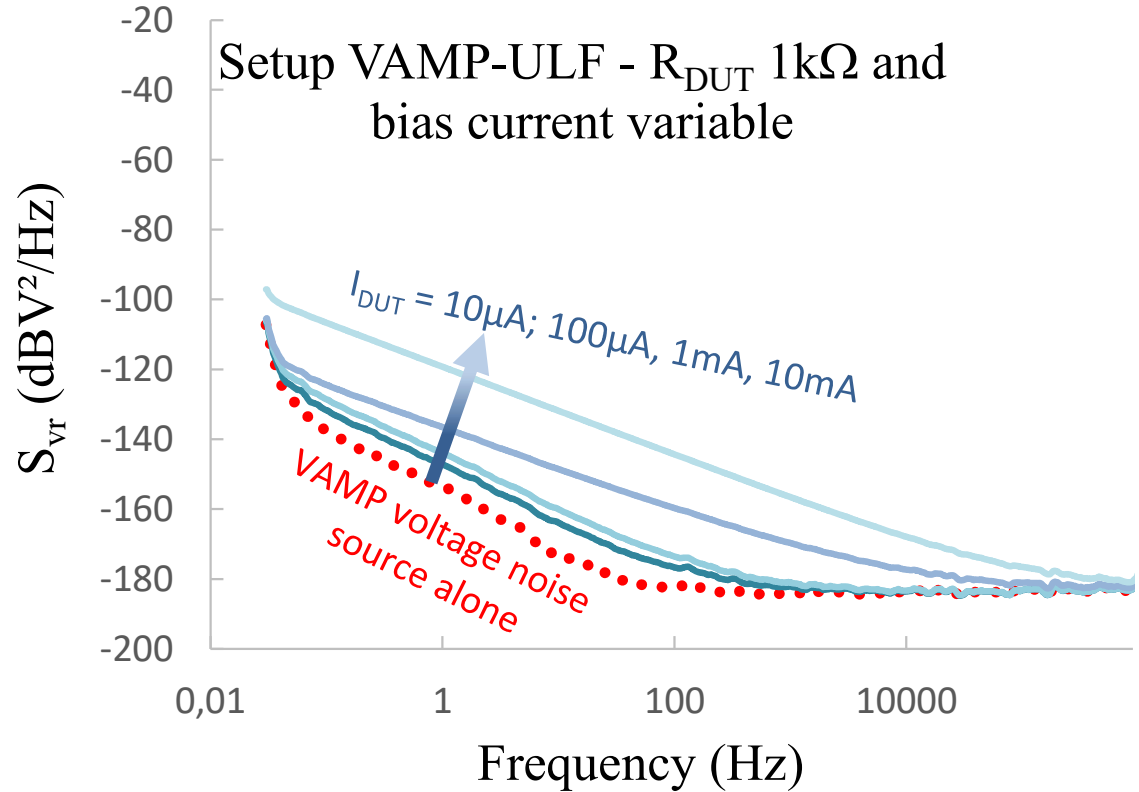
LFN EXPERIMENTAL SETUPS: a large variety of solutions E4727A from Keysight – with developments at LAAS



Université de Toulouse

Interval of confidence for LFN measurements with E4727A

Résistance (Ω)	VAMP	Courant (A)	R _{dut} (Ω)	R _{load} (Ω)	Fréquences (Hz)						S _v (dBV ² /Hz)		ΔS _v (dBV ² /Hz)		
					3	10	100	1k	10k	100k	900k	Mesuré		Théorique	
1k	VAMP-ULF	10μ	985,9	10k	6,58								-166,9	-167,93	-1,03
		100μ	987,5	10k		13,92							-167,1	-167,92	-0,82
		1m	987,9	10k				1,186k					-168,6	-167,92	0,68
		10m	983,3	10k					9,572k				-167	-167,94	-0,94
	VAMP-LF	10μ	987,8	10k			73,83						-167,5	-167,92	-0,42
		100μ	989,2	10k			34,88						-166,6	-167,91	-1,31
		1m	990,3	10k				297,1					-167,5	-167,91	-0,41
		10m	986,3	10k					5,649k				-166,3	-167,93	-1,63
	VAMP-HF	10μ	990,7	10k				135,5					-166,8	-167,91	-1,11
		100μ	992,8	10k				119,5					-165,9	-167,90	-2,00
		1m	994,7	10k					227,3				-165	-167,89	-2,89
		10m	989,9	10k						9,479k			-166,2	-167,91	-1,71
10k	VAMP-ULF	1μ	9,831E+03	100k	6,70				62,29k				-157,6	-157,94	-0,34
		10μ	9,849E+03	100k	5,13				62,19k				-156,7	-157,93	-1,23
		100μ	9,881E+03	100k		12,07			62,01k				-156,3	-157,92	-1,62
		1m	9,830E+03	100k			300		68,30k				-155,3	-157,94	-2,64
	VAMP-LF	1μ	9,809E+03	100k			10		62,42k				-157,9	-157,95	-0,05
		10μ	9,833E+03	100k			10		62,28k				-157,3	-157,94	-0,64
		100μ	9,885E+03	100k			10		61,98k				-157	-157,92	-0,92
		1m	9,867E+03	100k				1,481k	62,09k				-156,5	-157,93	-1,43
	VAMP-HF	1μ	9,849E+03	100k			19,70		96,81k				-155,5	-157,93	-2,43
		10μ	9,864E+03	100k			18,02		96,68k				-157,1	-157,93	-0,83
		100μ	9,901E+03	100k			57,50		96,35k				-159,9	-157,91	1,99
		1m	9,839E+03	100k				751,60	96,90k				-154,2	-157,94	-3,74
100k	VAMP-ULF	100m	9,774E+04	1M	3				6,759k				-147,2	-147,97	-0,77
		1μ	9,808E+04	1M	3				6,740k				-147,2	-147,95	-0,75
		10μ	9,842E+04	1M		19,55			6,720k				-146,5	-147,94	-1,44
		100μ	9,820E+04	1M									-	-147,95	-
	VAMP-LF	100n	9,804E+04	1M			10		6,742k				-146,8	-147,95	-1,15
		1μ	9,824E+04	1M			10		6,730k				-147,2	-147,94	-0,74
		10μ	9,880E+04	1M			10		6,699k				-146,6	-147,92	-1,32
		100μ	9,727E+04	1M									-	-147,99	-
	VAMP-HF	100n	9,798E+04	1M					10,50k				-147,8	-147,96	-0,16
		1μ	9,820E+04	1M			10		10,48k				-146,8	-147,95	-1,15
		10μ	9,915E+04	1M			17,39		10,40k				-147,6	-147,90	-0,30
		100μ	9,789E+04	1M									-	-147,96	-



- measurements made with 2 SMUs : HP4142 and HP4156C
- Resistance ranging from 100Ω, 470Ω,..., 100kΩ, 470kΩ, 1MΩ
- 2 Diodes : PH4148 & 1N 4007

Example for V-AMP LF configuration

Set the interpretable and reliable measurement limits



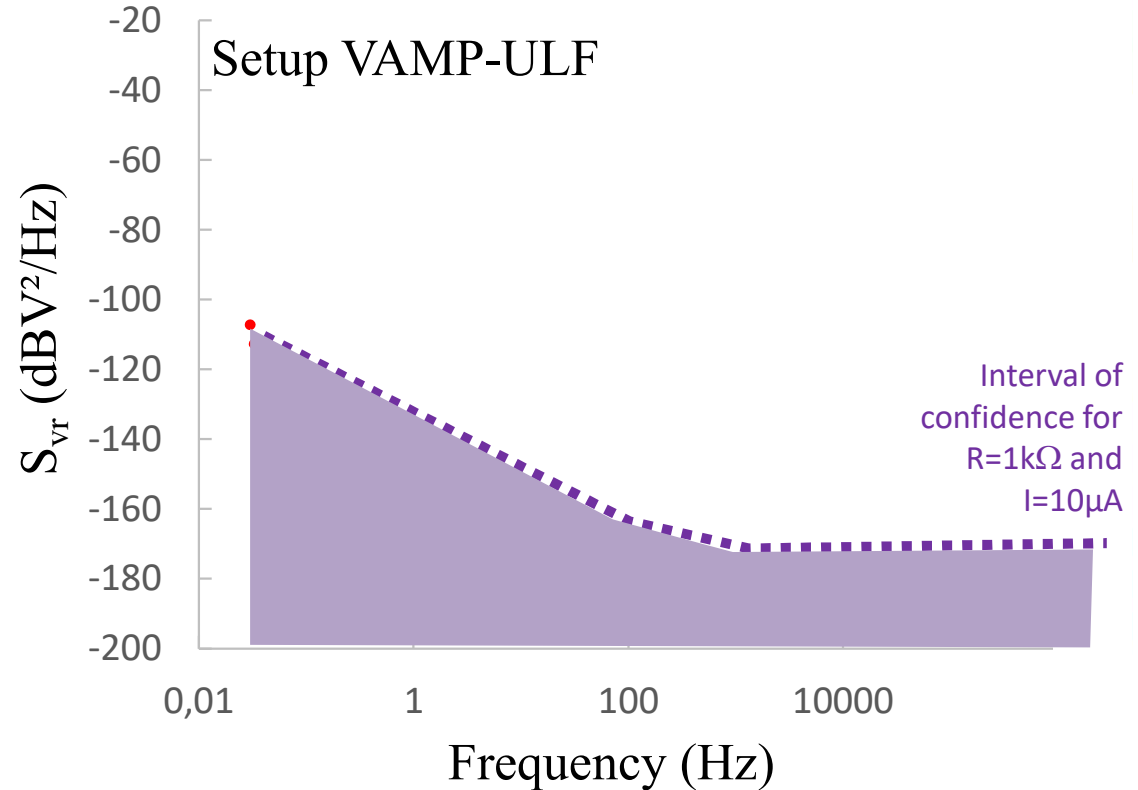


LFN EXPERIMENTAL SETUPS: a large variety of solutions E4727A from Keysight – with developments at LAAS



Interval of confidence for LFN measurements with E4727A

Résistance (Ω)	VAMP	Courant (A)	Rdut (Ω)	Rload (Ω)	Fréquences (Hz)						Sv (dBV ² /Hz)		ΔSv (dBV ² /Hz)		
					3	10	100	1k	10k	100k	900k	Mesuré		Théorique	
1k	VAMP-ULF	10μ	985,9	10k	6,58								-166,9	-167,93	-1,03
		100μ	987,5	10k		13,92							-167,1	-167,92	-0,82
		1m	987,9	10k				1,186k					-168,6	-167,92	0,68
		10m	983,3	10k					9,572k				-167	-167,94	-0,94
	VAMP-LF	10μ	987,8	10k			73,83						-167,5	-167,92	-0,42
		100μ	989,2	10k			34,88						-166,6	-167,91	-1,31
		1m	990,3	10k				297,1					-167,5	-167,91	-0,41
		10m	986,3	10k					5,649k				-166,3	-167,93	-1,63
	VAMP-HF	10μ	990,7	10k				135,5					-166,8	-167,91	-1,11
		100μ	992,8	10k				119,5					-165,9	-167,90	-2,00
		1m	994,7	10k					227,3				-165	-167,89	-2,89
		10m	989,9	10k						9,479k			-166,2	-167,91	-1,71
10k	VAMP-ULF	1μ	9,831E+03	100k	6,70				62,29k				-157,6	-157,94	-0,34
		10μ	9,849E+03	100k	5,13				62,19k				-156,7	-157,93	-1,23
		100μ	9,881E+03	100k		12,07			62,01k				-156,3	-157,92	-1,62
		1m	9,830E+03	100k			300		68,30k				-155,3	-157,94	-2,64
	VAMP-LF	1μ	9,809E+03	100k		10			62,42k				-157,9	-157,95	-0,05
		10μ	9,833E+03	100k		10			62,28k				-157,3	-157,94	-0,64
		100μ	9,885E+03	100k		10			61,98k				-157	-157,92	-0,92
		1m	9,867E+03	100k				1,481k	62,09k				-156,5	-157,93	-1,43
	VAMP-HF	1μ	9,849E+03	100k		19,70			96,81k				-155,5	-157,93	-2,43
		10μ	9,864E+03	100k		18,02			96,68k				-157,1	-157,93	-0,83
		100μ	9,901E+03	100k		57,50			96,35k				-159,9	-157,91	1,99
		1m	9,839E+03	100k			751,60		96,90k				-154,2	-157,94	-3,74
100k	VAMP-ULF	100n	9,774E+04	1M	3				6,759k				-147,2	-147,97	-0,77
		1μ	9,808E+04	1M	3				6,740k				-147,2	-147,95	-0,75
		10μ	9,842E+04	1M		19,55			6,720k				-146,5	-147,94	-1,44
		100μ	9,820E+04	1M									-	-147,95	-
	VAMP-LF	100n	9,804E+04	1M		10			6,742k				-146,8	-147,95	-1,15
		1μ	9,824E+04	1M		10			6,730k				-147,2	-147,94	-0,74
		10μ	9,880E+04	1M		10			6,699k				-146,6	-147,92	-1,32
		100μ	9,727E+04	1M									-	-147,99	-
	VAMP-HF	100n	9,798E+04	1M					10,50k				-147,8	-147,96	-0,16
		1μ	9,820E+04	1M					10,48k				-146,8	-147,95	-1,15
		10μ	9,915E+04	1M					10,40k				-147,6	-147,90	-0,30
		100μ	9,789E+04	1M									-	-147,96	-



- measurements made with 2 SMUs : HP4142 and HP4156C
- Resistance ranging from 100Ω, 470Ω,..., 100kΩ, 470kΩ, 1MΩ
- 2 Diodes : PH4148 & 1N 4007

Set the interpretable and reliable measurement limits

Example for V-AMP LF configuration





LFN EXPERIMENTAL SETUPS: a large variety of solutions from home-made to commercial solutions



Université de Toulouse

		W7802B PathWave WaferPro Express A-LFNA Measurement and Programing bundle	W7801B PathWave WaferPro Express WGFMU Measurement bundle	Home made setup LAAS-CNRS (batteries)
Measurement Hardware		E4727B A-LFNA	B1500A with B1530A WGFMU	x
Target Device		FET, BJT, Diode, Resistor, Circuit	FET	FET, HBT (BJT), Diode, circuit (depending on RF-DC decoupling)
Device Terminal Number		3, 4, 5, 6	3	3
Maximum Bias Voltage		±200 V	±10 V	Limited by batteries (60 V) - SMUs can be used with degraded perf.
Maximum Bias Current		±100 mA	±10 mA	250 mA
Noise Floor		S_1 1E-28 A ² /Hz	1E-25 A ² /Hz	S_1 : typ 1E -24 A ² /Hz, down to 2E -28 A ² /Hz <small>S_v: typ 1E -17 V²/Hz Downto 1E-19V²/Hz</small>
Analog Frequency Bandwidth		30 mHz – 100 MHz	1 mHz – 16 MHz	1 Hz – 100 MHz
Frequency Domain Measurement	Min Frequency	30 mHz	1 mHz	1 Hz
	Max Frequency	100 MHz	16 MHz	100 MHz
Time Domain Measurement	Max Sampling Frequency	500 MHz	200 MHz	FFT on with Signal Analyzer (Takeda)
	Min Sampling Interval	2 ns	5 ns	
	Max Sampling Number	16,777,216(=2 ²⁴)	2,097,152(=2 ²¹)	
Controller PC		M9037A Embedded Controller	Windows PC	Windows – C++
GP-IB Interface		M9037A Built-in GP-IB interface (Micro-D 25pin)	USB GP-IB Interface (Keysight 82357B, NI GPIB-USB-HS)	GP-IB interface

According to the gain of each V or I amplifier (feedback)

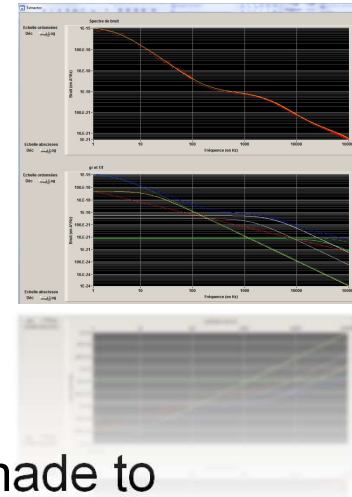
S_1 1E-28 A²/Hz

SRS preamplifier SR570 gives S_1 as low as $25 \cdot 10^{-30} \text{ A}^2/\text{Hz}$ (limited to 1-60 Hz bandwidth!)

Noise floor must be carefully interpreted ! This is without DUT / biasing systems



- ELECTRONIC NOISE: in France and at LAAS-CNRS
- LOW FREQUENCY NOISE (LFN) : metrological niche ? Not only !
- LFN EXPERIMENTAL SETUPS: a large variety of solutions from home-made to commercial solutions
- **APPLICATIONS OF LFN MEASUREMENTS : defect detection, reliability analysis, non-linear RF circuit design (VCOs, Mixers).**



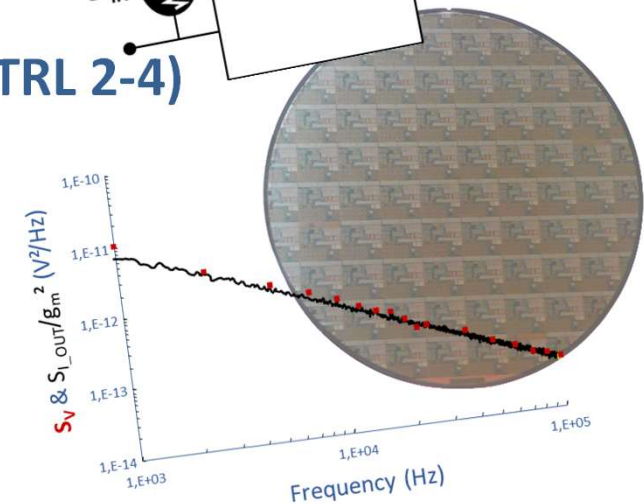
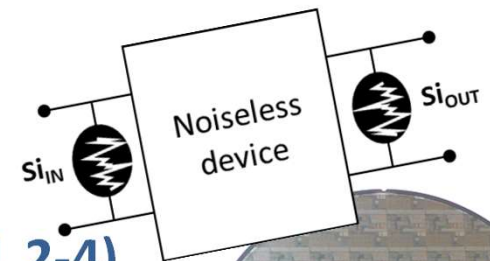
Emerging Technologies / Defect detection & Reliability Analysis

#1 : Noise Theory, is there some new 'hot' topics ?

#2 : Defect Detection for Technological development (TRL 2-4)

#3 : Failure Analysis in RF Devices (TRL 3-7)

#4 : Failure Analysis in RF Devices (part 2)

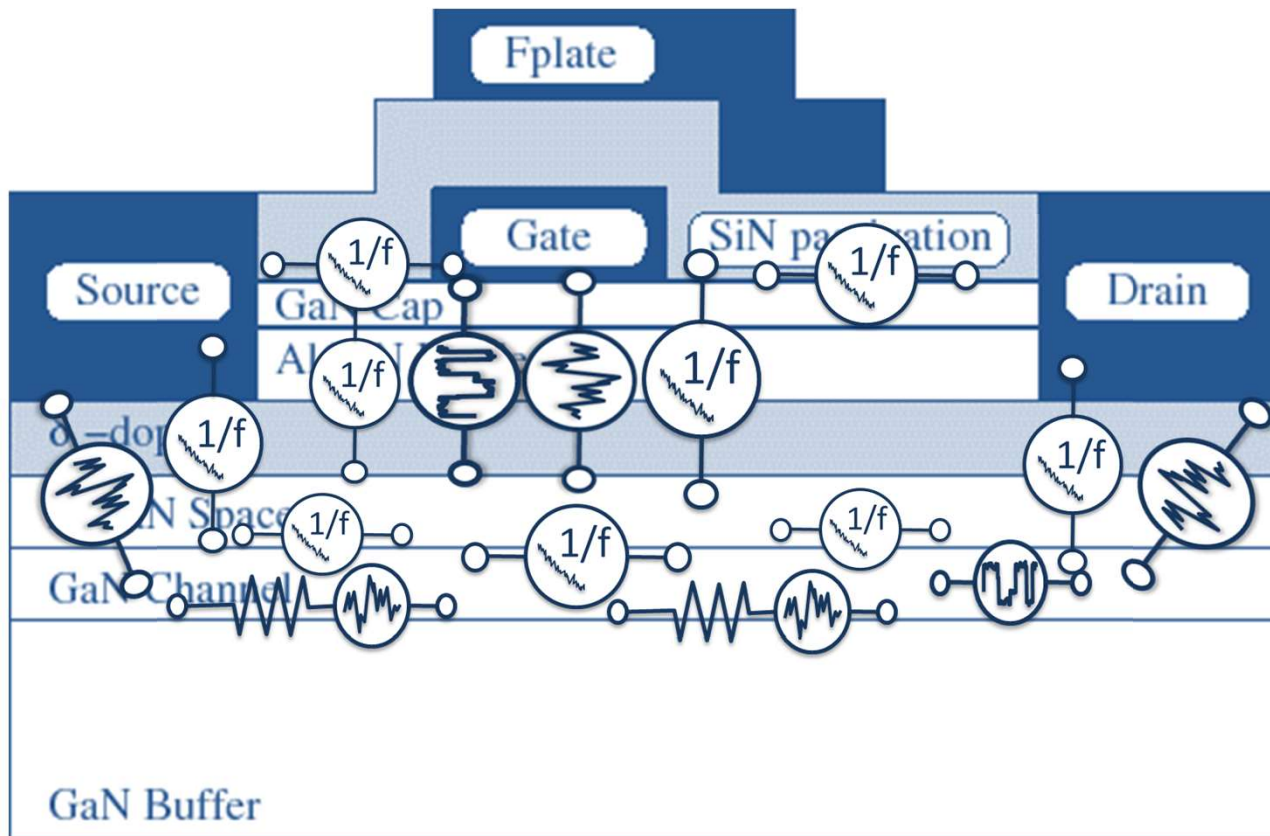


LFN for non-linear RF circuit design (VCOs, Mixers).

Electrical improvement by frequency & power increase

→ various technologies (III-V, SiGe, GaN, ...)

→ various active devices (HBT, LDMOS, MESFET, HEMT, m/pHEMT, FinFET, nanoFET...)



NOISE REVEALS EVENTS (DEFECTS) THAT :

- SET THE LIMIT OF ELECTRICAL PERF.
- REVEAL WEAKNESSES OF A DEVICE

MEASUREMENTS TOOLS

NON-INVASIVE DETECTION TOOLS OF MICROSCOPIC DEFECTS



STARTING POINT OF OUR STUDIES !

... and opportunities to play with the latest technologies !

Electrical improvement by frequency & power increase

→ various technologies (III-V, SiGe, GaN, ...)

→ various active devices (HBT, LDMOS, MESFET, HEMT, m/pHEMT, FinFET, nanoFET...)



BLIND TEST ON TECHNOLOGY

NOISE REVEALS EVENTS (DEFECTS) THAT :

- SET THE LIMIT OF ELECTRICAL PERF.
- REVEAL WEAKNESSES OF A DEVICE

MEASUREMENTS TOOLS

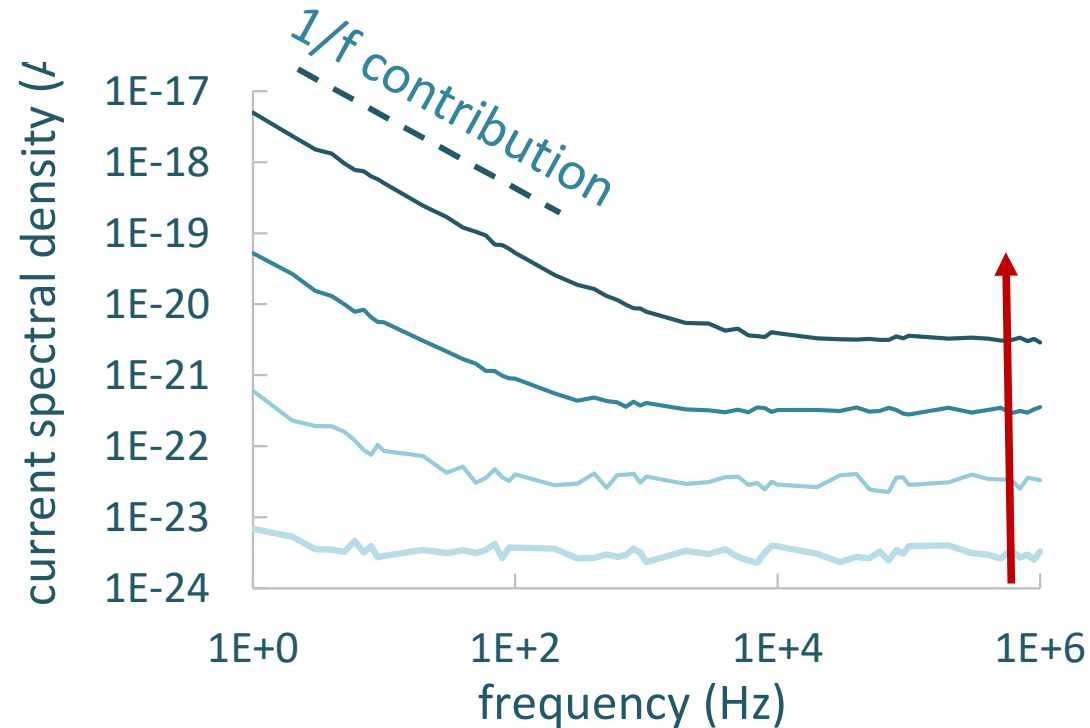
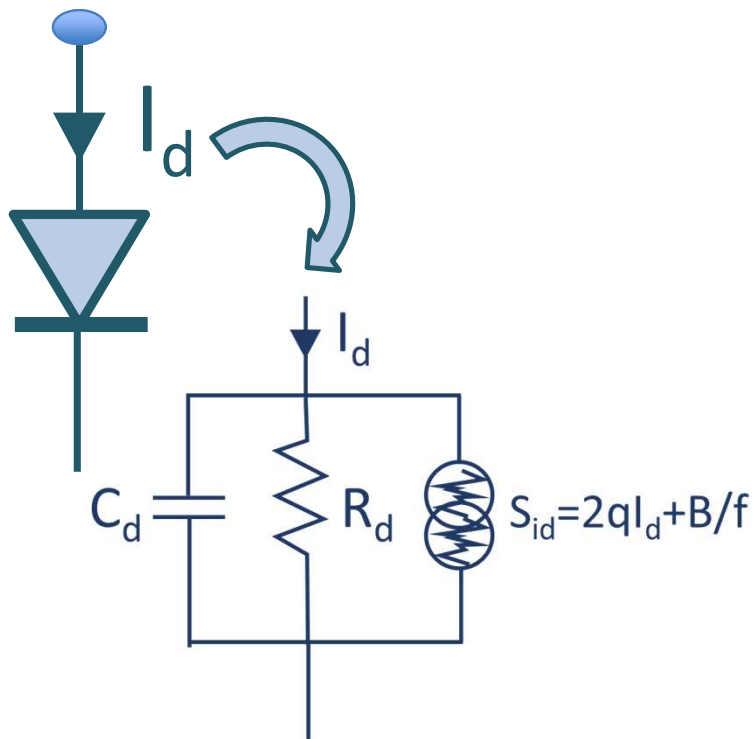
NON-INVASIVE DETECTION TOOLS OF MICROSCOPIC DEFECTS



STARTING POINT OF OUR STUDIES !

... and opportunities to play with the latest technologies !

Shot noise is massively used for noise design in (complex) solid state devices, and very easy to formulate if frequency is not very high



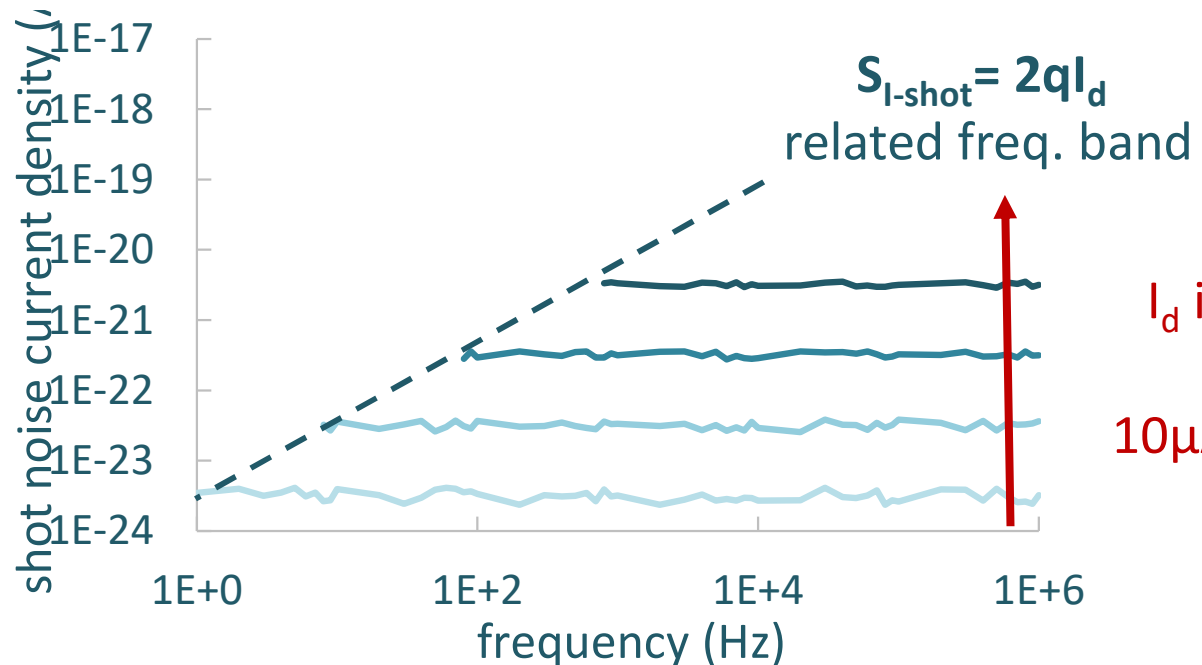
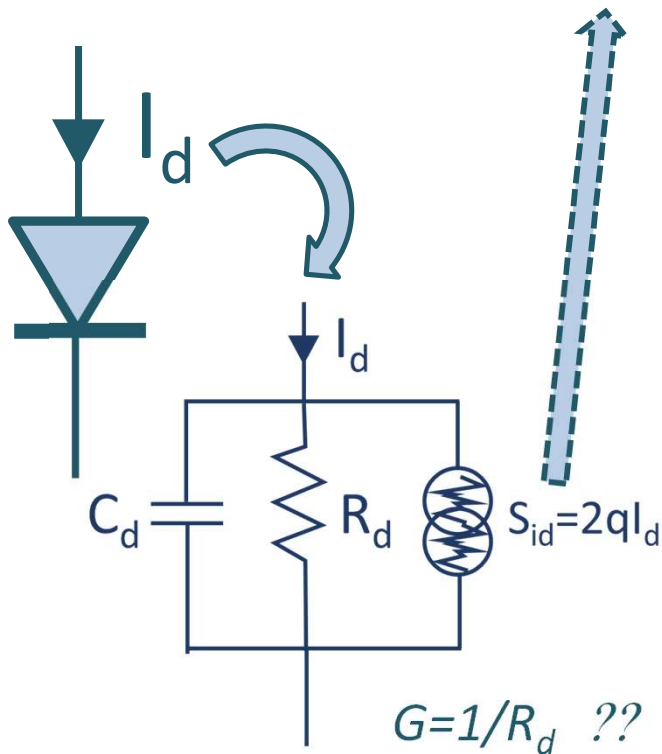
I_d increases from $10\mu A$ to $10mA$

Nota: graphics are not extracted from measurements in this slide

Ref: Graffeuil, Escotte, Tartarin, IEEE ICNF 2019

...and once 1/f contributor is corrected, the plateau matches with theory

Generalized Van der Ziel's expression
 $S_{id} = 4.k.T/R_d - 2qI_d = 2qI_d$ if using constant R_d

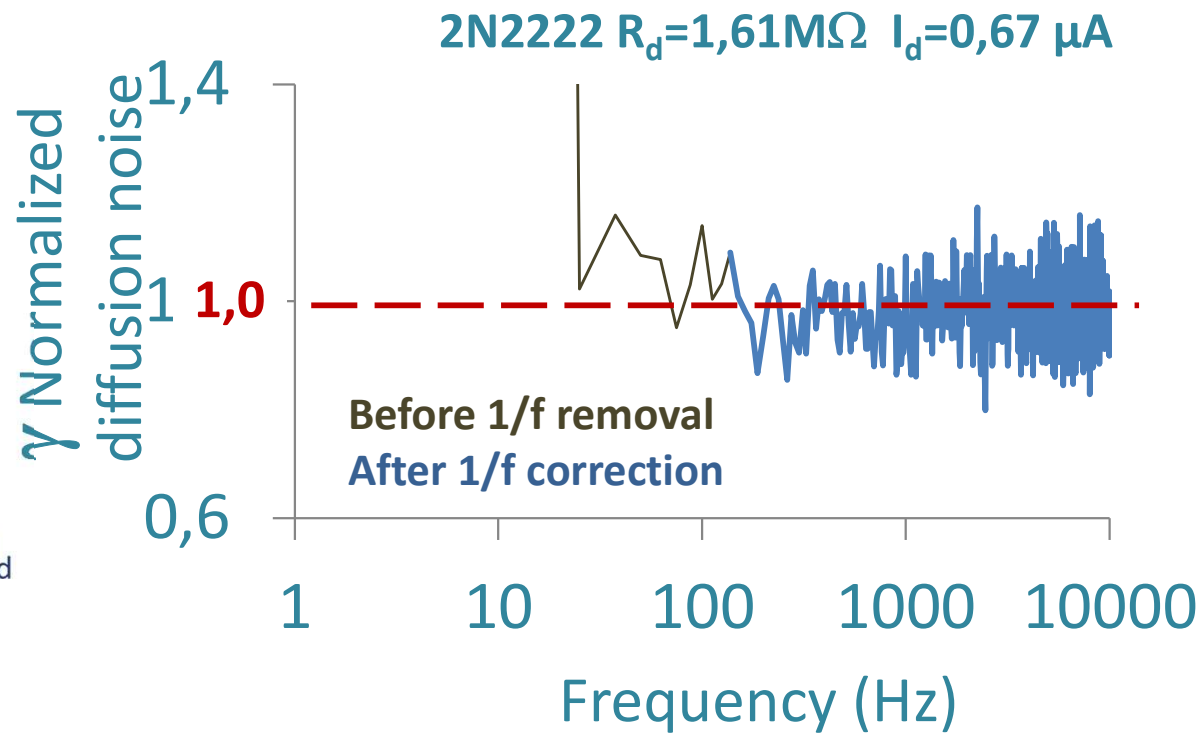
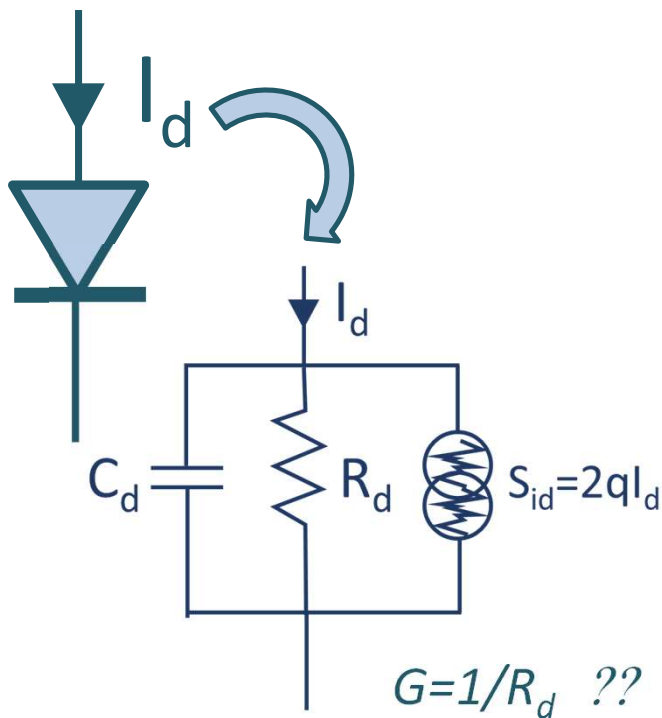


Nota: graphics are not extracted from measurements in this slide

Ref: Graffeuil, Escotte, Tartarin, IEEE ICNF 2019

...and once 1/f contributor is corrected, the plateau matches with theory

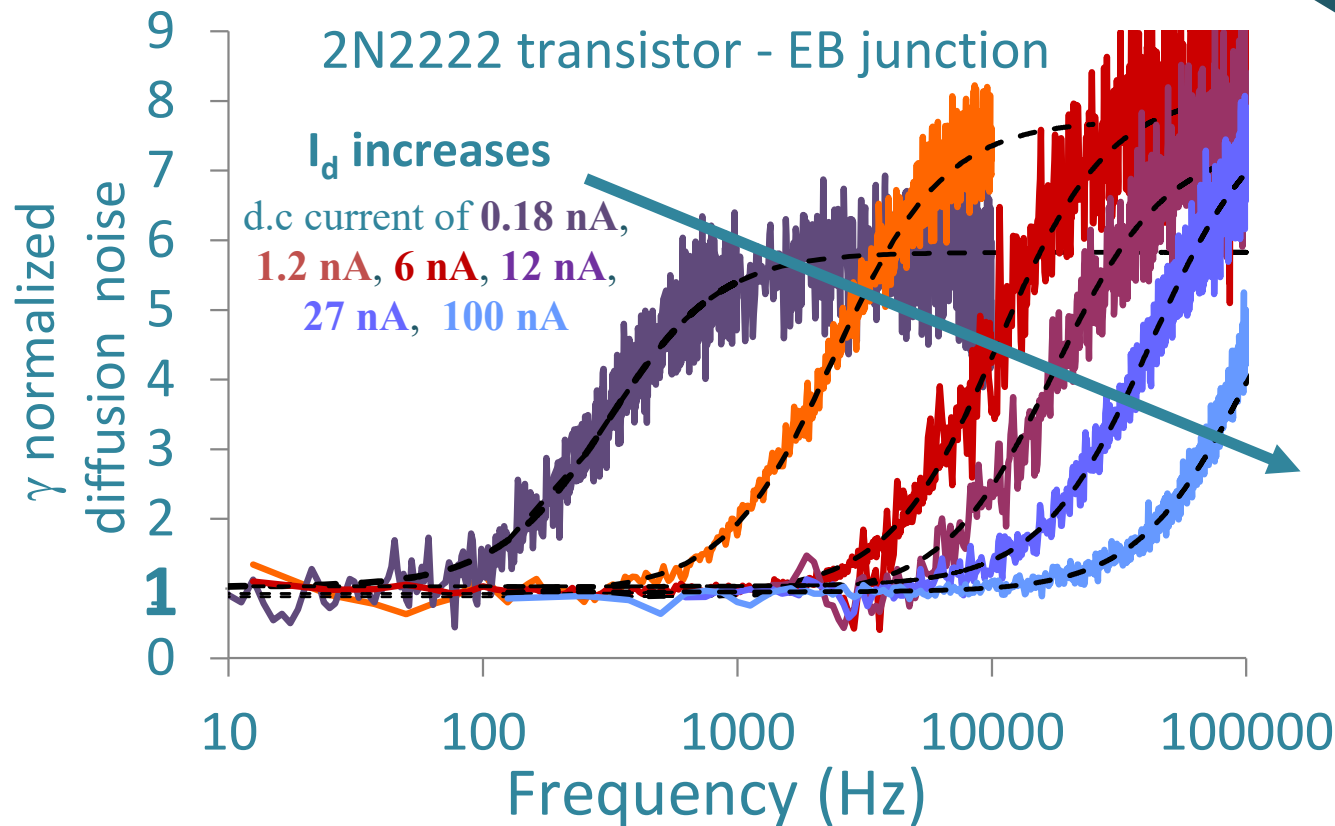
$$\gamma = \frac{S_{id}(f)}{2 \cdot q \cdot I_d} = 2 \cdot U_t \cdot G / I_d - 1 = 1 \text{ @ LF}$$



Here 1/f has no impact over 200 Hz and disappears at lower current (as in our study case)

Ref: Graffeuil, Escotte, Tartarin, IEEE ICNF 2019

But under specific very low biasing conditions, an enhancement occurs vs frequency ! Using the normalized form



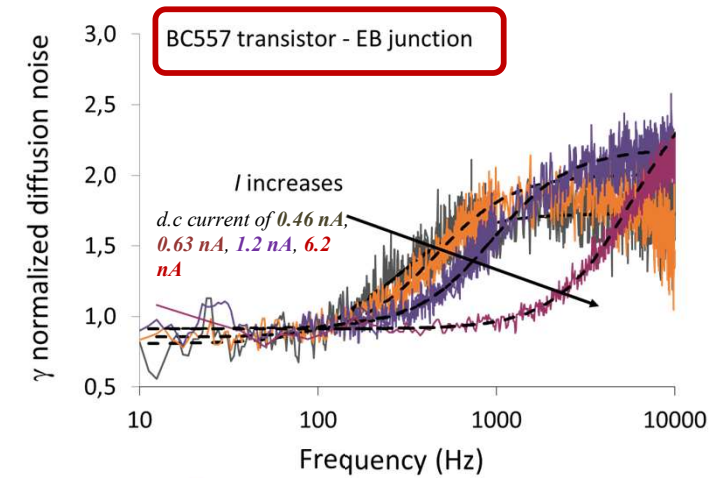
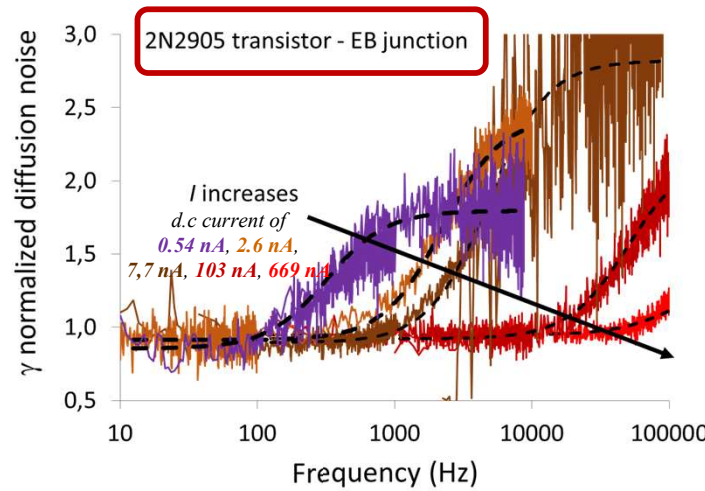
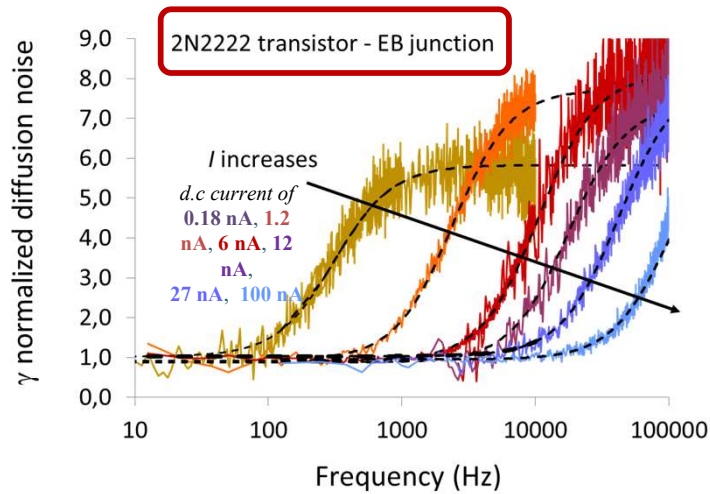
$$\gamma = \frac{S_i(f)}{2 \cdot q(I_d + 2I_s)}$$

Nota: saturation current is considered as in Van der Ziel' expression

Ref: Graffeuil, Escotte, Tartarin, IEEE ICNF 2019

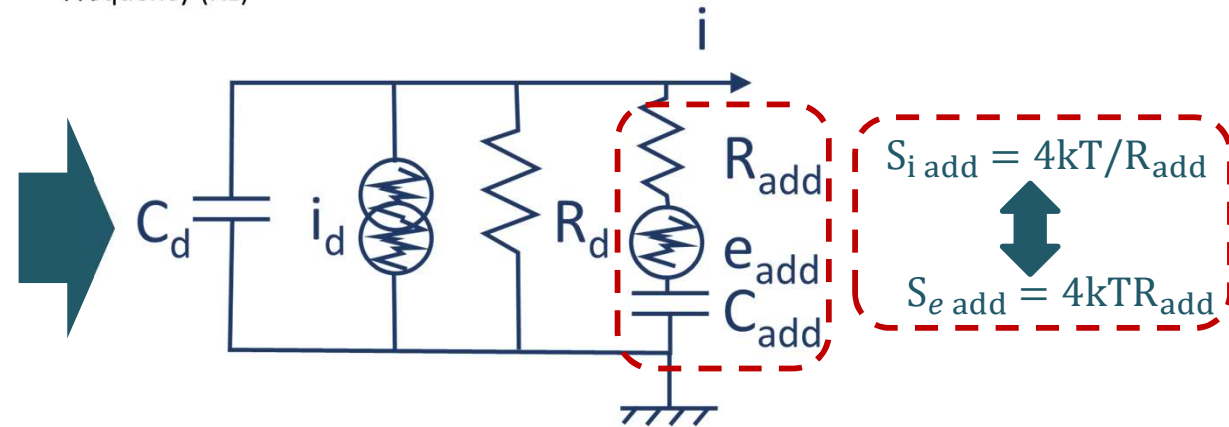
Measurement of various diodes; model of the noise floor enhancement phenomenon

Evolution of the plateau magnitude and corner frequency with I_d



$$\gamma = \frac{S_i(f)}{2 \cdot q \cdot I_d}$$

A noise model can be developed to satisfy the LFN measurements with noisy R_{add} in parallel with C_{add}



Ref: Graffeuil, Escotte, Tartarin, IEEE ICNF 2019

Measurement of various diodes; model of the noise floor enhancement phenomenon

Expression of S_i

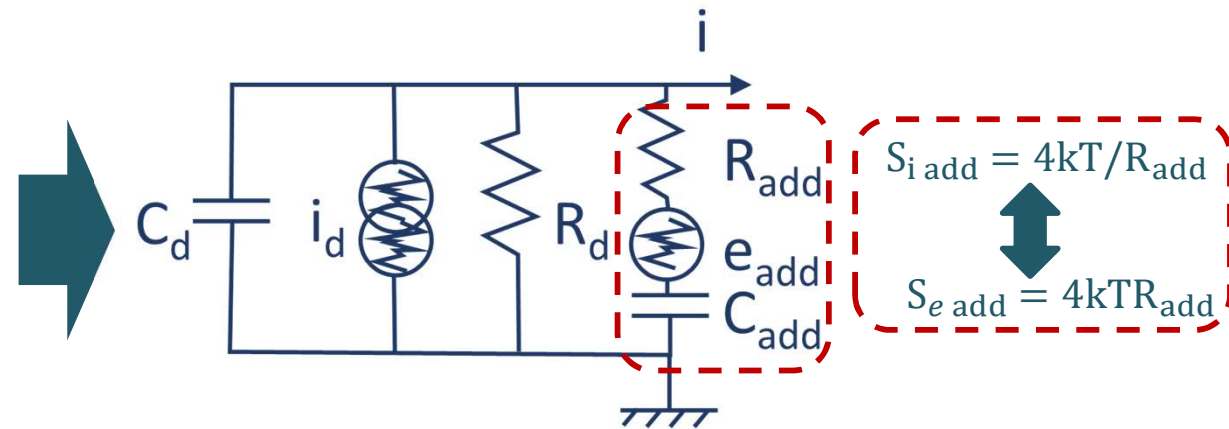
$$S_i(f) = S_{id} + \frac{(C_{add} \cdot \omega)^2 S_{i\ add}}{(1 + (R_{add} C_{add} \omega)^2)}$$

for $\omega \rightarrow 0$ $S_i(f) = S_{id}$
 for $\omega \rightarrow \infty$ $S_i(f) = S_{id} + S_{i\ add} = S_{id} + 4kT/R_{add}$

R_{add} is noisy and associated in a serial representation with C_{add}

So $R_{add}-C_{add}$ cannot be attributed to a (deep) trap phenomenon (Veddel 1997, Jensen 2006)

A noise model can be developed to satisfy the LFN measurements with noisy R_{add} in parallel with C_{add}



Ref: Graffeuil, Escotte, Tartarin, IEEE ICNF 2019

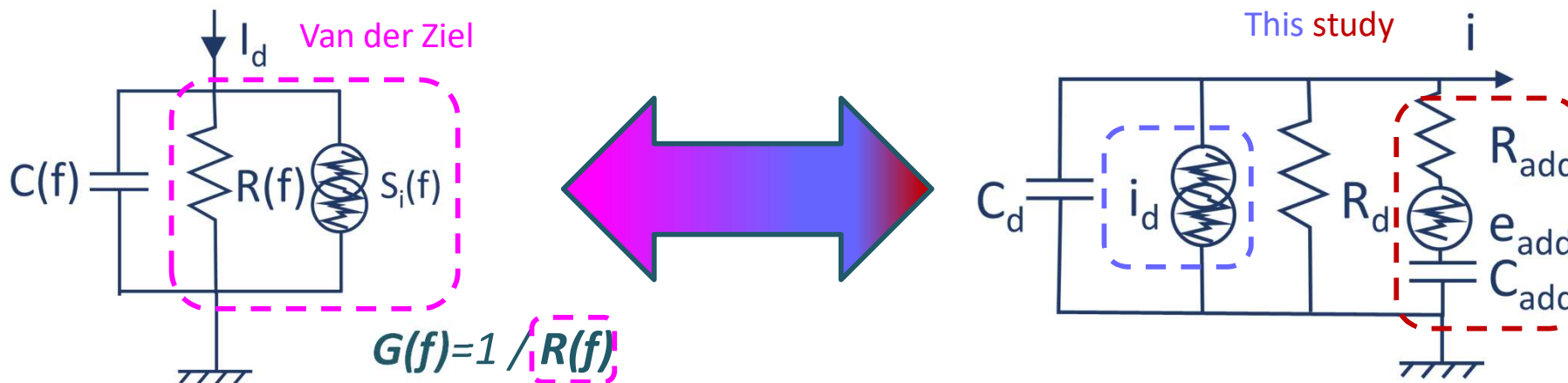
This model is fully compatible with the Van Der Ziel expression

Generalized Van der Ziel's expression

$$S_i(f) = 4 \cdot k \cdot T / R(f) - 2qI_d$$

$R(f)$ stands for the frequency behavior of the $R_d, C_d, R_{add}, C_{add}$ network

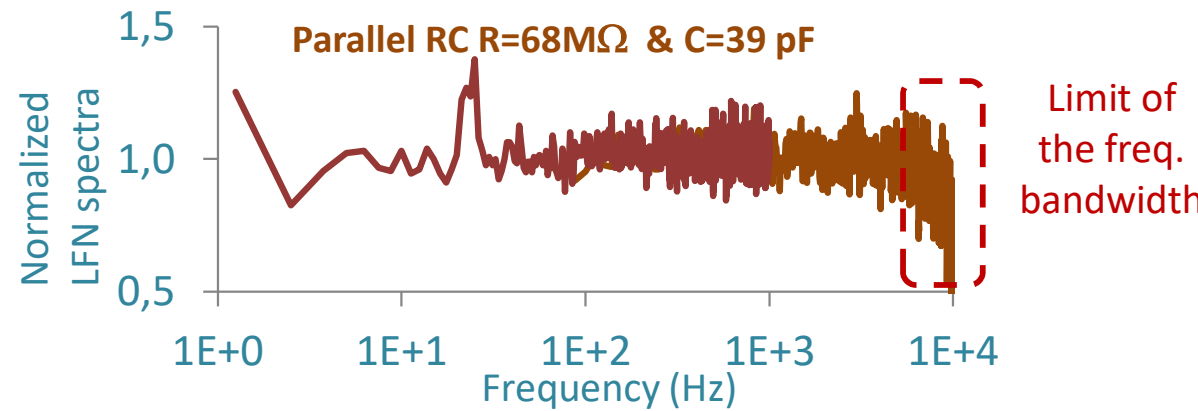
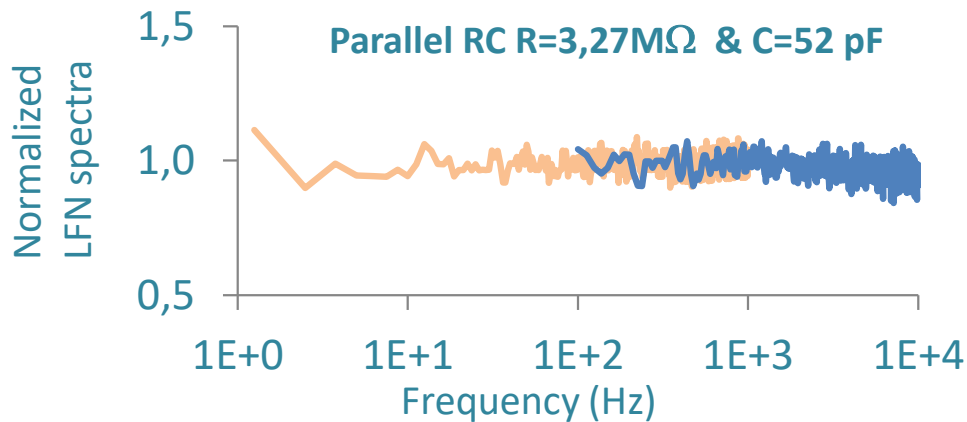
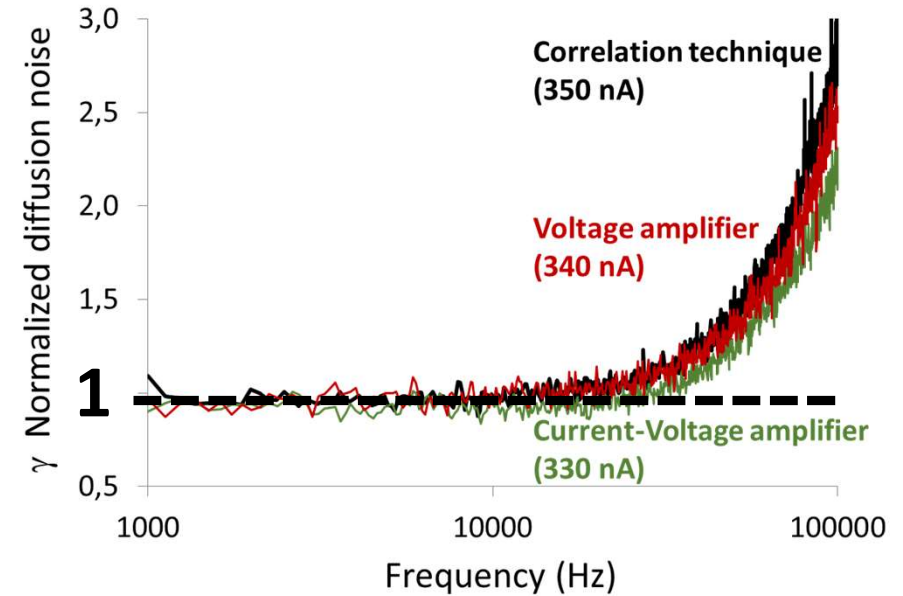
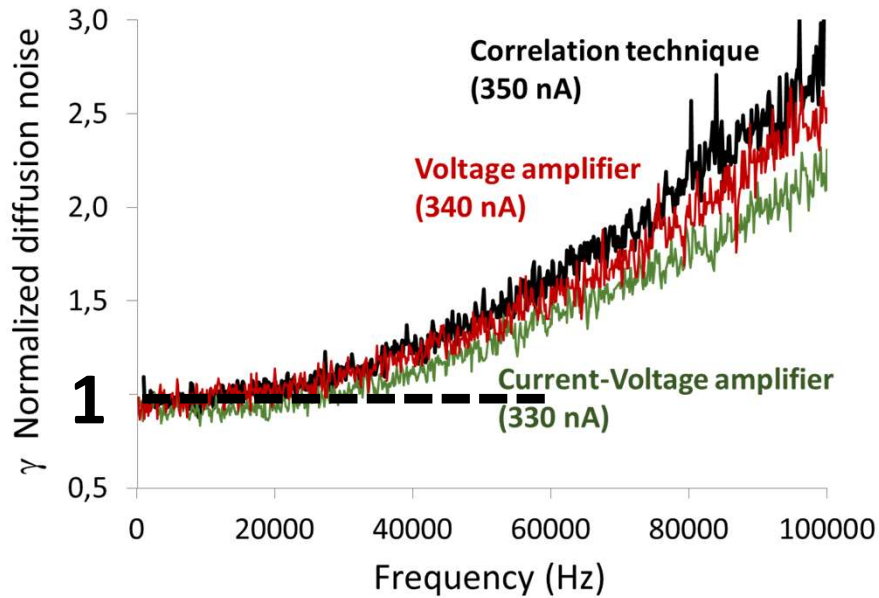
But is not used neither in the CAD soft. (noise models of diodes), nor in the usual models (-it was not necessary to use it till then-) where $S_{id} = 2qI_d$ applies



This model allowed interpretation about such signature: consistent with impedance(freq) spectroscopy with temperature

Ref: Graffeuil, Escotte, Tartarin, IEEE ICNF 2019

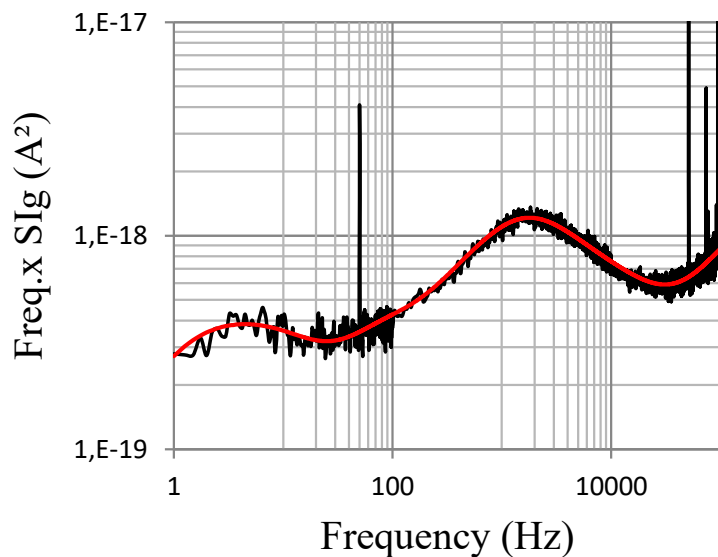
Experimental setups and measurement validation



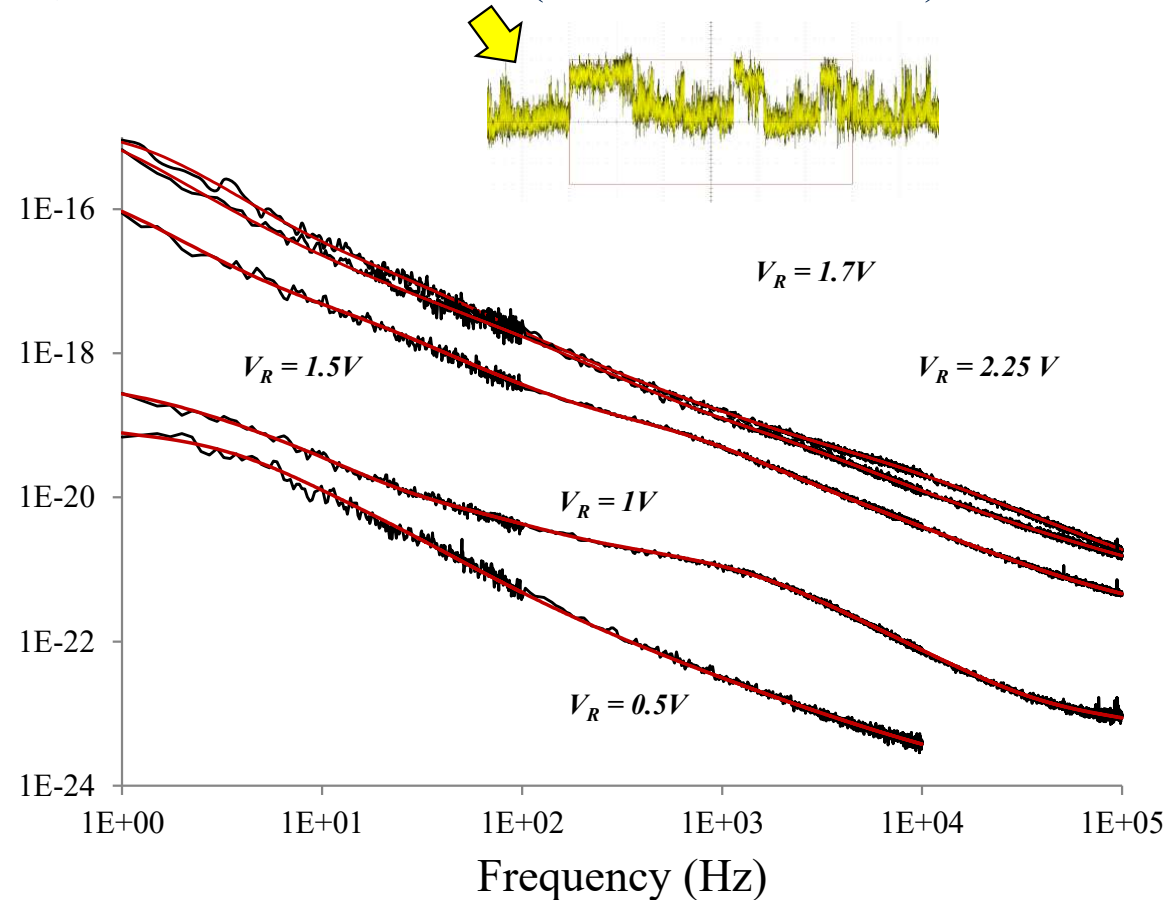
Ref: Graffeuil, Escotte, Tartarin, IEEE ICNF 2019

LFN on gate terminal: the command of the HEMT GaN high frequency transistors

- Gate access : charges distribution under the gated zone affects I_{DS} (and I_{GS})
- Transient and harmonic evaluation of charges , GR centers and RTN (not discussed here).



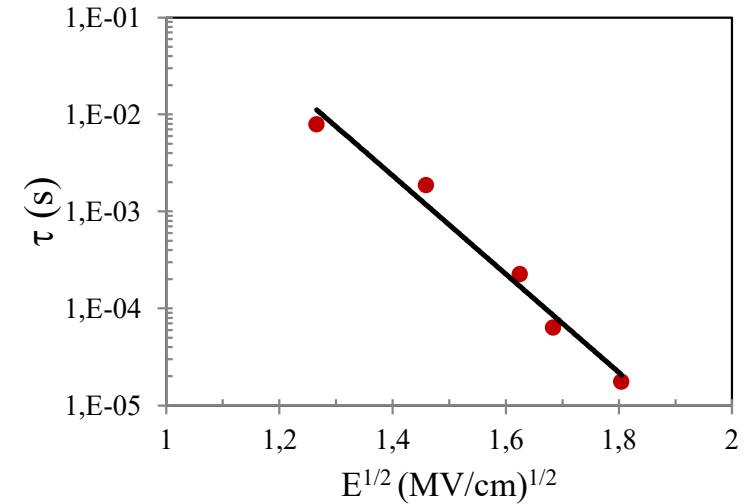
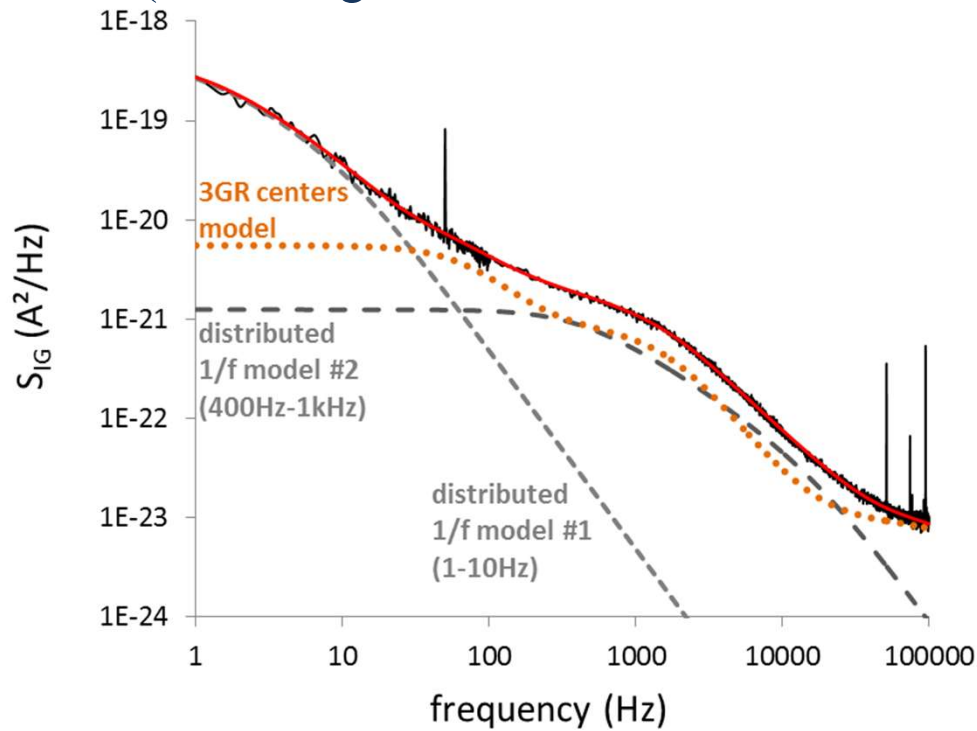
SI_G (A^2/Hz)



Ref: Tartarin, IEEE ICNF 2015

LFN on gate terminal : the command of the HEMT GaN high frequency transistors

- GR centers tracking : identification of bias dependant time constants ranging between 10 μ s and 10 ms (also using C-V measurements to extract E-field)



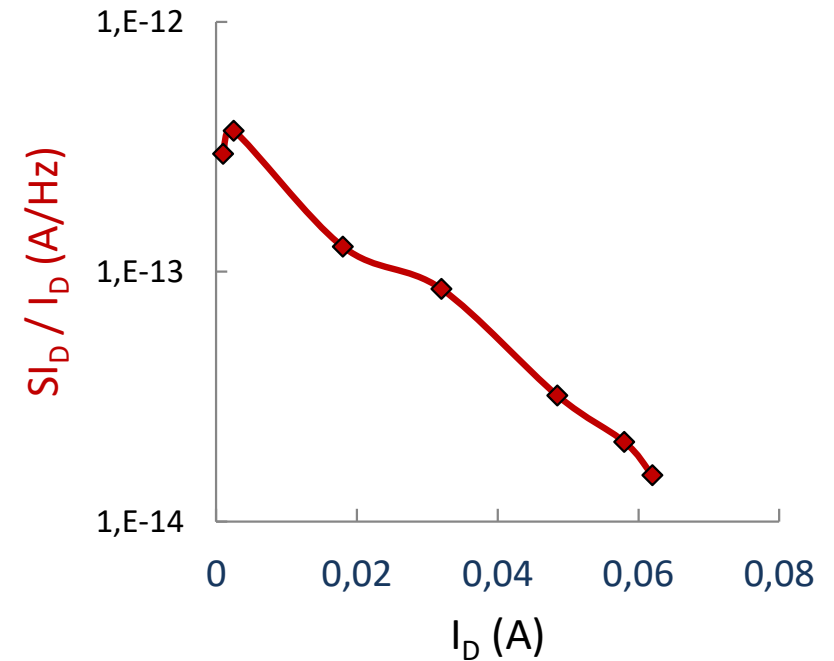
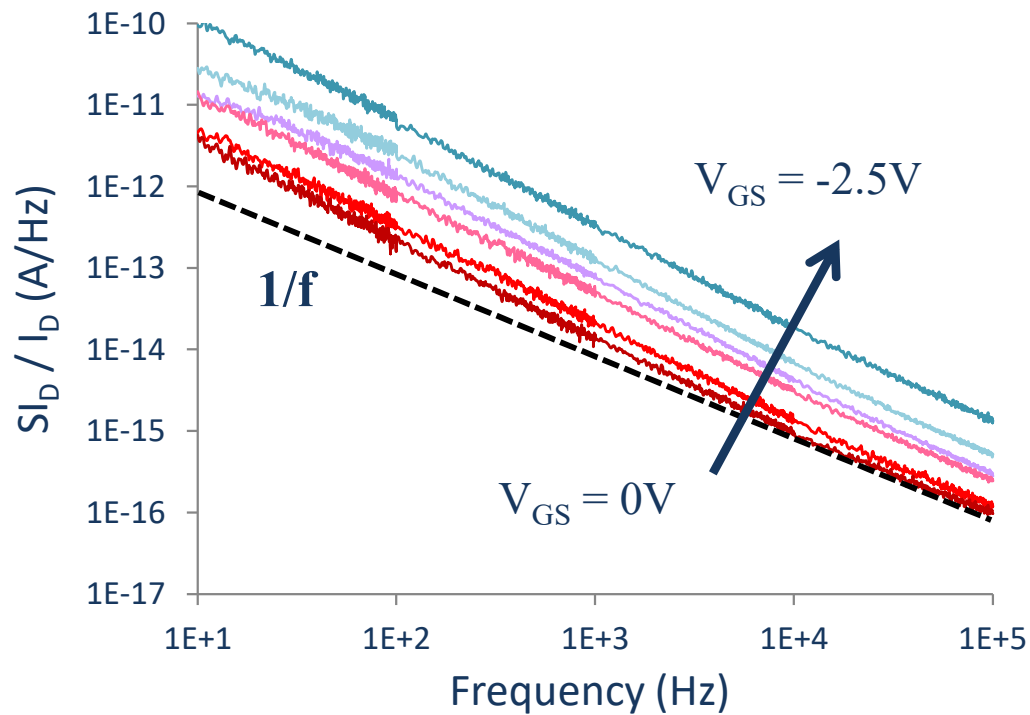
$$\tau(E) = \tau_0 \exp\left(-\frac{1}{kT} \sqrt{q^3 / \pi \epsilon_0 \epsilon_s} * \sqrt{E}\right)$$

Here evidencing Poole-Frenkel effect with \sqrt{E} dependency

$$S_{IG} = \sum_{i=1}^n \frac{A_i \tau_i}{1 + (2\pi f \tau_i)^2} + \sum_{j=1}^m \frac{B_j [\text{Arctg}(2\pi f \tau_{j1}) - \text{Arctg}(2\pi f \tau_{j0})]}{f \ln(\tau_{j1} / \tau_{j0})}$$

LFN on drain terminal: defects in the 2DEG, but is this detrimental to proper functioning?

- S_{ID} vs V_{GS} and V_{DS} also reveals the presence of distributed GR centers : which impact ?

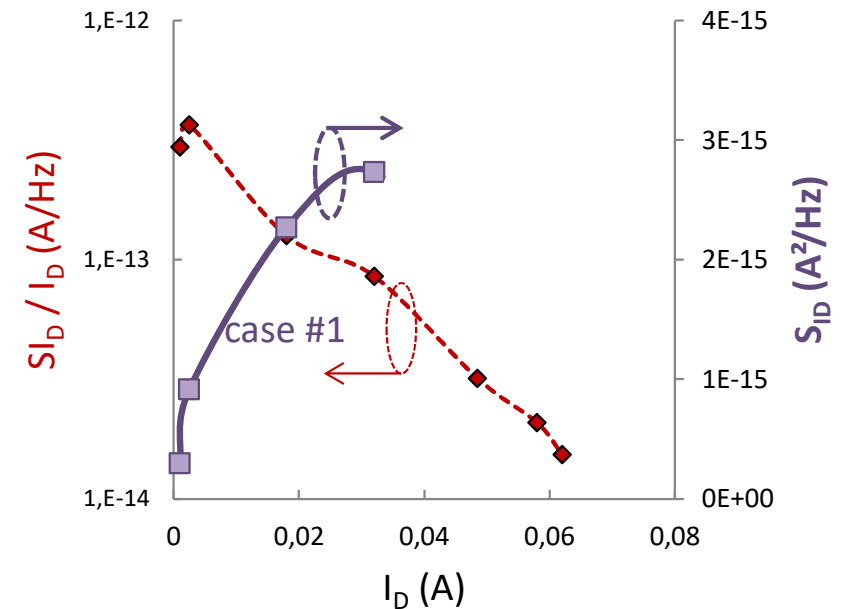
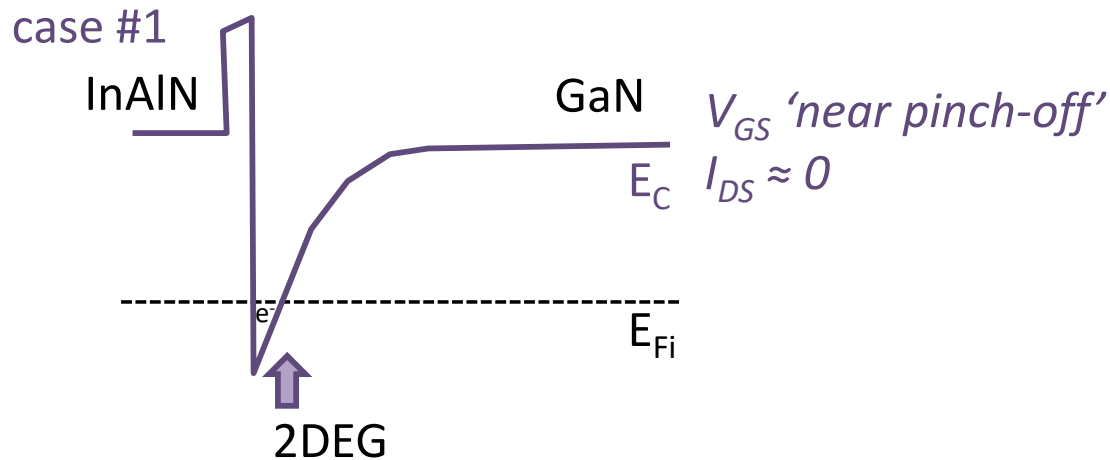


Neither a $1/f$ trend, nor $1/f^\gamma$ frequency dependency

S_{ID}/I_D decreases when I_{DS} increases
 → monotoneous behavior

LFN on drain terminal: defects in the 2DEG, but is this detrimental to proper functioning?

- S_{ID} vs V_{GS} and V_{DS} also reveals the presence of distributed GR centers : which impact ?



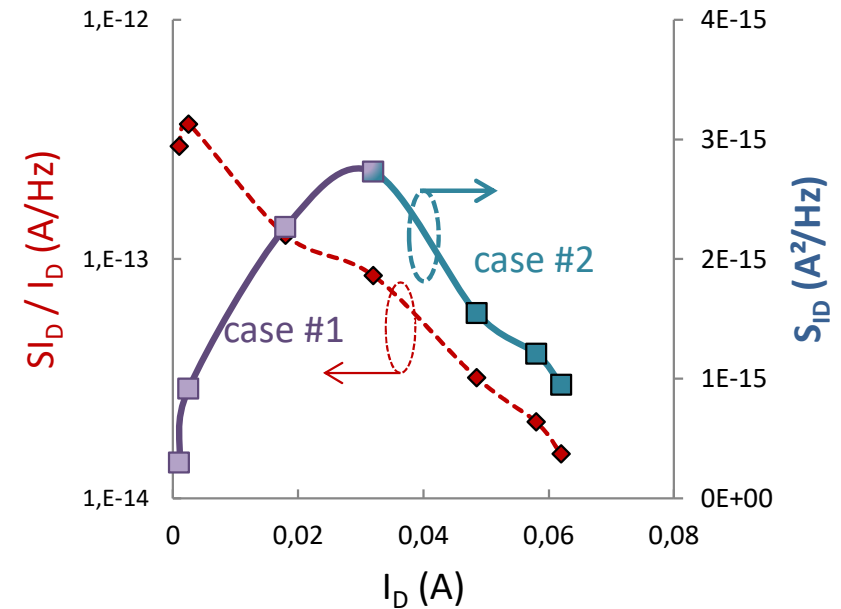
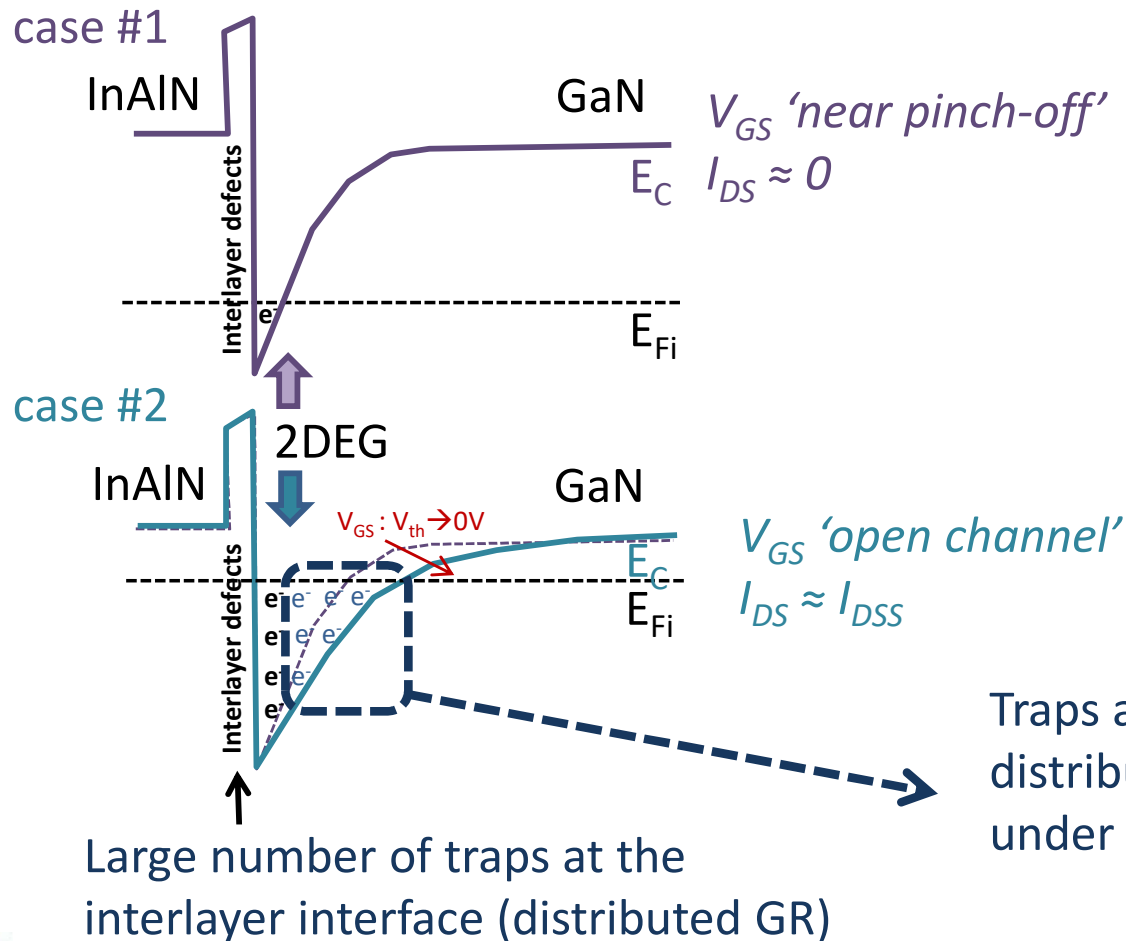
S_{ID} increases when I_{DS} increases

But S_{ID}/I_D decreases (effects of 'defects' on carriers in the 2DEG are less effective !)

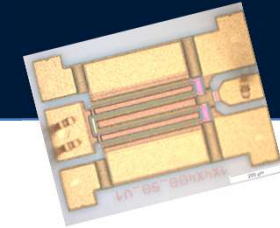
WHY ?

LFN on drain terminal: defects in the 2DEG, but is this detrimental to proper functioning?

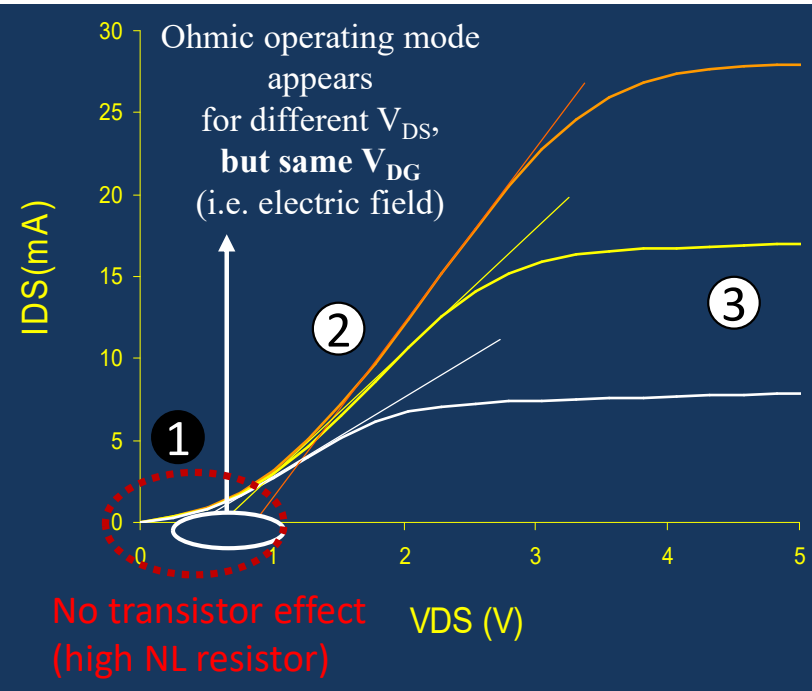
- S_{ID} vs V_{GS} and V_{DS} also reveals the presence of distributed GR centers : which impact ?



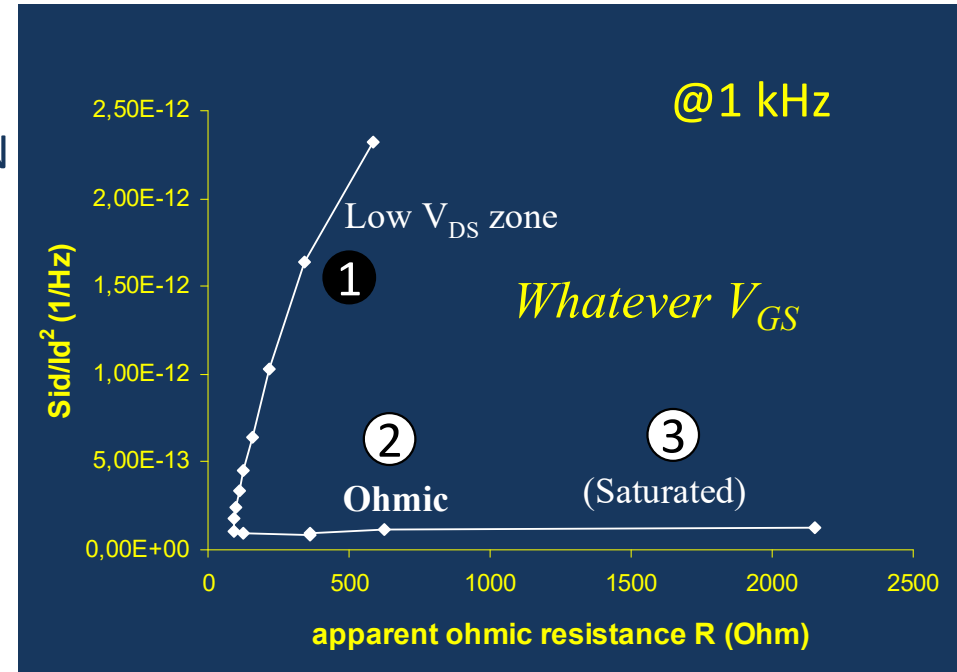
Traps are less sensitive when n_i distribution is more in the 'bulk' of GaN under open channel conditions (case #2)



First generation of GaN HEMTs: Thales Research Technologies

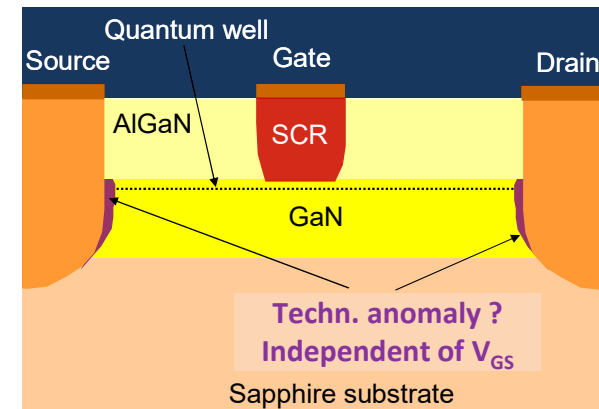


Also strongly noticeable by LFN measurements



Ohmic operating mode appears for different V_{DS} but same V_{DG} (i.e. electric field)

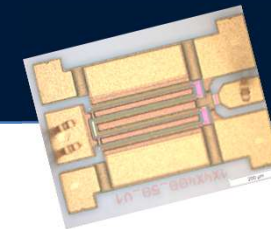
The carriers can't go through this thin layer...



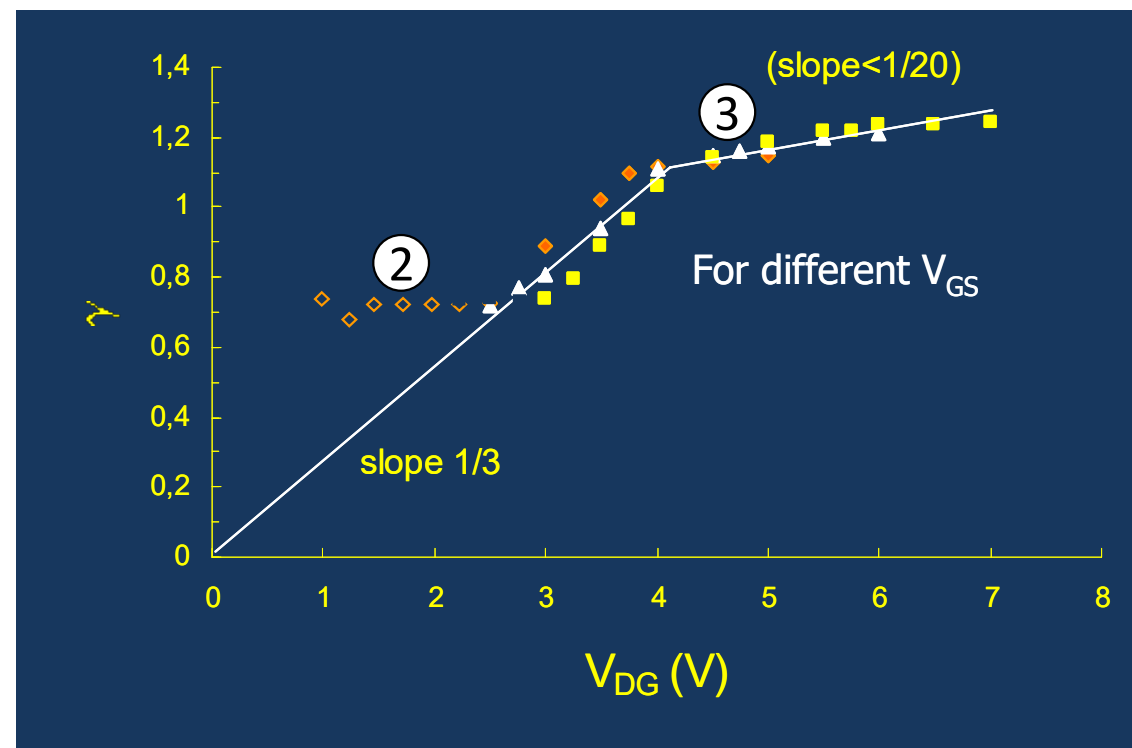
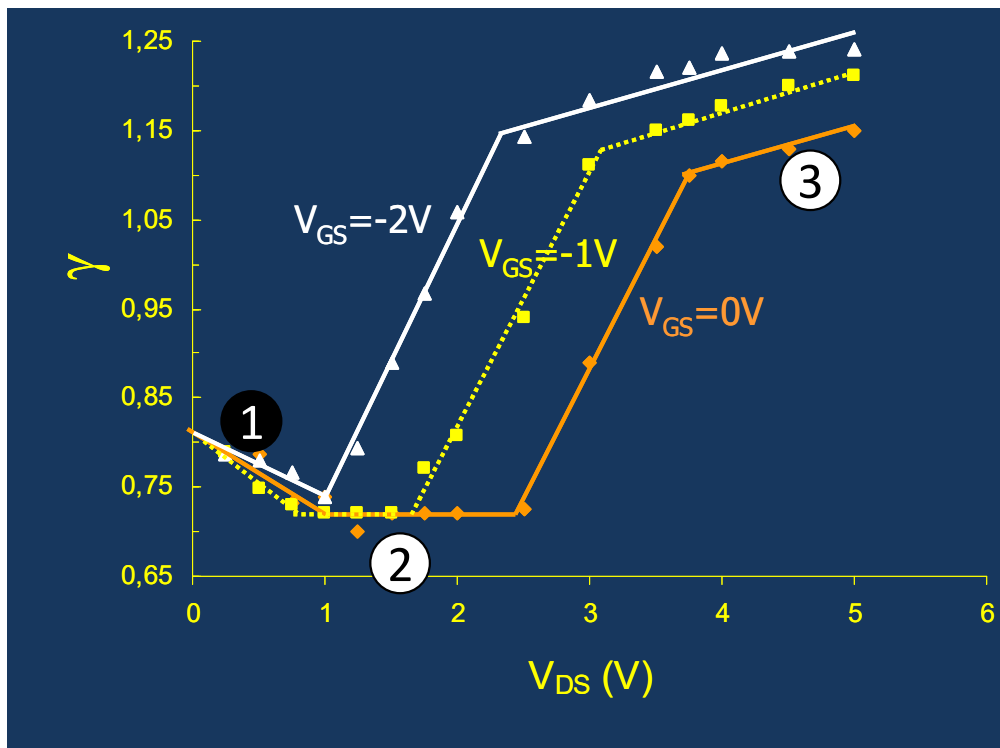
what is their path?

European funding [ESA AO/1-3916/01/NL/CK](#)

Ref: Tartarin, Fluctuation And Noise 2004



First generation of GaN HEMTs: Thales Research Technologies

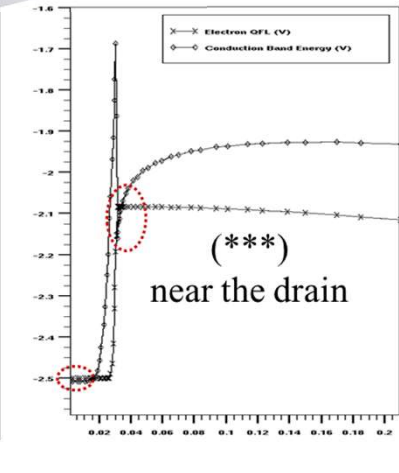
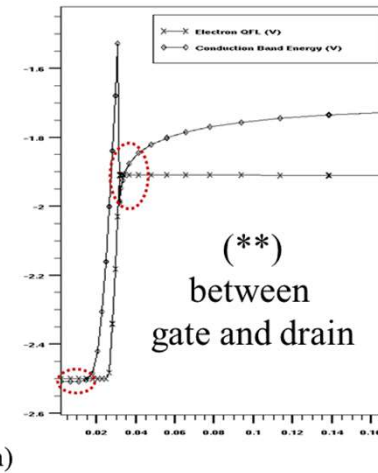
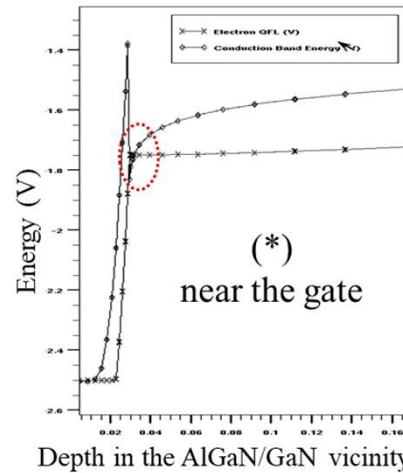
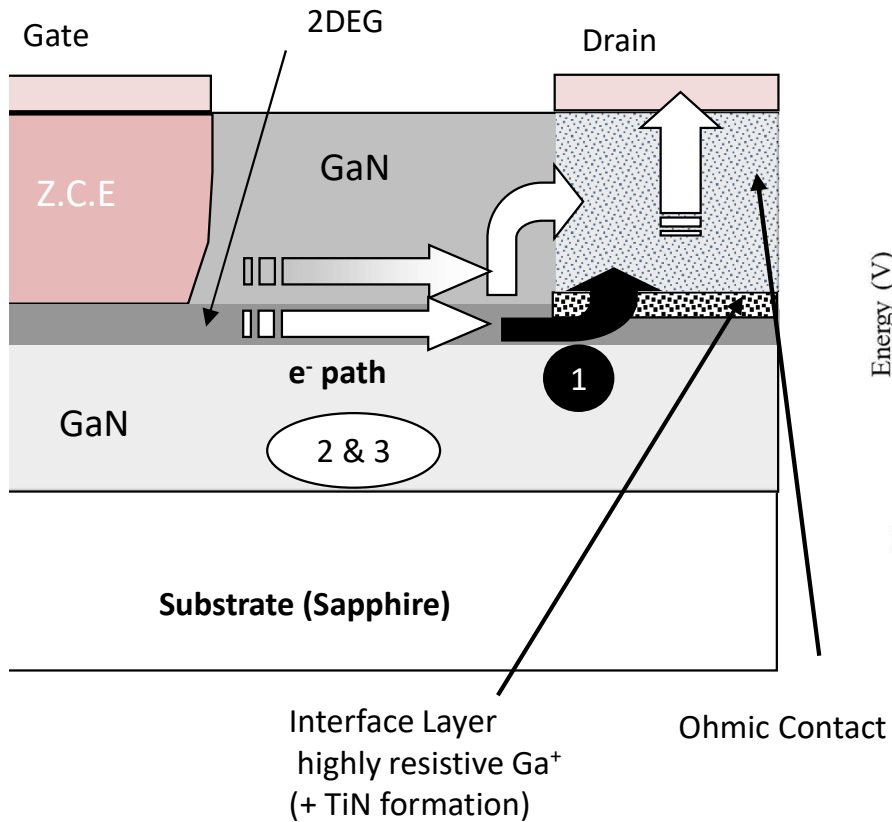


Index factor γ ($1/f^\gamma$) lower than 1 (noticed for the first time)

Study on mechanisms of conduction in parallel layers

European funding ESA AO/1-3916/01/NL/CK

Ref: Tartarin, Fluctuation And Noise 2004



Models developed with TCAD software
 → Process correction

Example for LFN for defect detection and technological development

Also used for HBT (GaInP/GaAs, GaAlAs/GaAs, SiGe, CMOS...), and FET (GaN HEMT)

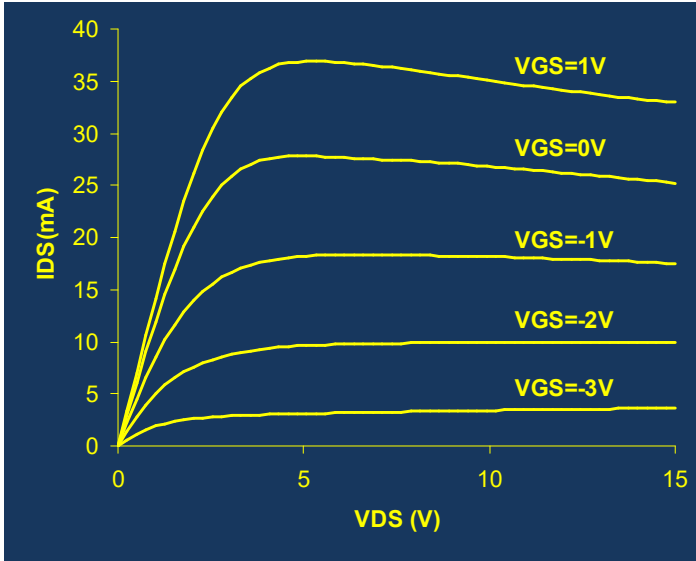
European funding ESA AO/1-3916/01/NL/CK

Ref: Tartarin, Fluctuation And Noise 2004

3 European Programs and 10 National Programs

Cooperations with foundries from the United States, Canada and Taiwan

First generation of GaN HEMTs: Thales Research Technologies

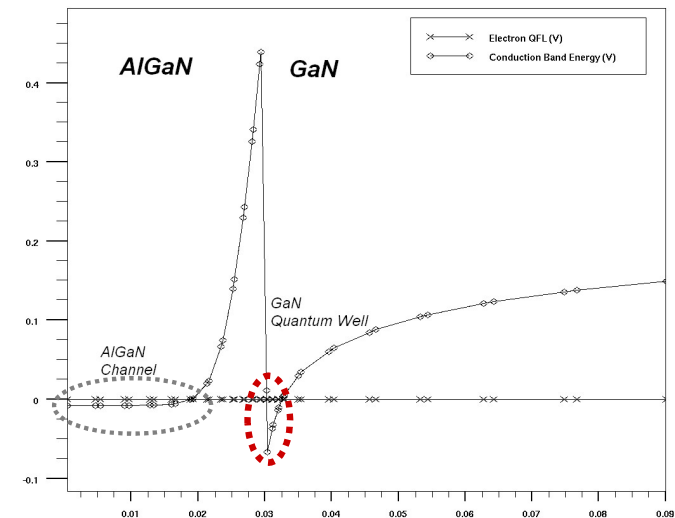
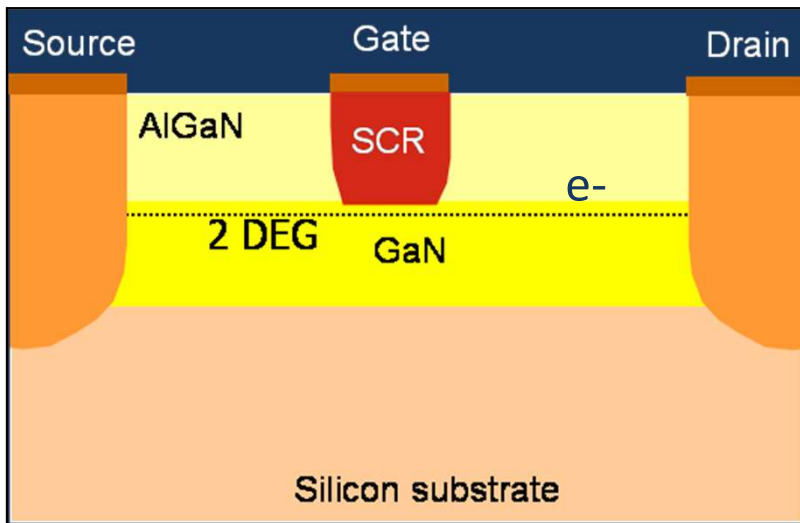
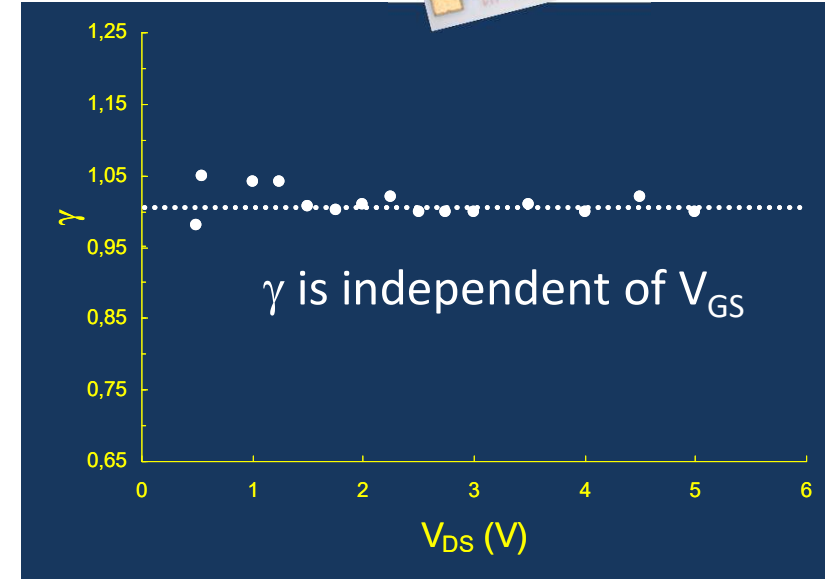


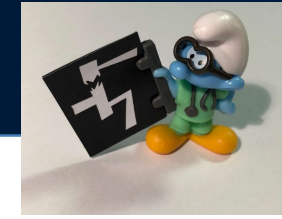
Devices on SiC substrate
LFN $1/f^\gamma$ feat.

$$\gamma = 1$$

Whatever V_{DS} , conduction between gate and drain in the 2DEG GaN

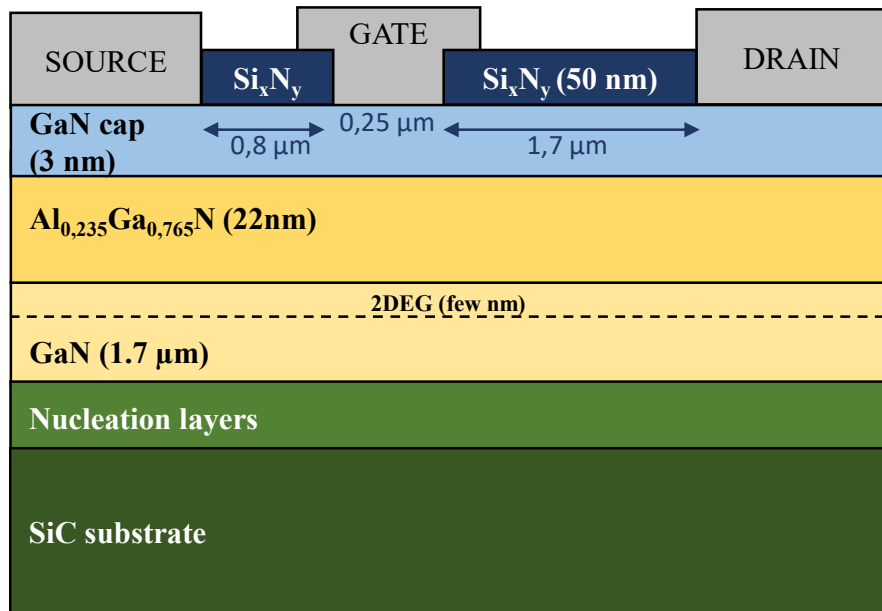
(no parasitic MESFET)





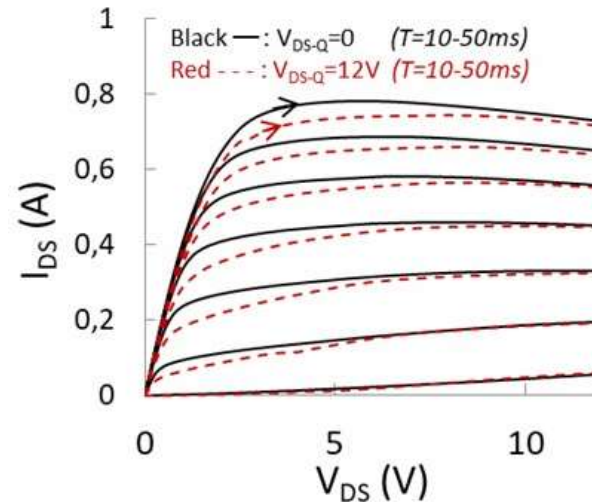
> GaN HEMT structure

→ Process during development phase (Now qualified & commercially available)

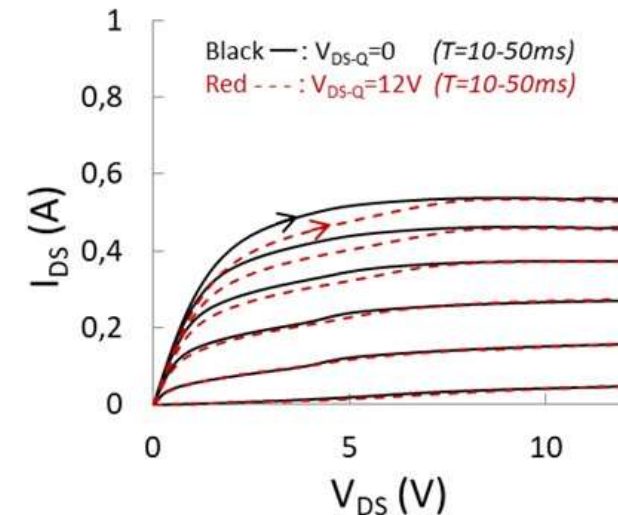


gate lag degrades by $\Delta(GL_{\%})=3\%$

drain lag degrades by $\Delta(DL_{\%})=5\%$ (4% to 12%)



a) Virgin device



b) HTOL stressed device

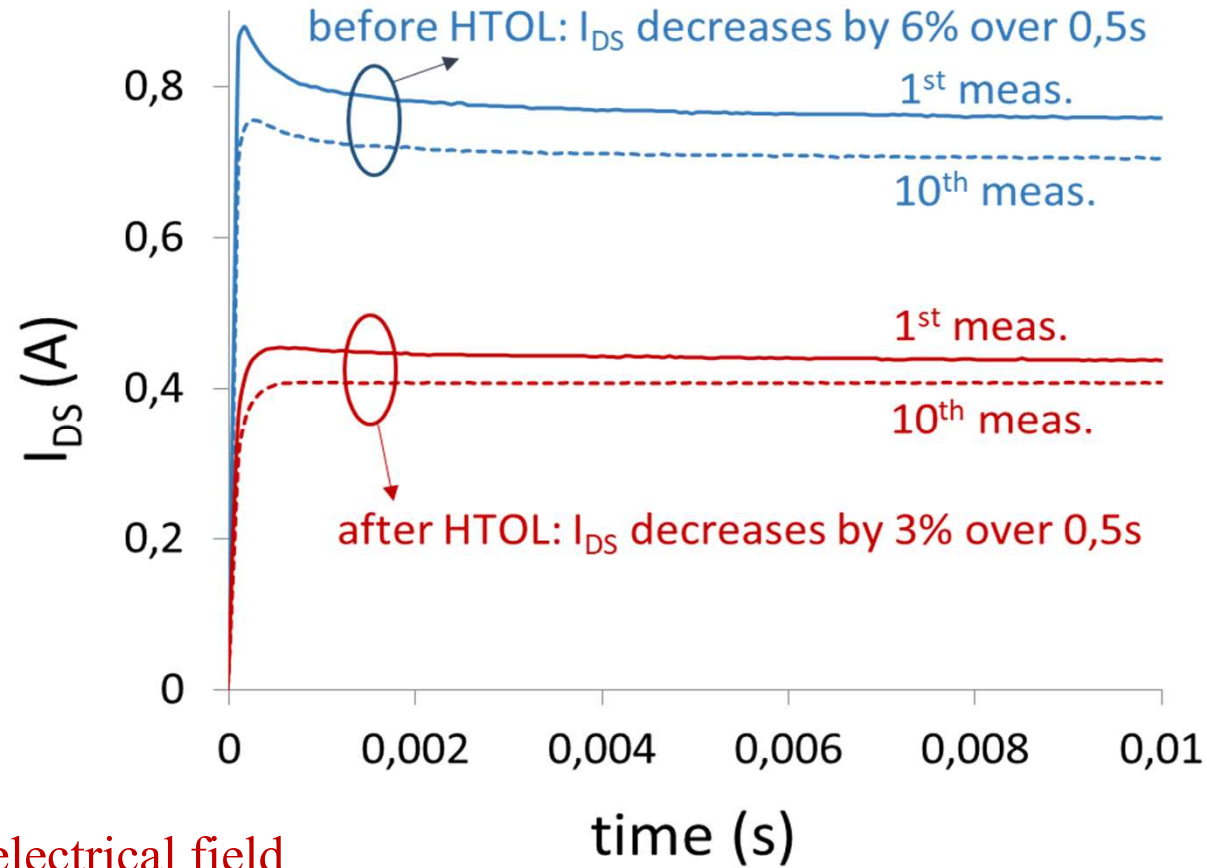
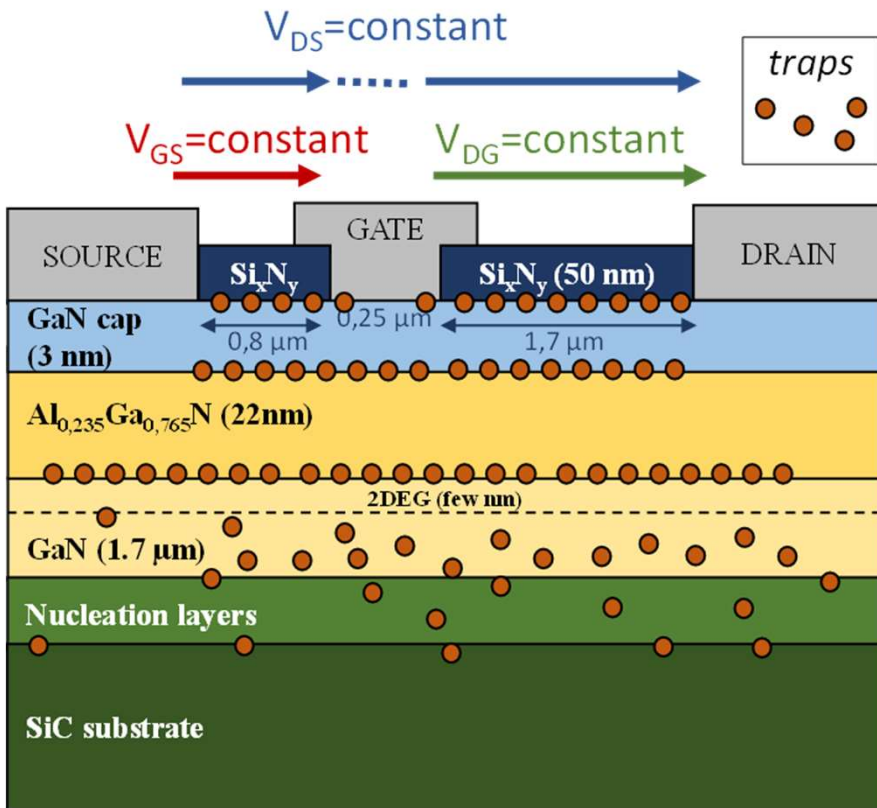
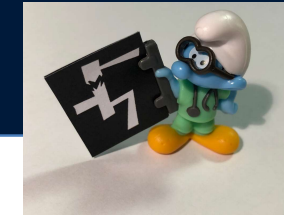
> The devices feature 8 gate fingers of 125 μm width (gate length 0.25 μm) grown on SiC substrate, and with 25% of Al content.

$$GL_{\%} = 100 \times \frac{\Delta I \Delta U(V_{GS-Q} < V_{th} \& V_{DS-Q} = 0V) - \Delta I \Delta U(V_{GS-Q} = 0V \& V_{DS-Q} = 0V)}{\Delta I \Delta U(V_{GS-Q} = 0V \& V_{DS-Q} = 0V)}$$

$$DL_{\%} = 100 \times \frac{\Delta I \Delta U(V_{GS-Q} < V_{th} \& V_{DS-Q} \neq 0V) - \Delta I \Delta U(V_{GS-Q} = 0V \& V_{DS-Q} = 0V)}{\Delta I \Delta U(V_{GS-Q} = 0V \& V_{DS-Q} = 0V)}$$

ANR Funding, French DoD funding

Ref: Tartarin, Elsevier Microelectronics Reliability Volume 114, November 2020



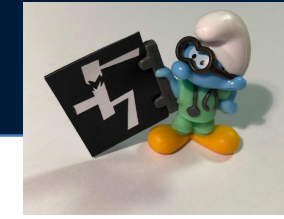
I_{DS} current constant (V_{GS} constant) vs variable electrical field

Drain-source electrical field constant vs variable electron density (V_{GS} variable)

Mixed biasing : constant V_{DS} (variable V_{DG} and V_{GS} – thus I_{DS})

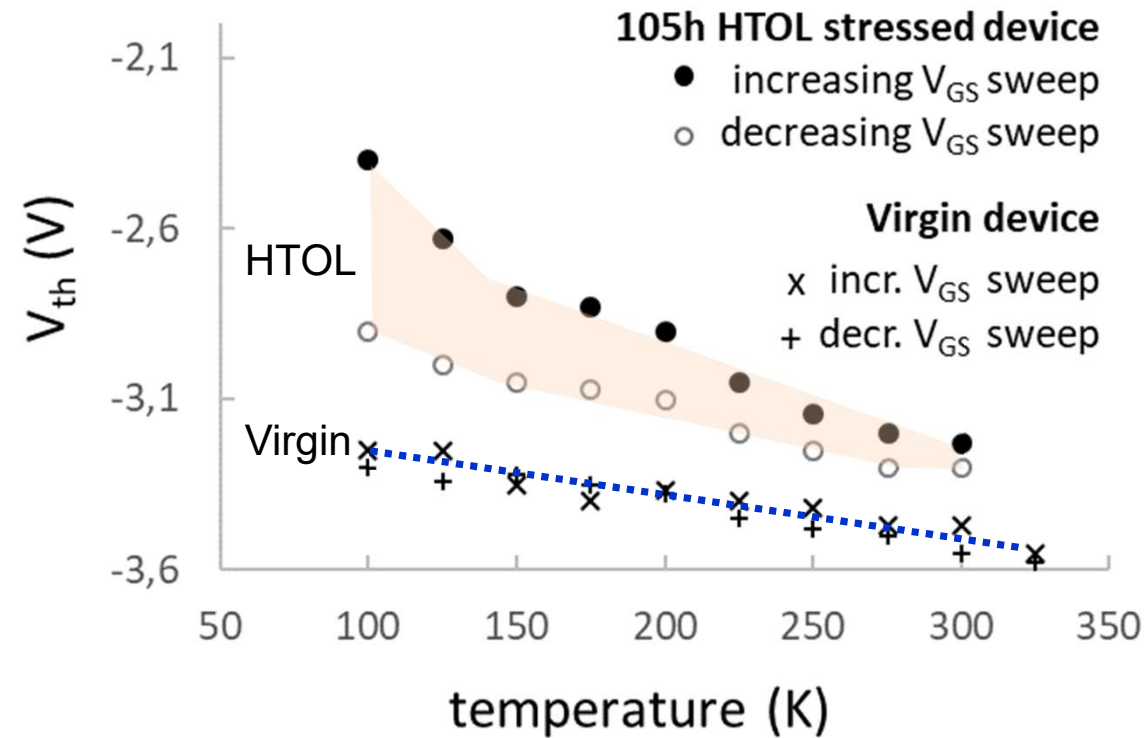
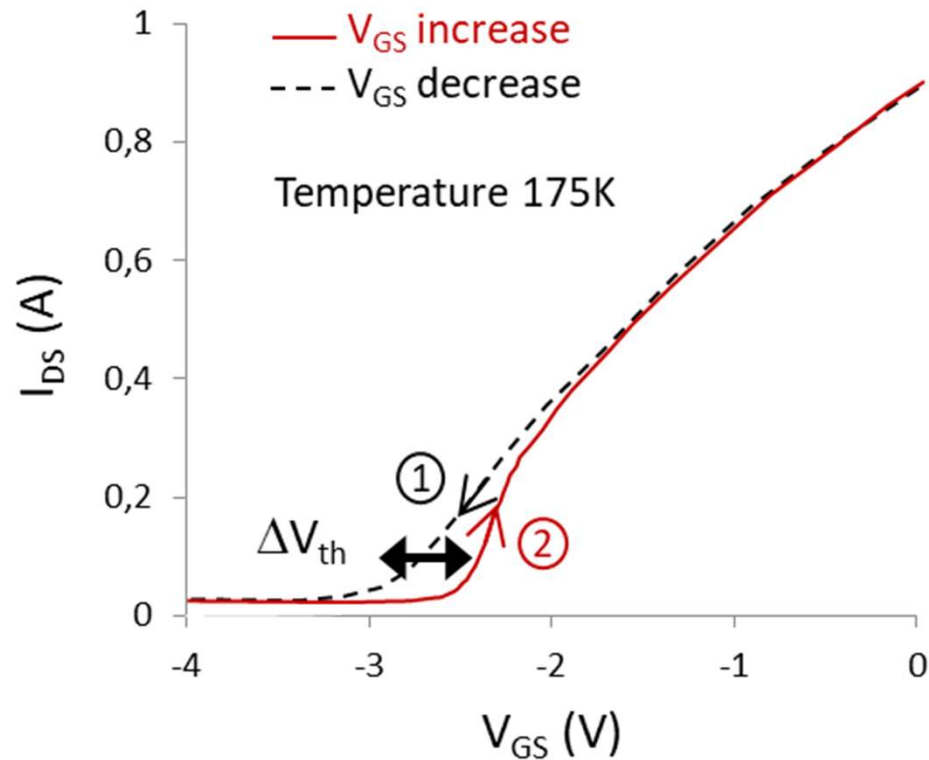
ANR Funding, French DoD funding

Ref: Tartarin, Elsevier Microelectronics Reliability Volume 114, November 2020



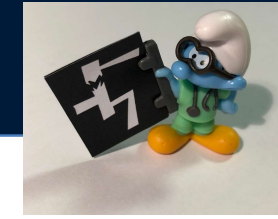
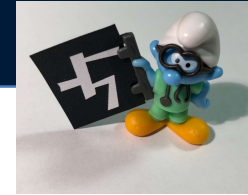
Thermal characterization: V_{th} drift (increasing and decreasing V_{GS} sweeps)

- V_{th} also depends on the sweeping conditions for V_{GS} (increasing/decreasing V_{GS})



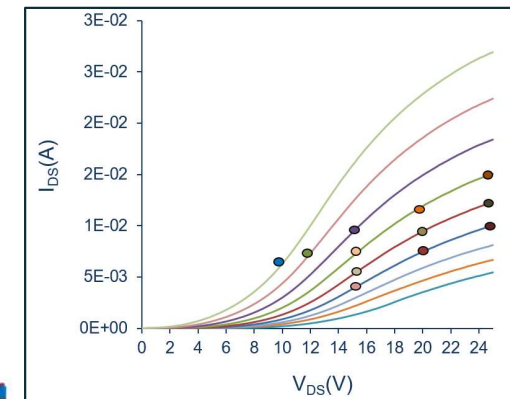
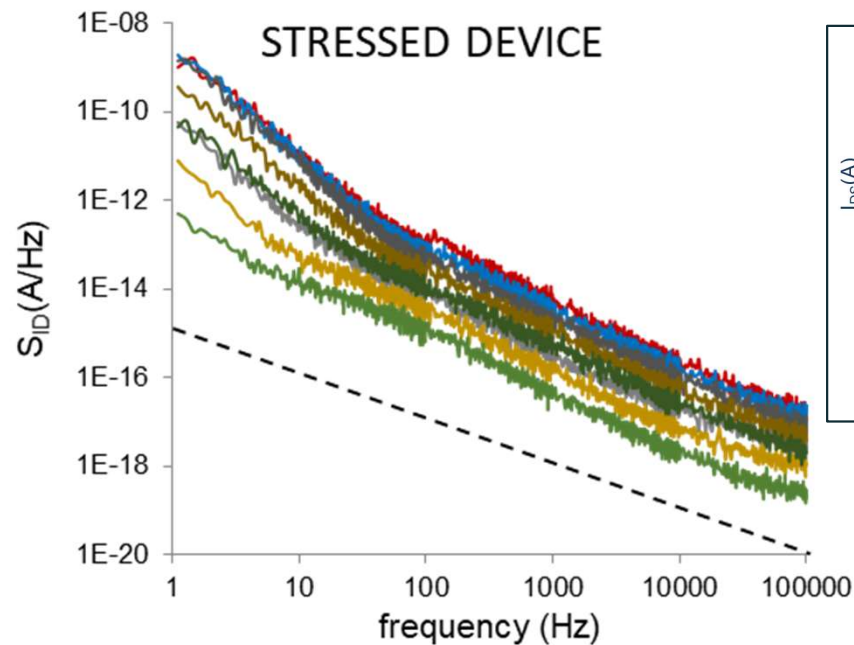
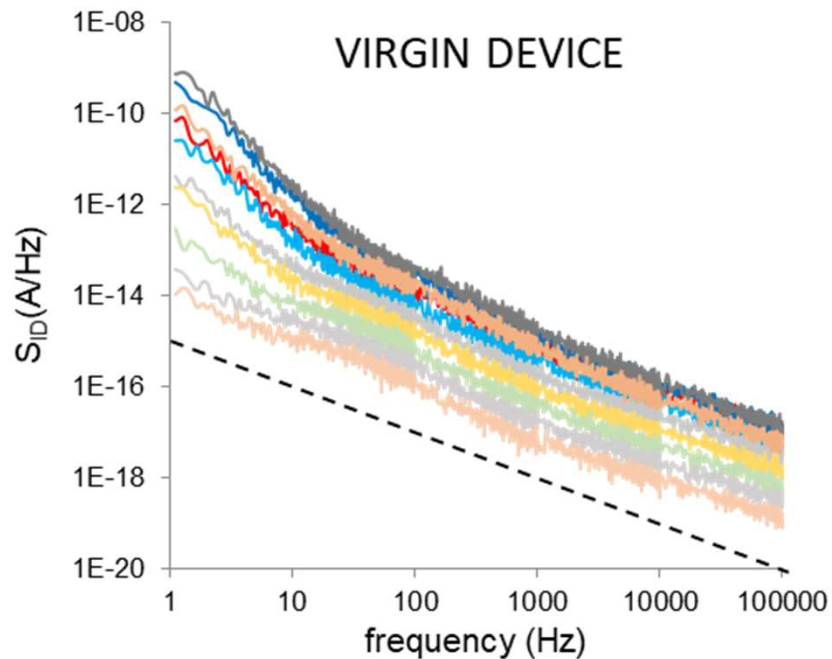
ANR Funding, French DoD funding

Ref: Tartarin, Elsevier Microelectronics Reliability Volume 114, November 2020



Evidence of traps with LFN & RTN characterization (study on PBTI drifts in HEMT GaN devices).

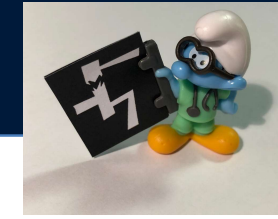
- LFN & RTN characterizations on **Drain** and Gate ports



Presence of traps in the 2DEG but no major influence of the HTOL stress on their evolution

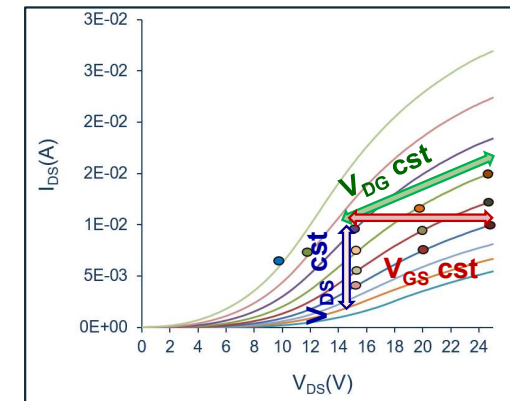
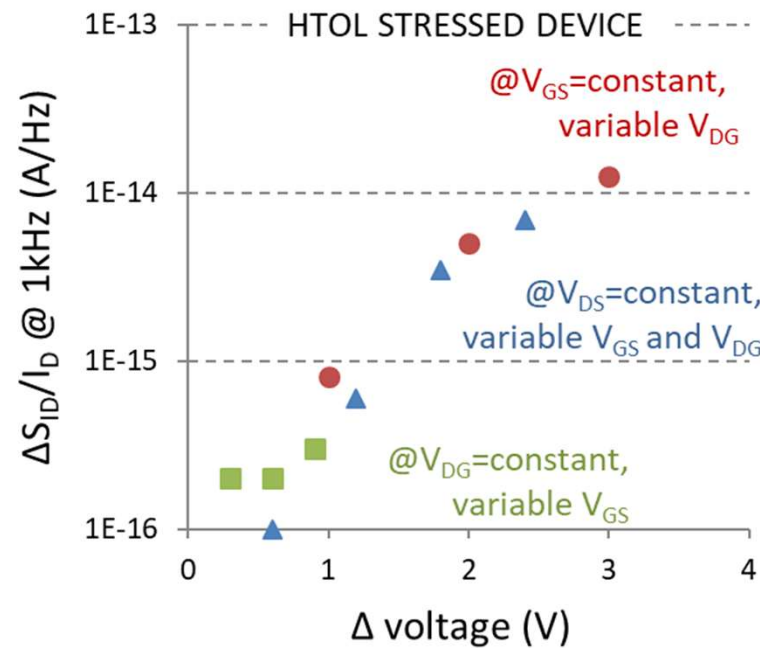
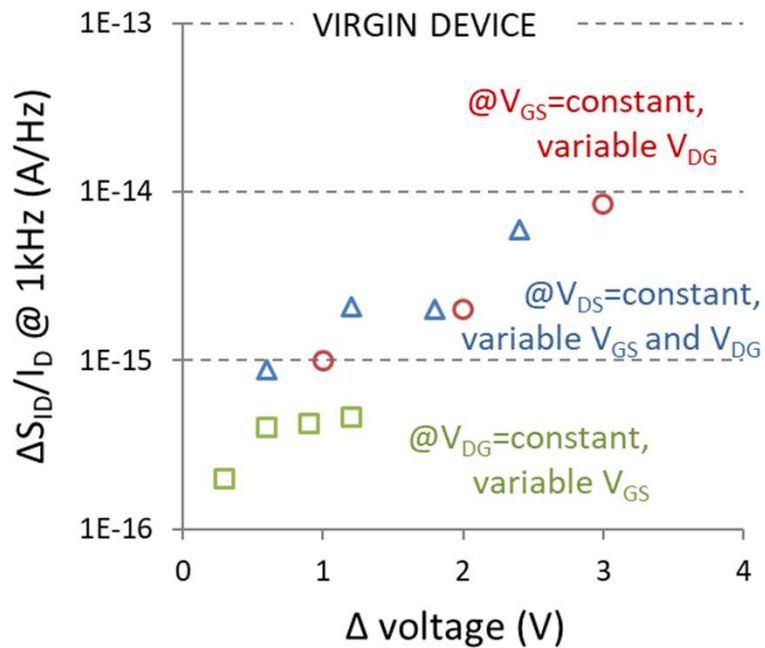
ANR Funding, French DoD funding

Ref: Tartarin, Elsevier Microelectronics Reliability Volume 114, November 2020



Evidence of traps with LFN & RTN characterization (study on PBTI drifts in HEMT GaN devices).

• LFN & RTN characterizations on Drain and Gate ports



Activation of traps (normalized spectral density) in the 2DEG with electrical field distribution **G-D** (& G-S)
 BUT no major difference between VIRGIN & STRESSED devices

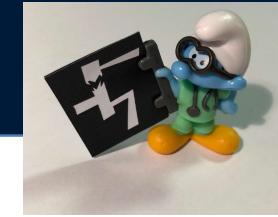
I_{DS} current constant (V_{GS} constant) vs variable electrical field

Drain-source electrical field constant vs variable electron density (V_{GS} variable)

Mixed biasing : constant V_{DS} (variable V_{DG} and V_{GS} – thus I_{DS})

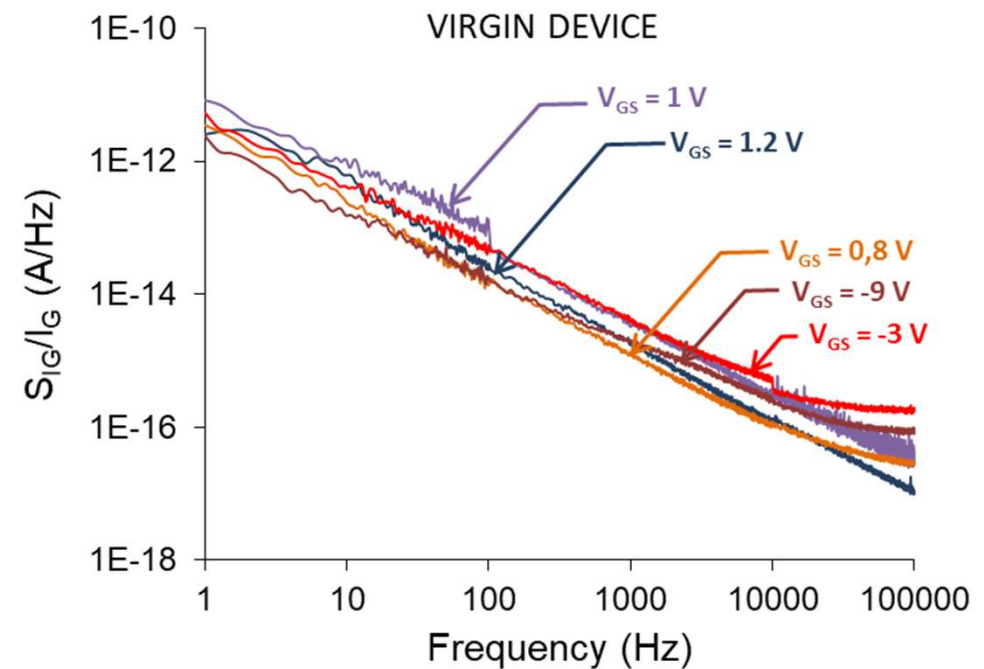
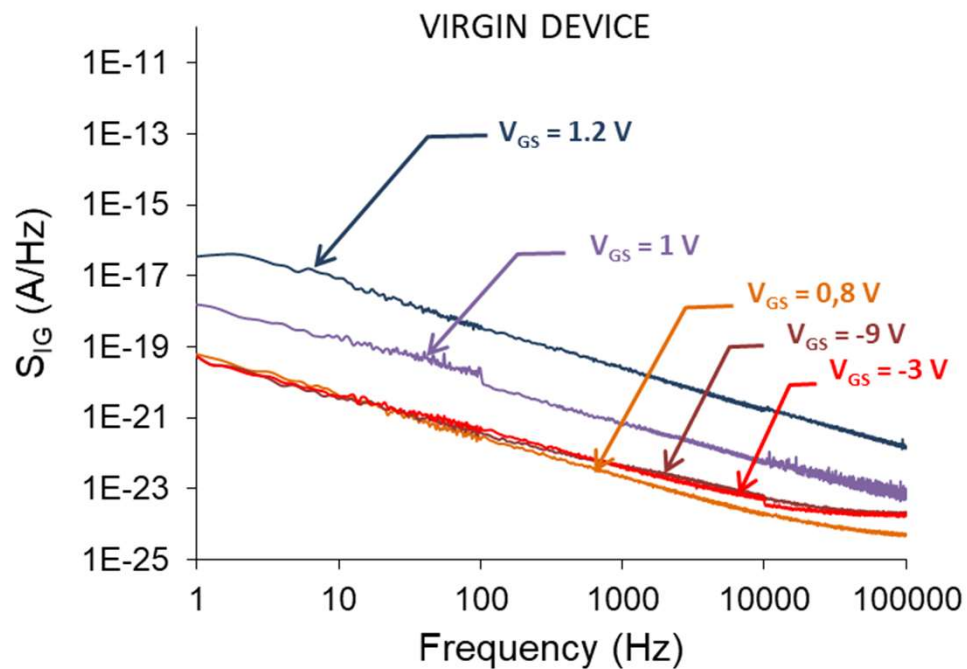
ANR Funding, French DoD funding

Ref: Tartarin, Elsevier Microelectronics Reliability Volume 114, November 2020



Evidence of traps with LFN & RTN characterization (study on PBTI drifts in HEMT GaN devices).

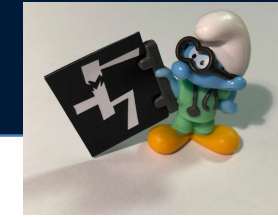
- LFN & RTN characterizations on Drain and **Gate** ports



Normalized S_{IG} LFN spectral density features almost stable signature on VIRGIN devices vs V_{GS}

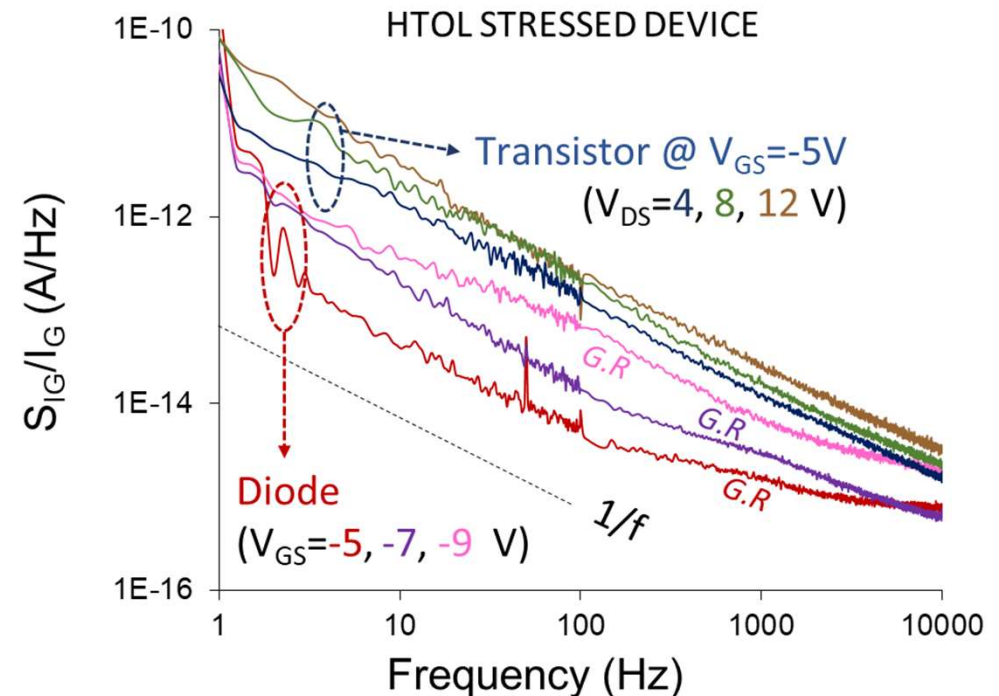
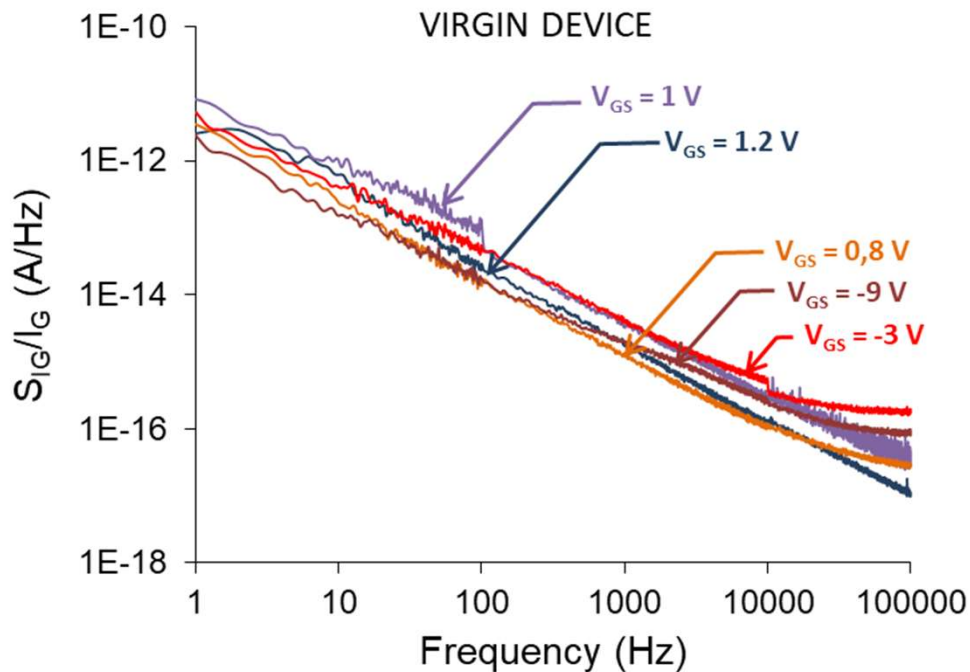
ANR Funding, French DoD funding

Ref: Tartarin, Elsevier Microelectronics Reliability Volume 114, November 2020



Evidence of traps with LFN & RTN characterization (study on PBTI drifts in HEMT GaN devices).

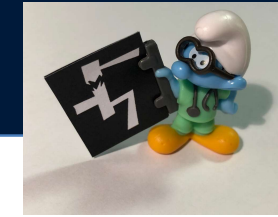
- LFN & RTN characterizations on Drain and **Gate** ports



Normalized S_{IG} LFN spectral density features scattered signature on STRESSED devices vs V_{GS}
Evidence of new traps activated on the G-S path, with various act. mode (diode/transistor)

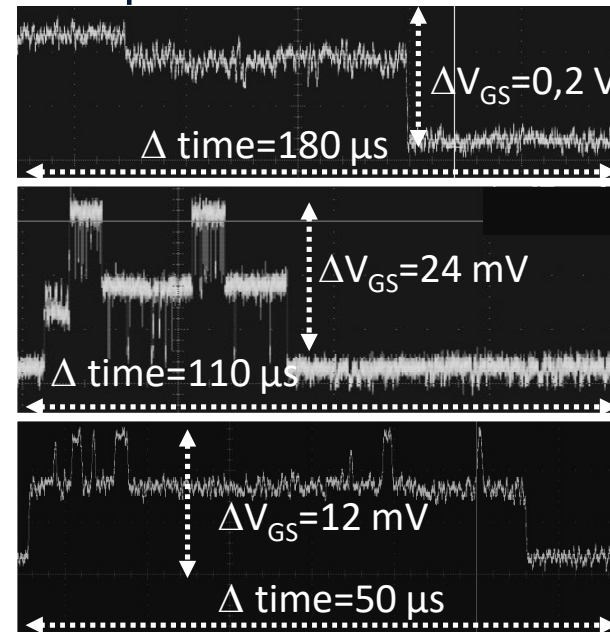
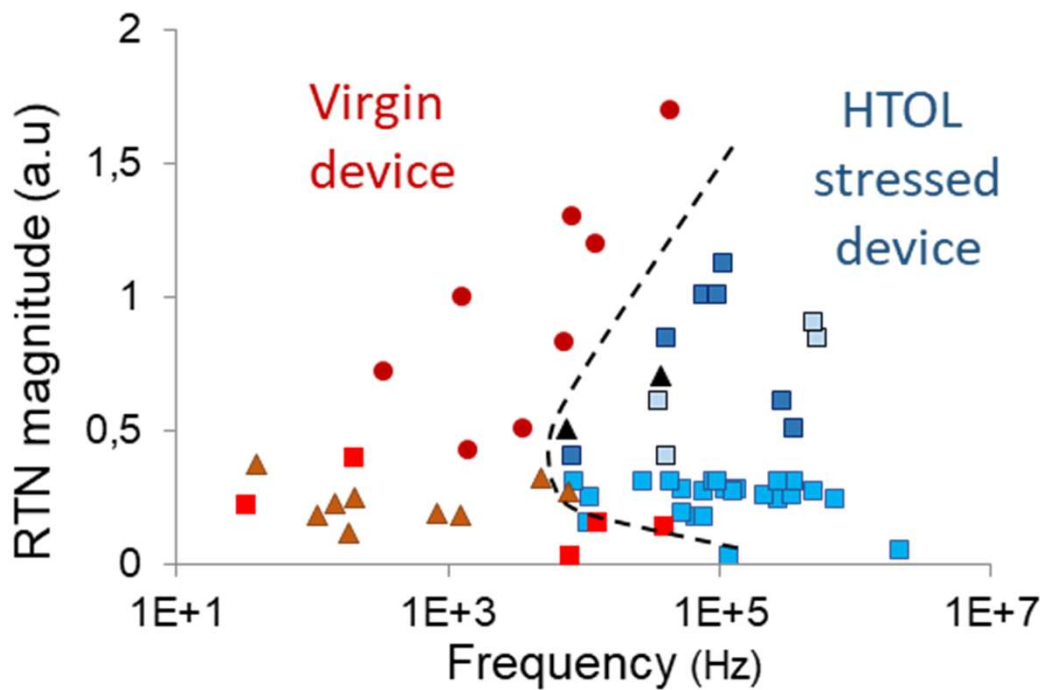
ANR Funding, French DoD funding

Ref: Tartarin, Elsevier Microelectronics Reliability Volume 114, November 2020



Evidence of traps with LFN & RTN characterization (study on PBTI drifts in HEMT GaN devices).

- LFN & RTN characterizations on Drain and **Gate** ports



Trap energy

$$\frac{\langle \tau_c \rangle}{\langle \tau_e \rangle} = g \exp\left(\frac{E_T - E_F}{kT}\right)$$

Corner frequency (time constant)

$$\frac{1}{\bar{\tau}} = \frac{1}{\bar{\tau}_e} + \frac{1}{\bar{\tau}_c}$$



$$S(f) = \frac{2(\Delta I)^2 \bar{\tau}}{4 + (2\pi f \bar{\tau})^2}$$

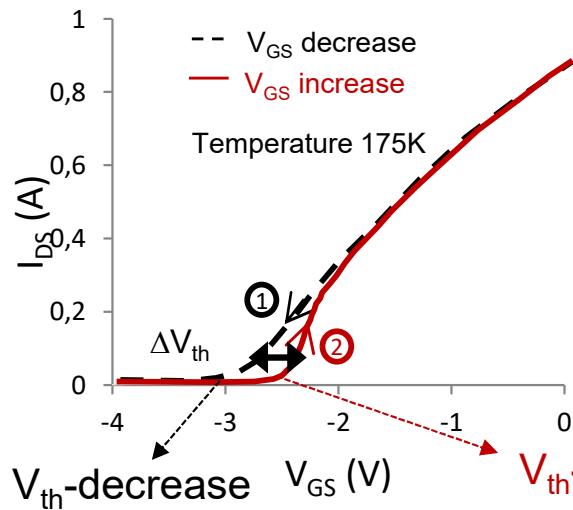
RTN time constants (noise corner frequency) delimitation between VIRGIN and STRESSED devices

ANR Funding, French DoD funding

Ref: Tartarin, Elsevier Microelectronics Reliability Volume 114, November 2020



Evidence of traps with LFN & RTN characterization (study on PBTI drifts in HEMT GaN devices.)



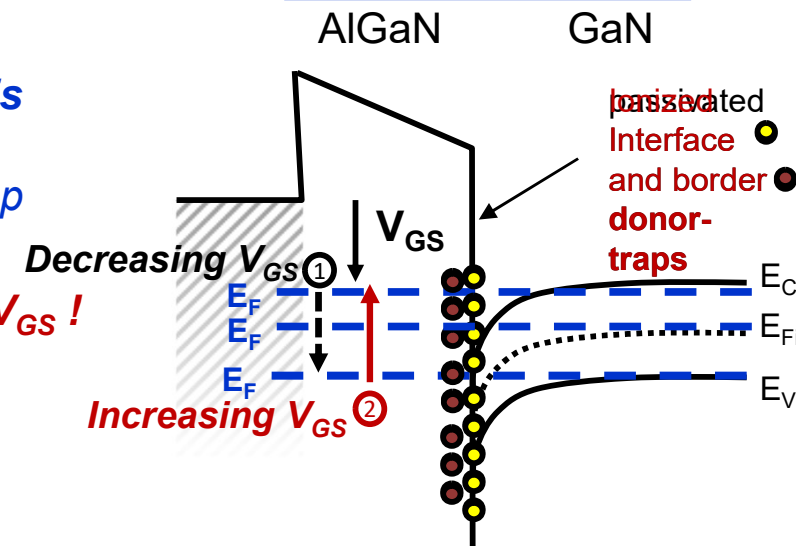
① donor-traps are passivated at positive V_{GS}

Decreasing V_{GS} from +3V to -6V:
Donor remain passivated till the 2DEG is fully depleted
 → $V_{th-decr.}$ is not modified during V_{GS} sweep (so $n_{i-decr.}$ in the 2DEG)

Donor becomes ionized under reverse V_{GS} !

@ reverse V_{GS} , donors are ionized

$\Delta V_{th} = 0,1V @ 200 K$
 $\Delta V_{th} = 0,5 @ 100 K$



② donor-traps are ionized at very negative V_{GS}

Increasing V_{GS} from -6V to +3V:

Donor are ionized (N_D^+) at very low V_{GS} . These positive charges act as an internal generator which field is opposite to the applied voltage V_{GS} , and $V_{th-incr.} > V_{th-decr.}$ (thus $n_{i-incr.} < n_{i-decr.}$), till $V_{th-incr.}$. When the 2DEG starts to conduct electrons, **ionized donor-traps recombine with electrons from the 2DEG (few electrons that do not change n_i), and **become passivated**. The internal generator disappears and V_{th} changes to a lower value as for the decreasing sweep)**

ANR Funding, French DoD funding

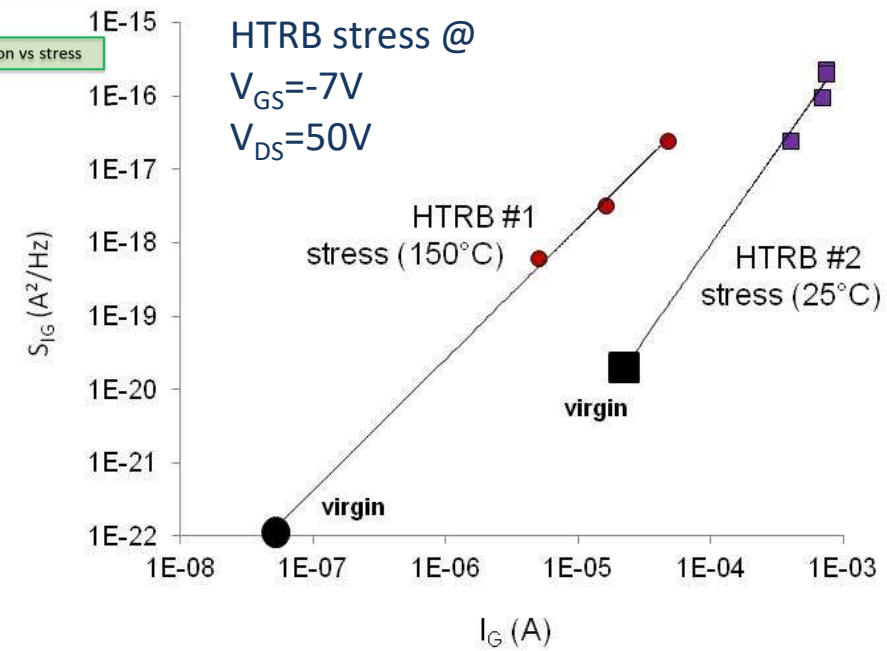
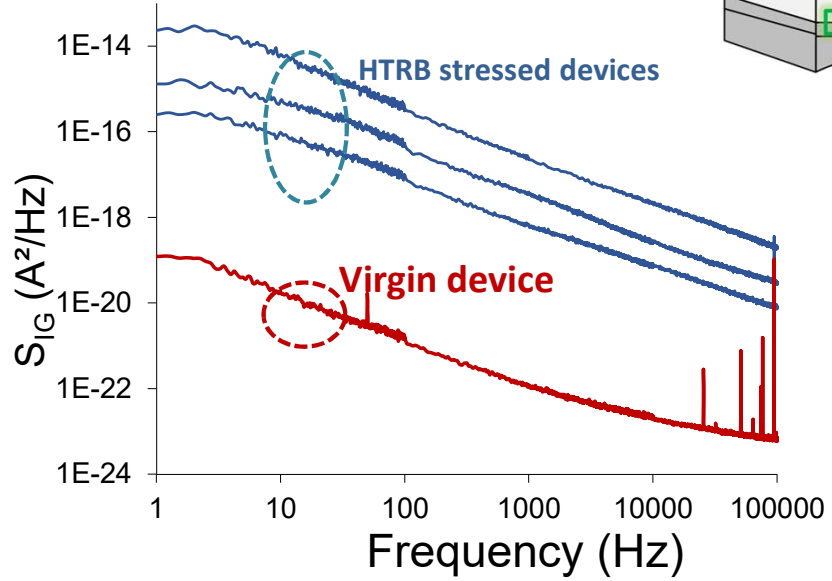
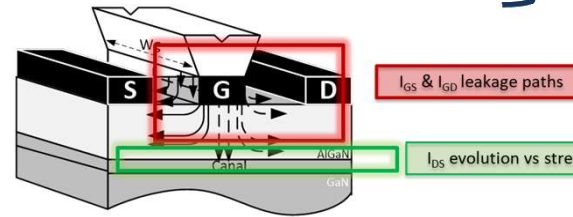
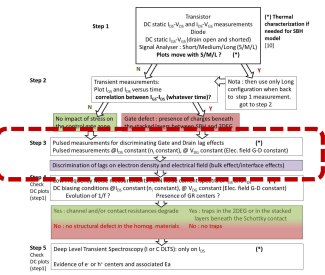
Ref: Tartarin, Elsevier Microelectronics Reliability Volume 114, November 2020

▶ CASE STUDY: AlGaN/GaN GH50 & GH25-10 (UMS) under HTRB stresses

noise spectroscopy

-diode alone
-transistor mode

Ref : Tartarin et al. IEEE ICNF 2017

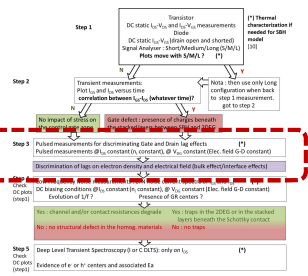


Leakage current as marker of failure events ! S_{ig} also gives a finest signature of carrier's path/interactions in the control zone and lateral/vertical leakage zones

ANR Funding, French DoD funding

Ref: Int. Conference on Noise and Fluctuation (ICNF) 2011, Toronto, invited paper

▶ CASE STUDY: AlGaIn/GaN GH50 & GH25-10 (UMS) under HTRB stresses

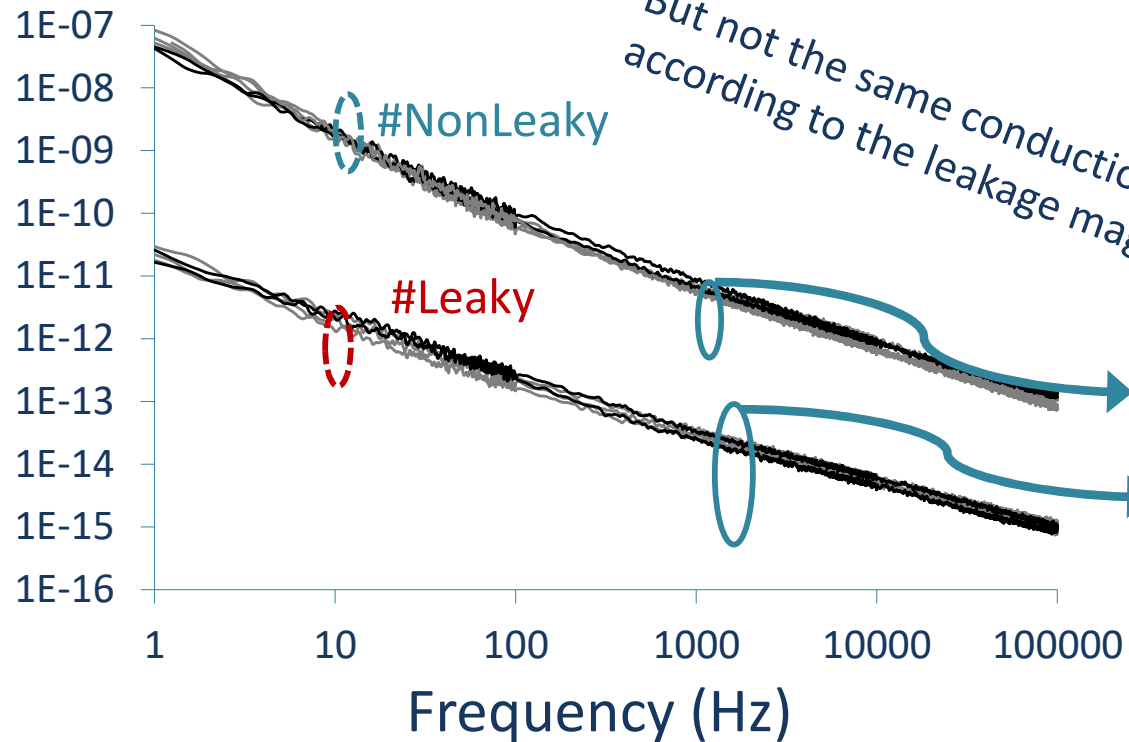


noise spectroscopy

-diode alone
-transistor mode

Ref : Tartarin et al. IEEE ICNF 2017

$$S_{IG}/I_G^x \text{ (A}^{2-x}\text{/Hz)}$$



▶ LFN

(#Leaky and #NonLeaky)

dim. 0,5x4x400 μ m²

-diode alone

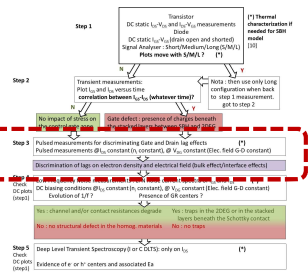
-transistor (saturated) mode

i.e. same leakage mechanisms, same defects in **Transistor and Diode** biasing mode

ANR Funding, French DoD funding

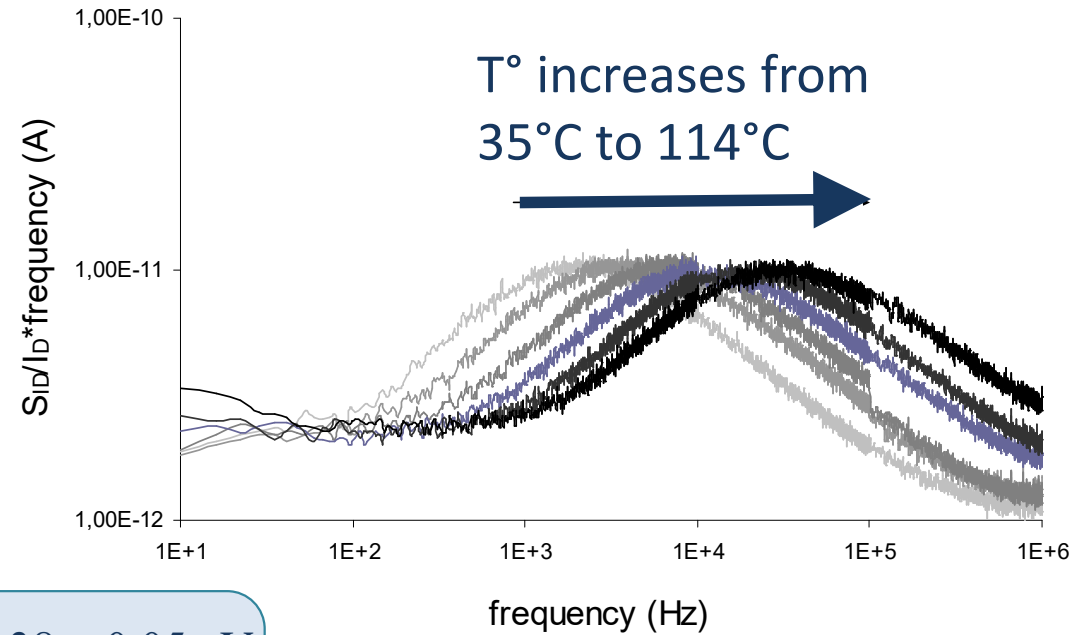
Ref: Tartarin, invited paper IEEE ICNF 2010

▶ CASE STUDY: AlGaIn/GaN GH50 & GH25-10 (UMS) under HTRB stresses



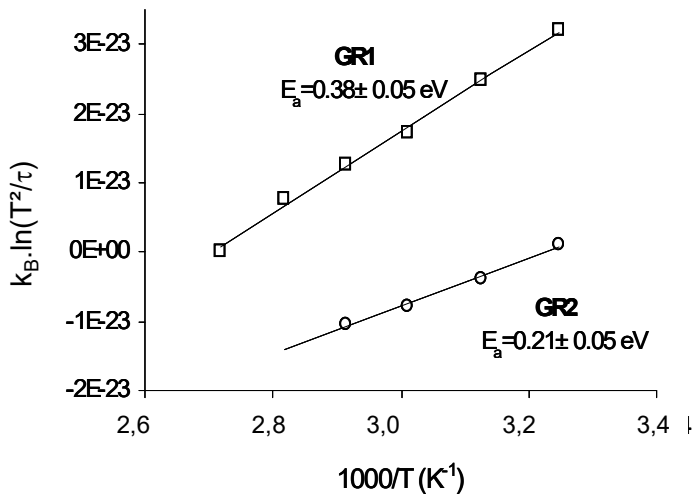
noise spectroscopy GR centers evolution vs temperature (saturated zone)

- ▶ The magnitude of $S_{ID} \times \text{frequency}$ is constant
- ▶ Extraction of GR_1 and GR_2 from each GR 'bulge' (T°)
- ▶ Extraction of E_A from Arrhenius plots



$$E_{A1} = 0.38 \pm 0.05 \text{ eV}$$

$$E_{A2} = 0.21 \pm 0.05 \text{ eV}$$



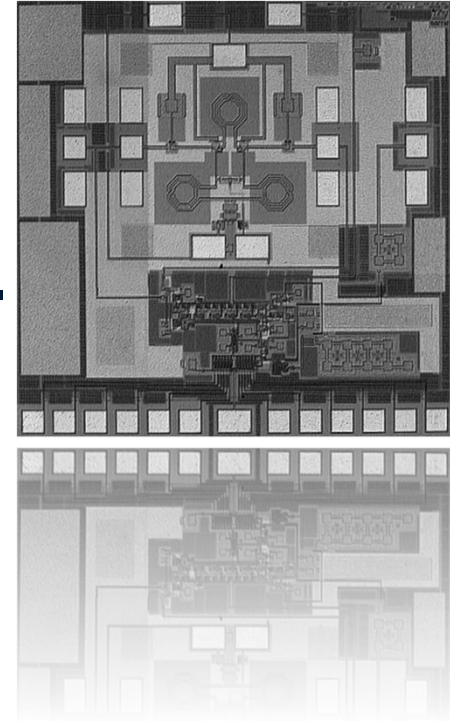
ANR Funding, French DoD funding

Ref: Int. Conference on Noise and Fluctuation (ICNF) 2011, Toronto, invited paper

Ref: Soubercaze IEEE MTTs 2006

- Emerging Technologies / Defect detection & Reliability Analysis

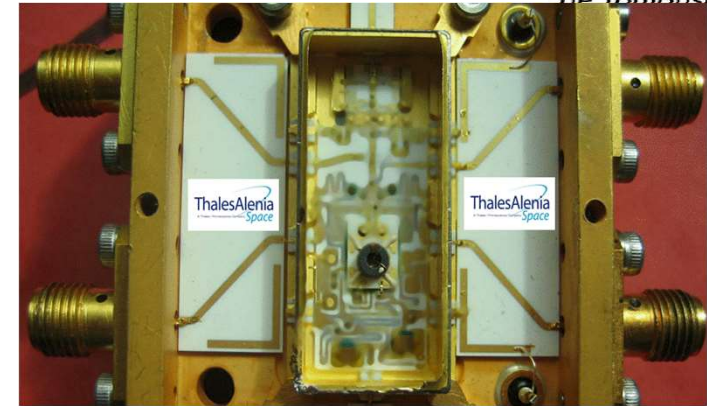
- **LFN for non-linear RF circuit design (VCOs, Mixers).**



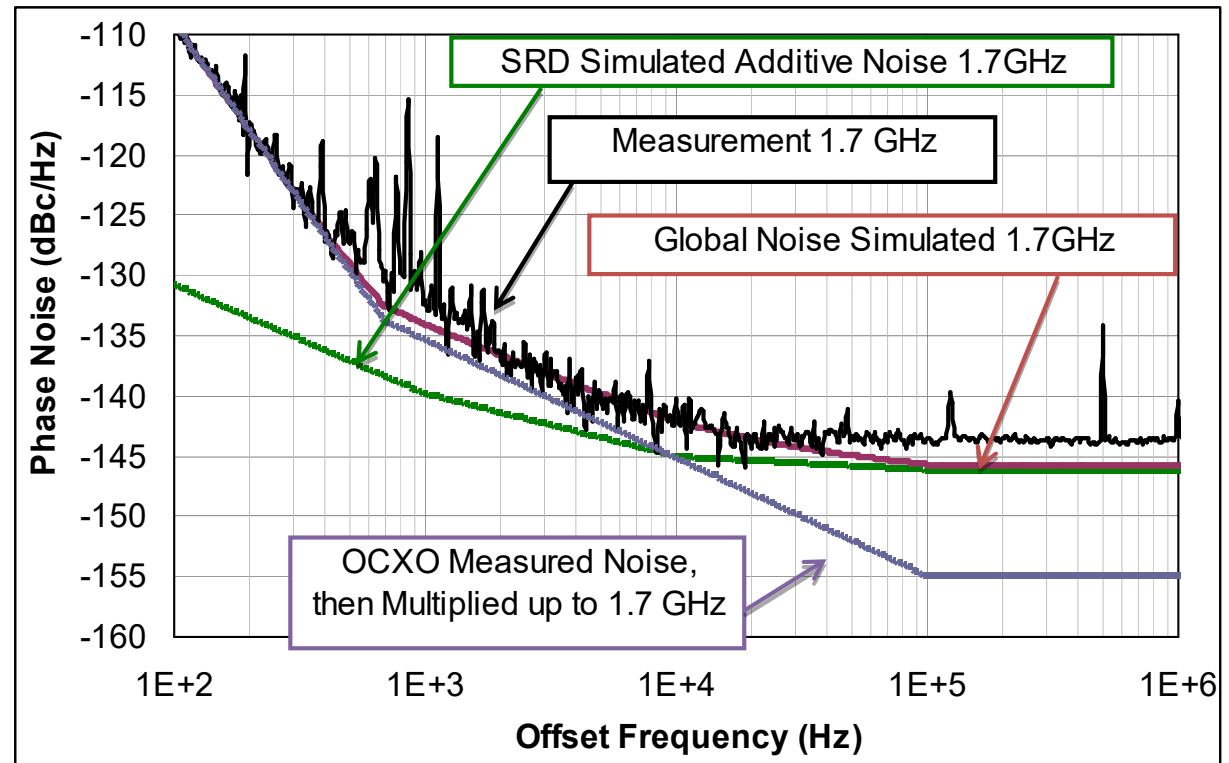
- LFN for Sampling Phase Detectors
- LFN conversion for Low Phase Noise Frequency Synthetizers (VCOs)

Low phase noise systems

Heterogen systems, with embedded RF and Optic carriers,
and/or digital / analog functions,
and/or high number of harmonics or non-linearities
and/or new generation/high performances (reliable ?) devices

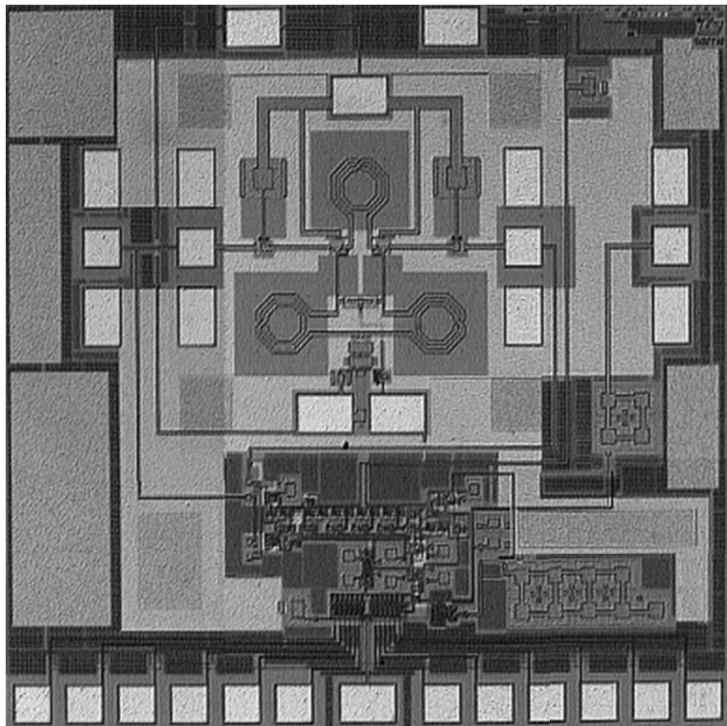


Example : Noise simulation
 around harmonic 17th
 of a sampling phase detector

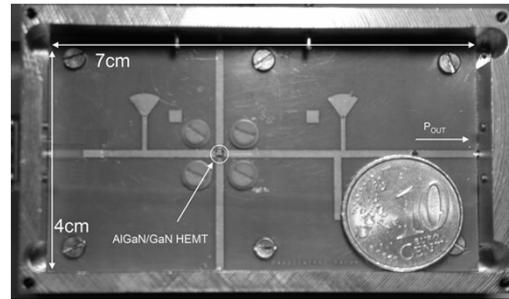


Ref: Cyclostationary shot noise measurements in RF Schottky barrier diode detectors, *IEEE Electron Devices Letters*, Vol.31, N°1, pp.74-76, Janvier 2010.

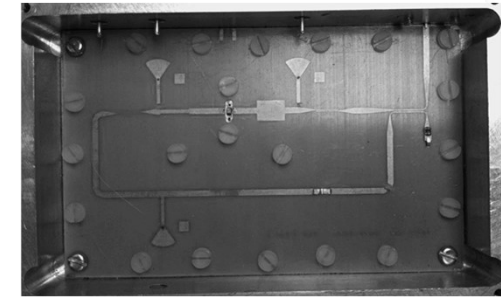
Ref: Proc. of the 2009 European Microwave Conf., Rome, oct. 2009, pp. 480-483, J. Graffeuil.



PLL 20 GHz, Tournier-Tartarin

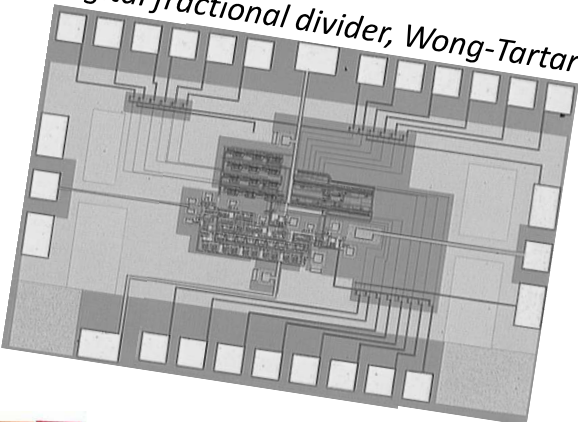


10GHz Hybrid GaN oscillators
Soubercaze-Tartarin

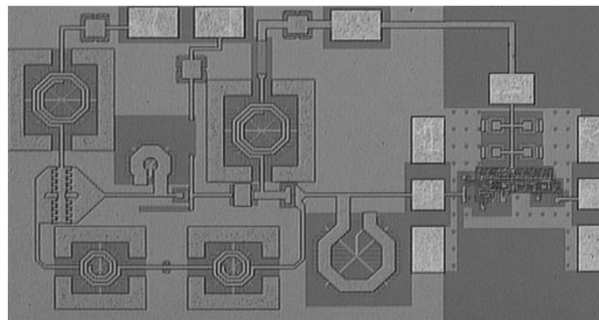


10GHz Reflexion and
transmission VCOs
Wong-Tartarin

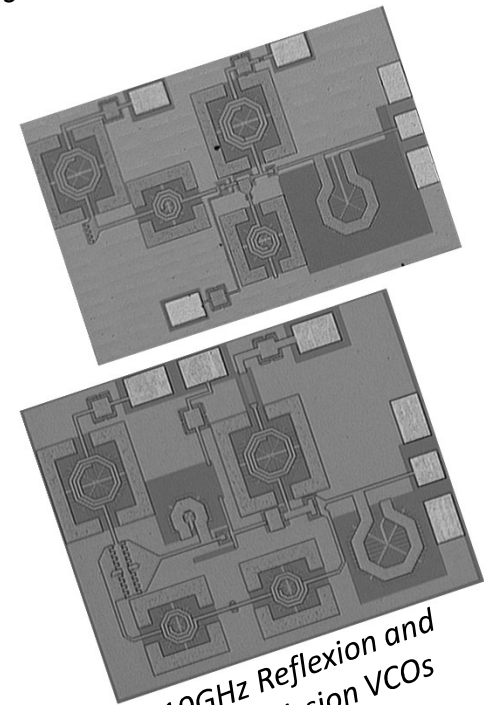
Digital fractional divider, Wong-Tartarin



10GHz VCO with divider, Wong-Tartarin



20GHz push-push VCO
Wong-Tartarin

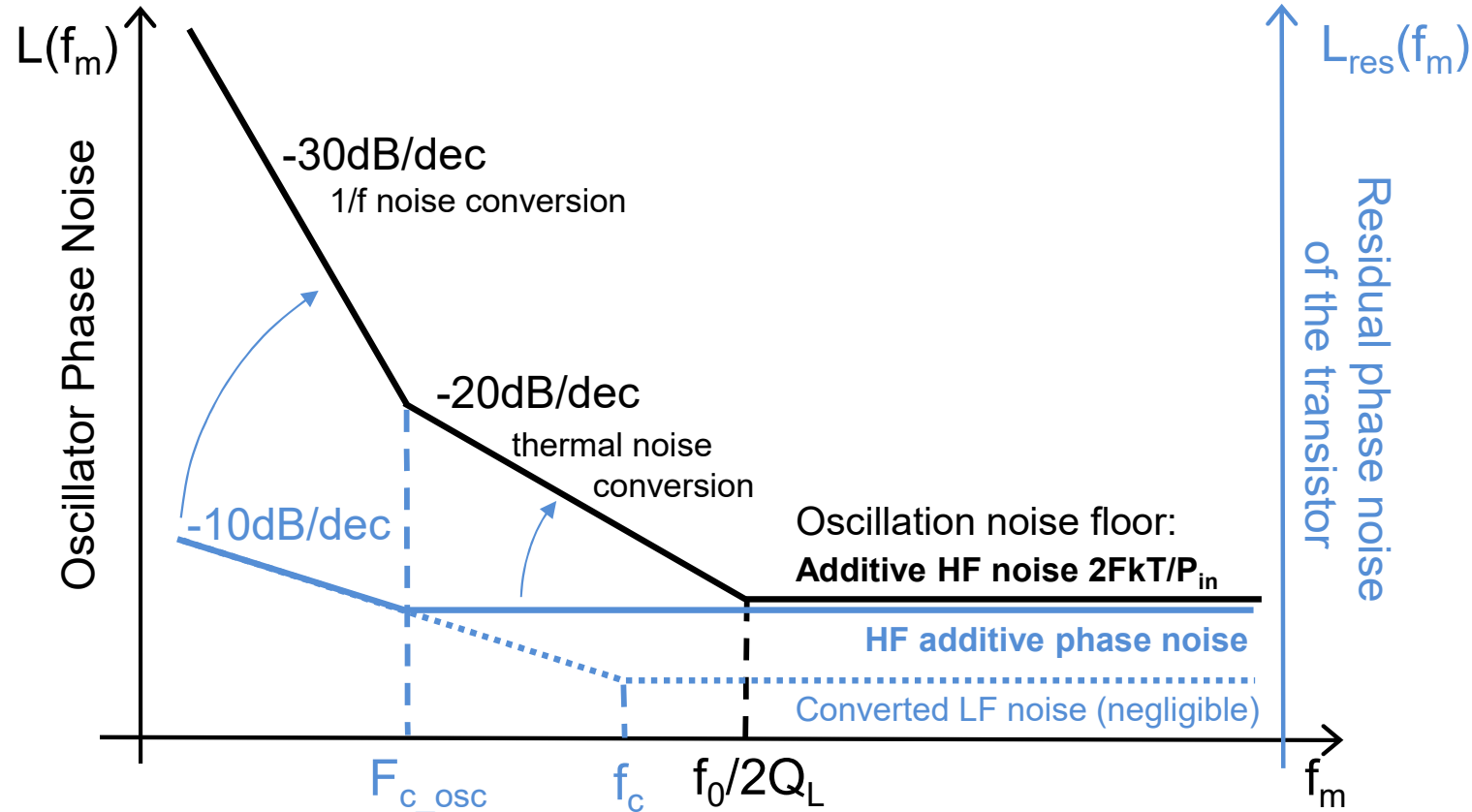


Kurokawa :

$$\Delta f = \frac{\frac{\partial X_t}{\partial A} \frac{\partial R_t}{\partial V_0} \frac{\partial R_t}{\partial A} \frac{\partial X_t}{\partial V_0}}{\frac{\partial R_t}{\partial A} \frac{\partial X_t}{\partial f_0} - \frac{\partial X_t}{\partial A} \frac{\partial R_t}{\partial f_0}} \Delta V_0$$



$$\Delta f = -\frac{\frac{\partial X_t}{\partial V_0}}{\frac{\partial X_t}{\partial f_0}} \Delta V_0$$



Leeson :

$$L(f_m) = 20 \log \left[\frac{f_0}{2\sqrt{2}Q_L f_m} \right] + 20 \log(\Delta\bar{\Phi}_A) \quad dBc/Hz$$

$P_{in-ampli}$ high
(highly non-linear regime)

Ref: Tartarin, invited talk, Univ. Of Chalmers, 2014

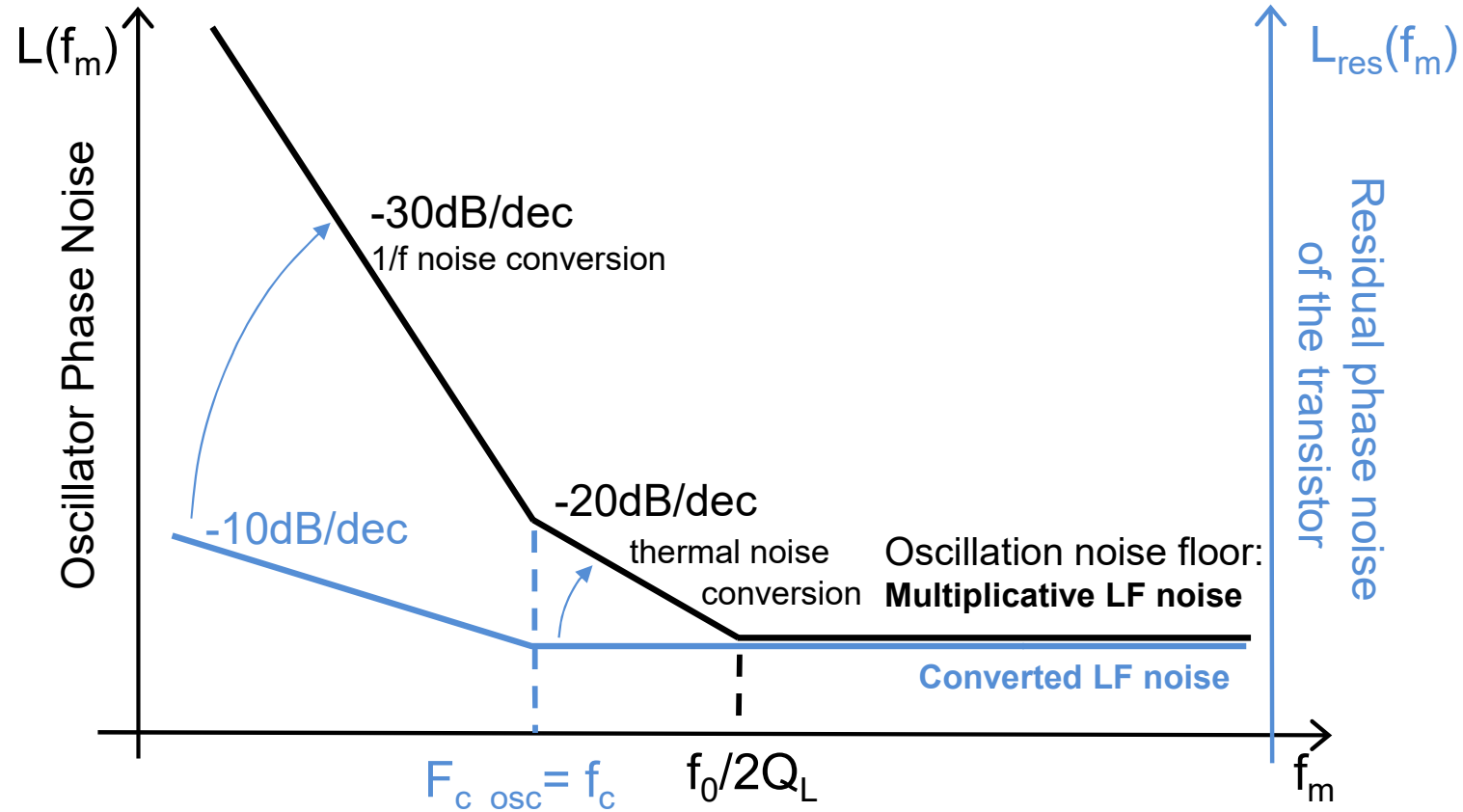
Design of low phase noise VCOs on BiCMOS technology (ST microelectronics)

Kurokawa :

$$\Delta f = \frac{\frac{\partial X_t}{\partial A} \frac{\partial R_t}{\partial V_0} \frac{\partial R_t}{\partial A} \frac{\partial X_t}{\partial V_0}}{\frac{\partial R_t}{\partial A} \frac{\partial X_t}{\partial f_0} \frac{\partial X_t}{\partial A} \frac{\partial R_t}{\partial f_0}} \Delta V_0$$



$$\Delta f = \frac{-\frac{\partial X_t}{\partial V_0}}{\frac{\partial X_t}{\partial f_0}} \Delta V_0$$



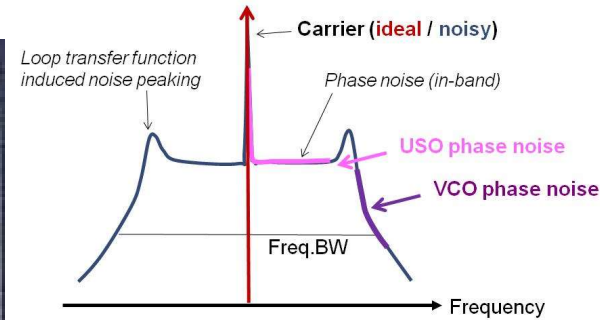
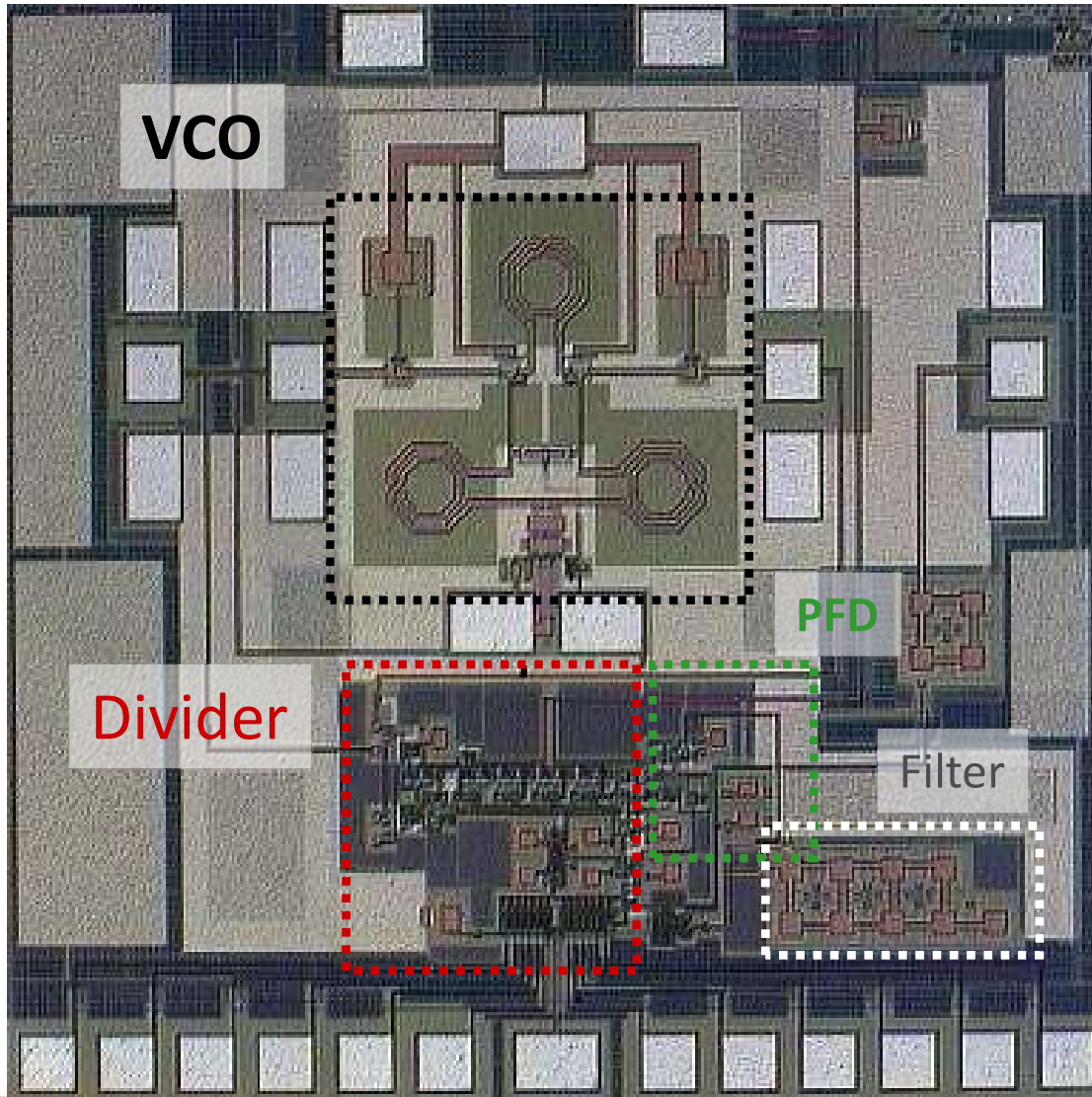
Leeson :

$$L(f_m) = 20 \log \left[\frac{f_0}{2\sqrt{2}Q_L f_m} \right] + 20 \log(\Delta\bar{\Phi}_A) \quad dBc/Hz$$

$P_{in-ampli}$ **low**
(weak non-linear regime)

Ref: Tartarin, invited talk, Univ. Of Chalmers, 2014

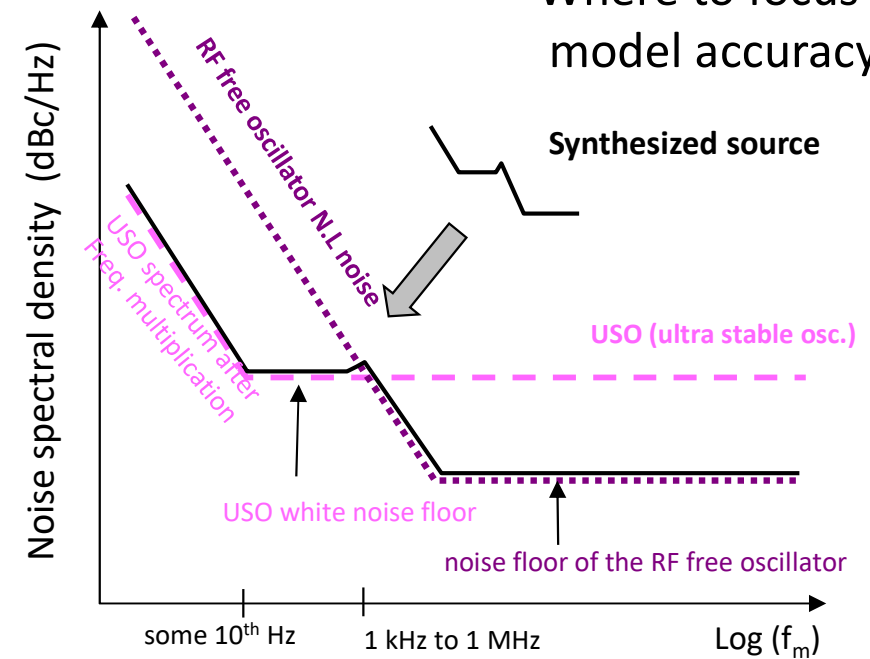
First Fully integrated MMIC PLL @ 20 GHz



Where to optimize (phase) noise in RF free oscillator?

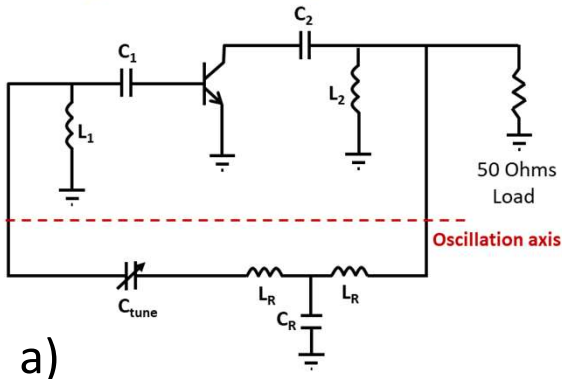


Where to focus on model accuracy?

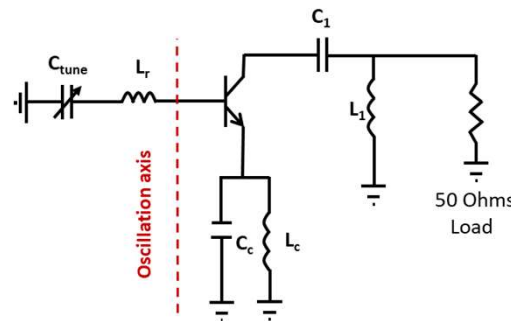


Distance f_m to the carrier (Hz) (SSB)

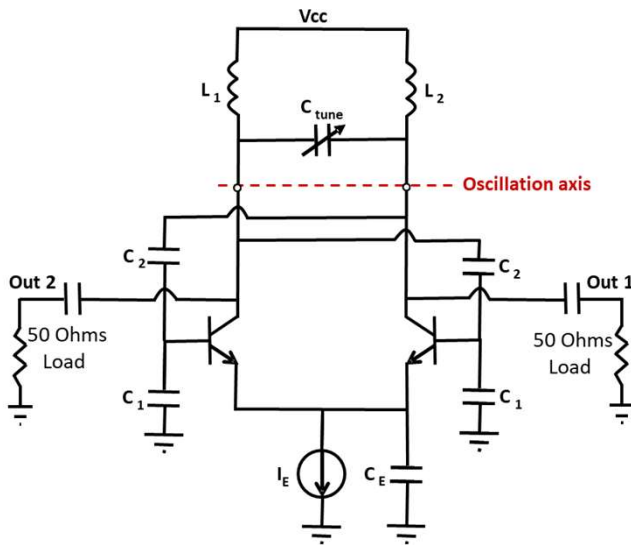
Design of low phase noise VCOs on BiCMOS technology (ST microelectronics)



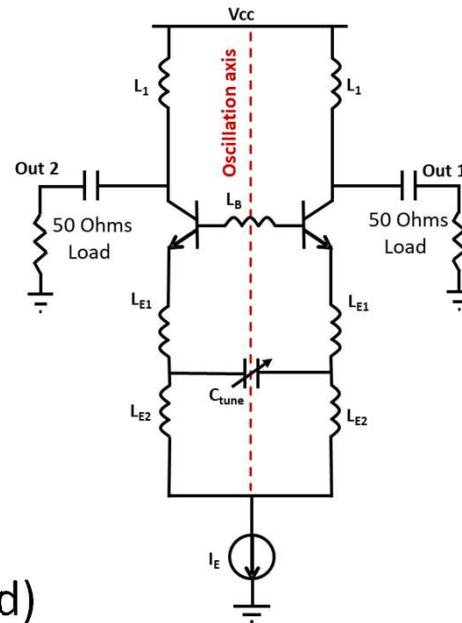
a)



b)



c)



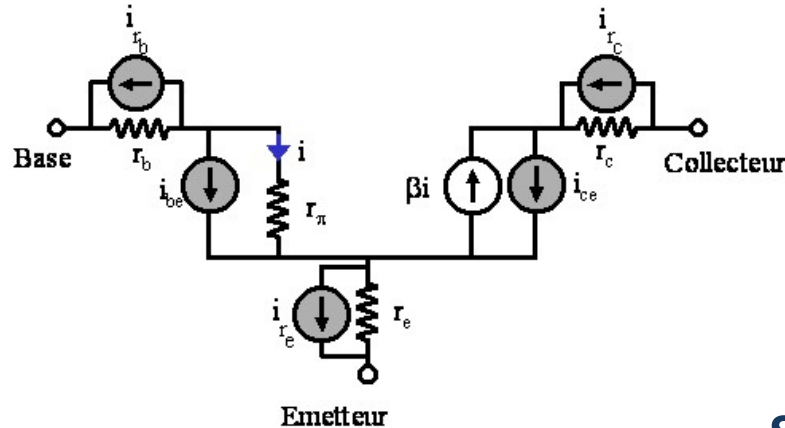
d)

- Device LFN modeling
- Analysis of noise conversion.
- Topology selection prior to design: according to which metrics or FoM?
- Design of the resonator (Q) and of the amplifier (LFN) : reflection or transmission
- Measurement and refinement of the model (if necessary)

Ref: Ph. D. Thesis W. Wong, University of Toulouse, France, 2003

All noise models were developed from our LFN measurement campaigns

HBTs



$$S_{i_{be}} = 2qI_B + B_{1/f} \frac{I_B^{\alpha_f}}{A_E \cdot f}$$

$$S_{i_{ce}} = 2qI_C$$

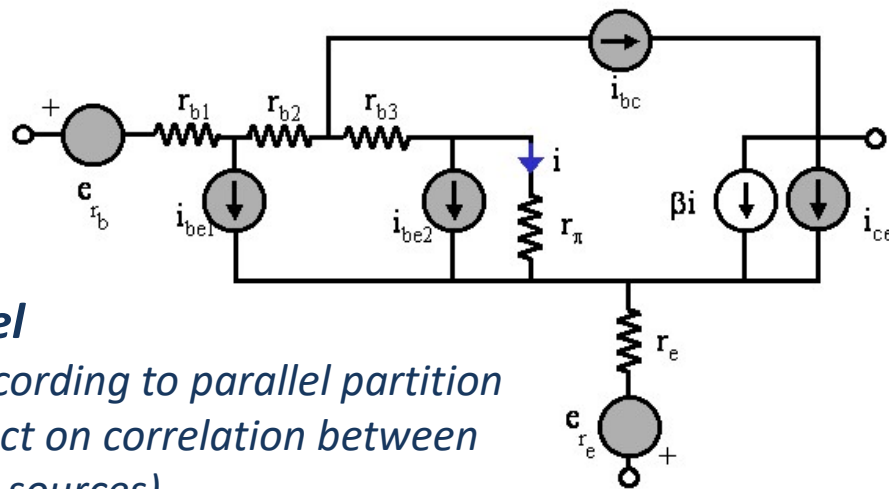
$$S_{i_{r_b}} = 4kT/r_b$$

$$S_{i_{r_e}} = 4kT/r_e$$

$$S_{i_{r_c}} = 4kT/r_c$$

SPICE model

SS model with associated LF noise sources



$$R_{cor} = \frac{\Re\{S_{VI^*}\}}{S_{I_1}}$$

$$S_{I_1} = S_{i_{be}} + \frac{1}{\beta^2} \cdot S_{i_{ce}}$$

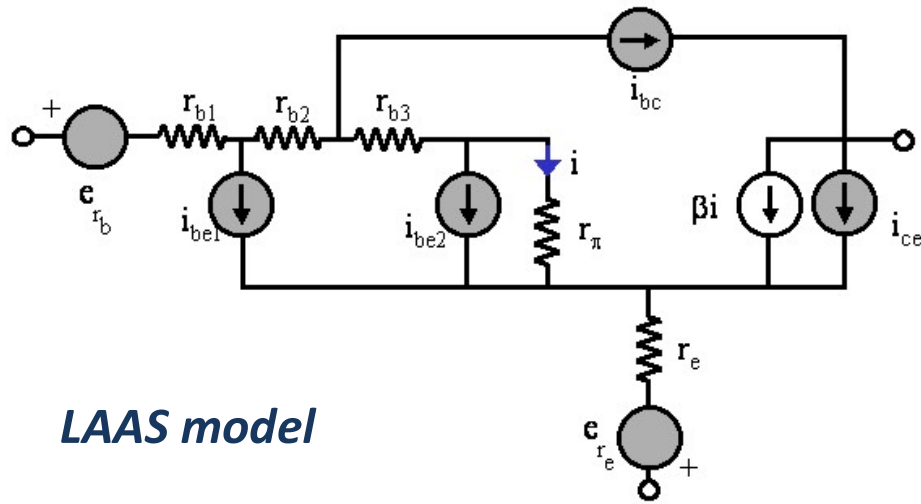
$$S_{VI^*} = (r_b + r_e) S_{i_{be}} + (r_b + r_e + r_\pi) \frac{1}{\beta^2} \cdot S_{i_{ce}}$$

$$R_{cor} = \frac{(r_b + r_e) S_{i_{be}} + (r_b + r_e + r_\pi) \frac{1}{\beta^2} \cdot S_{i_{ce}}}{S_{i_{be}} + \frac{1}{\beta^2} \cdot S_{i_{ce}}}$$

LAAS model

evolutive according to parallel partition of I_{bc} - impact on correlation between In-Out noise sources)

All noise models were developed from our LFN measurement campaigns



LAAS model

Noise partition, according to specific technological developments

$$S_V = (S_{rb} + S_{re}) + (r_{b1} + r_e)^2 \cdot S_{ibel} + (r_b + r_e)^2 \cdot S_{ibe2} + (r_b + r_e + r_{\Pi})^2 \cdot \frac{S_{ice}}{\beta^2} + \left(\frac{Z_{\text{entrée}}}{\beta} + r_{b1} + r_{b2} \right)^2 S_{ibc}$$

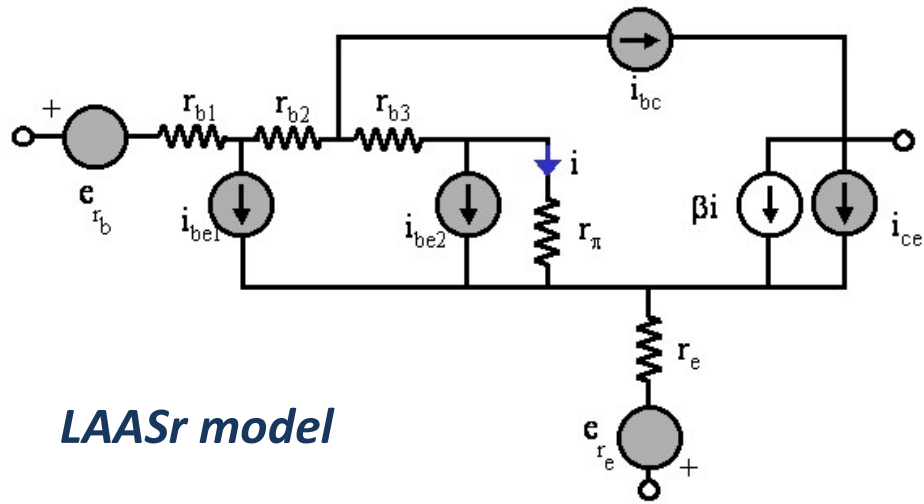
$$S_I = S_{ibel} + S_{ibe2} + \left(1 + \frac{1}{\beta} \right)^2 \cdot S_{ibc} + \frac{S_{ice}}{\beta^2}$$

$$S_{IV^*} = (r_{b1} + r_e) S_{ibel} + (r_b + r_e) S_{ibe2} + (r_b + r_e + r_{\Pi}) \frac{S_{ice}}{\beta^2} + \left(\frac{Z_{\text{entrée}}}{\beta} + r_{b1} + r_{b2} \right) S_{ibc}$$

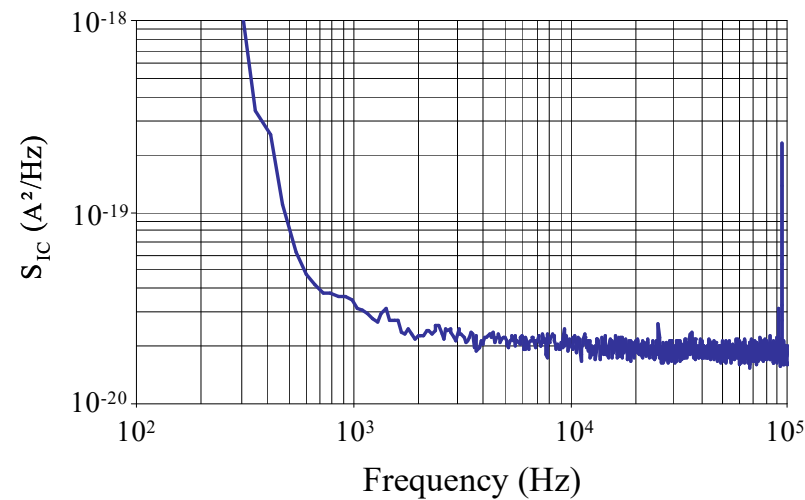
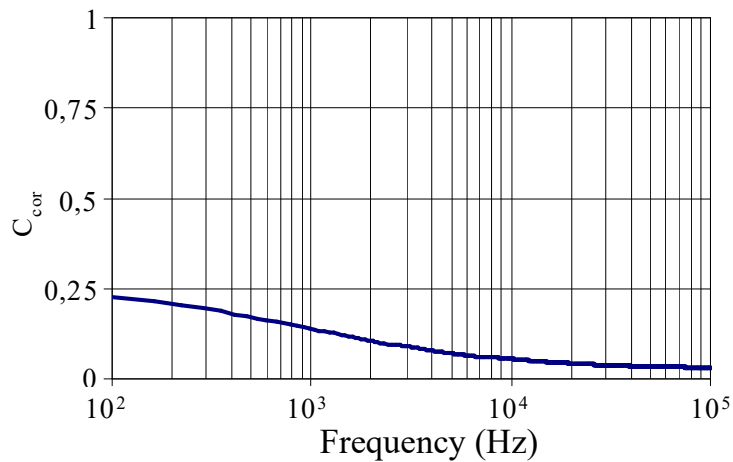
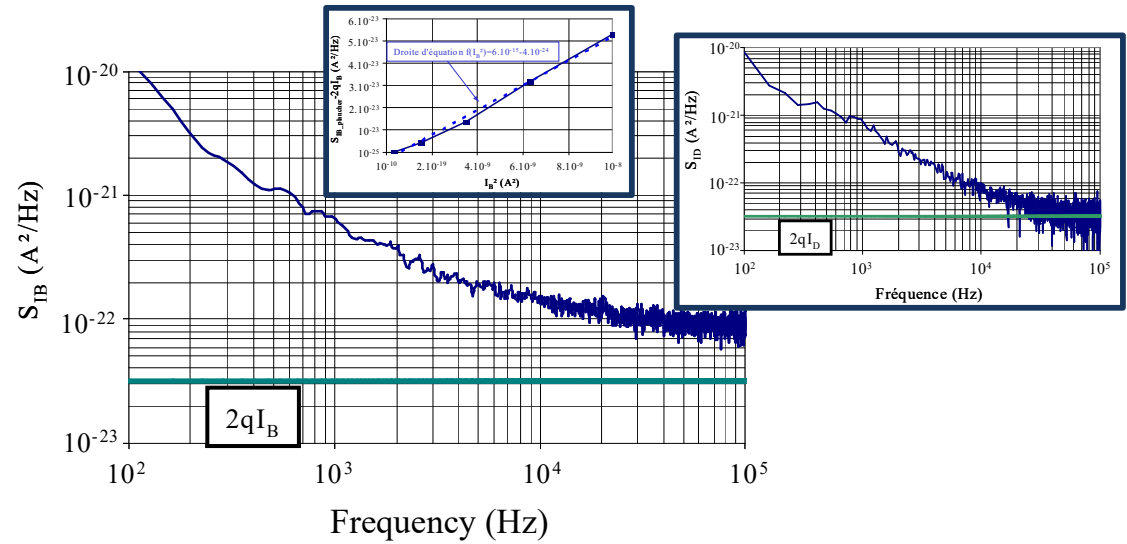
$$R_{\text{cor}} = \frac{(r_{b1} + r_e) S_{ibel} + (r_b + r_e) S_{ibe2} + (r_b + r_e + r_{\Pi}) \frac{S_{ice}}{\beta^2} + \left(\frac{Z_{\text{entrée}}}{\beta} + r_{b1} + r_{b2} \right) S_{ibc}}{S_{ibel} + S_{ibe2} + \left(1 + \frac{1}{\beta} \right)^2 \cdot S_{ibc} + \frac{S_{ice}}{\beta^2}}$$

	e_{r_b}	e_{r_e}	i_{be2}	i_{ce}	i_{be1}	i_{bc}
$R_{\text{cor}} < (r_e + r_b)$	∇	∇	∇	○	∇	∇
$R_{\text{cor}} = (r_e + r_b)$	∇	∇	∇	○	○	○
$R_{\text{cor}} > (r_e + r_b)$	∇	∇	∇	∇	○	○

All noise models were developed from our LFN measurement campaigns

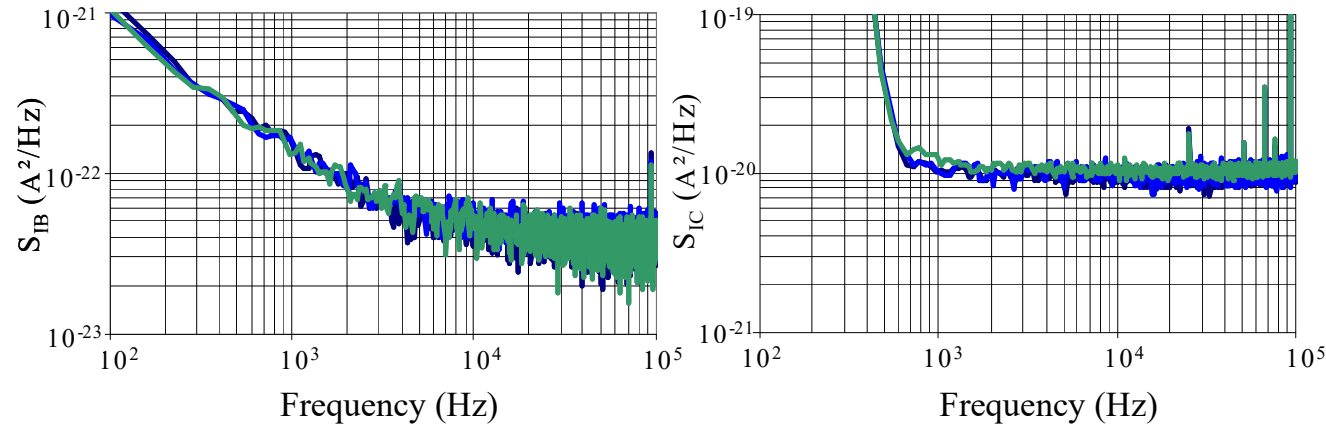


LAASr model

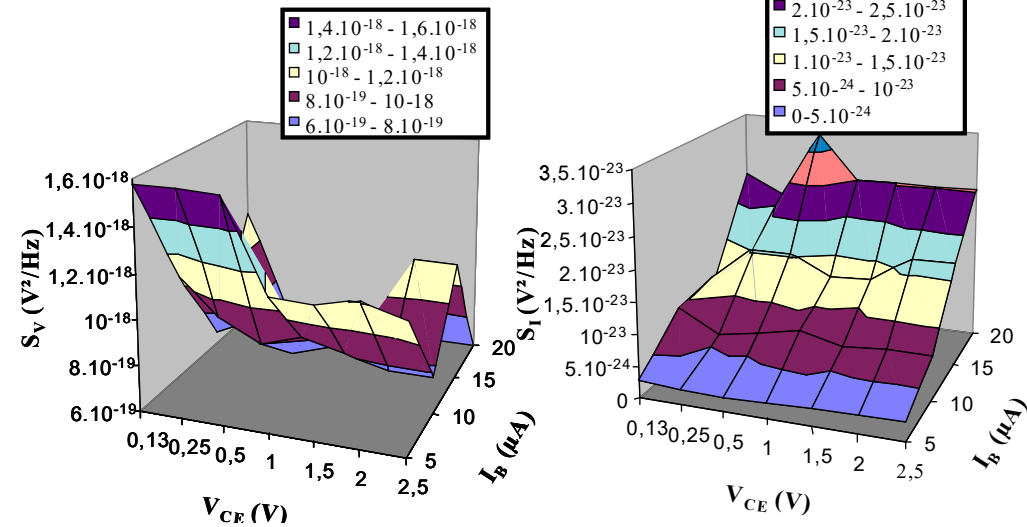
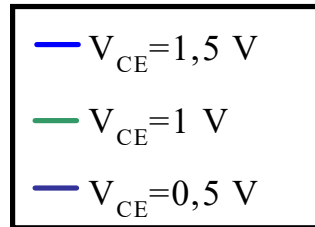
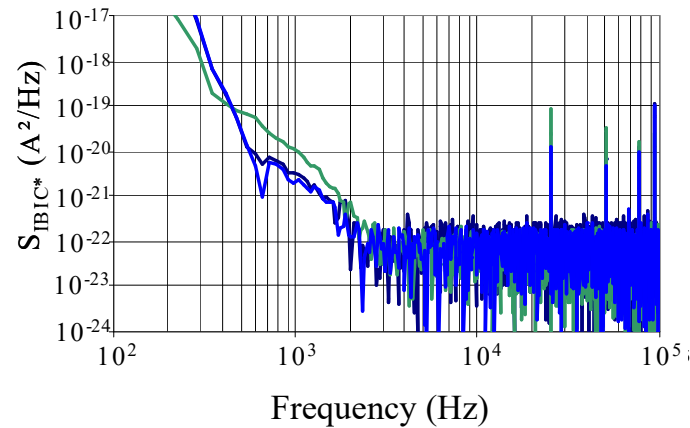


Ref: Ph. D. Thesis L. Bary, University of Toulouse, France, 2001

All noise models were developed from our LFN measurement campaigns

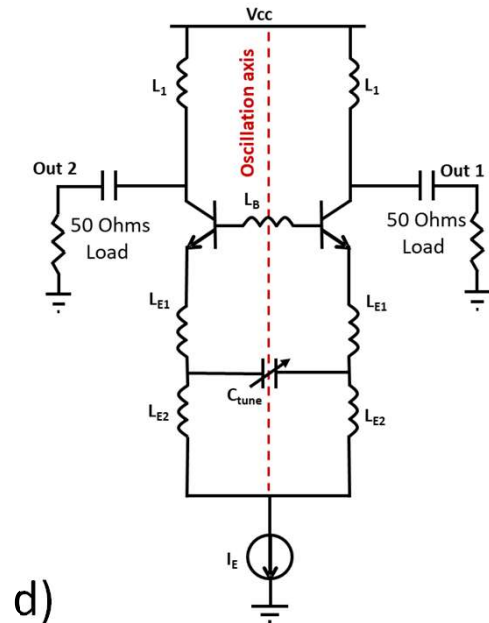
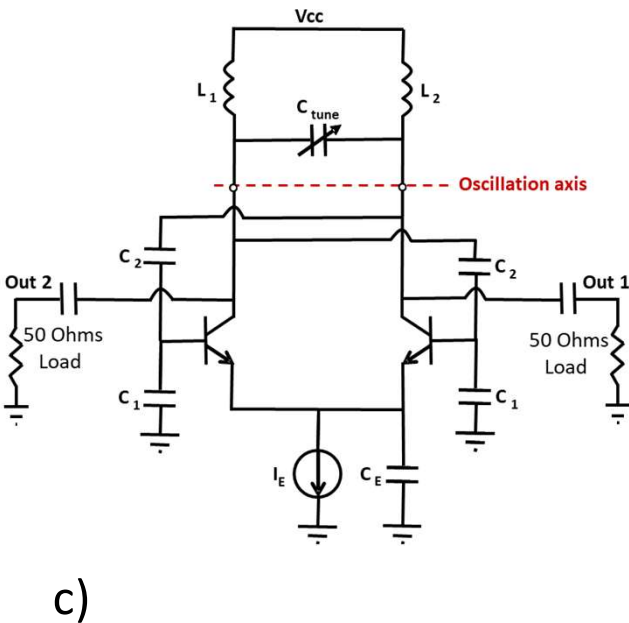
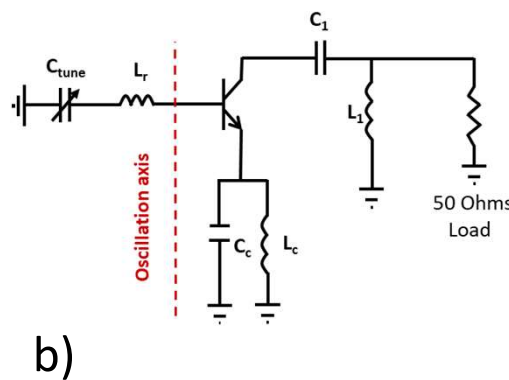
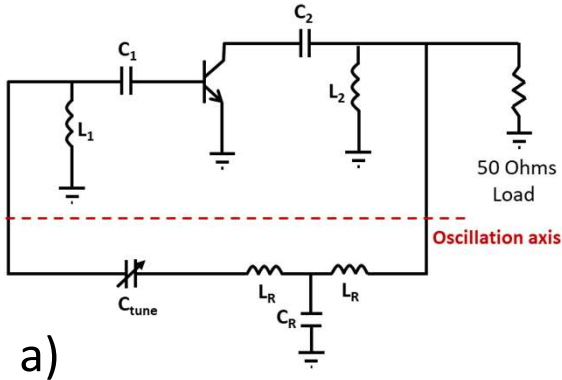


MAPPING OF THE:
-biasing conditions
-sizing conditions



Ref: Ph. D. Thesis L. Bary, University of Toulouse, France, 2001

Design of low phase noise VCOs on BiCMOS technology (ST microelectronics)

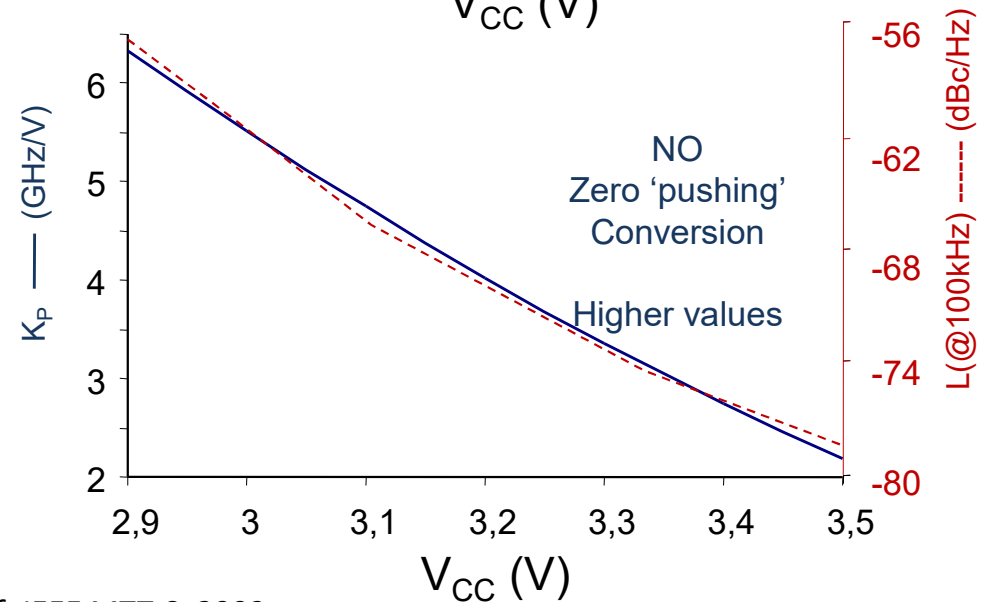
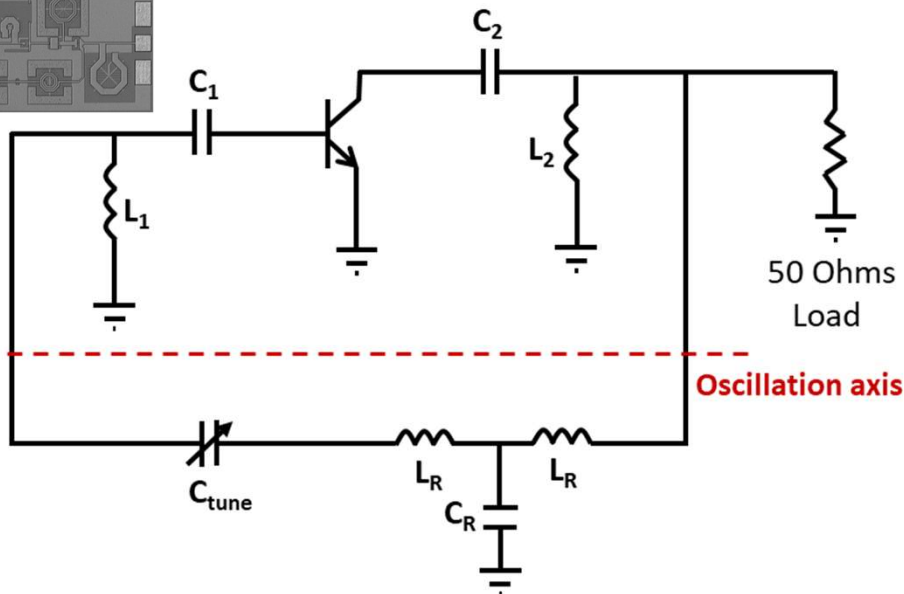
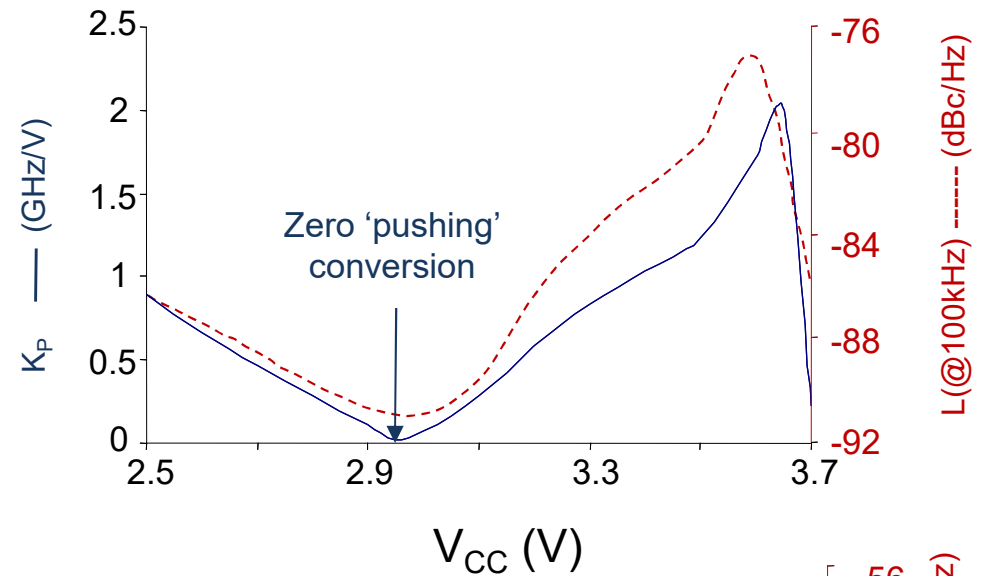
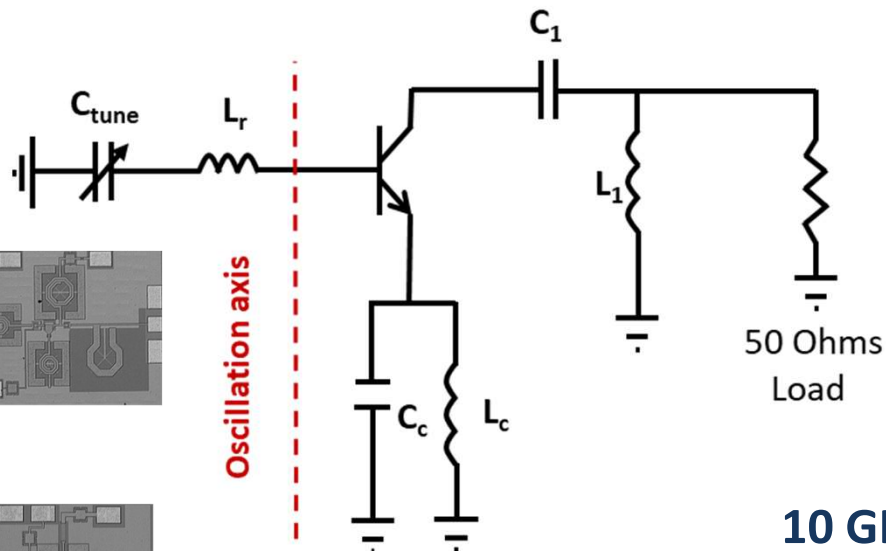


- Device LFN modeling
- **Analysis of noise conversion.**
- **Topology selection prior to design: according to which metrics or FoM?**
- **Design of the resonator (Q) and of the amplifier (LFN) : reflection or transmission**
- **Measurement and refinement of the model (if necessary)**

$$L(f_m) = 10 \times \log \left(\left(\frac{f_0}{f_m} \right)^2 \left(\frac{R_L F k T}{Q_L^2 V_O^2} \right) \right)$$

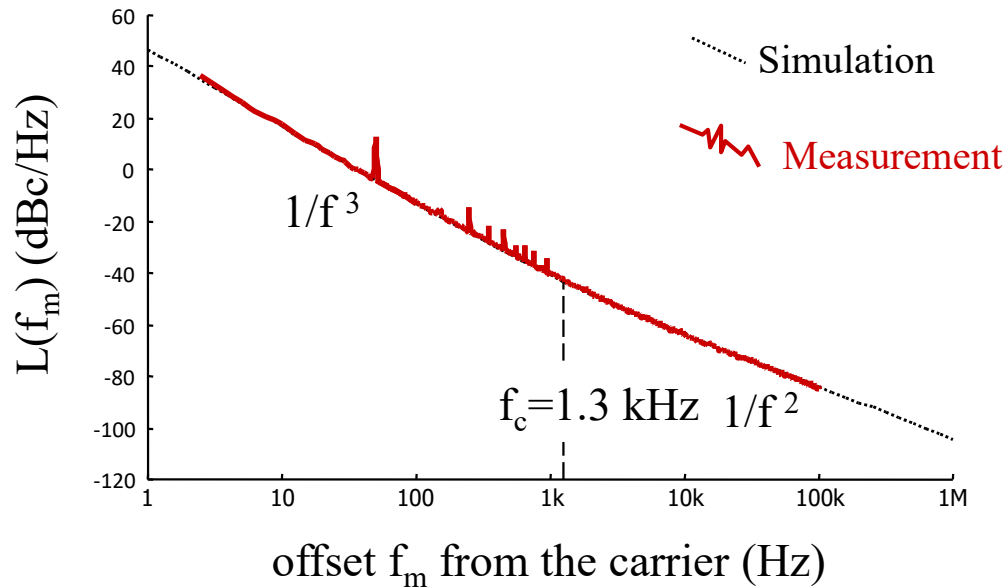
Ref: Tartarin et al. Journal of MDPI, 2022, Evolution Trends and Paradigms of Low Noise Frequency Synthesis and Signal Conversion Using Silicon Technologies

Ref: Ph. D. Thesis W. Wong, University of Toulouse, France, 2003



Ref: Ph. D. Thesis W. Wong, University of Toulouse, France, 2003

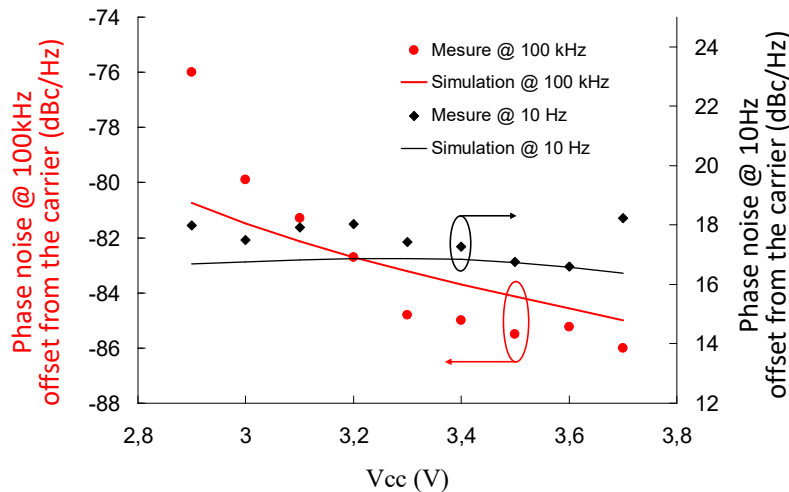
Ref: IEEE MTT-S, 2003



$$S_{i_{be}} = K \frac{I_{be_{DC}}^\alpha}{f^\beta} + 2qI_{be_{DC}}$$

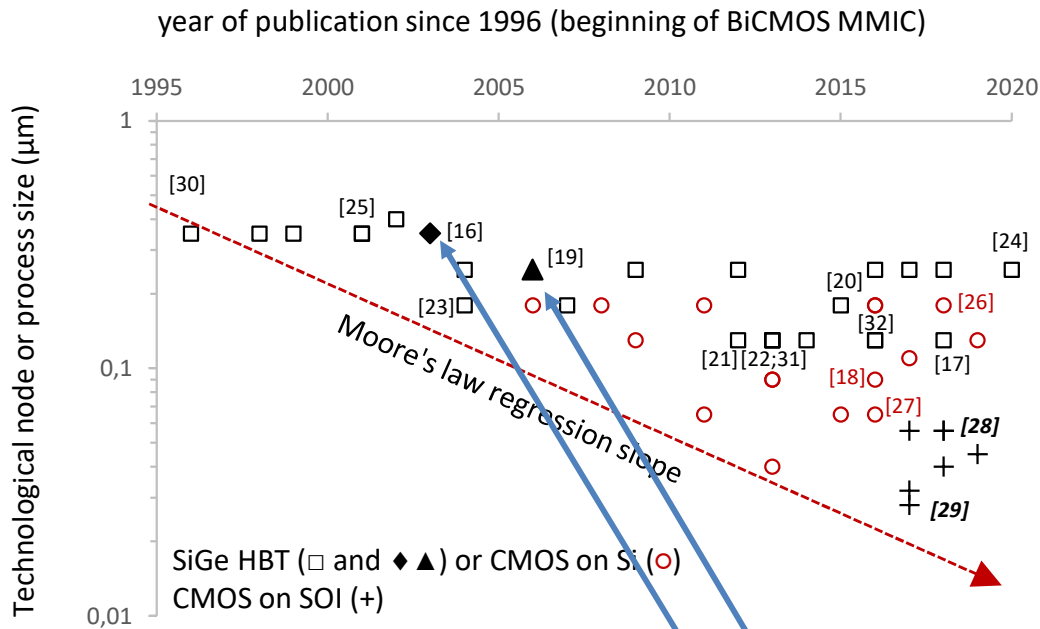
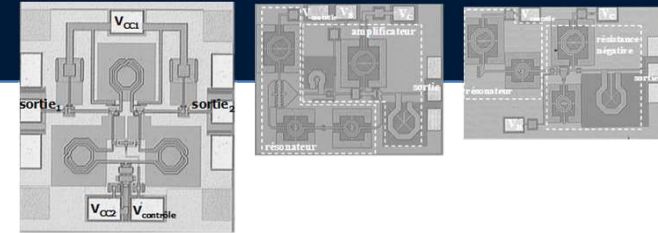
Phase noise computed with
ADS software (Keysight, prev. Agilent)

At the time, pnfm did not account for the
noise floor far from the carrier
→ pnm was also considered (matrix
conversion, account for the noise floor)

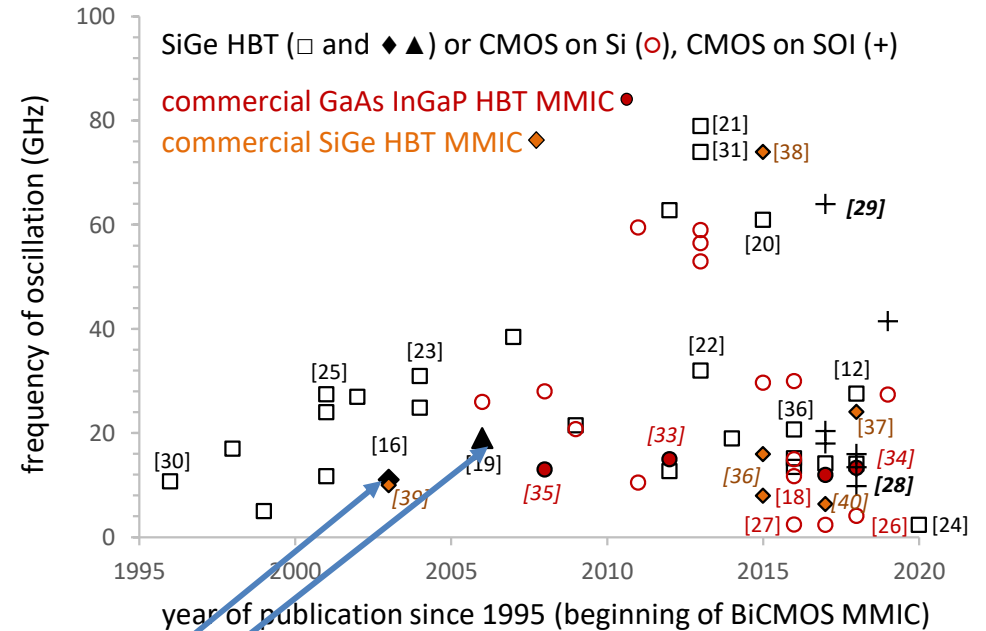


Less than 2dB error @10Hz
Less than 4.5dB error @100kHz

State of the Art of BiCMOS MMIC VCOs



Technological node :
evolution over time

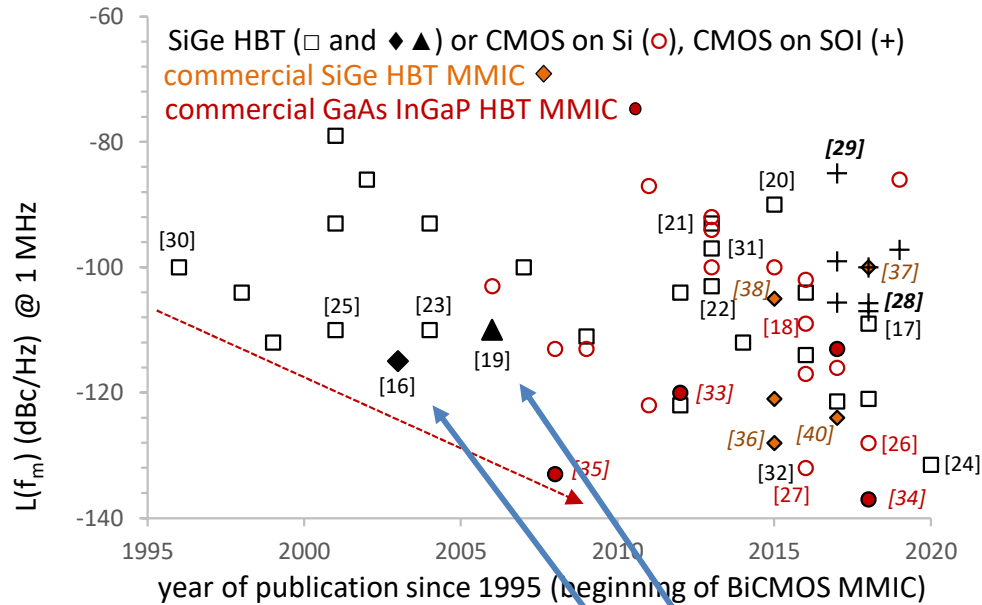
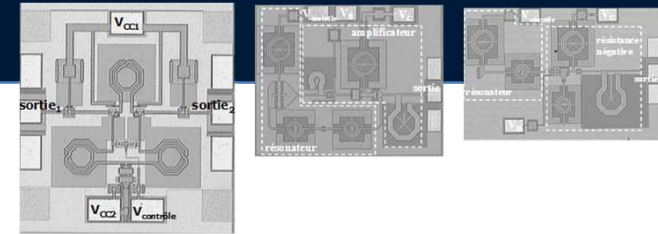


Freq. of oscillation:
evolution over time

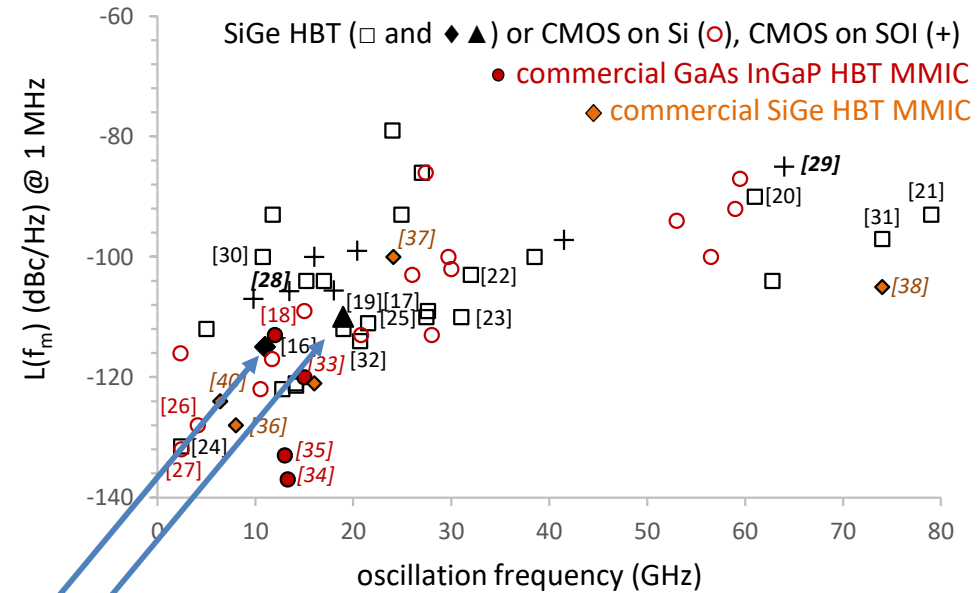
Our work

Ref: Tartarin et al. Journal of MDPI, 2022, Evolution Trends and Paradigms of Low Noise Frequency Synthesis and Signal Conversion Using Silicon Technologies

State of the Art of BiCMOS MMIC VCOs



Leeson's factor over time



Leeson's factor vs oscillation frequency

Our work

Ref: Tartarin et al. Journal of MDPI, 2022, Evolution Trends and Paradigms of Low Noise Frequency Synthesis and Signal Conversion Using Silicon Technologies

State of the Art of BiCMOS MMIC VCOs :

HOW TO DEFINE IT ? → **Figure of Merit**

ACCORDING TO WHICH METRICS ? → real use conditions AND easy to figure it out

$$L(f_m) = 10x\log \left(\left(\frac{f_0}{f_m} \right)^2 \left(\frac{R_L FkT}{Q_L^2 V_O^2} \right) \right)$$

Leeson: the fundamental !

$$FOM = L(f_m) - 10x\log \left(\left(\frac{f_0}{f_m} \right)^2 \frac{1}{P_{DC}} \right) = -10x\log \left(\left(\frac{R_L FkT}{Q_L^2 V_O^2} \right) x P_{DC} \right)$$

Adding P_{DC}. Not enough realistic (lower P_{DC} will lead to low output power, need of buffer amplifier → residual phase noise)

$$FOM_{PRF} = L(f_m) - 10x\log \left(\left(\frac{f_0}{f_m} \right)^2 \frac{P_{out}}{P_{DC}} \right)$$

Adding P_{RF}. Not enough realistic (does not account for controlled oscillator → Q factor largely impacts Leeson formula !)

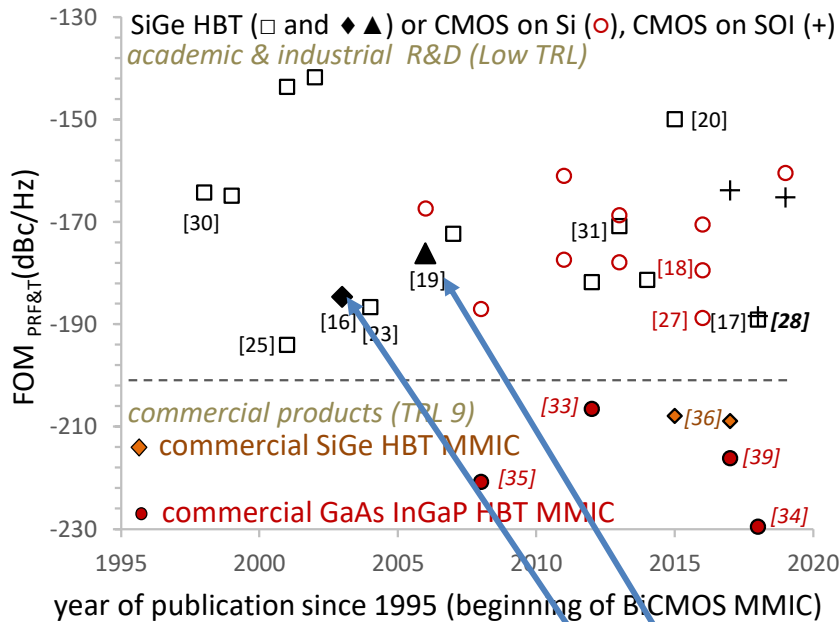
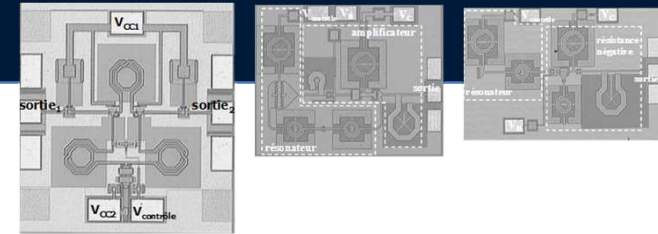
$$FOM_{PRF\&T} = L(f_m) - 10x\log \left(\left(\frac{f_0}{f_m} \right)^2 \left(\frac{TR\%}{10} \right)^2 \frac{P_{out}}{P_{DC}} \right)$$

Adding Δtune & P_{RF}. It seems quite realistic and not too elaborate

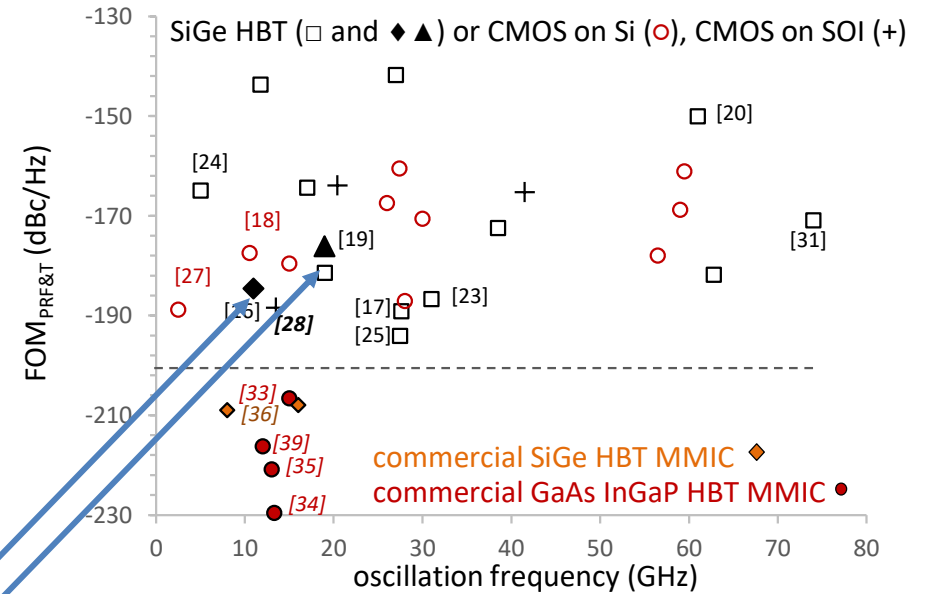
Ref: Tartarin et al. Journal of MDPI, 2022, Evolution Trends and Paradigms of Low Noise Frequency Synthesis and Signal Conversion Using Silicon Technologies

Ref: Ph. D. Thesis W. Wong, University of Toulouse, France, 2003

State of the Art of BiCMOS MMIC VCOs Proposed FOM with tuning range and RF output power



FOM_{RF&T} over time

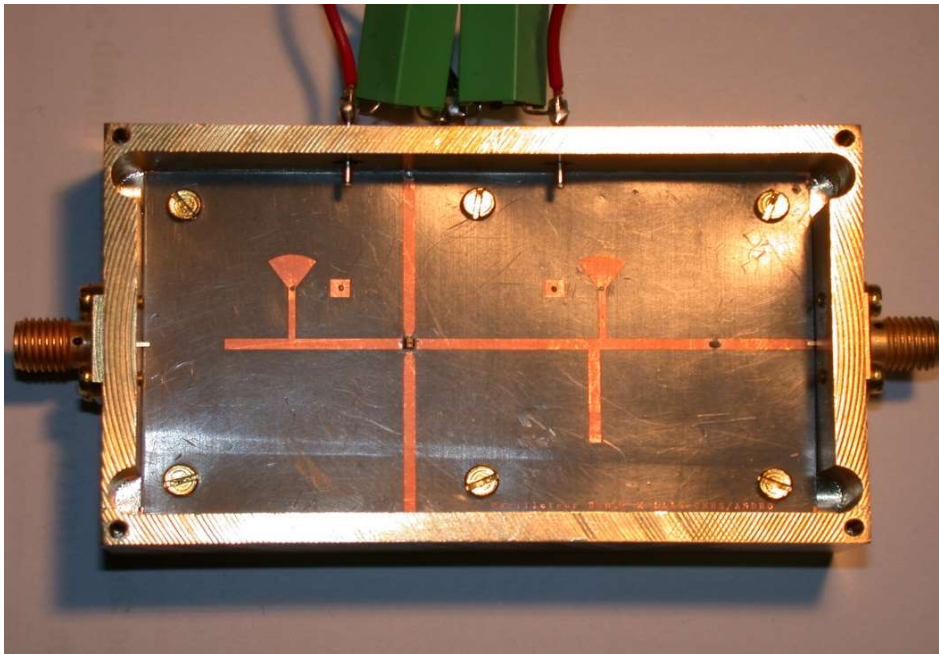


FOM_{RF&T} versus oscillation frequency

Our work

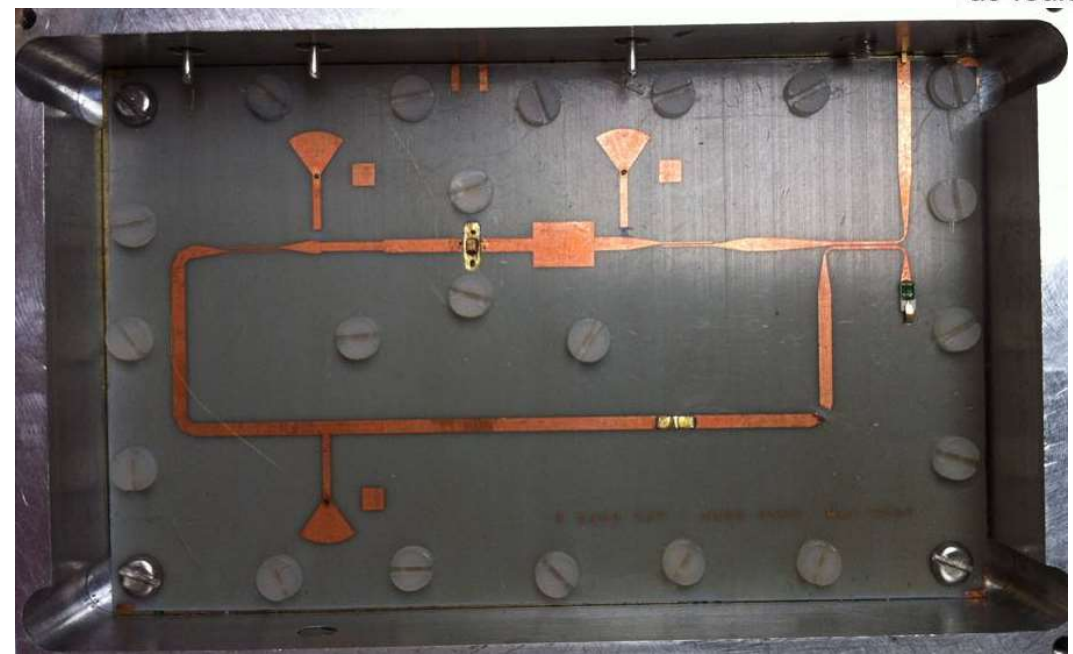
$$FOM_{PRFT} = L(f_m) - 10 \times \log \left(\left(\frac{f_0}{f_m} \right)^2 \left(\frac{TR\%}{10} \right)^2 \frac{P_{out}}{P_{DC}} \right)$$

Ref: Tartarin et al. Journal of MDPI, 2022, Evolution Trends and Paradigms of Low Noise Frequency Synthesis and Signal Conversion Using Silicon Technologies



Fixed Oscillator (10 GHz)
(Soubercaze 2006)

$P_{out}=20\text{dBm}$
 $L(100\text{kHz})= -115\text{dBc/Hz}$

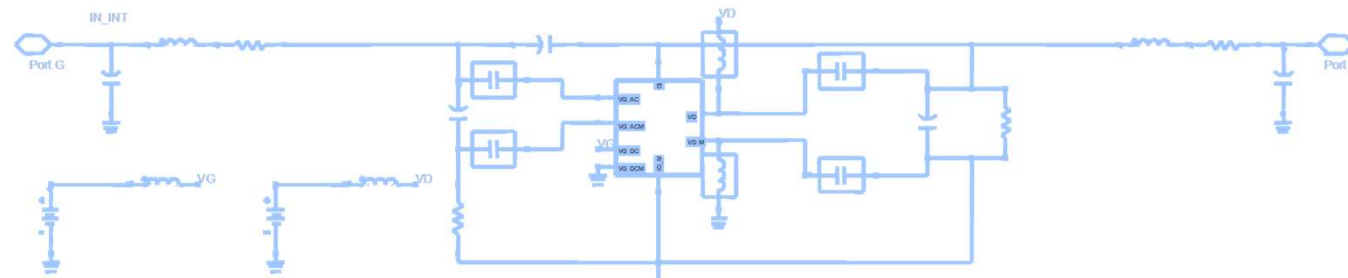
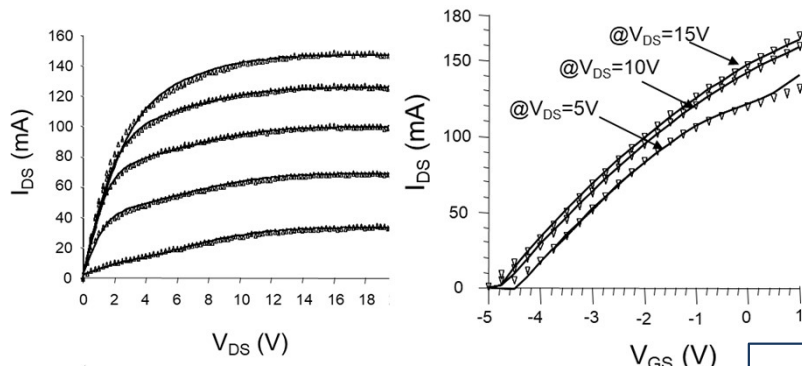


Voltage Controlled Oscillator (9.2 GHz)
(Tartarin 2008)

$P_{out}=23\text{dBm}$
 $L(100\text{kHz})= -92\text{dBc/Hz}$
2.5% tuning around f_0

Based on the same GaN HEMT chip: $2 \times 75\mu\text{m}$ gate width devices from Thales - TRT

The LS, SS and Noise model was developed from our LFN measurement campaigns



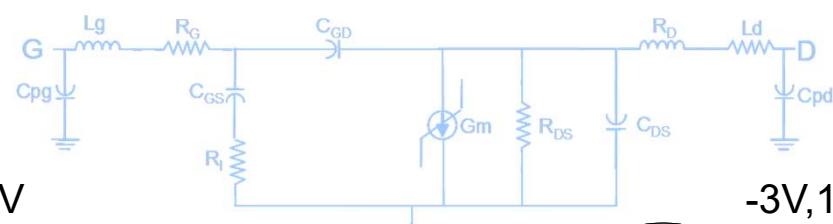
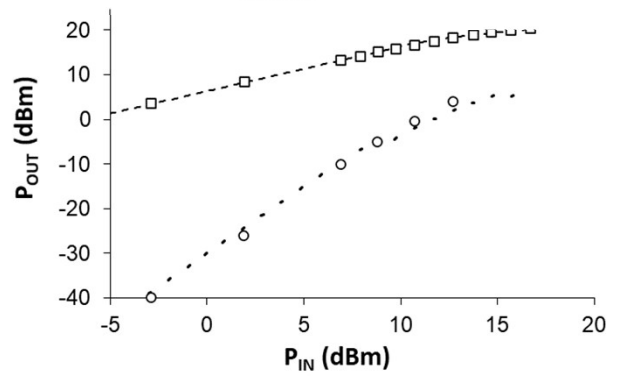
**Specific LS & SS model (multi-bias)
developed at LAAS-CNRS
Also with integrated LFN
 S_{IG} , S_{ID} and correlation**

$$I_D = (I_{Fager} + I_{Correction}) * K_{Correction}$$

$$I_{Fager} = I_S(V_{GS}) * \text{Tanh}(P_S(V_{GS}) * V_{DS})$$

$$I_{Correction} = A_P * \text{Tanh}(P_P(V_{DS} - V_{TP}) + A_P)$$

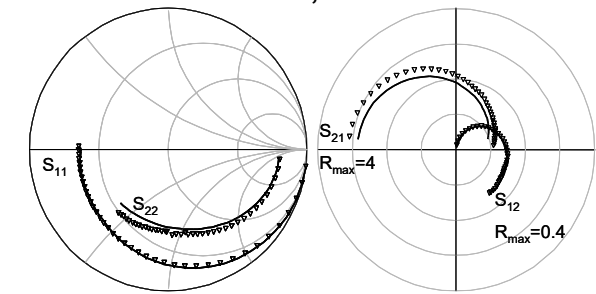
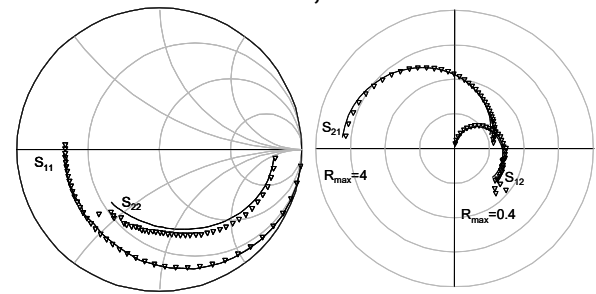
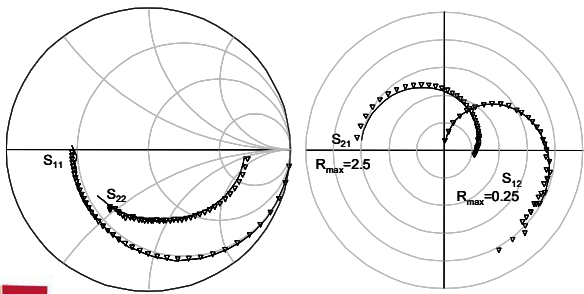
$$K_{Correction} = A_C * \text{Tanh}(P_C(V_{GS} - V_{TC}) + P_C)$$



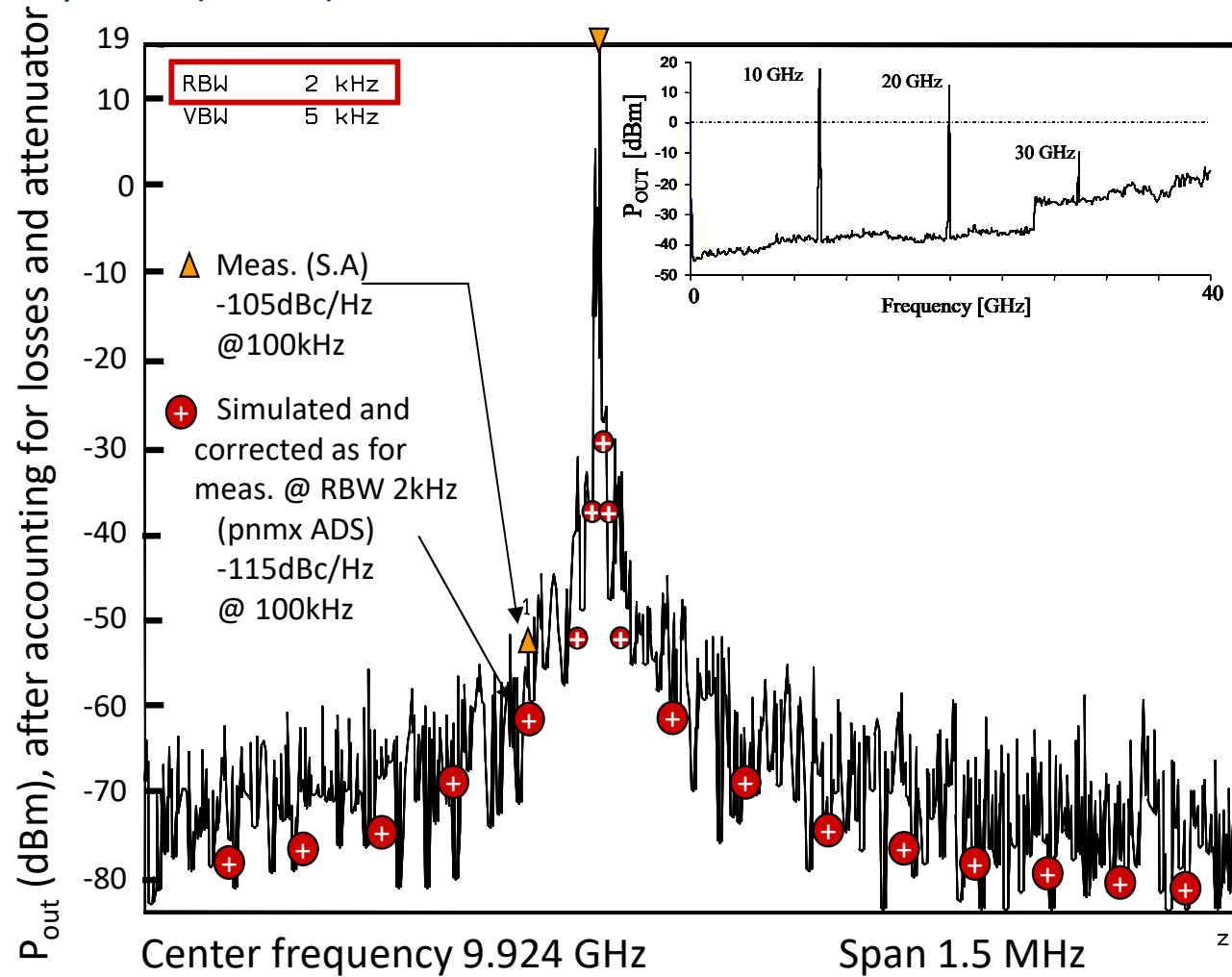
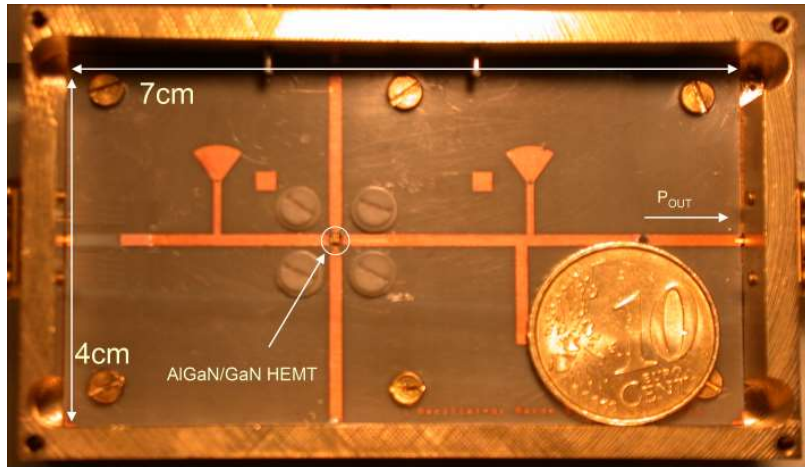
0V,10V

-4V,10V

-3V,10V

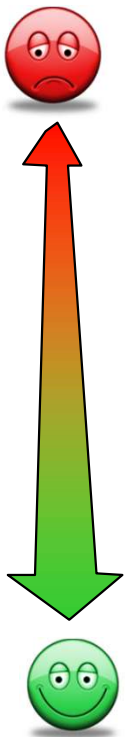


→ High output power(19 dBm), no buffer amplifier (Radar)

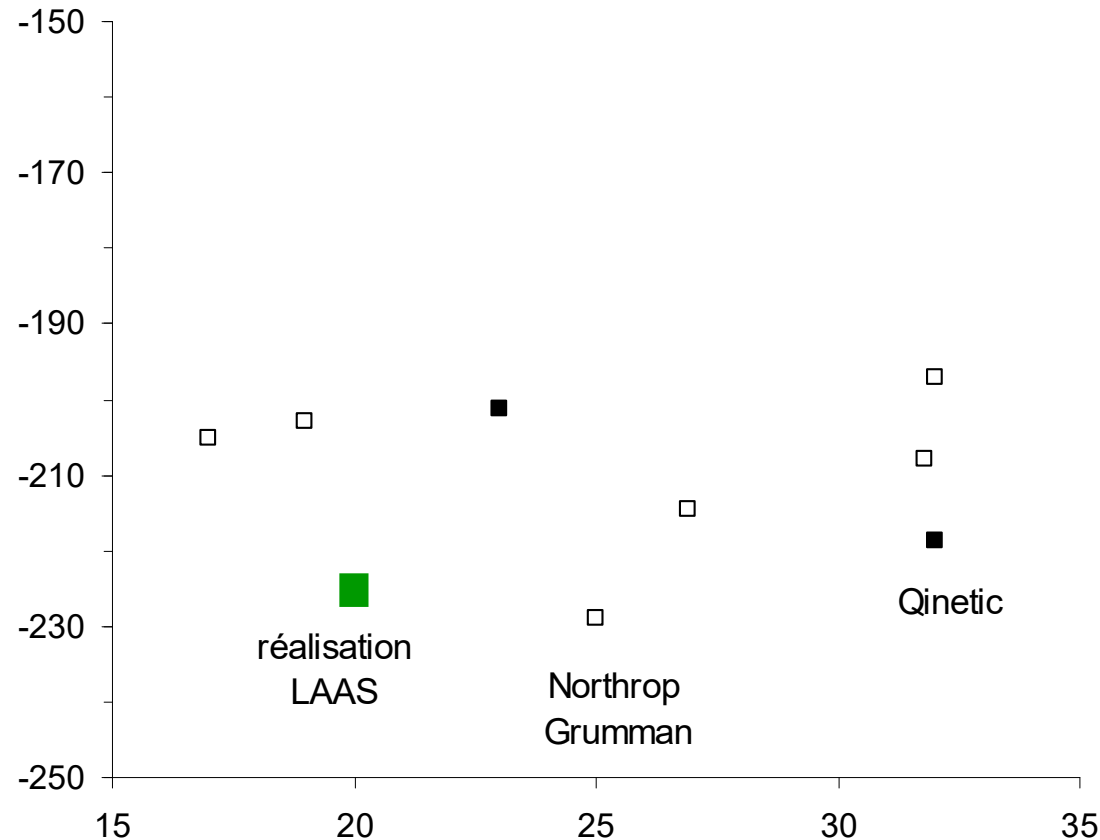


GaN oscillators @ 10 GHz (till 2016)

→ State of the art



$L(f_m) - 20 \log(f_0/f_m) - P_{out_dBm}$

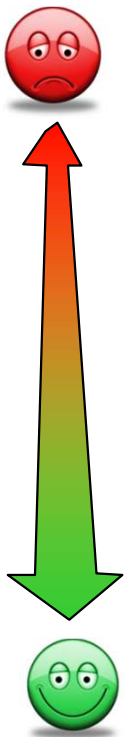


□ OCT

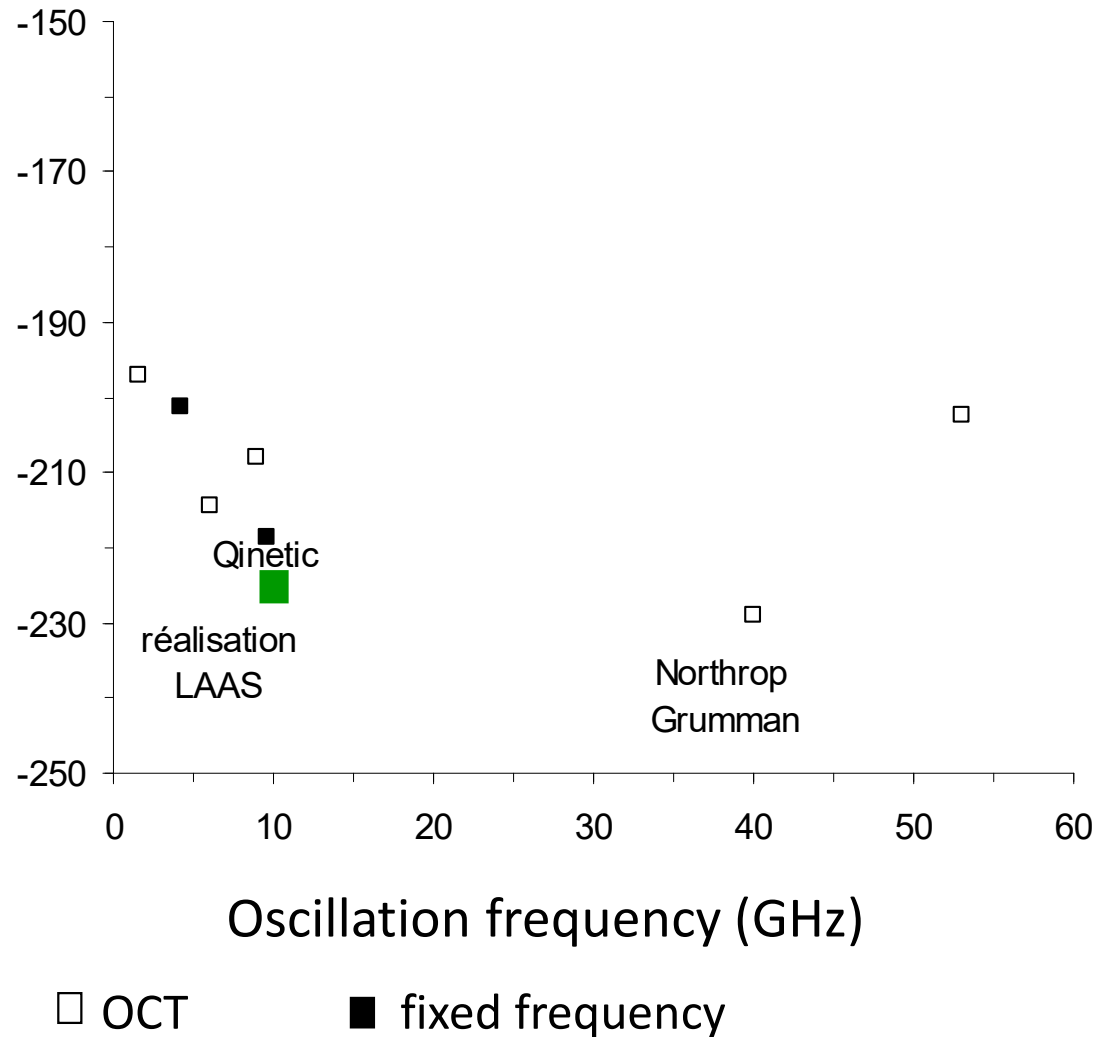
■ fixed frequency

GaN oscillators @ 10 GHz (till 2016)

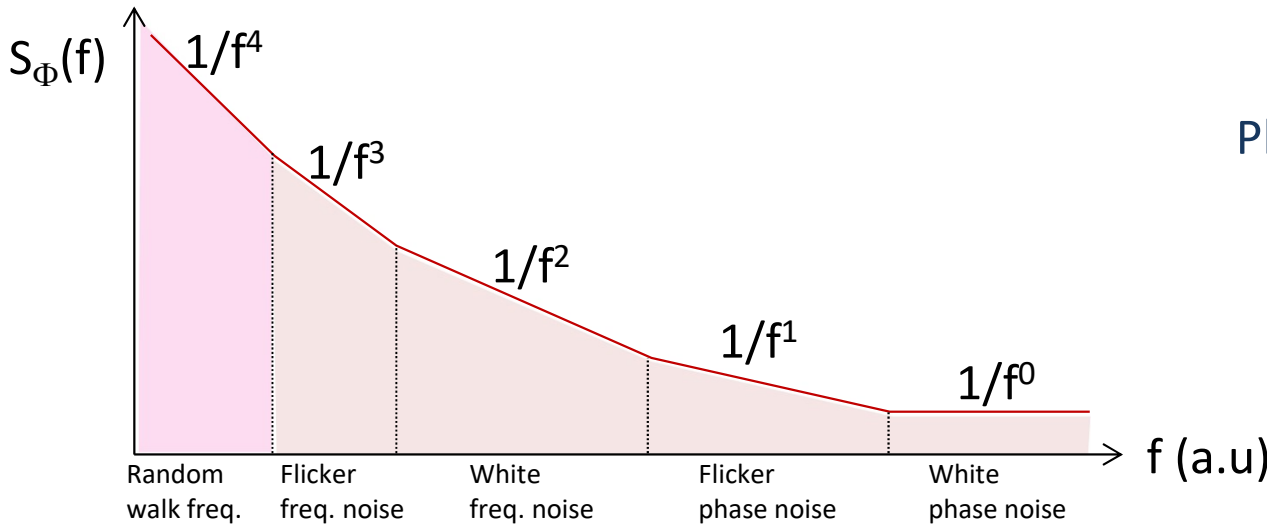
→ State of the art



$L(f_m) - 20 \log(f_0/f_m) - P_{out_dBm}$

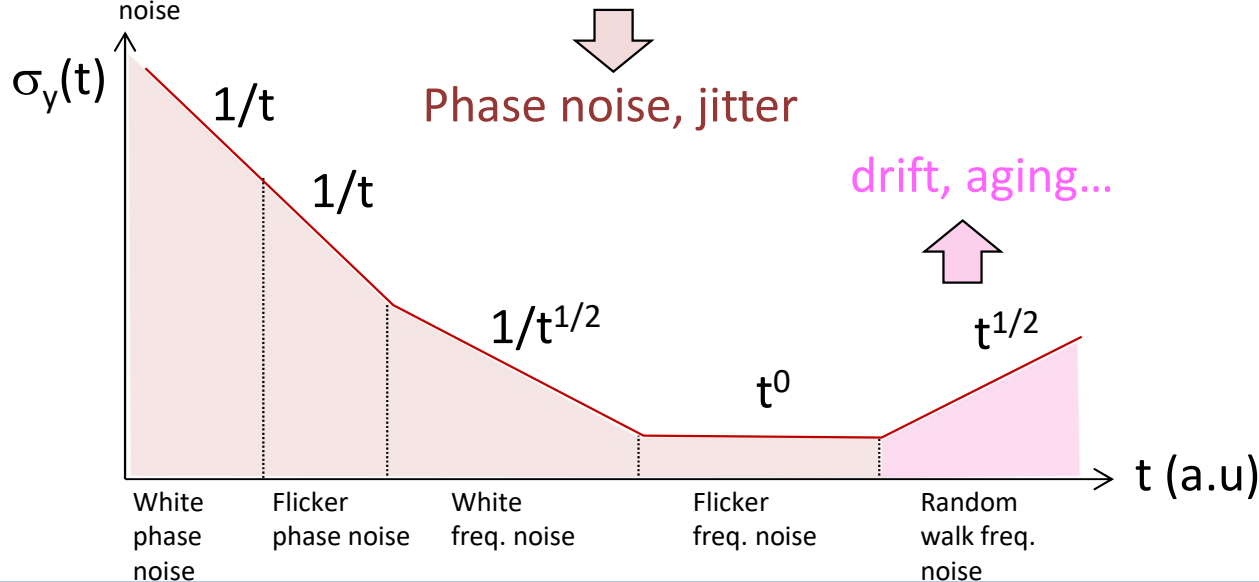


Frequency instabilities can be represented in harmonic domain or time domain



Phase noise spectrum in harmonic domain representation

Ranging from some Hz to MHz



Root-Allan variance plot in time domain representation

Short-long term stability : more than 1s (1Hz and under), to days-months...

This was my first question for Chat GPT !!!



ChatGPT

Q1 JGT : How has low-frequency noise metrology been an accelerator in microelectronics research?



Low-frequency noise metrology has played a crucial role in microelectronics research by providing insights into the behavior of electronic devices at a fundamental level. It has helped researchers understand the origin and mechanisms of low-frequency noise in semiconductor devices, leading to improvements in device performance, reliability, and design. By characterizing and quantifying low-frequency noise, researchers have been able to identify and address issues related to device miniaturization, process variations, and material defects, ultimately driving advancements in microelectronics technology. Additionally, low-frequency noise metrology has contributed to the development of new materials, device structures, and fabrication techniques, further accelerating progress in microelectronics research. *For more in-depth information on this topic, I recommend consulting specialized sources or experts in the field.*

TRL 3-4 for technological & reliability improvement

This was my second question for Chat GPT !!!



ChatGPT

Q2 JGT : Tell me about Low Frequency electronic noise, for what use in applied research in the decades to come?



Low-frequency electronic noise has many potential applications in applied research for the coming decades. It is used in fields such as **spectroscopy, wireless communication, weak signal detection, environmental monitoring and fundamental physics research**. Additionally, it could be leveraged for emerging applications such as quantum technology, biotechnology and quantum communications. *However, for more detailed information on this topic, I recommend consulting specialized sources or experts in the field.*

For sure, if Chat GPT exists, and when it evolves in the future – it will be partly thanks to LFN studies on quantum electronics.

LFN still in the race from low to high TRL contexts

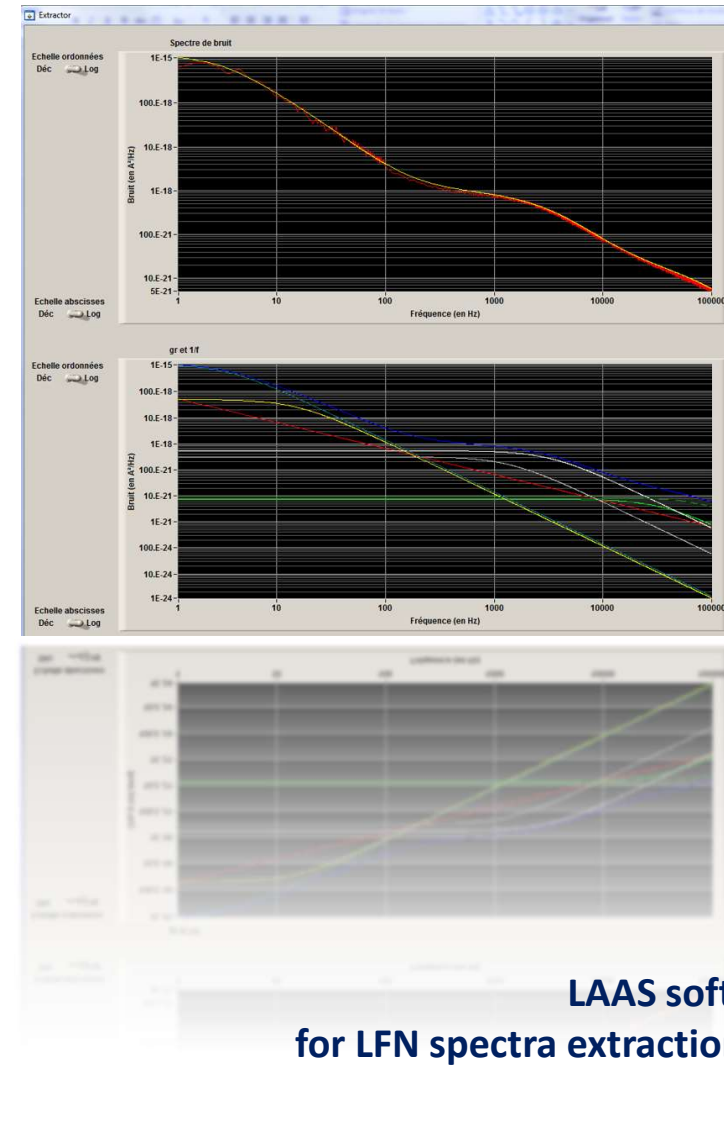
(2/3-5)

- Case of study
- Physics and Theory
- Technology exploration

(6-8)

- Industry quality
- Device selection

Time for questions



LAAS soft.
for LFN spectra extraction

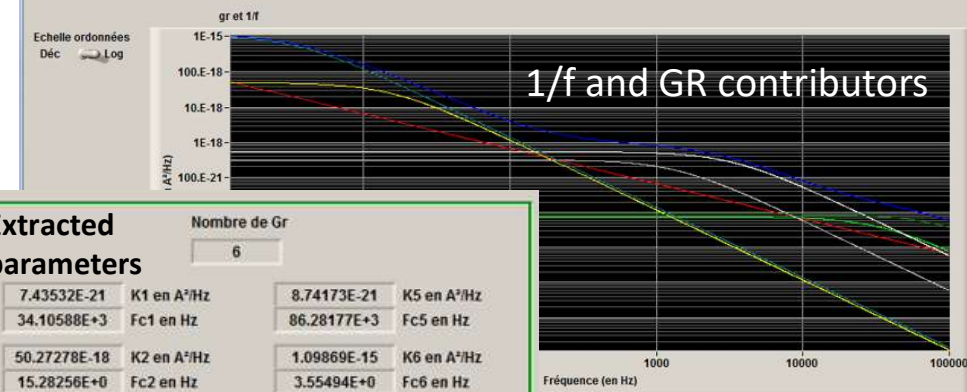
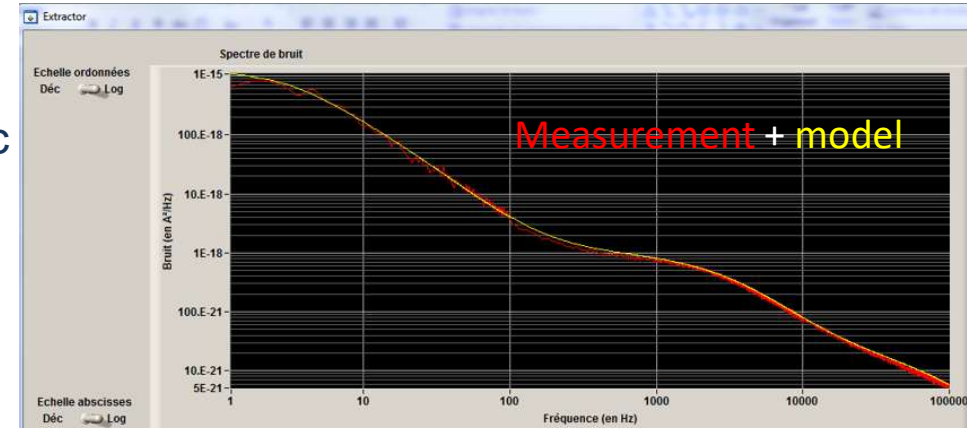
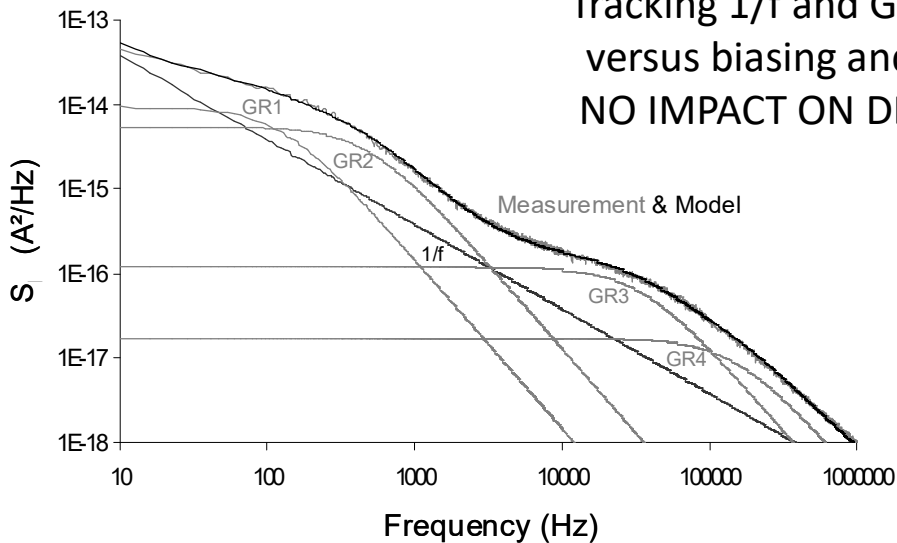
Low Freq. Noise spectroscopy for the detection and tracking of defects – degradation mechanisms

- SiGe HBT technologies Stmicro / IBM / SiGeMicrosystems
- GaN HEMT UMS GH50-GH25, TRT III-V Lab, IEMN, Ommic

$$S_l(f) = B \frac{I^2}{f^\gamma} + \sum_i K_i^2 \frac{I^2 \times \tau_i}{1 + (2\pi f)^2 \tau_i^2} \quad [A^2/Hz]$$

(Ohmic zone)

Tracking 1/f and GR centers (RTN ?) versus biasing and geometry with NO IMPACT ON DEVICE INTEGRITY



Gr

Extracted parameters		Nombre de Gr	
		6	
7.43532E-21	K1 en A ² /Hz	8.74173E-21	K5 en A ² /Hz
34.10588E+3	Fc1 en Hz	86.28177E+3	Fc5 en Hz
50.27278E-18	K2 en A ² /Hz	1.09869E-15	K6 en A ² /Hz
15.28256E+0	Fc2 en Hz	3.55494E+0	Fc6 en Hz
316.17628E-21	K3 en A ² /Hz	83.82504E-21	K7 en A ² /Hz
1.36308E+3	Fc3 en Hz	15.43718E+3	Fc7 en Hz
539.87735E-21	K4 en A ² /Hz	3.05500E-21	K8 en A ² /Hz
3.26904E+3	Fc4 en Hz	178.05139E+3	Fc8 en Hz

LAAS soft. for LFN spectra extraction

LAAS : labelled by KEYSIGHT as European platform for LF Noise and RT Noise measurement